

AD-A185 035

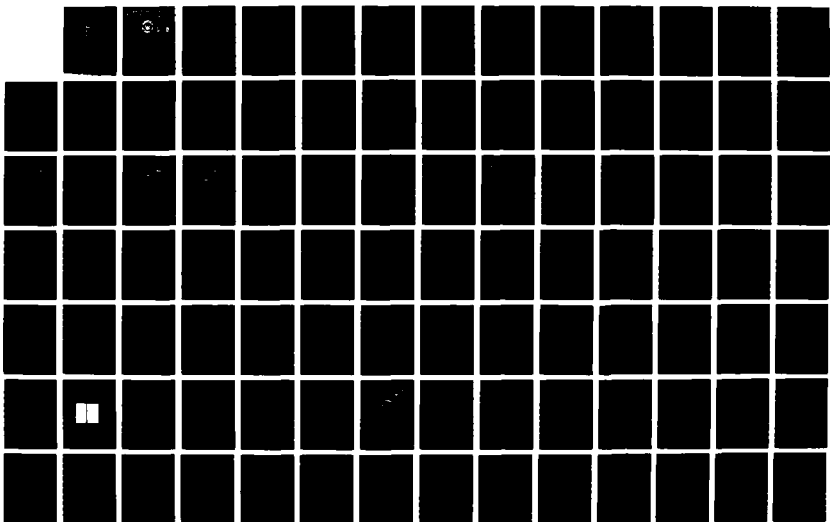
CONTROL OF A FLEXIBLE ONE-LINK MANIPULATOR(U) NAVAL  
POSTGRADUATE SCHOOL MONTEREY CA I E ZOUZIAS JUN 87

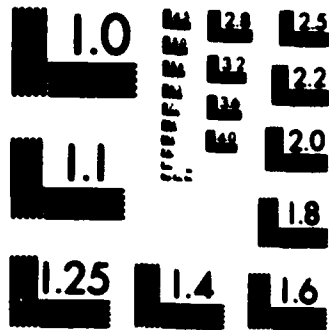
1/2

UNCLASSIFIED

F/G 13/9

NL





MICROCOPY RESOLUTION TEST CHART  
NATIONAL BUREAU OF STANDARDS 1963-A

AD-A185 035

# NAVAL POSTGRADUATE SCHOOL

Monterey, California

2

DTIC FILE COPY



DTIC  
ELECTE  
OCT 06 1987  
S D

## THESIS

CONTROL OF A FLEXIBLE ONE-LINK  
MANIPULATOR

by

Ioannis E. Zouzias

June 1987

Thesis Advisor:

George J. Thaler

Approved for public release; distribution is unlimited

87 9 20 047

UNCLASSIFIED

SECURITY CLASSIFICATION OF THIS PAGE

REPORT DOCUMENTATION PAGE

1a REPORT SECURITY CLASSIFICATION <b>UNCLASSIFIED</b>			1b RESTRICTIVE MARKINGS			
2a SECURITY CLASSIFICATION AUTHORITY			3 DISTRIBUTION/AVAILABILITY OF REPORT <b>Approved for public release; distribution is unlimited</b>			
2b DECLASSIFICATION/DOWNGRADING SCHEDULE						
4 PERFORMING ORGANIZATION REPORT NUMBER(S)			5 MONITORING ORGANIZATION REPORT NUMBER(S)			
6a NAME OF PERFORMING ORGANIZATION <b>NAVAL POSTGRADUATE SCHOOL</b>		6b OFFICE SYMBOL (if applicable) <b>62</b>	7a NAME OF MONITORING ORGANIZATION <b>NAVAL POSTGRADUATE SCHOOL</b>			
6c ADDRESS (City, State, and ZIP Code) <b>Monterey, California 93943-5000</b>			7b ADDRESS (City, State, and ZIP Code) <b>Monterey, California 93943-5000</b>			
8a NAME OF FUNDING/SPONSORING ORGANIZATION		8b OFFICE SYMBOL (if applicable)	9 PROCUREMENT INSTRUMENT IDENTIFICATION NUMBER			
8c ADDRESS (City, State, and ZIP Code)			10 SOURCE OF FUNDING NUMBERS			
			PROGRAM ELEMENT NO	PROJECT NO	TASK NO	WORK UNIT ACCESSION NO
11 TITLE (Include Security Classification) <b>CONTROL OF A FLEXIBLE ONE-LINK MANIPULATOR</b>						
12 PERSONAL AUTHOR(S) <b>ZOUZIAS IOANNIS E.</b>						
13a TYPE OF REPORT <b>Master's Thesis</b>		13b TIME COVERED FROM _____ TO _____		14 DATE OF REPORT (Year, Month, Day) <b>1987 JUNE</b>		15 PAGE COUNT <b>188</b>
16 SUPPLEMENTARY NOTATION						
17 COSATI CODES			18 SUBJECT TERMS (Continue on reverse if necessary and identify by block number) <b>Robotics, Robot arm, Flexible manipulator, Flexible arm, Curve following system.</b>			
FIELD	GROUP	SUB-GROUP				
19 ABSTRACT (Continue on reverse if necessary and identify by block number)  <b>The feasibility of controlling a flexible one-link manipulator with an adaptive computer simulation model, called a curve following system, is investigated. At the beginning a very flexible unloaded arm is used. Later the stiffness of the arm is increased, until we reach the case of a flexible arm that can be used in practice. Finally load is added to the arm and its behavior is studied.</b>						
20 DISTRIBUTION/AVAILABILITY OF ABSTRACT <input checked="" type="checkbox"/> UNCLASSIFIED/UNLIMITED <input type="checkbox"/> SAME AS RPT <input type="checkbox"/> DTIC USERS				21 ABSTRACT SECURITY CLASSIFICATION <b>UNCLASSIFIED</b>		
22a NAME OF RESPONSIBLE INDIVIDUAL <b>George J. Thaler</b>			22b TELEPHONE (Include Area Code) <b>(408) 646-2056</b>		22c OFFICE SYMBOL <b>Code 62Tr</b>	

Approved for public release; distribution is unlimited

Control Of A Flexible One-Link  
Manipulator

by

Ioannis Zouzas  
Lieutenant JG, Hellenic Navy  
B.S., Hellenic Naval Academy, 1979

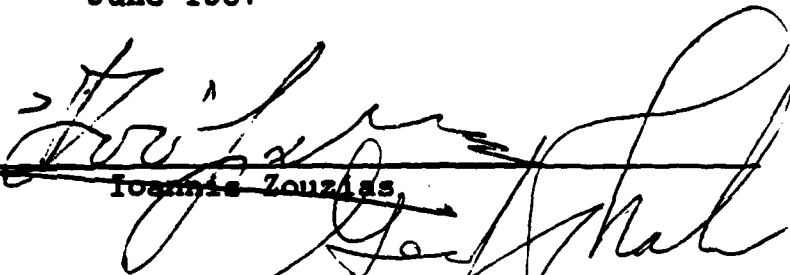
Submitted in partial fulfillment of the  
requirements for the degree of

MASTER OF SCIENCE IN ENGINEERING SCIENCE

from the


NAVAL POSTGRADUATE SCHOOL  
June 1987


Author:


  
Ioannis Zouzas

Approved by:

  
George J. Thaler, Thesis Advisor

  
Harold A. Titus, Second Reader

  
John P. Powers, Chairman, Department of  
Electrical and Computer Engineering

  
Gordon E. Schacher,  
Dean of Science and Engineering

ABSTRACT

The feasibility of controlling a flexible one-link manipulator with an adaptive computer simulation model, called a curve following system, is investigated. At the beginning a very flexible unloaded arm is used. Later the stiffness of the arm is increased, until we reach the case of a flexible arm that can be used in practice. Finally load is added to the arm and its behavior is studied.



Accession For	
NTIS CRA&I	<input checked="" type="checkbox"/>
DTIC TAB	<input type="checkbox"/>
Unannounced	<input type="checkbox"/>
Justification	
By	
Distribution	
Availability Codes	
Dist	Avail and/or Spec
A-1	

## TABLE OF CONTENTS

I.	INTRODUCTION.....	14
A.	BACKGROUND.....	14
B.	REVIEW OF PREVIOUS WORK.....	16
C.	OBJECTIVE OF THE THESIS.....	17
D.	THESIS ORGANIZATION.....	18
II.	MATHEMATICAL MODEL OF THE ARM.....	20
A.	OVERVIEW.....	20
B.	DERIVATION OF THE MATHEMATICAL MODEL.....	21
III.	PRELIMINARY STUDIES ON THE FLEXIBLE ARM.....	25
A.	INTRODUCTION.....	25
B.	ANALYSIS OF THE MODEL OF THE ARM.....	25
1.	Frequency Response.....	25
2.	Time Response Of The Arm.....	30
IV.	VELOCITY CURVE FOLLOW CONTROL SCHEME.....	36
A.	INTRODUCTION.....	36
B.	DESCRIPTION OF THE BASIC SYSTEM.....	37
C.	CURVE DESIGN.....	39
D.	SIMULATION STUDIES OF THE BASIC MODEL.....	41
E.	THE ADAPTIVE ALGORITHM.....	50
V.	APPLICATION OF THE CURVE FOLLOWING SYSTEM FOR THE CONTROL OF THE FLEXIBLE ARM.....	54
VI.	CONTROL OF THE TIP OF THE ARM.....	71
A.	USE OF A SIMPLE COMPENSATOR.....	71
B.	POSI-CAST CONTROL.....	77

C.	USE OF A SHAPED INPUT.....	83
D.	FEEDBACK COMPENSATION.....	92
1.	Overview.....	92
2.	Design Of The Feedback Compensator.....	93
3.	Simulation Of The System.....	96
VII.	EFFECT OF THE ARM'S STIFFNESS ON THE CURVE FOLLOWING SYSTEM.....	107
A.	INTRODUCTION.....	107
B.	BASIC THEORY OF ELASTICITY.....	108
C.	CHANGE OF THE STIFFNESS OF THE ARM.....	110
D.	BASIC STUDIES OF THE STIFFER ARMS.....	112
E.	USE OF THE CURVE FOLLOWING SCHEME WITH THE STIFFER ARMS.....	125
F.	LINEAR COMPENSATOR DESIGN FOR THE FINAL MOTION OF THE 100 TIMES STIFFER ARM.....	132
IX.	FLEXIBLE ARM WITH TIP LOAD.....	139
A.	OVERVIEW.....	139
B.	VERY FLEXIBLE LOADED ARM.....	140
C.	"FLEXIBLE PRACTICAL" LOADED ARM.....	149
IX.	CONCLUSIONS / AREAS FOR FUTURE STUDY.....	159
APPENDIX A:	SIMULATION PROGRAM FOR THE BASIC CURVE FOLLOWING SYSTEM.....	161
APPENDIX B:	SIMULATION PROGRAM FOR THE WHOLE SYSTEM USING CURVE FOLLOWING TECHNIQUE.....	162
APPENDIX C:	SIMULATION PROGRAM FOR THE WHOLE SYSTEM USING CURVE FOLLOWING TECHNIQUE FOR THE FIRST PART OF THE MOTION AND SWITCHING TO A SIMPLE LINEAR REGULATOR FOR THE FINAL MOTION.....	165
APPENDIX D:	SIMULATION PROGRAM FOR THE WHOLE SYSTEM USING CURVE FOLLOWING TECHNIQUE AND POSI-CAST CONTROL.....	168

APPENDIX E:	SIMULATION PROGRAM FOR THE SYSTEM USING CURVE FOLLOWING TECHNIQUE FOR THE FIRST PART OF THE MOTION AND SWITCHING TO A LINEAR SYSTEM CONTAINING A FEEDBACK COMPENSATOR FOR THE FINAL MOTION.....	171
APPENDIX F:	SIMULATION PROGRAM FOR THE SYSTEM USING CURVE FOLLOWING TECHNIQUE WITH THE ARM BEING 20 TIMES STIFFER.....	174
APPENDIX G:	SIMULATION PROGRAM FOR THE SYSTEM USING CURVE FOLLOWING TECHNIQUE WITH THE ARM BEING 50 TIMES STIFFER.....	177
APPENDIX H:	SIMULATION PROGRAM FOR THE SYSTEM USING CURVE FOLLOWING TECHNIQUE WITH THE ARM BEING 100 TIMES STIFFER.....	180
APPENDIX I:	SIMULATION PROGRAM FOR THE SYSTEM USING CURVE FOLLOWING TECHNIQUE FOR THE FIRST PART OF THE MOTION AND THEN SWITCHING TO A LINEAR REGULATOR FOR THE FINAL MOTION (THE ARM IS 100 TIMES STIFFER).....	183
	LIST OF REFERENCES.....	186
	INITIAL DISTRIBUTION LIST.....	187

## LIST OF FIGURES

2.1	Schematic Diagram Of The Arm.....	22
3.1	Open Loop Frequency Response Of The Hub Transfer Function (Arm Unloaded).....	26
3.2	Open Loop Frequency Response Of The Tip Transfer Function (Arm Unloaded).....	27
3.3	Open Loop Frequency Response Of The Hub Transfer Function (Arm Loaded).....	28
3.4	Open Loop Frequency Response Of The Tip Transfer Function (Arm Loaded).....	29
3.5	Step Response Of The Hub Transfer Function (Arm Unloaded).....	31
3.6	Step Response Of The Tip Transfer Function (Arm Unloaded).....	32
3.7	Step Response Of The Hub Transfer Function (Arm Loaded).....	33
3.8	Step Response Of The Tip Transfer Function (Arm Loaded).....	34
4.1	The Basic Velocity Curve Follow System.....	38
4.2	Phase Plane Trajectories Of The Model.....	42
4.3	Step Response Of The Model.....	43
4.4	Input Shape For Simulations Shown In Figures 4.5 And 4.6.....	44
4.5	Phase Plane Trajectories Of The Model For The Input Shown In Figure 4.4.....	45
4.6	Response Of The Model To The Input Shown In Figure 4.4.....	46
4.7	Input Shape For Simulations Shown In Figures 4.8 And 4.9.....	47

4.8	Phase Plane Trajectories Of The Model With Input As In Figure 4.7.....	48
4.9	Response Of The Model To The Input Shown In Figure 4.7.....	49
4.10	Block Diagram Of The Adaptive System.....	51
5.1	Phase Plane Trajectories Of The System With $K_1 = 0.7$ .....	55
5.2	Hub Motion With $K_1 = 0.7$ .....	56
5.3	Tip Motion With $K_1 = 0.7$ .....	57
5.4	Phase Plane Trajectories Of The System With $K_1 = 0.2$ .....	58
5.5	Hub Motion With $K_1 = 0.2$ .....	59
5.6	Tip Motion With $K_1 = 0.2$ .....	60
5.7	Phase Plane Trajectories Of The System With $K_1 = 0.06$ .....	61
5.8	Hub Motion With $K_1 = 0.06$ .....	62
5.9	Tip Motion With $K_1 = 0.06$ .....	63
5.10	Phase Plane Trajectories Of The System, Using Tip Position And Tip Velocity For The Adaptive Algorithm.....	64
5.11	Hub Motion When Tip Position And Tip Velocity Are Used For The Adaptive Algorithm.....	65
5.12	Tip Motion When Tip Position And Tip Velocity Are Used For The Adaptive Algorithm.....	66
5.13	Torque Applied To The Arm And Its Resulting Hub Motion.....	69
6.1	Use Of A Simple Compensator For The Tip Control.....	72
6.2	The Open Loop Bode Plot Of The Linear System.....	74
6.3	Step Response Of The Linear System (Hub Motion).....	75
6.4	Step Response Of The Linear System (Tip Motion).....	76
6.5	Hub Motion Switching To Linear Mode At 90% Of The Commanded Position.....	78

6.6	Tip Motion Switching To Linear Mode At 90% Of The Commanded Position.....	79
6.7	Hub Motion Switching To Linear Mode At 60% Of The Commanded Position.....	80
6.8	Tip Motion Switching To Linear Mode At 60% Of The Commanded Position.....	81
6.9	Posi-Cast Control (Hub Motion).....	84
6.10	Posi-Cast Control (Tip Motion).....	85
6.11	Posi-Cast Control (Hub Motion), Taking Into Account The 280 msec Delay Of The Tip's Response.....	86
6.12	Posi-Cast Control (Tip Motion), Taking Into Account The 280 msec Delay Of The Tip's Response.....	87
6.13	Input Shape For The Motions Shown In Figures 6.14 And 6.15.....	89
6.14	Hub Motion Subject To The Input Shown In Figure 6.13.....	90
6.15	Tip Motion Subject To The Input Shown In Figure 6.13.....	91
6.16	Control System For The Motion Of The Arm (Use Of Curve Following And Feedback Compensator)....	94
6.17	Step Response Of The Linear System.....	97
6.18	Hub Motion Using The System Shown In Figure 6.16 With $K_1 = 0.2$ (Small Motion).....	98
6.19	Tip Motion Using The System Shown In Figure 6.16 With $K_1 = 0.2$ (Small Motion).....	99
6.20	Hub Motion Using The System Shown In Figure 6.16 With $K_1 = 0.08$ (Small Motion).....	100
6.21	Tip Motion Using The System Shown In Figure 6.16 With $K_1 = 0.08$ (Small Motion).....	101
6.22	Hub Motion Using The System Shown In Figure 6.16 With $K_1 = 0.06$ (Small Motion).....	102
6.23	Tip Motion Using The System Shown In Figure 6.16 With $K_1 = 0.06$ (Small Motion).....	103

6.24	Hub Motion Using The System Shown In Figure 6.16 With $K_1 = 0.06$ (Large Motion).....	104
6.25	Tip Motion Using The System Shown In Figure 6.16 With $K_1 = 0.06$ (Large Motion).....	105
7.1	Open Loop Bode Plot Of The Hub Transfer Function Of The 20 Times Stiffer Arm.....	113
7.2	Open Loop Bode Plot Of The Tip Transfer Function Of The 20 Times Stiffer Arm.....	114
7.3	Step Response Of The Hub Transfer Function Of The 20 Times Stiffer Arm.....	115
7.4	Step Response Of The Tip Transfer Function Of The 20 Times Stiffer Arm.....	116
7.5	Open Loop Bode Plot Of The Hub Transfer Function Of The 50 Times Stiffer Arm.....	117
7.6	Open Loop Bode Plot Of The Tip Transfer Function Of The 50 Times Stiffer Arm.....	118
7.7	Step Response Of The Hub Transfer Function Of The 50 Times Stiffer Arm.....	119
7.8	Step Response Of The Tip Transfer Function Of The 50 Times Stiffer Arm.....	120
7.9	Open Loop Bode Plot Of The Hub Transfer Function Of The 100 Times Stiffer Arm.....	121
7.10	Open Loop Bode Plot Of The Tip Transfer Function Of The 100 Times Stiffer Arm.....	122
7.11	Step Response Of The Hub Transfer Function Of The 100 Times Stiffer Arm.....	123
7.12	Step Response Of The Tip Transfer Function Of The 100 Times Stiffer Arm.....	124
7.13	Hub Motion Of The 20 Times Stiffer Arm Using The Curve Following System.....	126
7.14	Tip Motion Of The 20 Times Stiffer Arm Using The Curve Following System.....	127
7.15	Hub Motion Of The 50 Times Stiffer Arm Using The Curve Following System.....	128

7.16	Tip Motion Of The 50 Times Stiffer Arm Using The Curve Following System.....	129
7.17	Hub Motion Of The 100 Times Stiffer Arm Using The Curve Following System.....	130
7.18	Tip Motion Of The 100 Times Stiffer Arm Using The Curve Following System.....	131
7.19	Open Loop Frequency Response Of The Linear System (Tip Feedback).....	134
7.20	Step Response of The Linear System.....	135
7.21	Hub Motion Using The Linear System For The Final Motion.....	136
7.22	Tip Motion Using The Linear System For The Final Motion.....	137
8.1	Tip Motion Of The Loaded Arm Using The Curve Following System Alone ( $K_1=0.06$ ).....	142
8.2	Tip Motion Of The Loaded Arm Using The Curve Following System Alone ( $K_1=0.02$ ).....	143
8.3	Hub Motion Of The Loaded Arm Using The Curve Following System Alone ( $K_1=0.06$ ).....	144
8.4	Hub Motion Of The Loaded Arm Using The Curve Following System Alone ( $K_1=0.02$ ).....	145
8.5	Hub Motion Of The Loaded Arm Using The System Shown In Figure 6.16 ( $K_1=0.06$ , Small Motion).....	146
8.6	Tip Motion Of The Loaded Arm Using The System Shown In Figure 6.16 ( $K_1=0.06$ , Small Motion).....	147
8.7	Tip Motion Of The Loaded Arm Using The System Shown In Figure 6.16 ( $K_1=0.06$ , Large Motion).....	148
8.8	Hub Motion Of The Loaded Arm Using The System Shown In Figure 6.16 ( $K_1=0.02$ , Small Motion).....	150
8.9	Tip Motion Of The Loaded Arm Using the System Shown In Figure 6.16 ( $K_1=0.02$ , Small Motion).....	151
8.10	Tip Motion Of The Loaded Arm Using The System Shown In Figure 6.16 ( $K_1=0.02$ , Large Motion).....	152
8.11	Hub Motion Of The 100 Times Stiffer Loaded Arm Using The Curve Following System Alone ( $K_1=0.06$ )....	154

8.12 Tip Motion Of The 100 Times Stiffer Loaded Arm  
Using The Curve Following System Alone ( $K_1=0.06$ )....155

8.13 Hub Motion Of The 100 Times Stiffer Loaded Arm  
Using The Linear System For The Final Motion  
( $K_1=0.06$ ).....156

8.14 Tip Motion Of The 100 Times Stiffer Loaded Arm  
Using The Linear System For The Final  
Motion ( $K_1=0.06$ ).....157

## ACKNOWLEDGMENT

I wish to express my deepest gratitude to my Thesis Advisor, Distinguished Professor, George J. Thaler who lead me so wisely in the course of this Thesis. Also I want to thank my wife Maria and my son Vagelis, whose help and support was very important during our stay in the Naval Postgraduate School.

## I. INTRODUCTION

### A. BACKGROUND

In recent years an increasing use of programmable manipulators, or robots as often called, has taken place, as a result of the need to increase industrial productivity. Beyond the use of these devices in manufacturing processes, they are also used to perform tasks in environments hazardous to humans, such as radioactive material handling, operations and maintenance inside nuclear reactors, etc. Furthermore the use of robots in space missions is a fact and their use in exploratory space missions, where a considerably high risk for the astronauts exists, is a necessity.

The trend towards "programmable manipulators" is dictated by the fact that such devices can perform a wide range of jobs, by simply changing the program that controls them, reducing considerably the overall cost.

Robots are essentially mechanical manipulators, with several degrees of freedom, typically six, to be capable of performing tasks similar to that of a human hand. They can be identified as consisting of three parts: the manipulator (arm), the controller and the power supply.

The manipulator of the robot performs the actual job. It essentially consists of links, joints and actuators. The

brain of the robot is the controller which directs the motion of the manipulator. Finally the power supply provides the energy required for the operation of the whole system.

Despite the amount of work done in the past in the field of robotics, one of the major drawbacks of today's robots is the low speed of operation. The speed is greatly limited by the weight of the manipulator arm. At present the ratio of arm weight to payload is of the order of 10 to 1. This excessive arm weight not only hampers the motion of the manipulator arm, but also increases the size of the required actuators as well as the power consumption. To overcome this problem, a lot of design effort nowadays is geared towards building of straight, stiff and light links, for which, however, the manufacturing cost is high.

A flexible manipulator is free of these drawbacks. It has slender links which are considerably more rigid in compression than in flexure and therefore requires less material, has less weight, consumes less power and has more maneuverability than traditional heavy manipulators. Furthermore with the lower power demand, smaller actuators can be used resulting in an overall lower cost and lower total weight for the system. This reduced weight enhances the transportability of the whole system, a feature very attractive for space applications.

In spite of these advantages, flexible manipulators have not been much favored in the production industries. Some of

the reasons are as follows: Manipulator arms require a reasonable accuracy in the response of the end point (tip), to commands applied at the joints. This accuracy is deteriorated by structural deformation when the arm is flexible, especially when the deformation is oscillatory. Traditionally, these oscillations have been eliminated by increasing the rigidity of the arms, and this is exactly what we want to avoid with the use of flexible arms, if we are not to sacrifice their advantage. Also the dynamics of flexible links is extremely complex and non-linear and obviously more difficult to analyze.

#### B. REVIEW OF PREVIOUS WORK

[Ref. 1] uses a very flexible arm on which control techniques are applied for the precise tip positioning. The controller used is linear and its design is based on optimal control theory. This control scheme results in a fast positioning of the tip of the arm, but it is only valid for small displacements, because otherwise the motor is driven to saturation limits. When the motor saturates the whole control scheme is rendered invalid.

Nevertheless the solution given in this reference works very well and the results have been verified experimentally.

[Ref. 2] presents the method for modelling a multi-link arm with all links being flexible. It uses series expansion about the operating point in order to obtain a linear model

for the manipulator. Application of optimal control theory is used for the control of a manipulator with two flexible links, without providing the intermediate steps followed.

[Ref. 3] uses an adaptive model for the positioning of a two-link rigid arm. This scheme results in a near minimum time solution, with very high accuracy of the end point position. The scheme used is customarily called velocity curve following, and it is widely used in high performance disk drives. The complete description of this scheme is given in [Ref. 4].

[Ref. 5] shows the implementation of the controller used in [Ref. 3] in a micro-computer, for an one-link rigid arm. The performance of the controller is excellent and verifies the theoretical results of [Ref. 3] and [Ref. 4] ensuring the applicability of the controller in actual hardware.

### C. OBJECTIVE OF THE THESIS

In this thesis a feasibility study of the application of the velocity curve follow technique to the flexible arms will be done. The advantage of this technique is its simplicity and as shown in [Ref. 4] and [Ref. 5], it can easily be implemented in a micro-computer. Another advantage of this technique is its adaptive nature. Through the adaptation procedure it accounts for modelling uncertainties, unpredictable environmental changes, and noise contamination of the signals.

The same arm used in [Ref. 1] will be used in this thesis in order to have a comparison basis for the results and because the model for this arm is well documented.

The effect of the arm's stiffness on the curve follow scheme will also be studied. This study is considered necessary in the sense that the arm we are going to use is an extremely flexible arm and not applicable in any practical situation. It is therefore necessary to have an idea--at least--of how the proposed scheme works with a more realistic flexible manipulator.

#### D. THESIS ORGANIZATION

In Chapter II the model of the arm will be given. As mentioned earlier the model used in [Ref.1] will be used in this thesis for it is well documented and will provide a comparison basis for the results.

Some preliminary studies on the model will be performed in Chapter III. These will include time and frequency response of the system which will help to reveal the prominent physical characteristics of the arm.

In Chapter IV the velocity curve following control system will be developed and simulated.

In Chapter V an investigation will be done on whether or not the curve follow scheme can be applied for the control of a flexible arm.

In Chapter VI some control schemes will be used and simulated as a supplement to the curve follow system for the accurate control of the tip of the arm.

The effect of the arm's stiffness on the curve follow scheme will be studied in Chapter VII.

While in all chapters the unloaded arm will be used, in Chapter IIX the simulation results of the motion of the arm with load will be presented. Some general remarks will be drawn and areas for future study will be outlined, which will help make the control scheme derived for the unloaded arm, to work with any load.

Chapter IX will conclude the thesis and recommendations for further study will be given in the same chapter.

## II. MATHEMATICAL MODEL OF THE ARM

### A. OVERVIEW

The modelling of a flexible arm is by no means an easy task. The dynamics of a robot arm, even in the case of a rigid body, is highly nonlinear and complex. The effective inertia of the whole system changes as the geometric configuration of the manipulator arm changes with its motion. When we use high speeds for the motion of the arm, coriolis effects cannot be neglected. Adding flexural dynamics makes the problem very complex.

The dynamics of a flexible arm can be most appropriately represented by a distributed (continuous) system model. This approach results in a set of partial differential equations of infinite dimensions. Such an infinite dimensional model cannot be used for the design of the controller of the system. The usual approach is to resort to a finite element representation in order to obtain a finite order system on which control design will be based. This, however, causes some problems, because we try to control the actual system with a controller whose design is based on an "incorrect" model.

Fortunately this finite order model produces reasonably accurate approximation for the low frequency structural mode. The accuracy for the higher mode frequencies and shapes is

often poor [Ref. 6], but with insignificant effects for the control design.

From Analytical Mechanics we see that the most commonly used methods to model complex structures with a distributed parameter nature is the Lagrange and the Hamiltonian methods.

[Ref. 7] describes these two methods and gives several illustrative examples for their use.

## B. DERIVATION OF THE MATHEMATICAL MODEL

[Ref. 1] uses both Hamilton's and Lagrange's formalism to derive the mathematical model of an experimental flexible arm, moving on the horizontal plane as shown in Figure 2.1. The mathematics involved are fairly complex and for the complete solution the reader is referred to [Ref. 1].

The resulting model is linear and, as mentioned in Chapter I, it is the model that will be used in the course of this thesis. In that experimental arm three sensors are used in order to measure various signals. One sensor is located at the hub of the arm (point O in Figure 2.1) which measures the hub angle of the arm. A Strain-gauge sensor is located close to the hub which measures the strain that the arm undergoes and a third sensor is located at the tip of the arm which measures the position of the tip of the arm.

The transfer functions from torque at the hub of the arm to the various sensors are as follows.

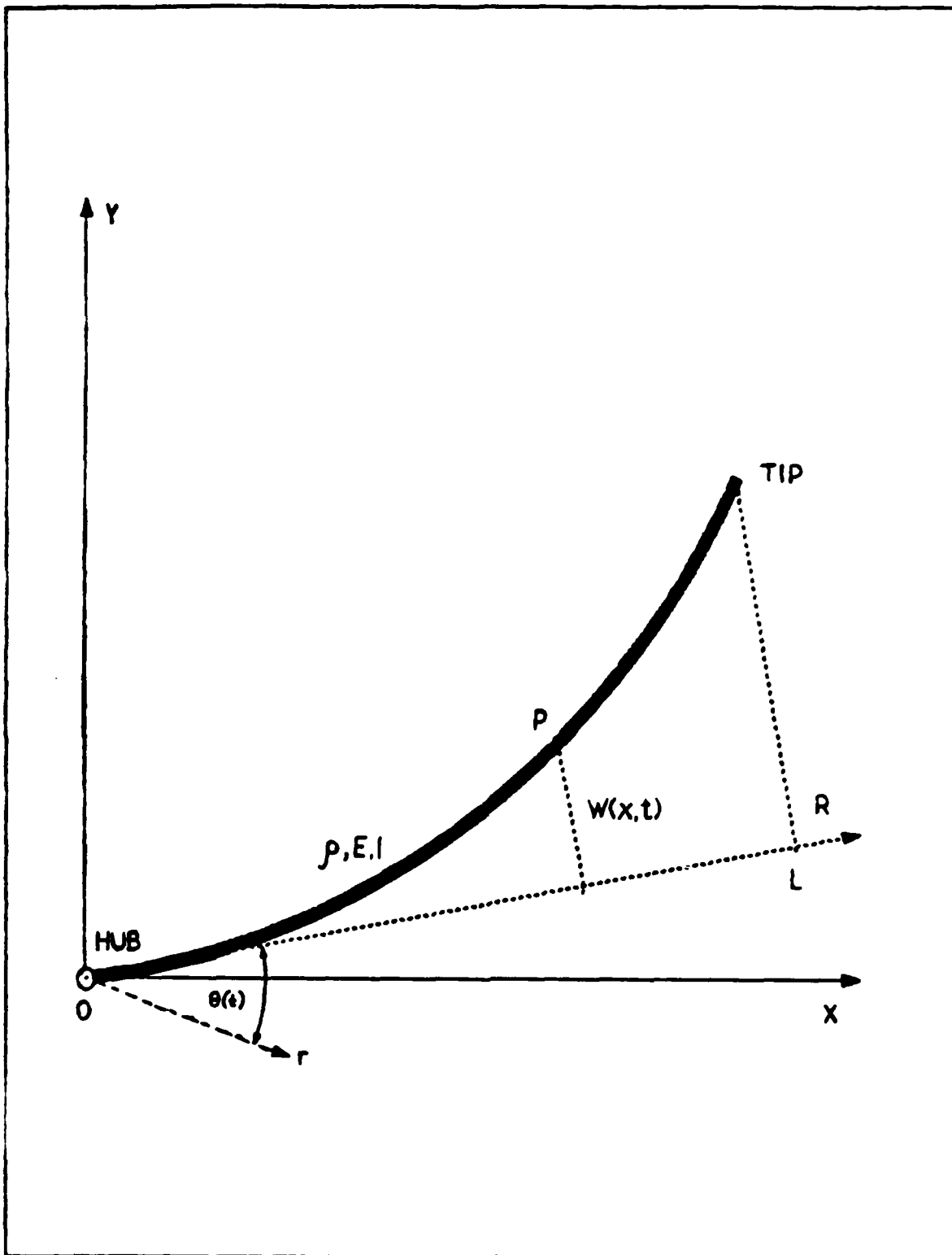


Figure 2.1 Schematic Diagram Of The Arm.

For the case of unloaded arm (no payload) we have.

Collocated hub angle sensor:

$$\frac{\theta(s)}{T(s)} = \frac{46.321(s+0.11+j3.34)(s+0.29+j17.47)(s+0.69+j46.44)}{s(s+0.2)(s+0.17+j11.79)(s+0.4+j21.61)(s+0.72+j48.07)}$$

Tip position sensor:

$$\frac{y_t(s)}{T(s)} = \frac{-2.177(s-12.04)(s+12.14)(s+22.38+j24.2)(s-21.52+j25.3)}{s(s+0.2)(s+0.17+j11.79)(s+0.4+j21.61)(s+0.72+j48.07)}$$

For the case of loaded arm with a tip mass equal to 0.229 Kg, the transfer functions are as follows.

Collocated hub angle sensor:

$$\frac{\theta(s)}{T(s)} = \frac{44.314(s+0.82+j41.7)(s+0.24+j14.509)(s+0.1+j2.47)}{s(s+0.2)(s+0.87+j43.53)(s+0.4+j19.4)(s+0.15+j10.1)}$$

Tip position sensor:

$$\frac{y_t(s)}{T(s)} = \frac{-0.714(s-12.74)(s+12.89)(s+20.7+j22.94)(s-19.9+j24.4)}{s(s+0.2)(s+0.87+j43.53)(s+0.4+j19.4)(s+0.1+j10.1)}$$

In both cases the transfer functions from torque to strain-gauge sensor are omitted because we are not going to use them throughout this thesis.

The units are: "rad" for hub angle, "meters" for tip position and "N·m" for torque.

The inertia of the unloaded arm (without the tip mass) is  $0.44 \text{ Kg}\cdot\text{m}^2$ , while for the loaded arm is  $0.73 \text{ kg}\cdot\text{m}^2$ , which corresponds to an increase of 66 %.

The physical dimensions and other parameters for the arm are given in Table 2.1.

TABLE 2.1. DIMENSIONS AND PARAMETERS OF THE ARM.

Beam length L (m)	1.13
Arm total mass $m_t$ (kg)	0.686
Hub moment of inertia $I_H$ ( $\text{kg}\cdot\text{m}^2$ )	0.023
Arm total moment of inertia $I_r$	0.44

### III. PRELIMINARY STUDIES ON THE FLEXIBLE ARM

#### A. INTRODUCTION

Before we proceed with the design of a controller for the flexible arm, it is helpful to perform some preliminary studies on the model of the arm, in order to obtain some feeling of the prominent physical properties of the system.

Without this physical insight of the system no reasonable control design can be done and the interpretation of the results, after the application of any control scheme will be difficult if not incorrect.

#### B. ANALYSIS OF THE MODEL OF THE ARM

##### 1. Frequency Response

In Figures 3.1 through 3.4 the frequency response for all transfer functions is given. For the derivation of these plots the software package "CONTROLS" was used.

In Figures 3.1 and 3.2 we see the open loop frequency response of the hub and tip motion, with the arm carrying no load. We observe that the hub motion has three resonance frequencies with the lower one at about 10 rad/sec. The two first resonant frequencies have magnitude greater than zero db. If the arm were modelled by an infinite element approach the resonant frequencies would be infinitely many. However,

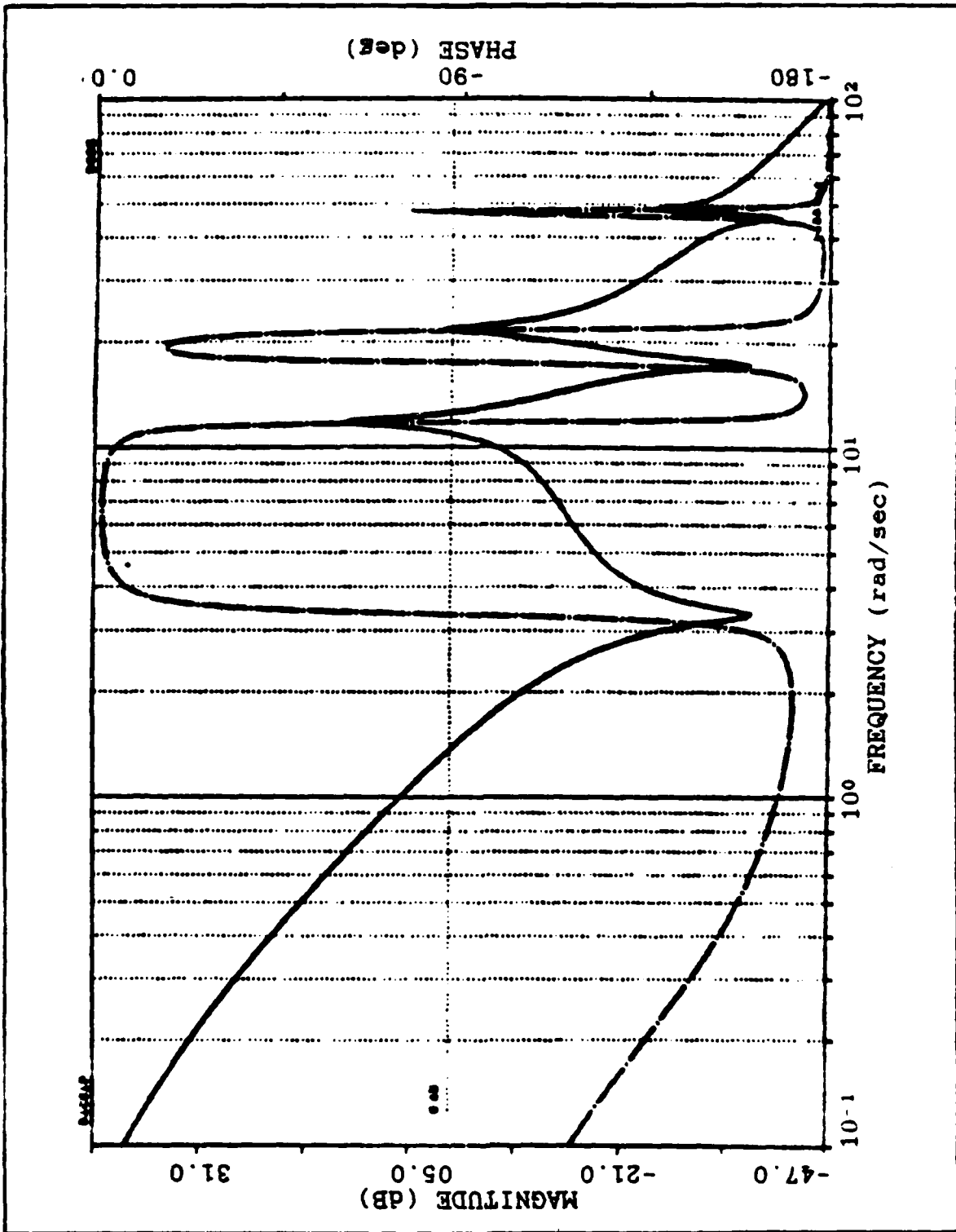


Figure 3.1 Open Loop Frequency Response Of The Hub Transfer Function (Arm Unloaded).

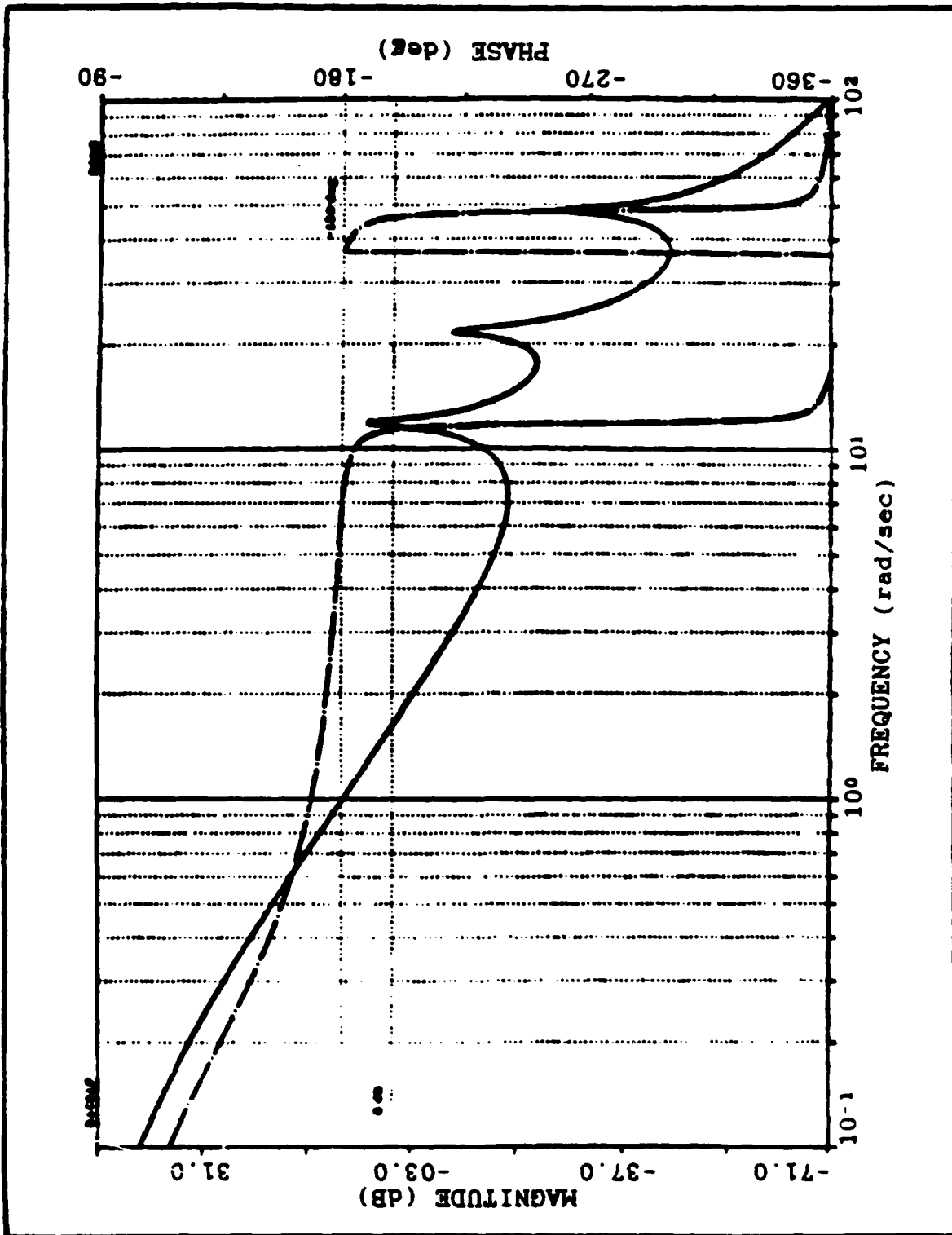


Figure 3.2 Open Loop Frequency Response Of The Tip Transfer Function (Arm Unloaded).

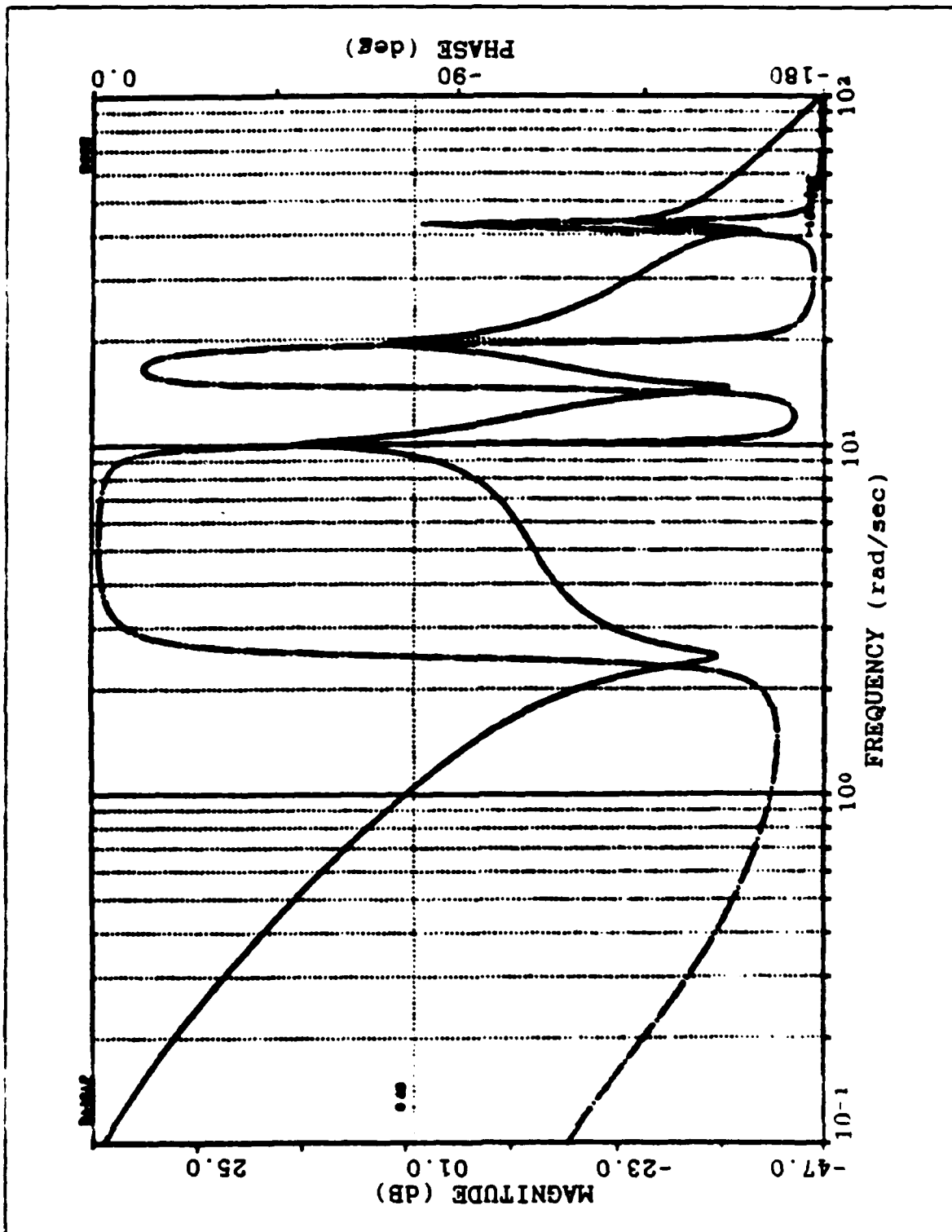


Figure 3.3 Open Loop Frequency Response Of The Hub Transfer Function (Arm Loaded).

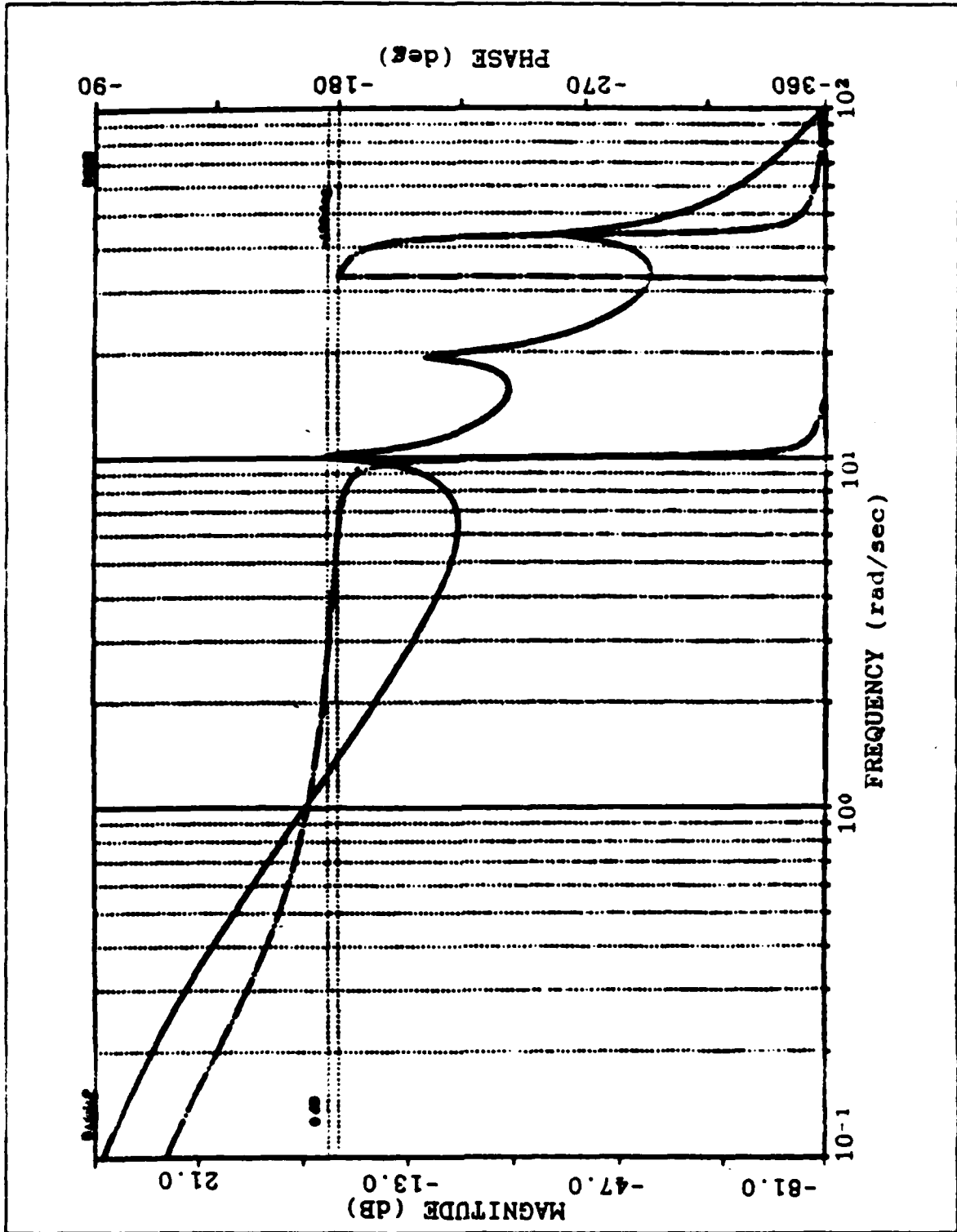


Figure 3.4 Open Loop Frequency Response Of The Tip Transfer Function (Arm Loaded).

we see that even the third resonant frequency is insignificant since its peak is at about -30 db, and we can say that the finite element approach used in Chapter II for the modelling of the flexible arm is sufficiently good. The phase margin for the hub transfer function is  $12^\circ$ .

From the open loop frequency response of the tip transfer function we see that only one resonant frequency exceeds the zero db level and it is at about 10 rad/sec, which is the same frequency as in the case of the hub transfer function. Therefore if a filter were to be used to eliminate the effects of this resonance, it would have the same good effects on both hub and tip transfer functions. Another significant observation on Figure 3.2 is its nonminimum phase character. In the lower frequencies, the magnitude has a slope of -40 db/dec but the phase does not pass through  $-180^\circ$ . This is the effect of the nonminimum phase zeros.

Similar observations hold for the open loop frequency response of the transfer functions that correspond to the loaded arm. The only difference is that the crossover frequencies as well as the resonances have been moved to the left by 0.4 rad/sec.

## 2. Time Response Of The Arm

The second set of preliminary studies of the arm is its time response and is presented in Figures 3.5 through 3.8. In Figures 3.5 and 3.6 the step response of the hub and

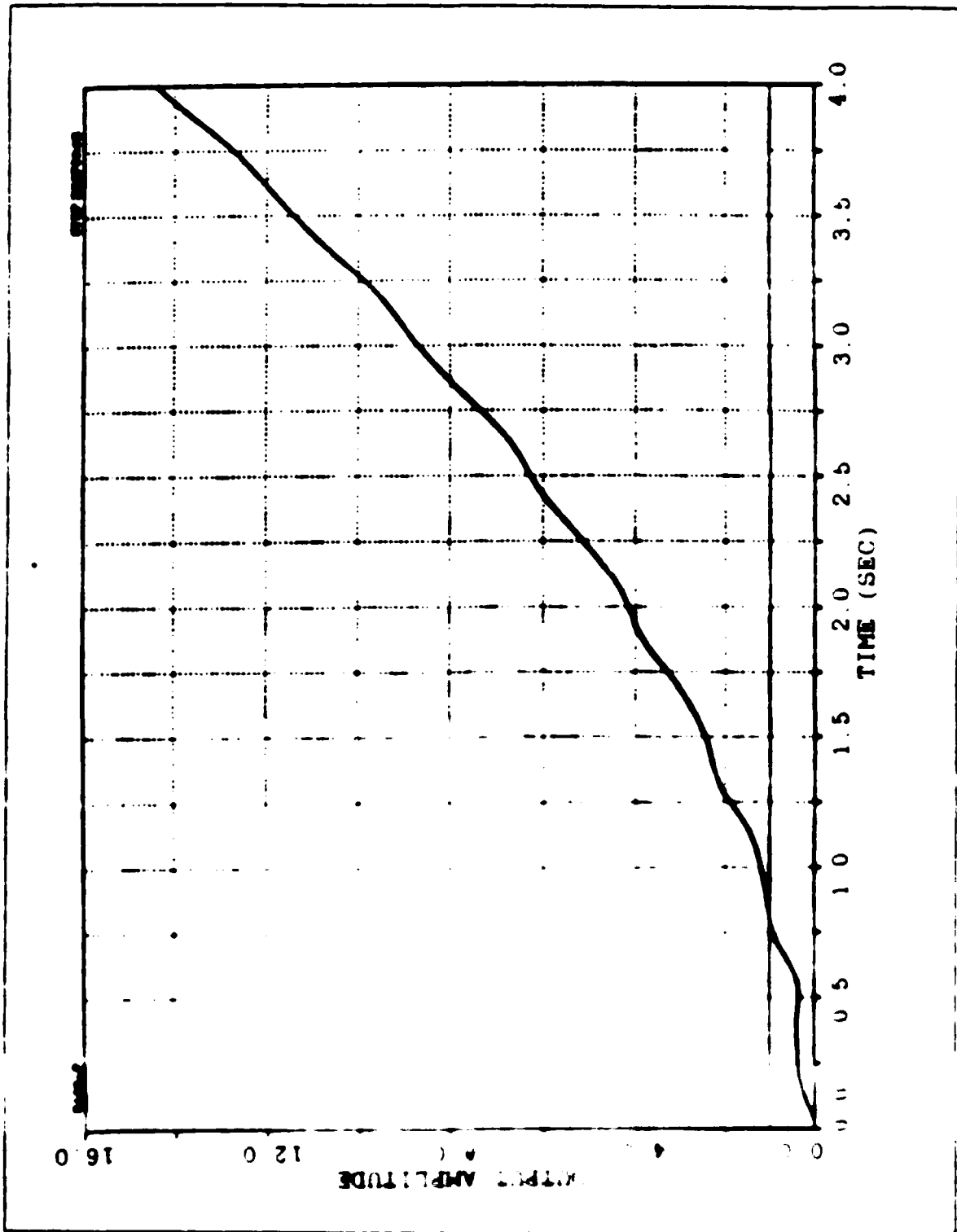


Figure 3.5 Step Response Of The Hub Transfer Function (Arm Unloaded)

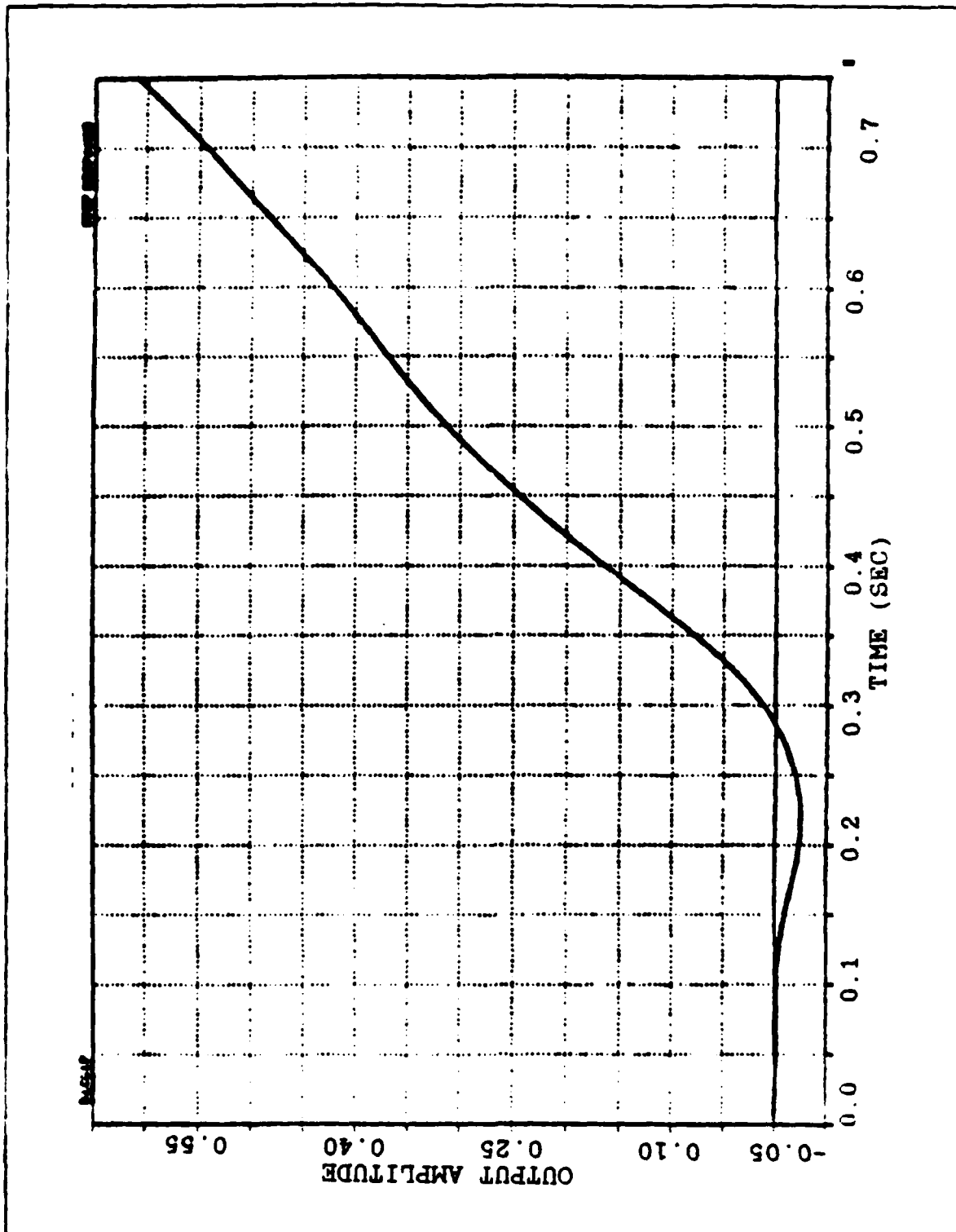


Figure 3.6 Step Response Of The Tip Transfer Function (Arm Unloaded).

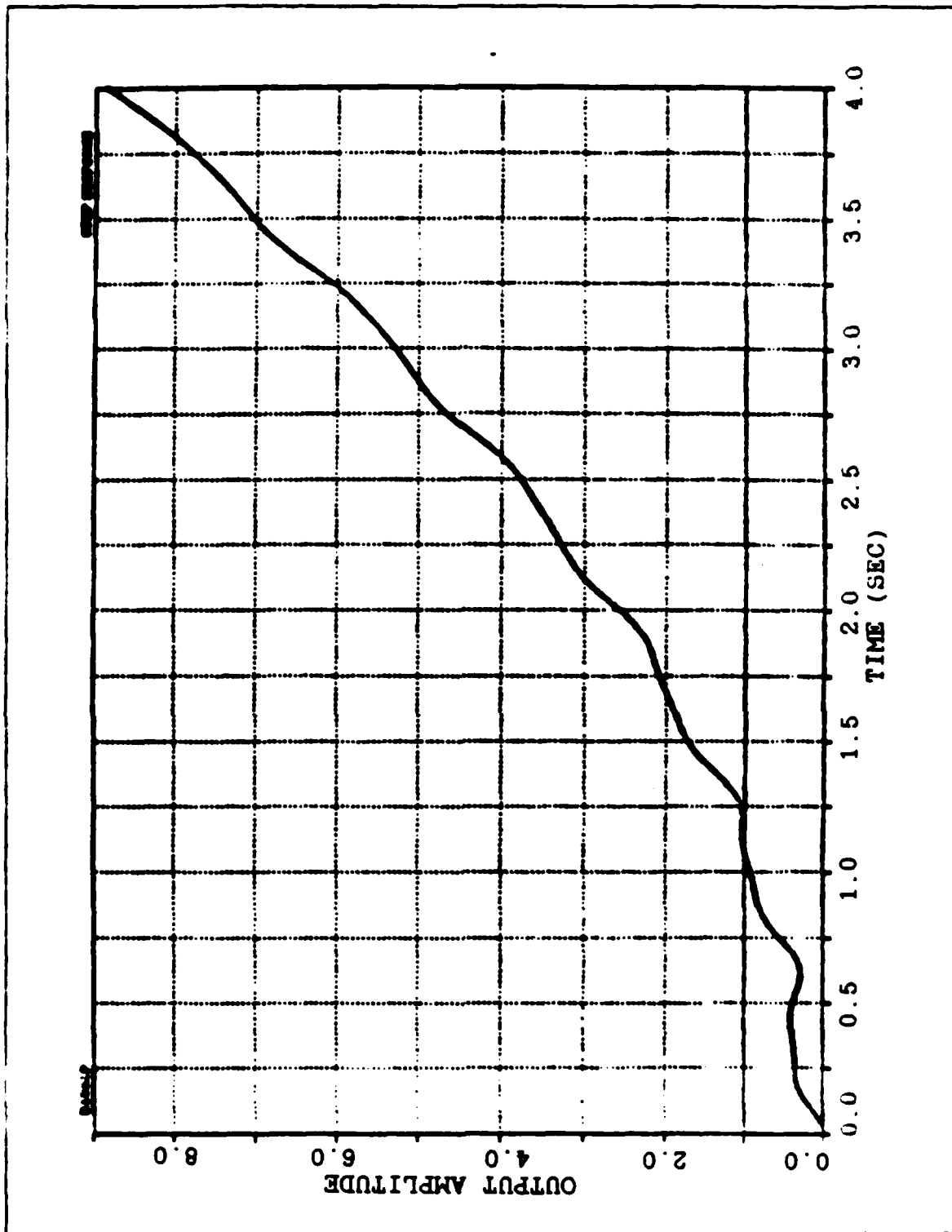


Figure 3.7 Step Response Of The Hub Transfer Function (Arm Loaded).

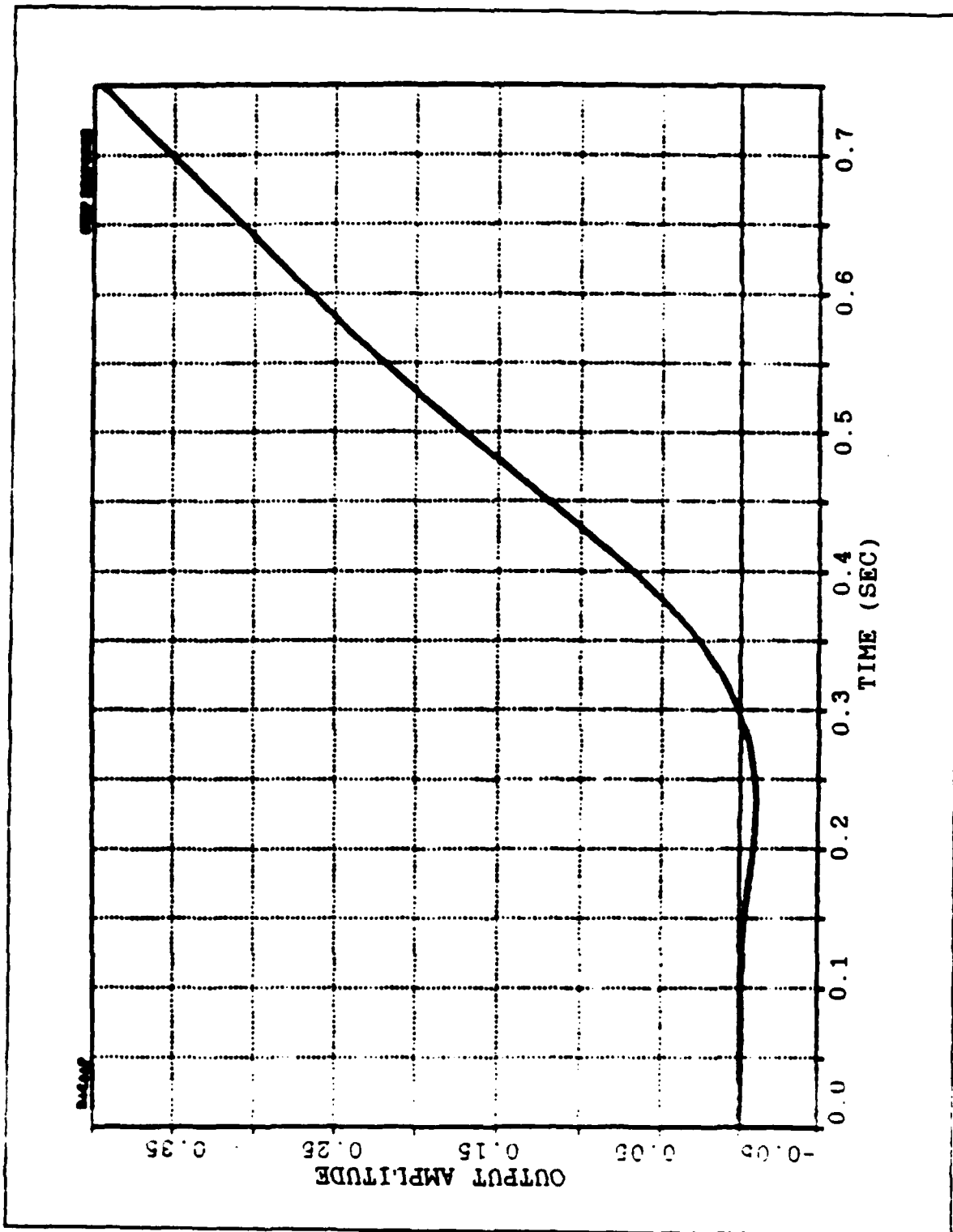


Figure 3.8 Step Response Of The Tip Transfer Function (Arm Loaded).

tip motion of the unloaded arm are shown. The oscillatory character of the arm is obvious. In Figure 3.6 we see the delay that the tip motion undergoes as a response to a torque at its hub, and also the initial motion of the tip in the opposite direction. This is an intuitive fact and is represented mathematically with the non-minimum phase zeros in the tip transfer functions.

In Figures 3.7 to 3.8 the step response for the case of the arm with a tip load are shown, and they do not differ appreciably from Figures 3.5 and 3.6.

#### IV. VELOCITY CURVE FOLLOW CONTROL SCHEME

##### A. INTRODUCTION

The velocity curve follow control scheme is a nonlinear adaptive system that has been used successfully for many years in disk drive systems. Recent studies [Ref. 3] show that this system is very effective in the control of rigid arms, yielding near minimum time positioning. The nice feature of this scheme is that we can take full advantage of all the power available in the motor which is being driven with full forward or full reverse power.

This feature is very important. In all linear controllers we have to avoid driving the amplifier to saturation, because this condition renders the controller ineffective [Ref. 1] and [Ref. 2], therefore only small loads are used and small displacements commanded.

In the case of the proposed control scheme we don't worry about this problem. We intentionally drive the amplifier to saturation limits so that we can take full advantage of the motor's capabilities.

Furthermore the system, being adaptive, eliminates errors due to noise, modelling uncertainties or change of the loads, and environment. Finally the system is simple and easily implemented in a micro-computer.

## B. DESCRIPTION OF THE BASIC SYSTEM

The curve follow scheme is shown in Figure 4.1. This scheme is described in [Ref. 4] and we will follow the same reasoning, making the necessary changes required for the application of the system to the control of the flexible arm.

The system operates in two modes for a step position command (the command has not necessarily to be a step as it will be shown later in this chapter): An initial full acceleration mode and a curve following mode. When the curve to be followed is chosen to be the deceleration curve for an idealized motor, the system will be practically the application of a bang-bang controller.

When a step input is applied to the system, the error signal ( $E$ ) will enter the curve and produce a commanded velocity input ( $\dot{X}$ ) to the velocity loop. The amplifier saturates and full forward signal is applied to the motor (full acceleration mode). As the position error signal decreases, the commanded velocity is reduced until it is equal to the velocity feedback signal ( $K\dot{C}$ ). Because the commanded velocity signal is decreasing, the velocity error ( $\dot{X}E$ ) will go negative and cause the voltage signal to the motor to reverse. Using a relatively high amplifier gain  $K_2$  we can make the system switch between positive and negative saturation limits and follow the curve down until it reaches the final position.



### C. CURVE DESIGN

It has been shown in [Ref. 4] that the curve can be derived from the idealized motor equations as follows:

$$\ddot{C} = K_m V_{sat} \quad (4.1)$$

$$\dot{C} = \int \ddot{C} dt = K_m V_{sat} t + \dot{C}(0), \quad (\dot{C}(0)=0) \quad (4.2)$$

$$C = \int \dot{C} dt = 1/2(K_m V_{sat} t^2) + C(0) \quad (4.3)$$

When we solve equation 4.3 for t and substitute in equation 4.3,

$$C = \frac{\dot{C}^2}{2 K_m V_{sat}} \quad (4.4)$$

For deceleration from initial conditions with the input

$$R = 0,$$

$$C = -E \quad (4.5)$$

$$\dot{C} = -\dot{E} \quad (4.6)$$

Finally when we combine equations 4.4, 4.5 and 4.6 we have:

$$E = \sqrt{2 K_m V_{sat}} \sqrt{E} \quad (4.7)$$

The parameters  $K_m$  and  $V_{sat}$  depend upon the motor and amplifier to be used. Letting:

$$A = \sqrt{2 K_m V_{sat}} \quad (4.8)$$

and

$$\dot{X} = \dot{E} \quad (4.9)$$

$$\dot{X} = A \sqrt{E} = \text{commanded velocity} \quad (4.10)$$

Thus the commanded velocity curve can be generated by an initial calculation of the parameter  $A$ , and then continuously multiplying this factor by the square root of the position error. The resulting commanded velocity is a parabola which corresponds to the deceleration curve of an ideal motor. As we will see in the simulation studies, for the case of the flexible arm, this curve has to be lowered by a factor of the order of 0.06, therefore we multiply the commanded velocity signal by  $K_1 = 0.06$ .

The parameters that are necessary for the calculation of the curve depend upon the specific actuator that we will use for the motion of the arm. The second order model gain constant ( $K_m$ ) is determined by the actuator parameters and the effective inertia seen by the actuator. This parameter is going to be updated through the adaptation algorithm as we

will see later and only an initial value need be given. As shown from the simulation studies the best value for  $K_m$  is 1.2 rad/volt. For the saturation limits of the amplifier we use  $V_{sat} = 50$  volt. Finally for the gain of amplifier  $K_2$  we have to use a large value so that the amplifier is driven into saturation limits even for very small input signals. As such  $K_2 = 10,000$  was chosen.

#### D. SIMULATION STUDIES OF THE BASIC MODEL

To demonstrate the ability of this scheme to follow the curve, the model was simulated using DSL/VS. The DSL/VS program is listed in Appendix A. For this simulation we used  $K_m = 17$  rad/volt and  $V_{sat} = 50$  volt. Figure 4.2 shows the phase plane trajectories (angular velocity  $\dot{C}$  versus angular position  $C$ ), for a step command of 0.1 rad. We observe that the angular velocity of the model increases with constant acceleration until the curve is reached. When this happens the velocity error applied to the amplifier changes sign the voltage to the motor reverses and the model velocity follows the curve until the commanded position is reached. The step response of the model is shown in Figure 4.3.

It was mentioned earlier in this chapter that the commanded input (position) need not be a step for the model to follow the curve. This is shown in Figures 4.4 through 4.9 for the case of the inputs shown in Figures 4.4 and 4.7.

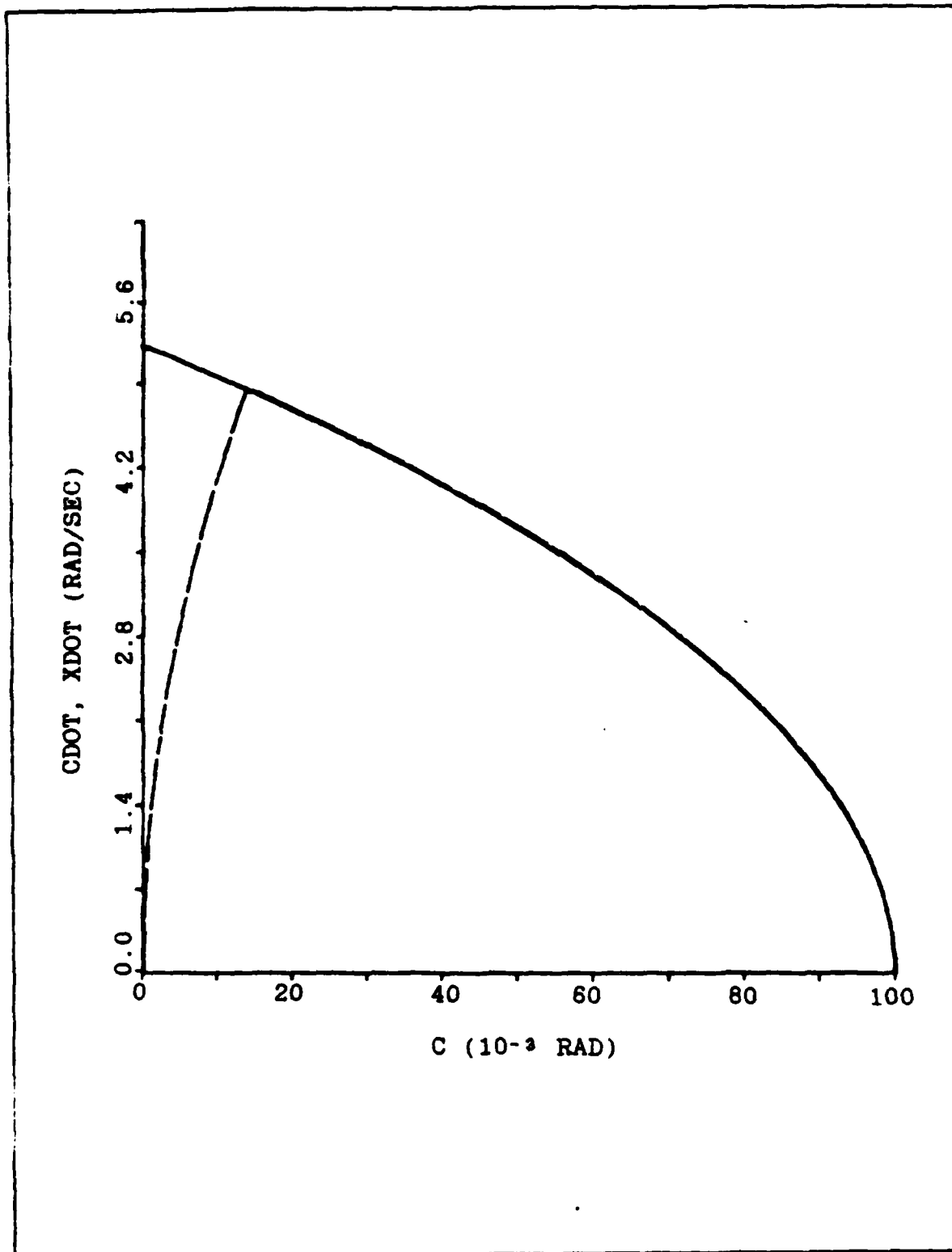


Figure 4.2 Phase Plane Trajectories Of The Model

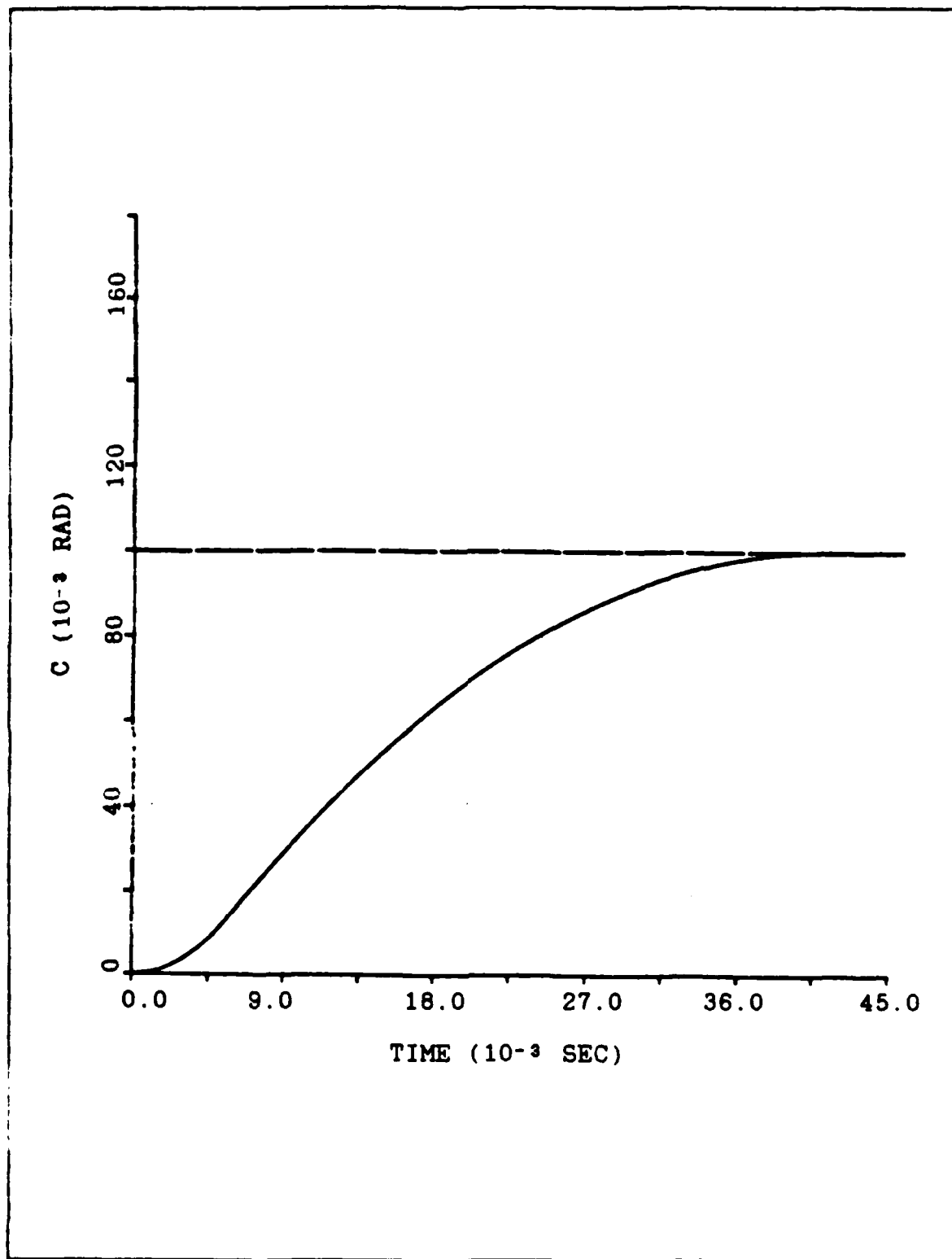


Figure 4.3 Step Response Of The Model

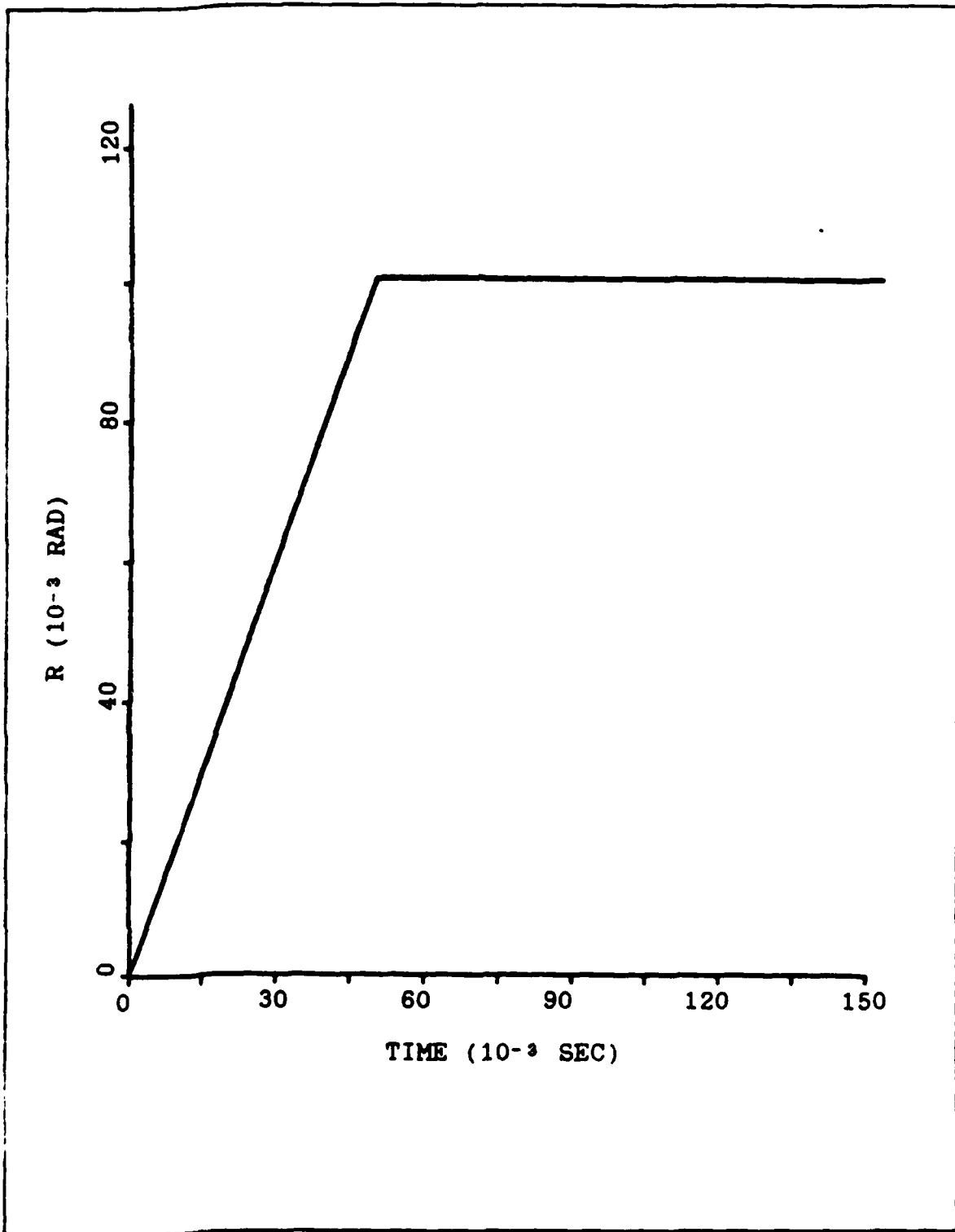


Figure 4.4 Input Shape For Simulations Shown In Figures 4.5 And 4.6.

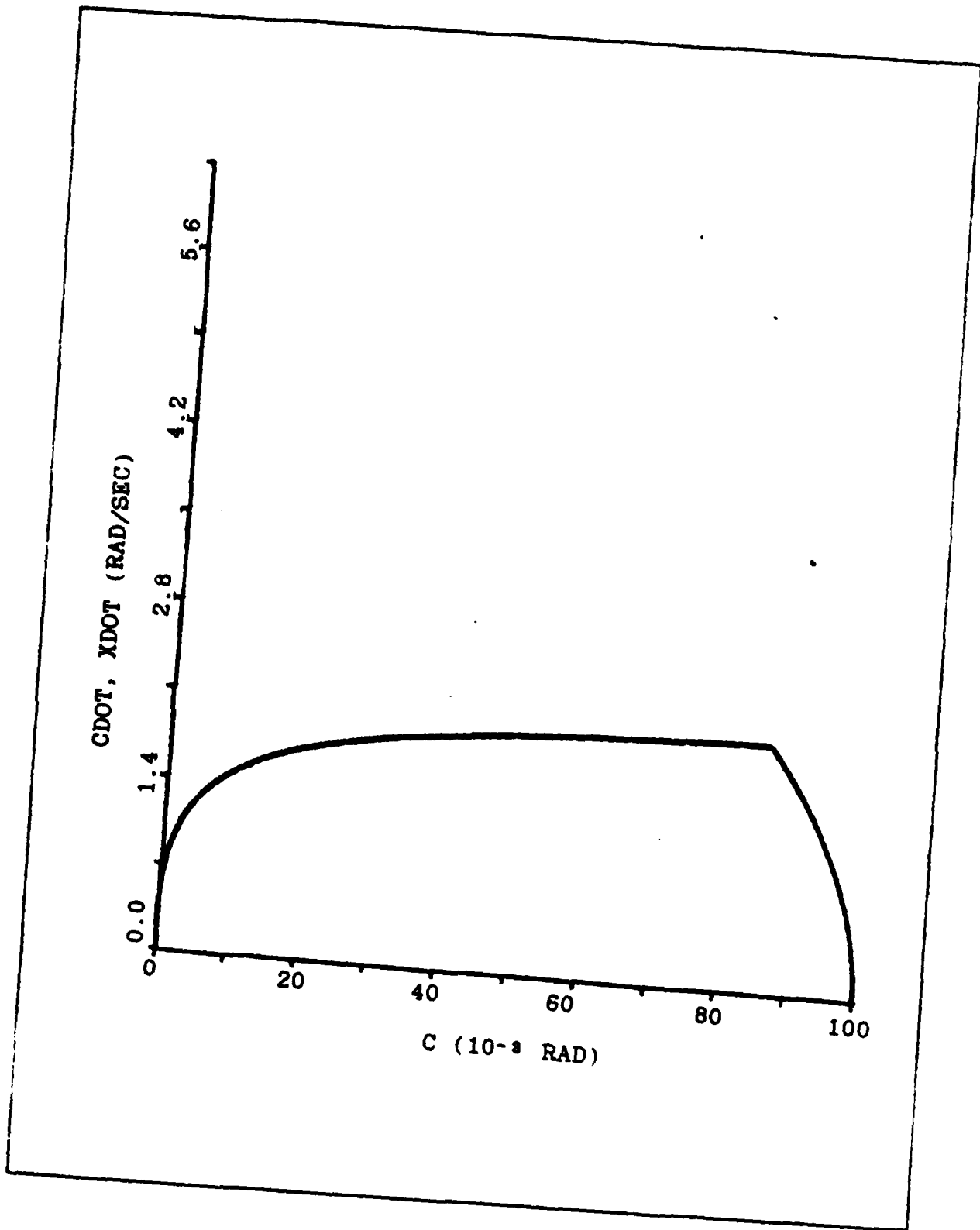


Figure 4.5 Phase Plane Trajectories Of The Model For The Input Shown In Figure 4.4.

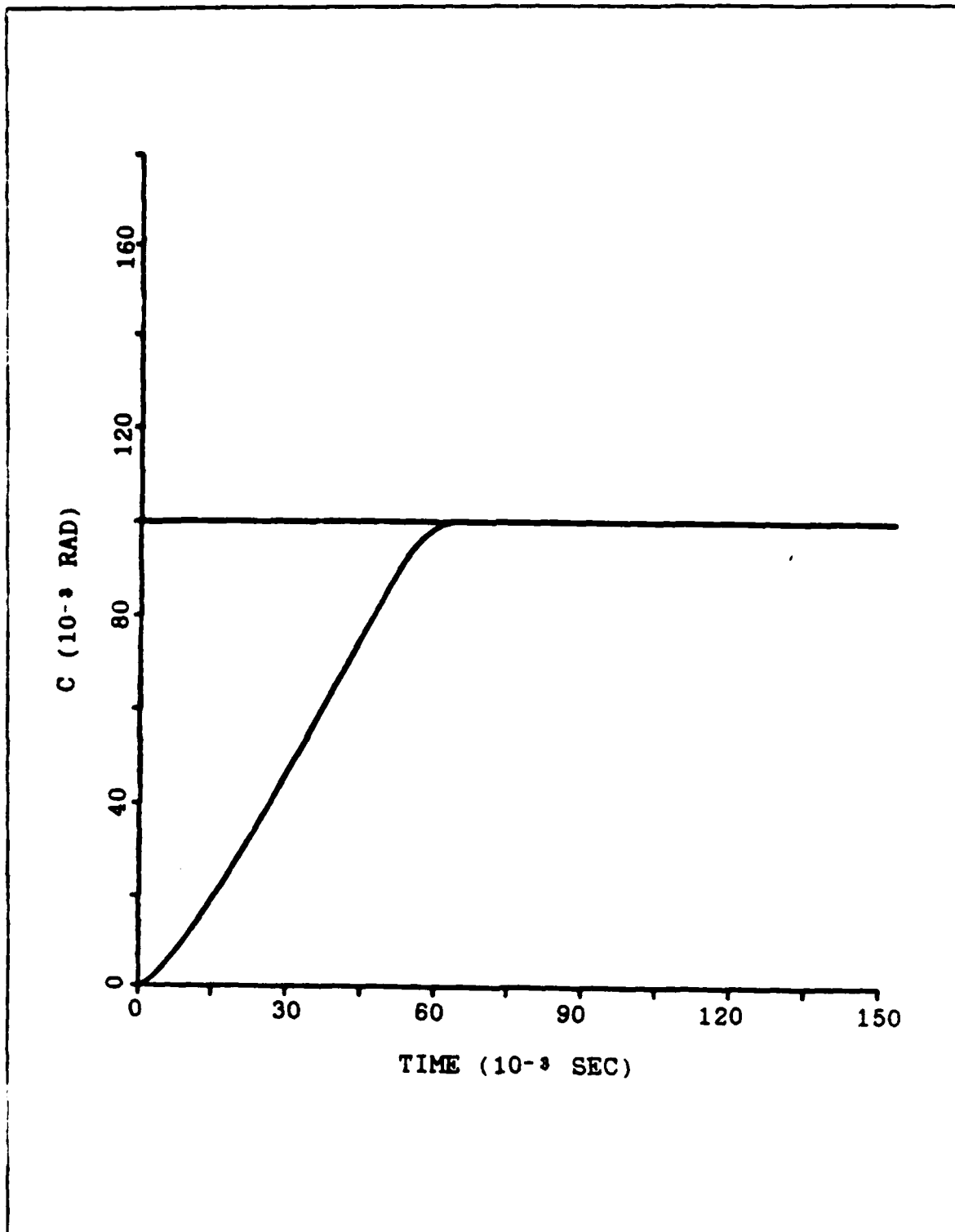


Figure 4.6 Response Of The Model To The Input  
Shown In Figure 4.4

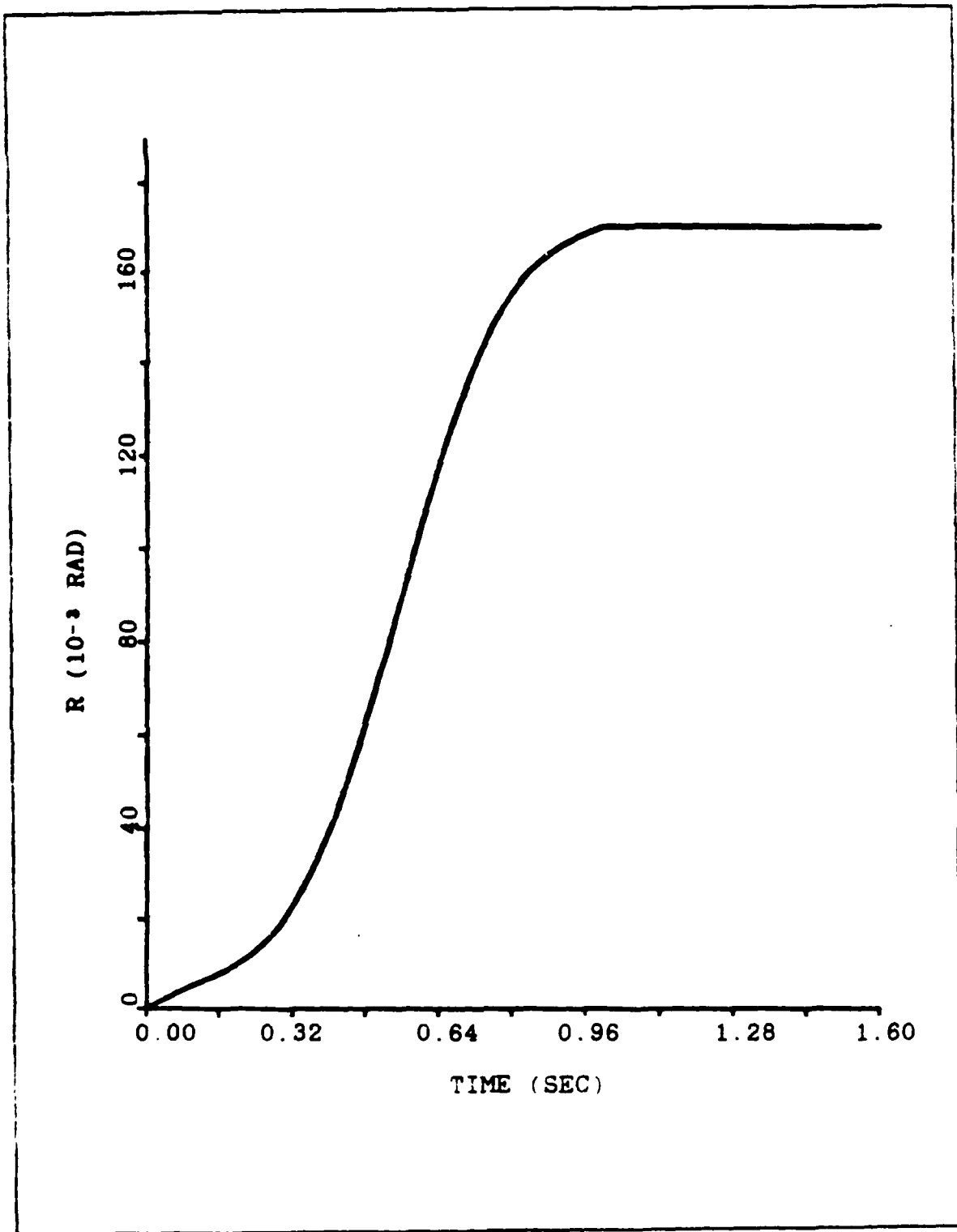


Figure 4.7 Input Shape For Simulations Shown In Figures 4.8 And 4.9.

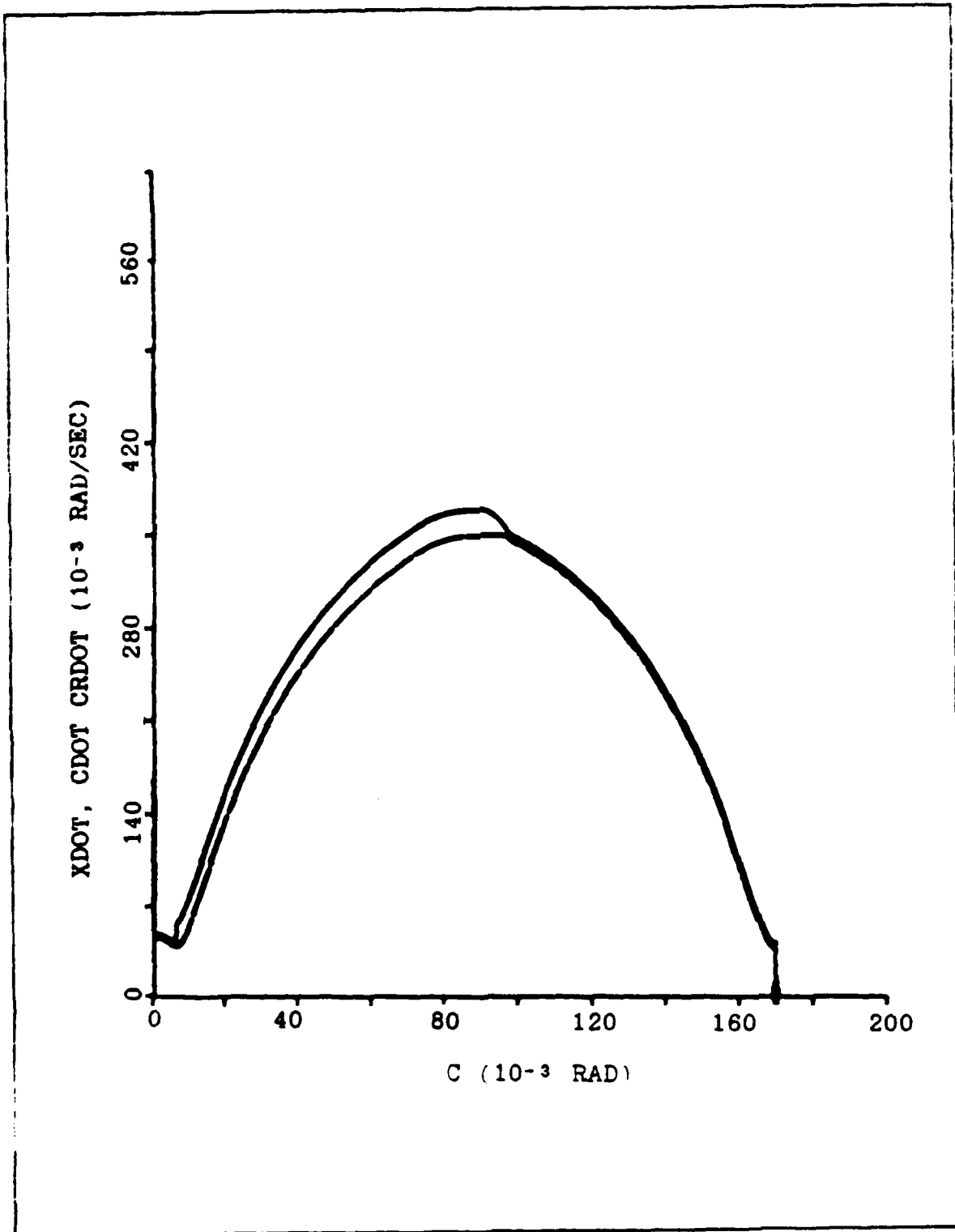


Figure 4.8 Phase Plane Trajectories Of The Model  
With Input As In Figure 4.7.

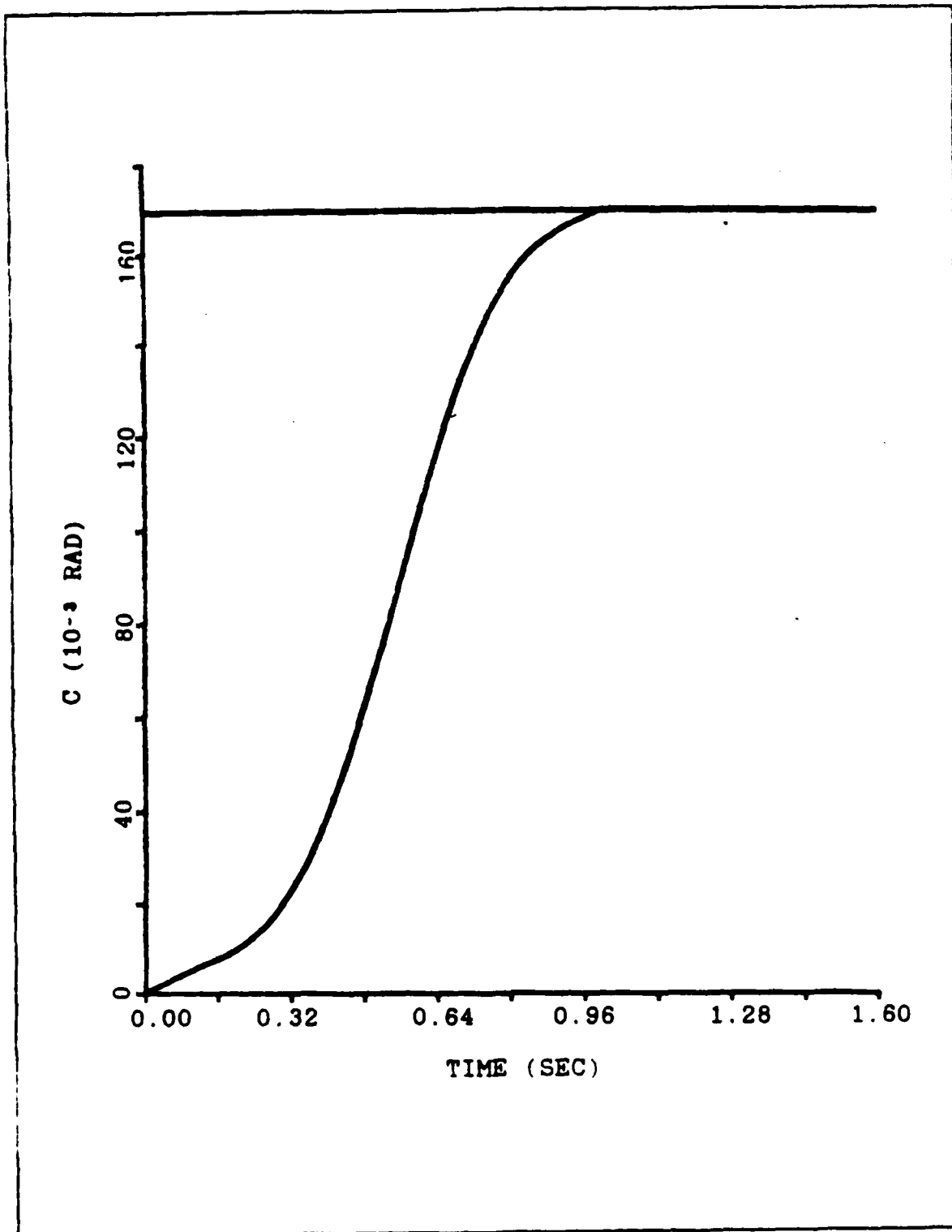


Figure 4.9 Response Of The Model To The Input Shown In Figure 4.7.

## E. THE ADAPTIVE ALGORITHM

The block diagram of the adaptive system for the flexible arm is shown in Figure 4.10. The signal that comes out of the switching amplifier (saturating amplifier), is common to both the second order model of the idealized motor and to the actual system (combination of real motor and flexible arm). This scheme is used to "force" the actual system to follow the ideal model which in turn is adaptive in nature.

The hub angle ( $CR$ ) and the hub angle rate ( $\dot{CR}$ ) are measured at specified time intervals (sampling intervals) and are fed back into the adaptive algorithm. This data is used to calculate the gain constant of the ideal model ( $K_m$ ), and to update the states of the ideal model.

The reason for using the hub angle and the hub angle rate as inputs to the adaptive algorithm will be made clear in the next chapter. At present it suffices to say that the tip position ( $YT$ ) and the tip velocity ( $\dot{YT}$ ) are not appropriate inputs for the adaptive algorithm, due to the delay in the response of the tip to torques applied at the hub as seen in Figures 3.6 and 3.8.

Due to that delay any attempt of the system to correct the tip position does not have instantaneous results on the tip motion. Therefore even though the system has applied the "correct torque" to move the tip as required, the tip does not move immediately and the system continues applying more torque "thinking" that the previously applied torque was not

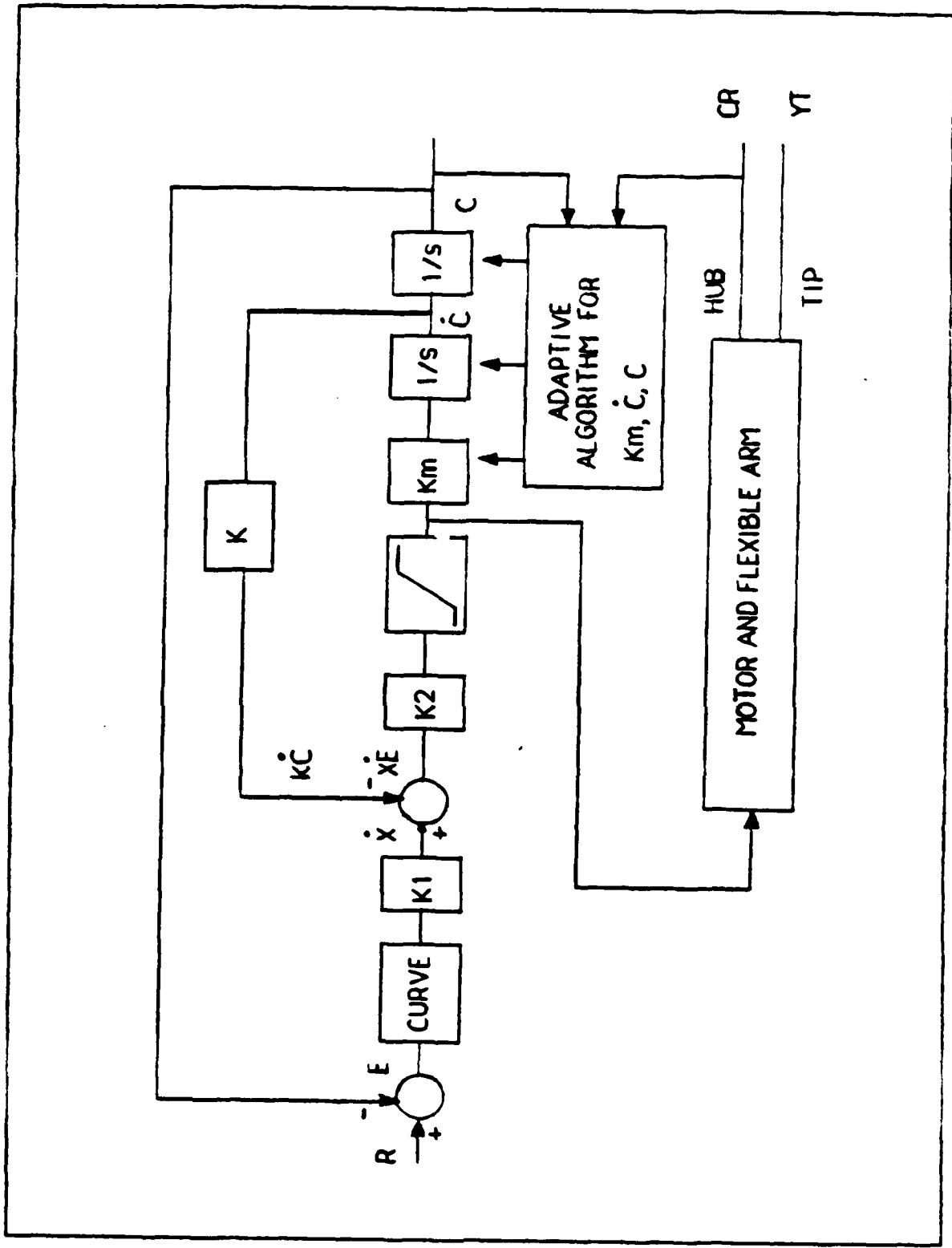


Figure 4.10 Block Diagram Of The Adaptive System.

sufficient. On the other hand when the tip has a position error in the opposite direction, the same process takes place in the opposite direction. This situation drives finally the system unstable as is shown in the next chapter.

The gain constant  $K_m$  of the model is not kept constant throughout the arm's motion but is adjusted so as to account for the inertia reflected back from the arm. The adaptation algorithm for  $K_m$  has to satisfy two basic criteria. One is that the calculations must be accurate enough in order that the second order model can approximate the trajectory of the arm as closely as possible. The second criterion is that the calculations must be simple to allow fast updating of  $K_m$ , and be easily programmed in a microprocessor.

There are several ways to satisfy the above criteria. For our purpose the method described in [Ref. 4] best satisfies both criteria.

Solving equation 4.3 for  $K_m$  we have:

$$K_m = \frac{2C}{V_{sat} t^2} \quad (4.11)$$

For discrete time intervals,

$$K_m = \frac{2C}{V_{sat} (NT)^2} \quad (4.12)$$

where  $T$  is the sampling interval and  $N$  the sample number.

Letting  $C = CR$ ,

$$K_m = \frac{2CR}{V_{sat} (NT)^2} \quad (4.13)$$

This equation for  $K_m$  is only valid for the full acceleration mode of the motor. Therefore we use it until the velocity of the actual system reaches the velocity curve and thereafter we keep  $K_m$  unchanged for the curve follow portion of the move.

## V. APPLICATION OF THE CURVE FOLLOWING SYSTEM FOR THE CONTROL OF THE FLEXIBLE ARM

The system shown in Figure 4.10 was simulated using DSL/VS. The simulation program derived for this purpose is given in Appendix B. The parameters used for this study were selected after exhaustive simulations on a trial and error basis. For the gain constant  $K_1$  the best value found was 0.06. It was found from the simulations that any value of the gain constant  $K_1 \leq 1$  is appropriate for the hub motion and the higher the gain the faster the positioning of the hub. However as  $K_1$  is increased higher the oscillations that the arm's tip undergoes also increase in amplitude.

The simulation results are shown in Figures 5.1 to 5.9 for values of  $K_1$  equal to 0.7, 0.2 and 0.06 and for a command of 0.17 rad (or  $10^\circ$ ). It is clear that the system follows the velocity curve, the hub is positioned quickly and accurately but the tip motion is unacceptable for all values of  $K_1$ . In Figures 5.10 to 5.12 tip position and tip velocity were used for the velocity curve following system (in other words the loop was closed around the tip). It is clearly shown that the system in this case cannot follow the curve (Figure 5.10) and the hub and tip motion are unstable (Figures 5.11 and 5.12). The reason for that was explained in Chapter IV.

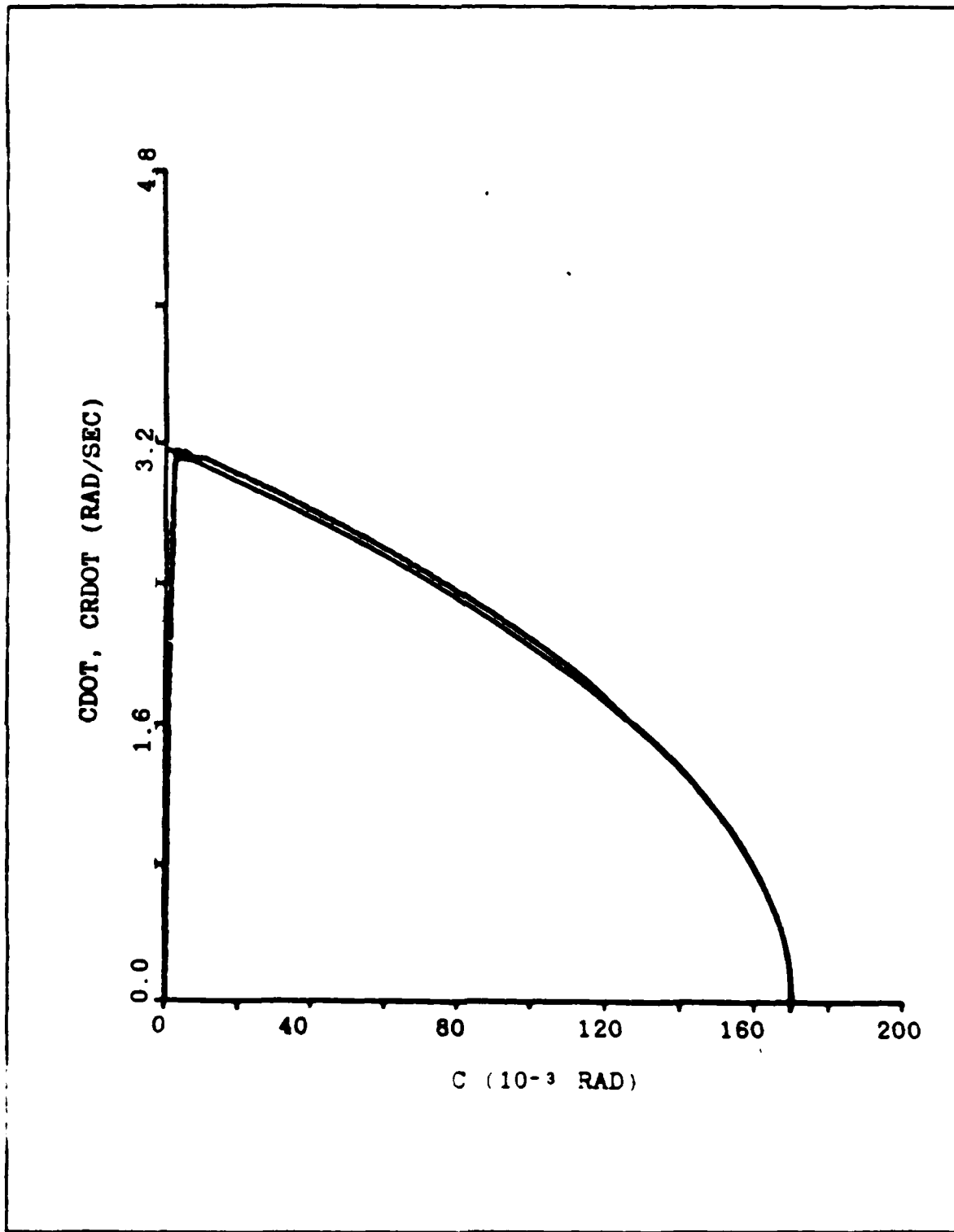


Figure 5.1 Phase Plane Trajectories Of The System With  $K_1 = 0.7$

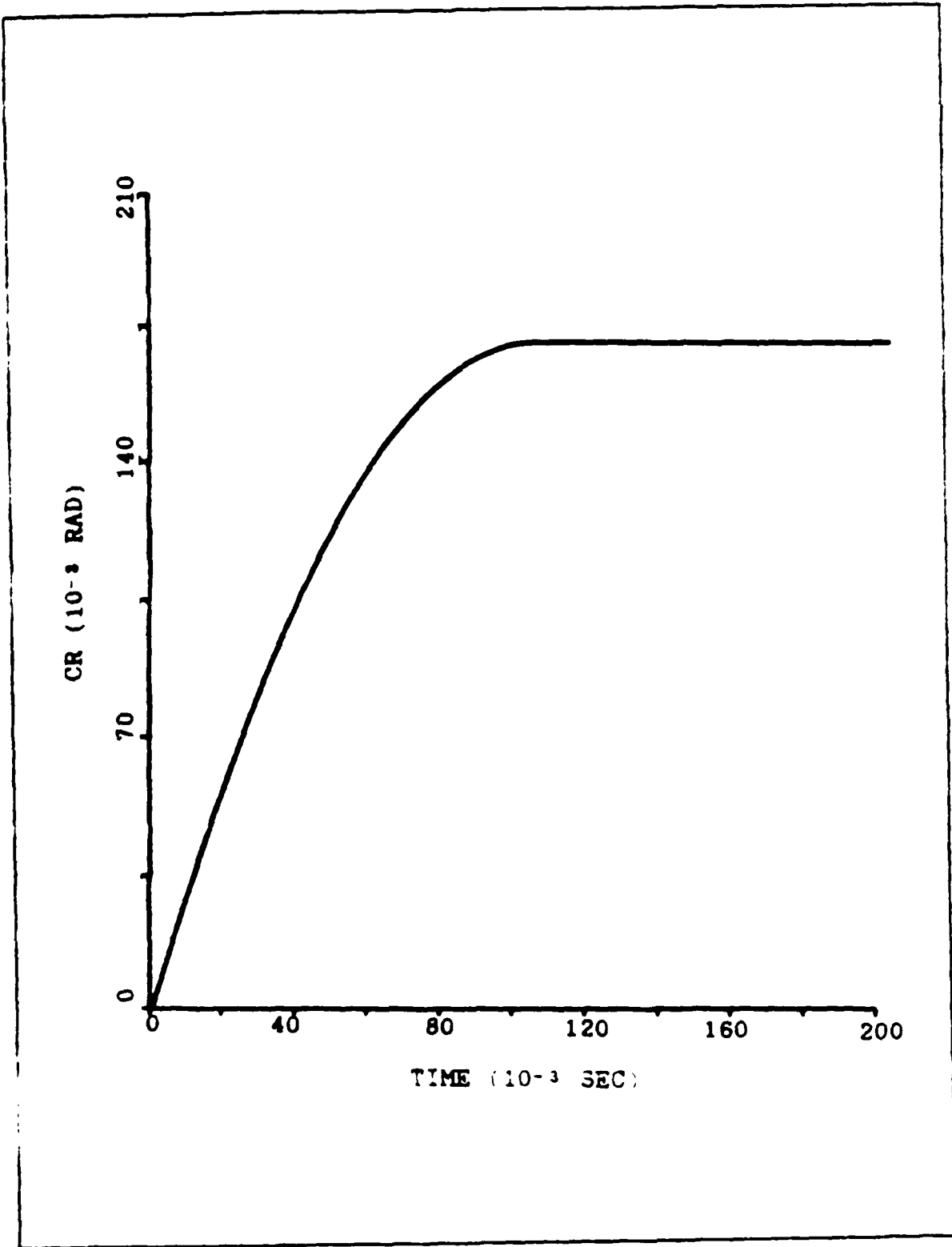


Figure 5.2 Hub Motion With  $K_1 = 0.7$

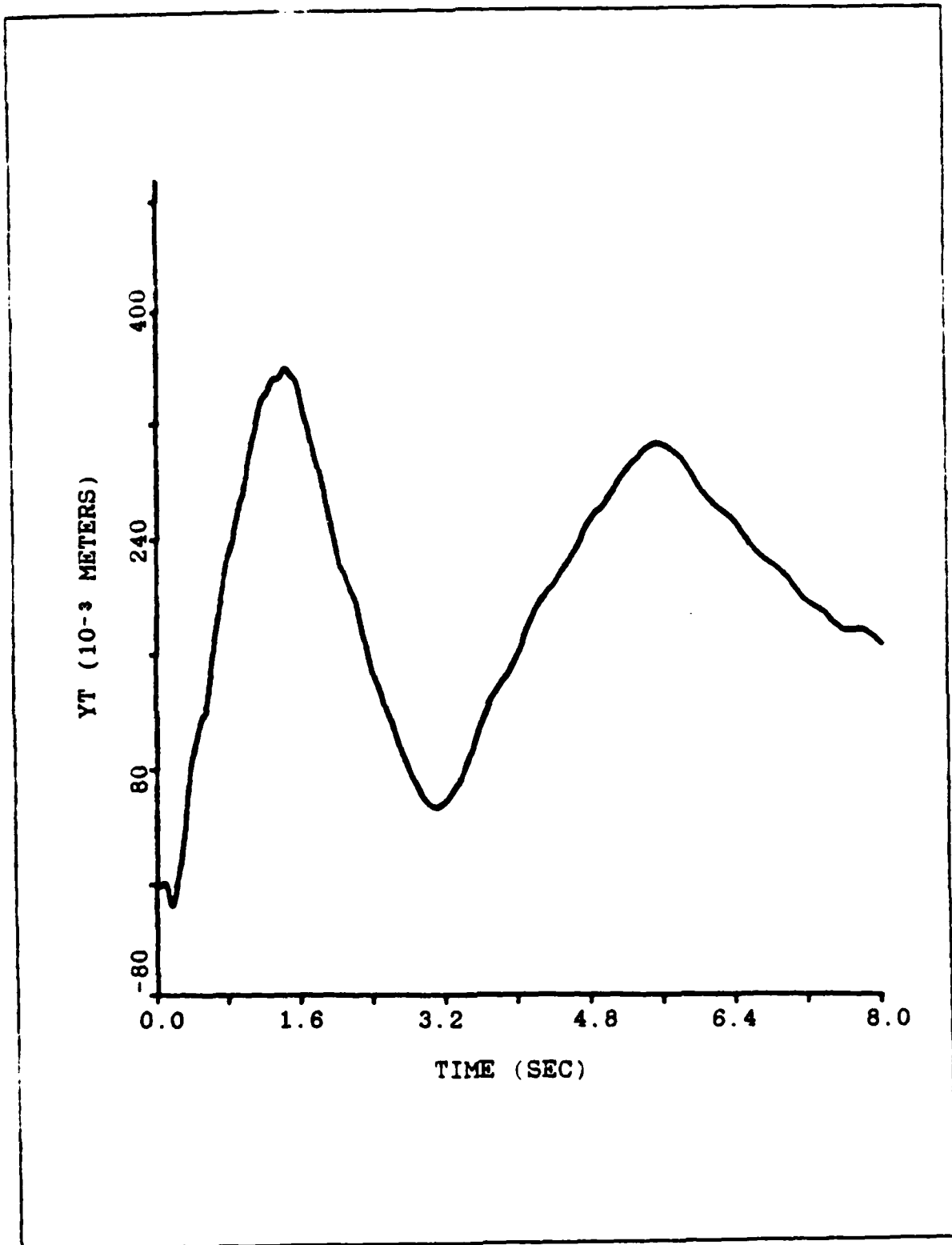


Figure 5.3 Tip Motion With  $K_1 = 0.7$

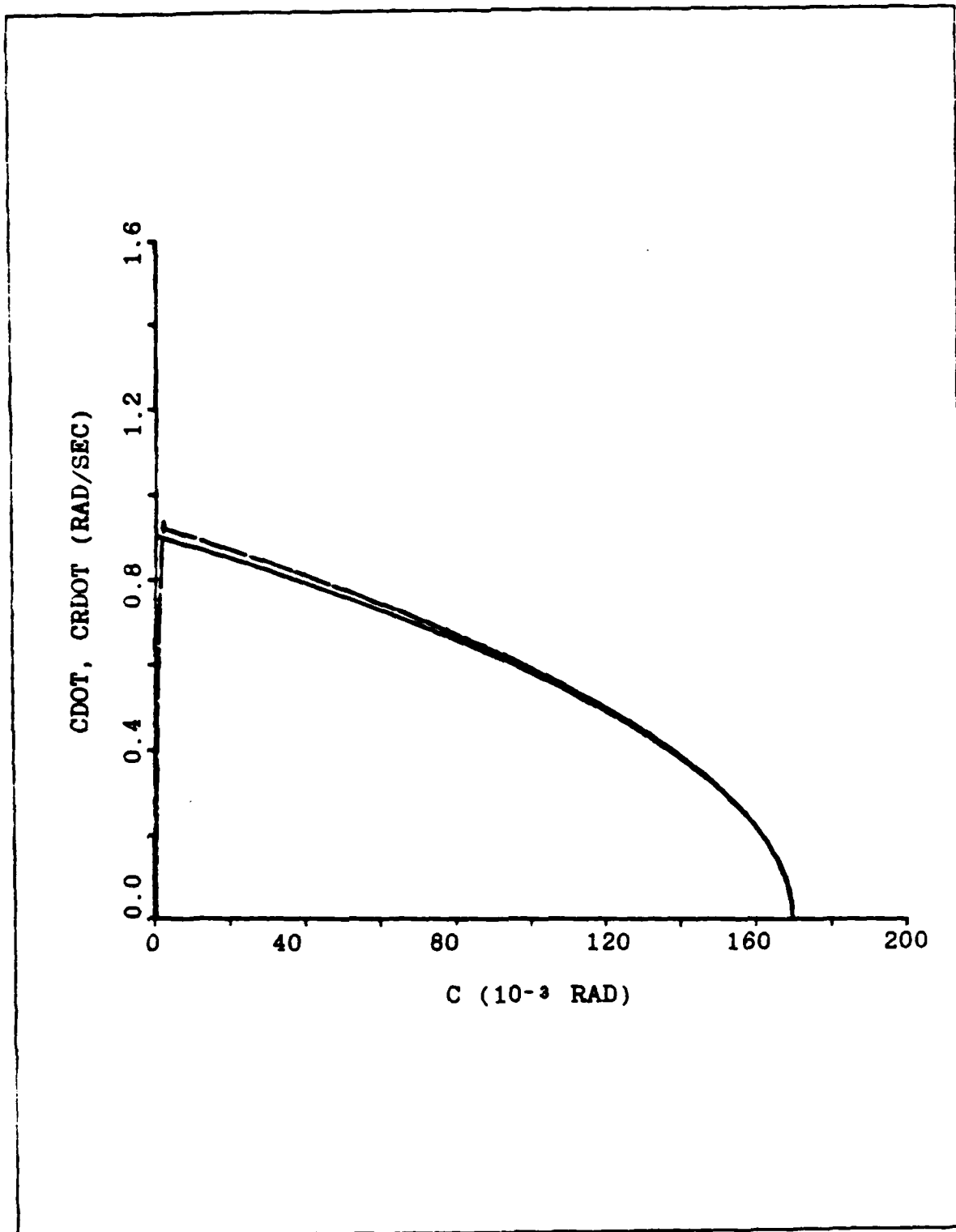


Figure 5.4 Phase Plane Trajectories Of The System With  $K_1 = 0.2$

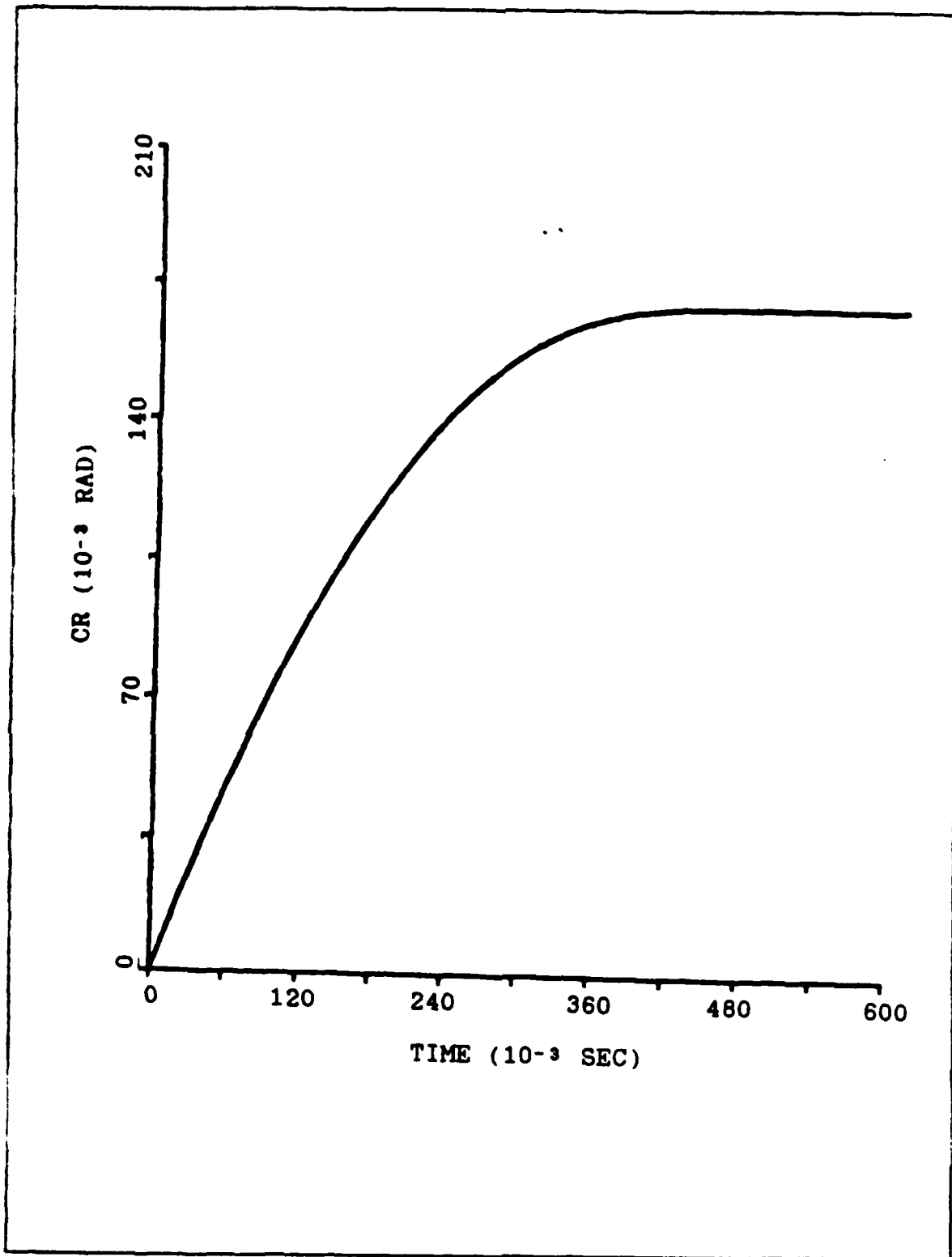


Figure 5.5 Hub Motion With  $K_1 = 0.2$

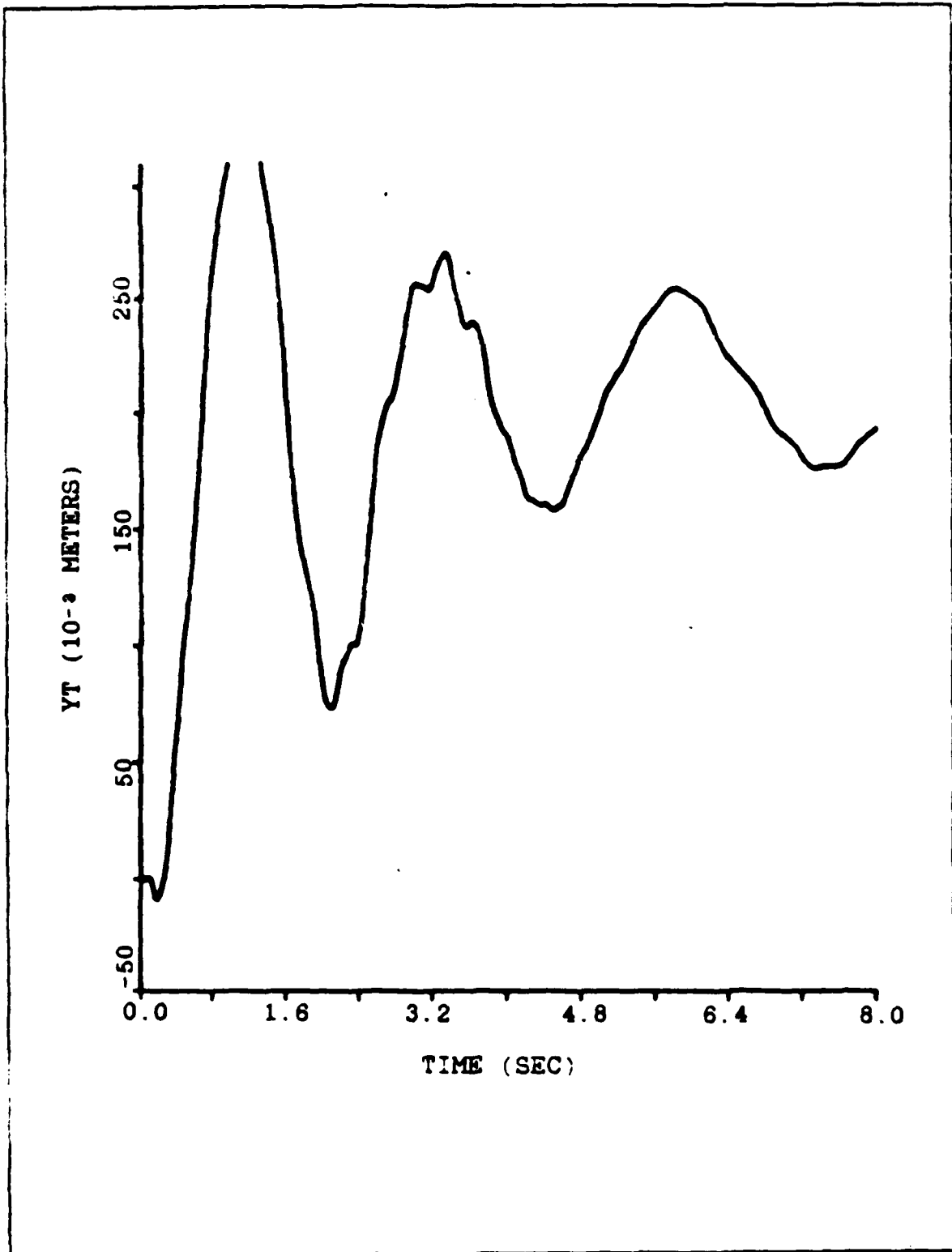


Figure 5.6 Tip Motion With  $K_1 = 0.2$

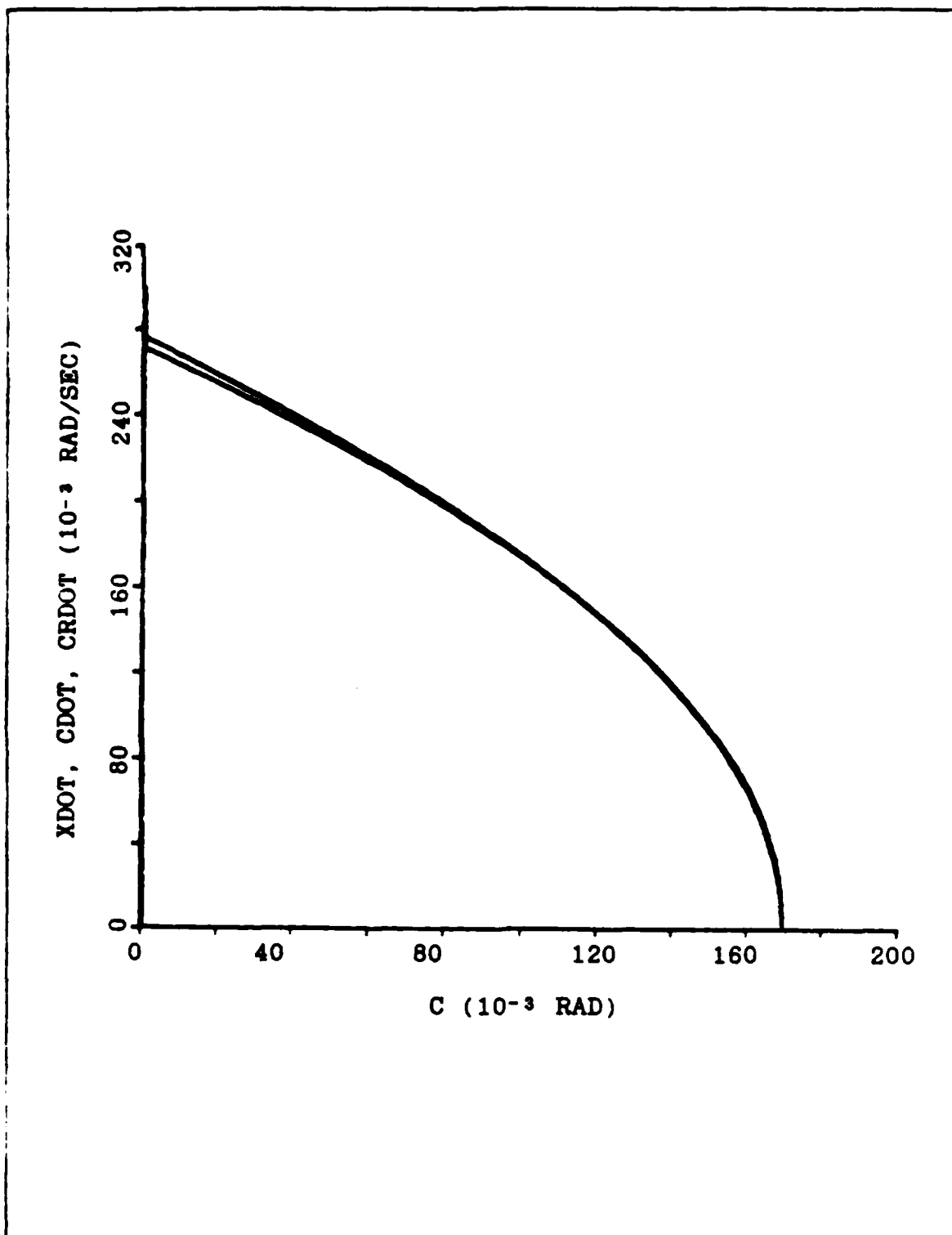


Figure 5.7 Phase Plane Trajectories Of The System With  $K_1 = 0.06$

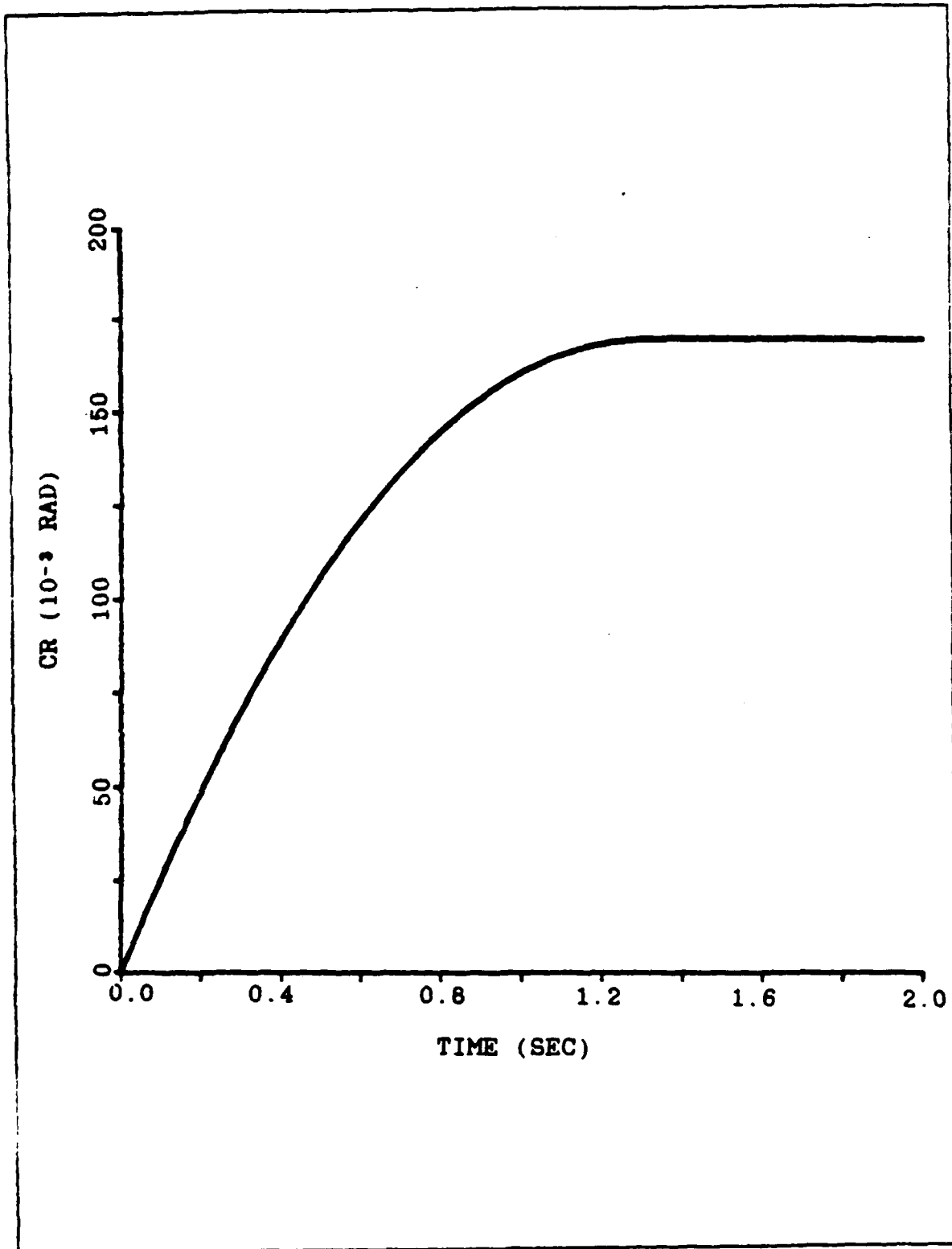


Figure 5.8 Hub Motion With  $K_1 = 0.06$

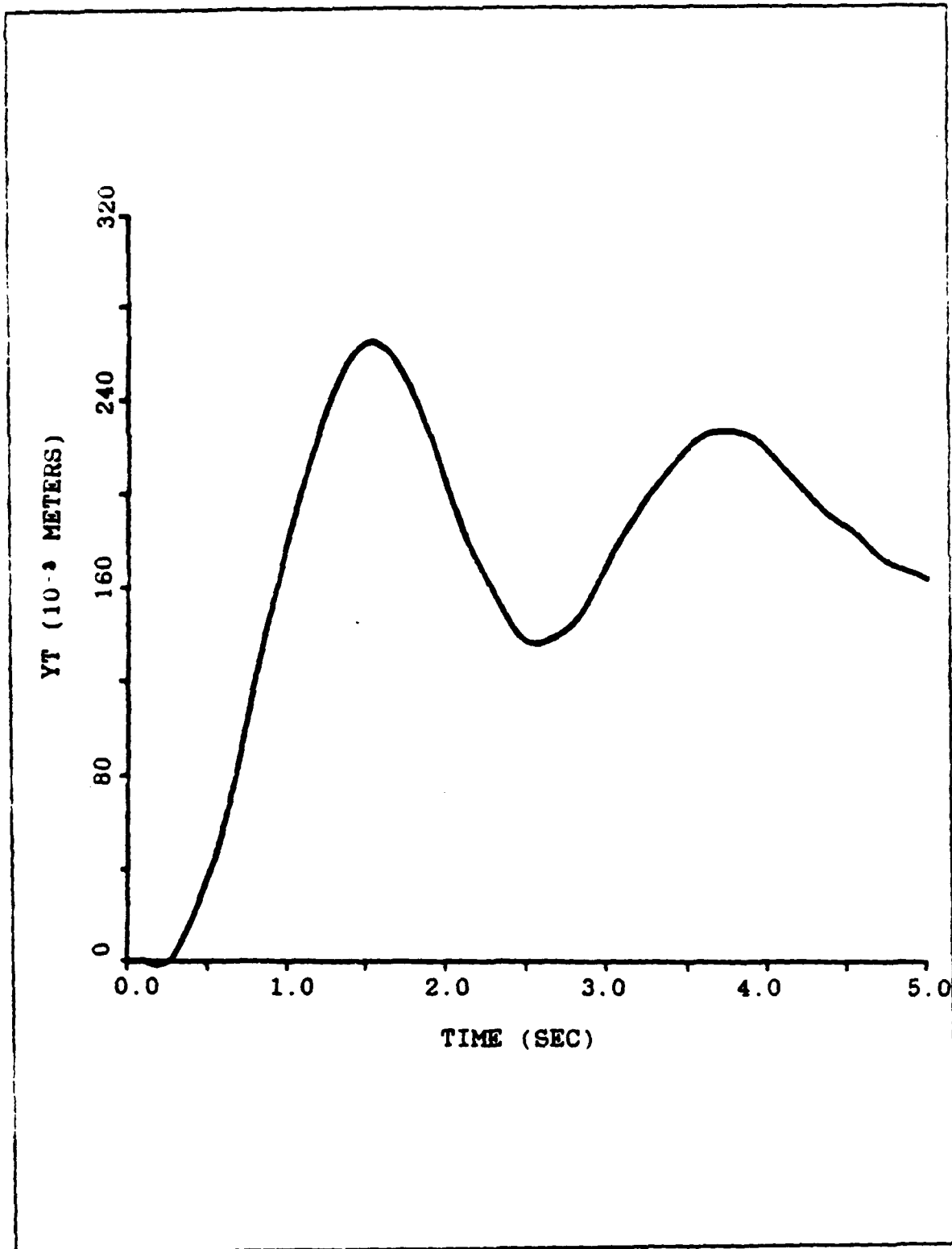


Figure 5.9 Tip Motion With  $K_i = 0.06$

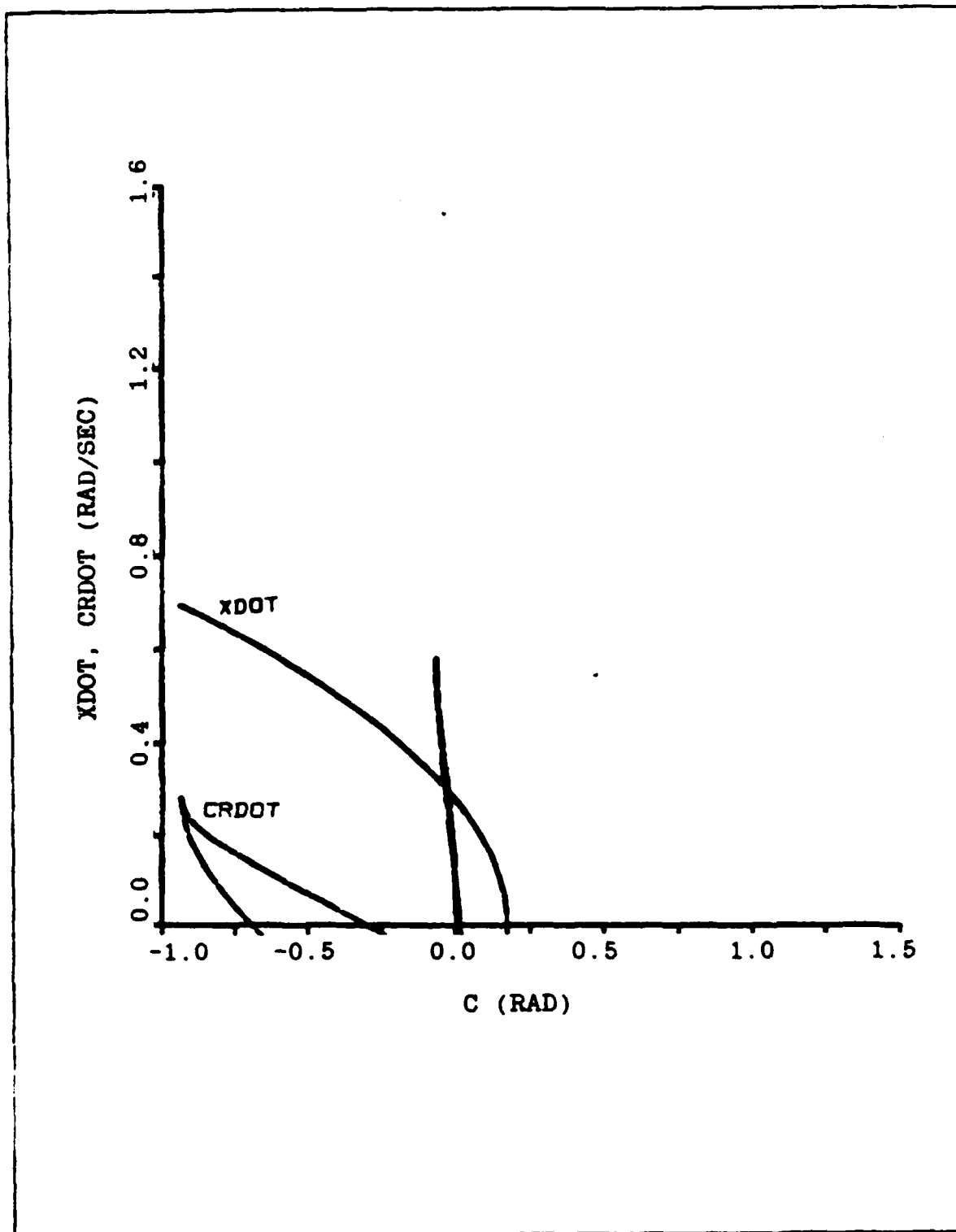


Figure 5.10 Phase Plane Trajectories Of The System, Using Tip Position And Tip Velocity For The Adaptive Algorithm.

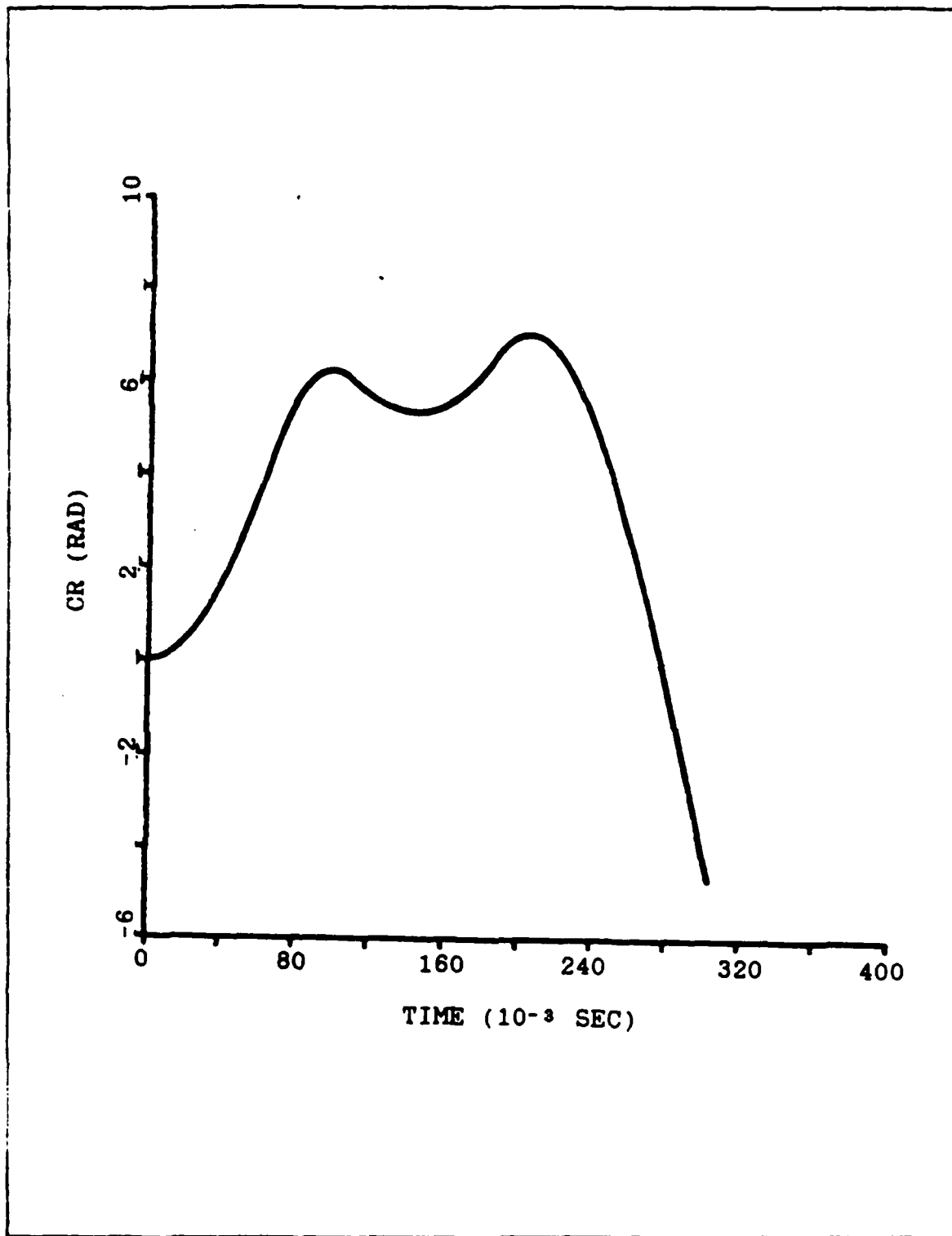


Figure 5.11 Hub Motion When Tip Position And Tip Velocity Are Used For The Adaptive Algorithm.

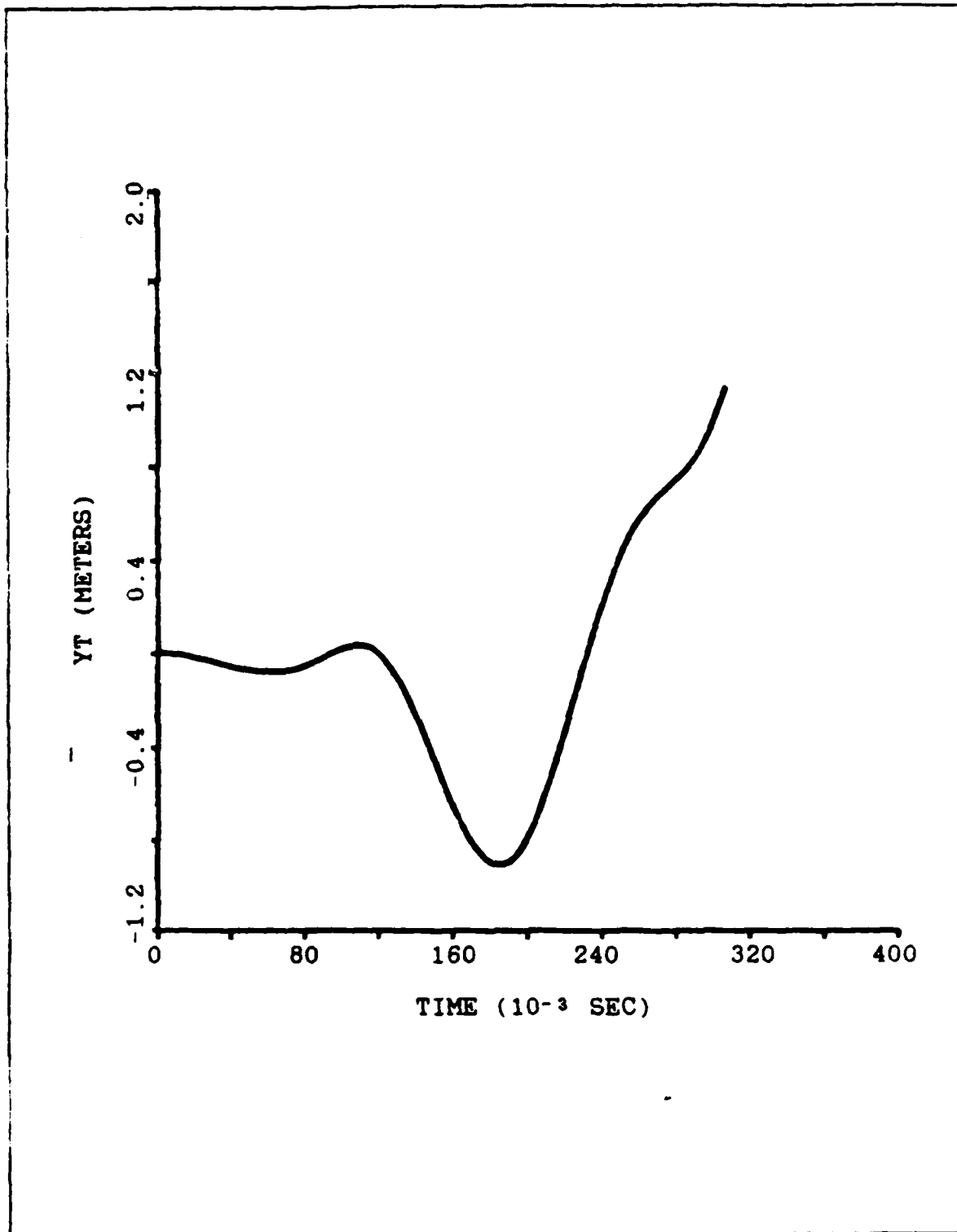


Figure 5.12 Tip Motion When Tip Position And Tip Velocity Are Used For The Adaptive Algorithm.

As mentioned previously the motion of the arm's tip is unacceptable. This is well explained physically if we consider the energy stored in the arm during the whole process.

When we give a command to the system to move the hub to a given position, the position error has its maximum value. Entering the curve with this large error we get out a high commanded velocity ( $\dot{X}$ ), which enters the velocity loop and drives the amplifier to its saturation limit and the motor operates at full forward acceleration, supplying to the arm the power required for its motion.

The motion of the hub starts immediately after the application of the torque. The motion of the tip, however, undergoes a delay of about 280 ms. This delay is seen in Figures 3.6 and 3.8 and it is intuitively expected. If we consider the arm as a combination of springs and masses, some energy is required for the spring to be "wound-up", and only when this energy has been given, a tension can arise at the tip and its motion will start. When the tip starts, finally, moving the motor is still in full forward mode supplying more power, until the error for the hub position becomes negative. When the hub reaches the commanded position the motor tries to keep it there switching from full forward to full reverse motion as necessary. The tip of the arm, on the other hand, does not stop but continues its motion, under the stored energy in the spring. The motion of the tip ceases only when

the physical damping of the arm dissipates all the stored energy in the spring.

The arm, however, is very flexible and its damping is very low and takes a long time to dissipate the energy stored during the process and this is why we have so long lasting oscillations as seen from Figures 5.3, 5.6 and 5.9.

We also see from these figures that the higher the gain constant  $K_1$  the longer the tip's oscillations and the higher the overshoot. This happens because when high gains are used, the system puts more energy into the arm.

At this point someone could expect that when the motor reverses, it would take out the energy stored into the system. This does not happen for the following reason: When the hub's velocity reaches the curve (commanded velocity), the system "tries" to follow it, switching the amplifier between the positive and the negative limits. The tip's oscillations, on the other hand, are reflected back to the hub, where the system senses them and they are another reason that causes this continuous switching of the amplifier. This switching results in a fixed position of the hub and good curve tracking, but it makes the average energy given to or taken out of the arm to be almost equal to zero. Therefore the reverse motion of the motor does not absorb any energy from the arm. The torque applied to the arm, with the hub motion superimposed is shown in Figure 5.13. We clearly see the fast switching of the torque after the hub's velocity has

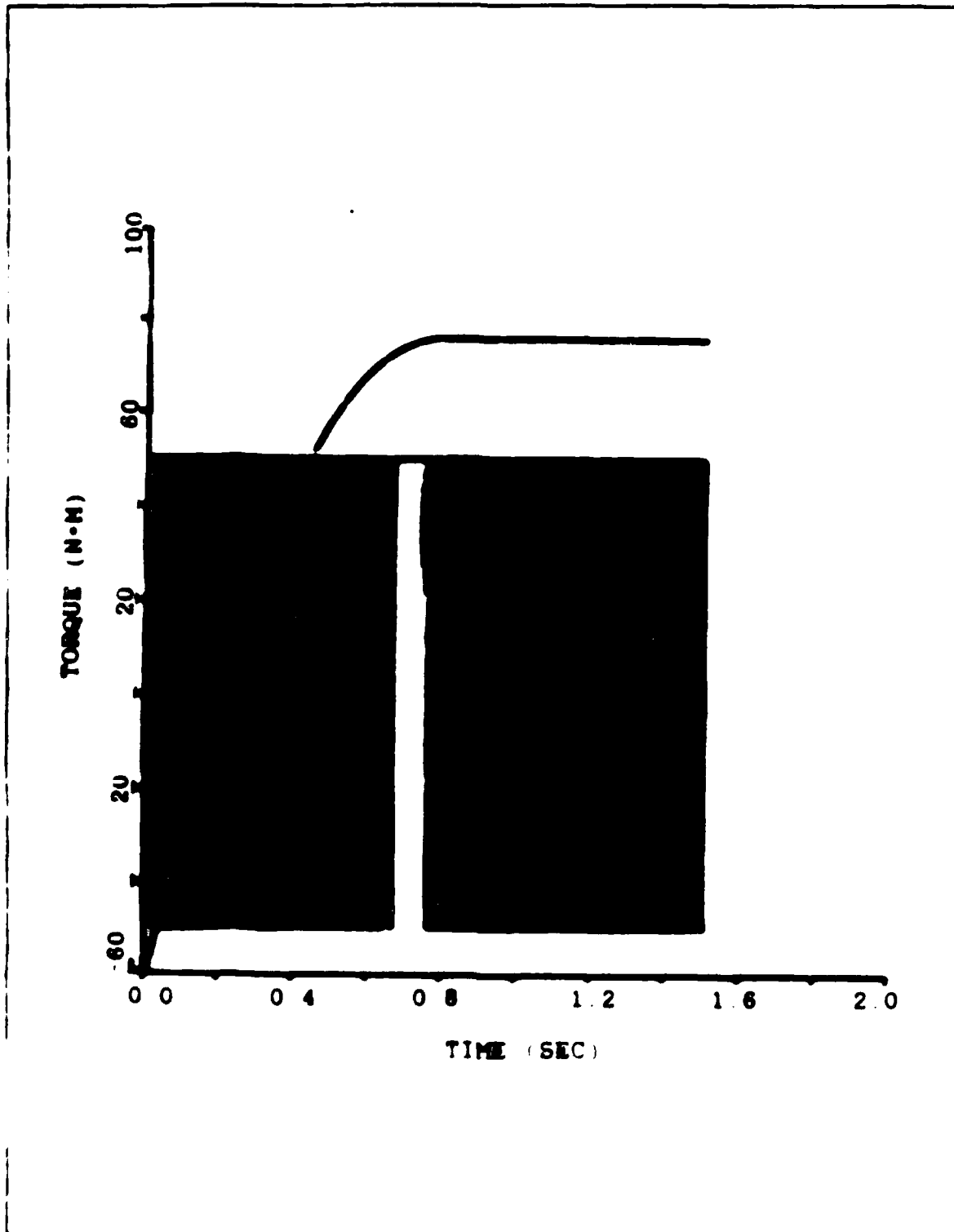


Figure 5.13 Torque Applied To The Arm And Its Resulting Hub Motion

reached the curve. This continued switching stops for a while when the hub reaches the commanded position in order to prevent a motion to the opposite direction.

Another observation drawn from the tip's motion is that the arm is extremely flexible. There is no engineering reason for using such an arm in a practical application. Actually the arm is about 100 times more flexible than a practical one, [Ref. 1]. Therefore if we had used a "practical flexible arm" with the above control scheme, its performance would have been 10 times better.

It is clear from the above considerations that we must find some way to remove the energy out of the system, in order to make the tip motion acceptable. In the next chapter four different methods will be used for the solution of this problem. In the first method a simple cascade compensator will be used for the final motion of the arm. In the second method an attempt to reduce the energy given to the arm will be made by shaping the input command. In the third method we will use posi-cast control. Finally as a last resort a complex feedback compensator based on optimal control theory will be used.

## VI. CONTROL OF THE TIP OF THE ARM

### A. USE OF A SIMPLE COMPENSATOR

As mentioned in Chapter V some way must be found to remove the energy stored in the arm, in order to make the tip's motion acceptable. As a first attempt to solve this problem, a simple compensator will be used. The resulting control scheme is shown in Figure 6.1. The arm is driven by the curve following system until a specific point off the final position is reached. Then we switch to the linear regulator, switching off the curve following system, for the final motion of the arm, by changing the position of the switch SW1. The compensator that will be used in the linear regulator must be designed in such a way that it can provide sufficient damping in order to dissipate the energy stored in the arm. If we consider the frequency response of the arm (Figures 3.1 and 3.2) we can see that this is not an easy task.

As we see from Figure 6.1 the linear regulator is a closed loop system, with feedback signal from the tip position of the arm.

The cascade compensator used in this linear system was derived using classical control techniques (frequency response method), on a trial and error basis. The ultimate task of the trials was to obtain the largest possible phase

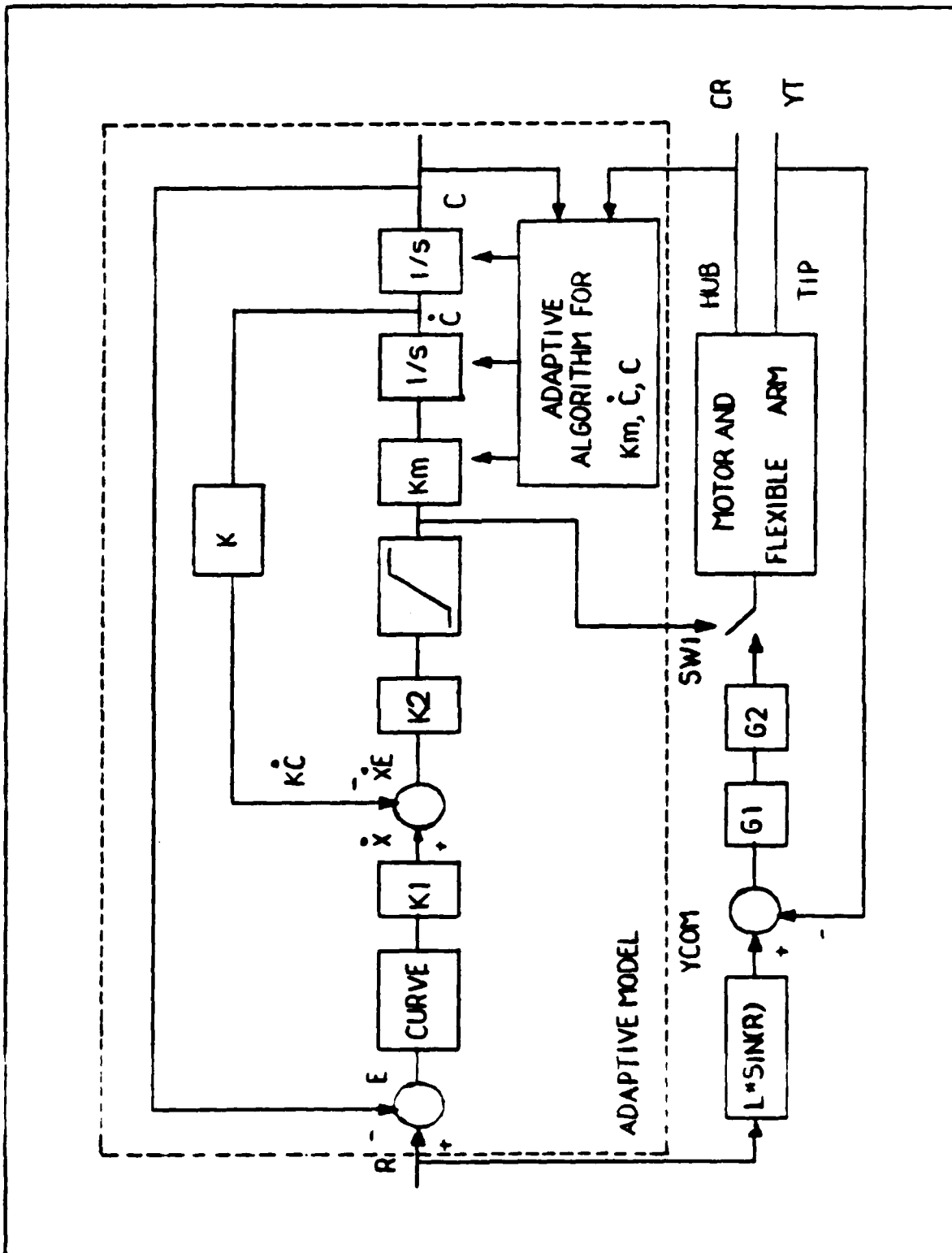


Figure 6.1 Use Of A Simple Compensator For The Tip Control.

margin for the open loop system, which would correspond to a large overall damping coefficient. Furthermore this compensator should be kept as simple as possible in order to be easily implemented in a microprocessor.

The resulted compensator consists of two filters. One phase lead filter and a second order filter with complex poles. The transfer function of the phase lead filter is:

$$G_1 = \frac{0.5S + 0.25}{0.5S + 1} \quad (6.1)$$

The transfer function of the second order filter is:

$$G_2 = \frac{16}{S^2 + 1.6S + 16} \quad (6.2)$$

The open loop frequency response of the linear regulator is shown in Figure 6.2, and the step response of the closed system in Figures 6.3 and 6.4, for the hub and tip motion respectively.

From Figure 6.2 we see that the phase margin is  $42^\circ$ , which corresponds to a damping coefficient of about 0.4. This is not a high damping and as seen in Figures 6.3 and 6.4, the resulting overshoot, for the tip motion, is of the order of 45% and the settling time very large 5 sec. These results are not acceptable for the motion of a robot arm where we strive for speed and accuracy.

Nevertheless the system is studied for various reasons. First it is very simple. Secondly we can have a baseline of

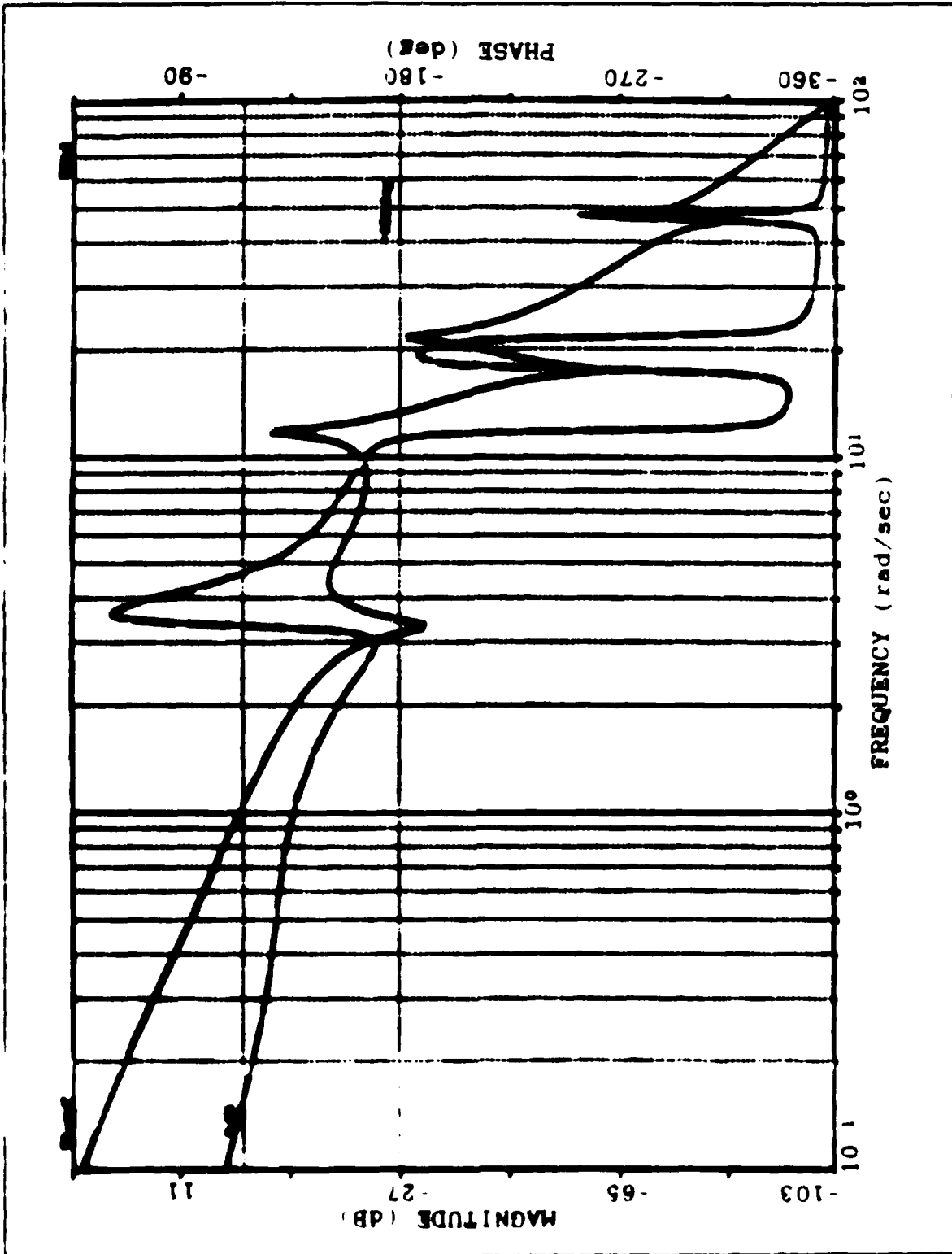


Figure 6.2 The Open Loop Bode Plot Of The Linear System.

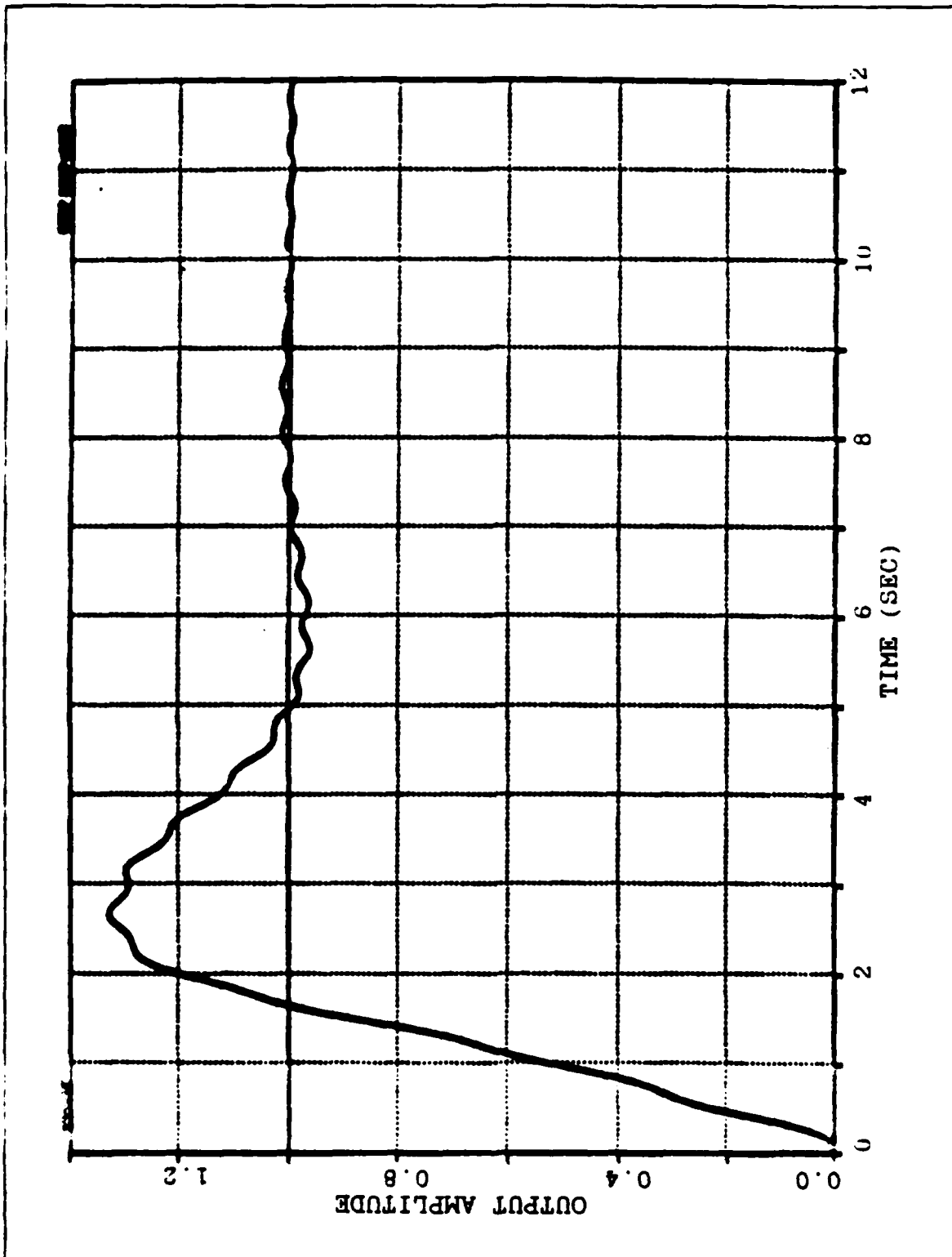


Figure 6.3 Step Response Of The Linear System (Hub Motion).

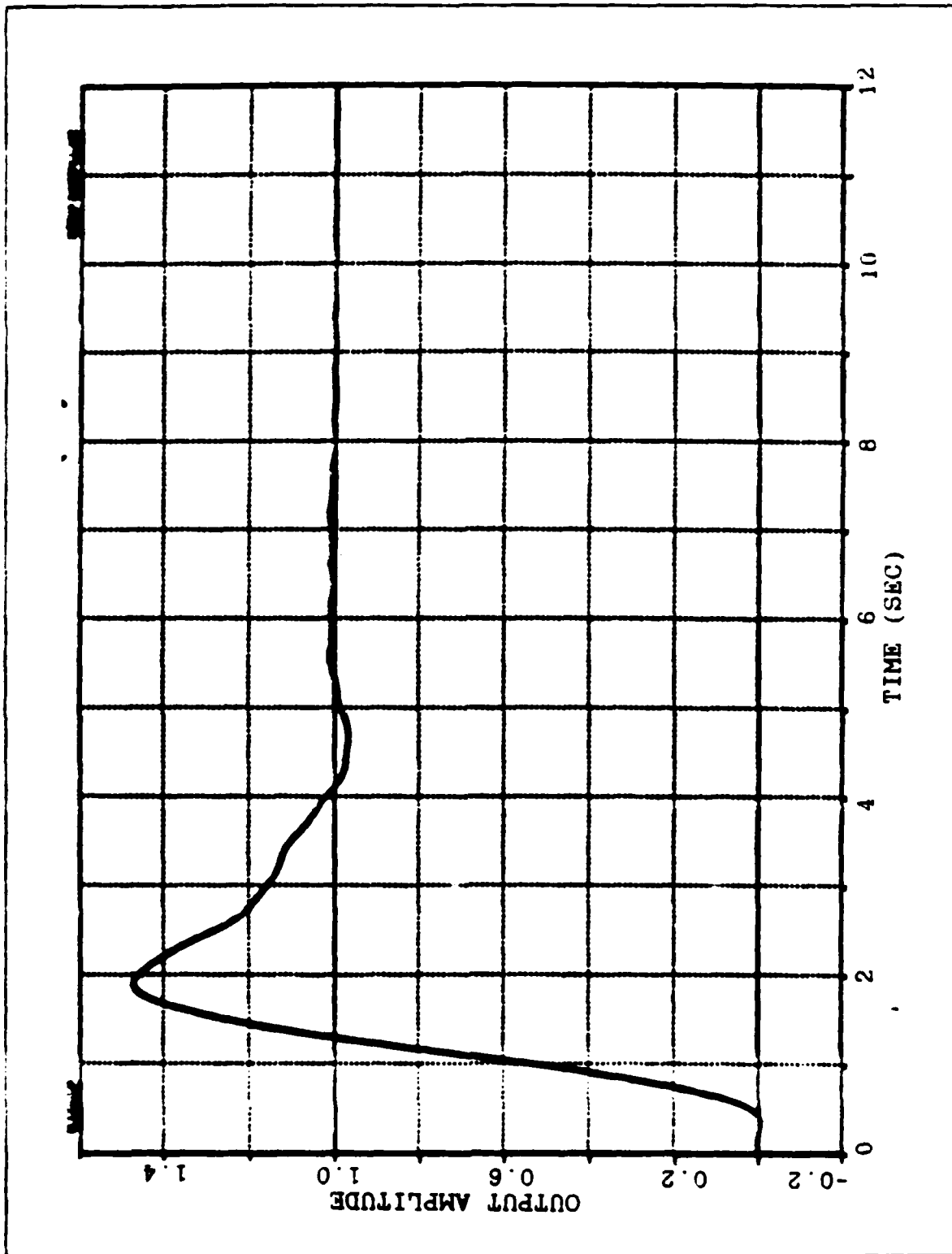


Figure 8.4 Step Response Of The Linear System (Tip Motion).

performance for future alternatives. Finally this system can be proven appropriate for the case where the arm is not so extremely flexible.

The resulting combination of the curve following and the linear regulator, shown in Figure 6.1, was simulated using the DSL/VS program listed in Appendix C. The results of the simulations are shown in Figures 6.5 through 6.8, where different switching points, from the curve following to the linear system have been used. We see that no matter at what point we make the switching to the linear mode, the arm (hub and tip) undergoes a large overshoot before it settles down to the commanded position.

It is obvious that this scheme does not work at least for the case of the very flexible arm.

#### B. POSI-CAST CONTROL

As a second attempt to control the arm's tip we will use posi-cast control.

The basic idea behind this scheme is very simple. Let's consider a system whose overshoot to a step input is known (from previous simulations or tests). Instead of applying the desired command to the system at once, we can apply it in two or more specified steps. The rule that is used to determine the steps, for the case where only two steps are used is the following: We apply the first fraction of the command, whose magnitude is calculated in such a way that at the peak

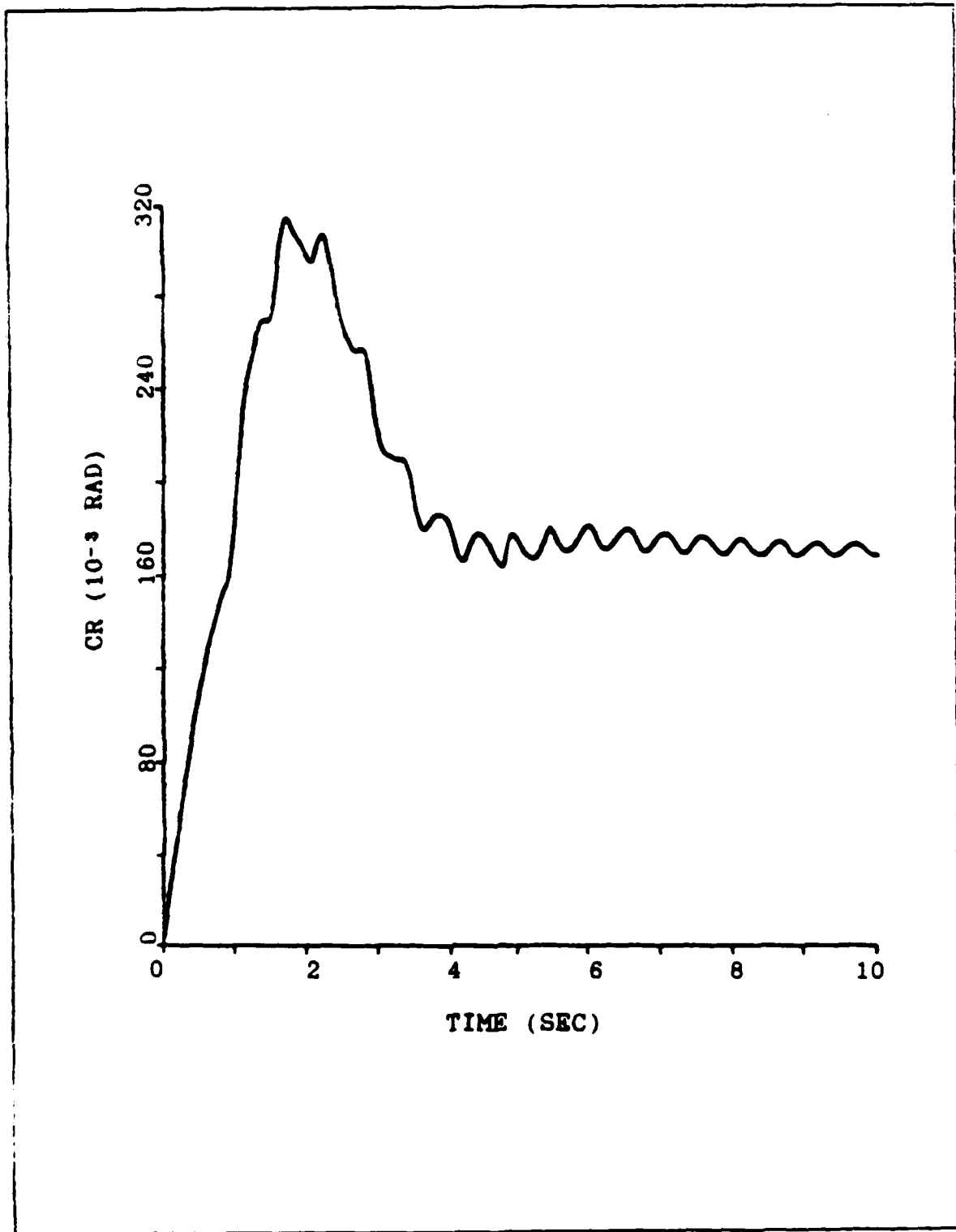


Figure 6.5 Hub Motion Switching To Linear Mode  
At 90% Of The Commanded Position.

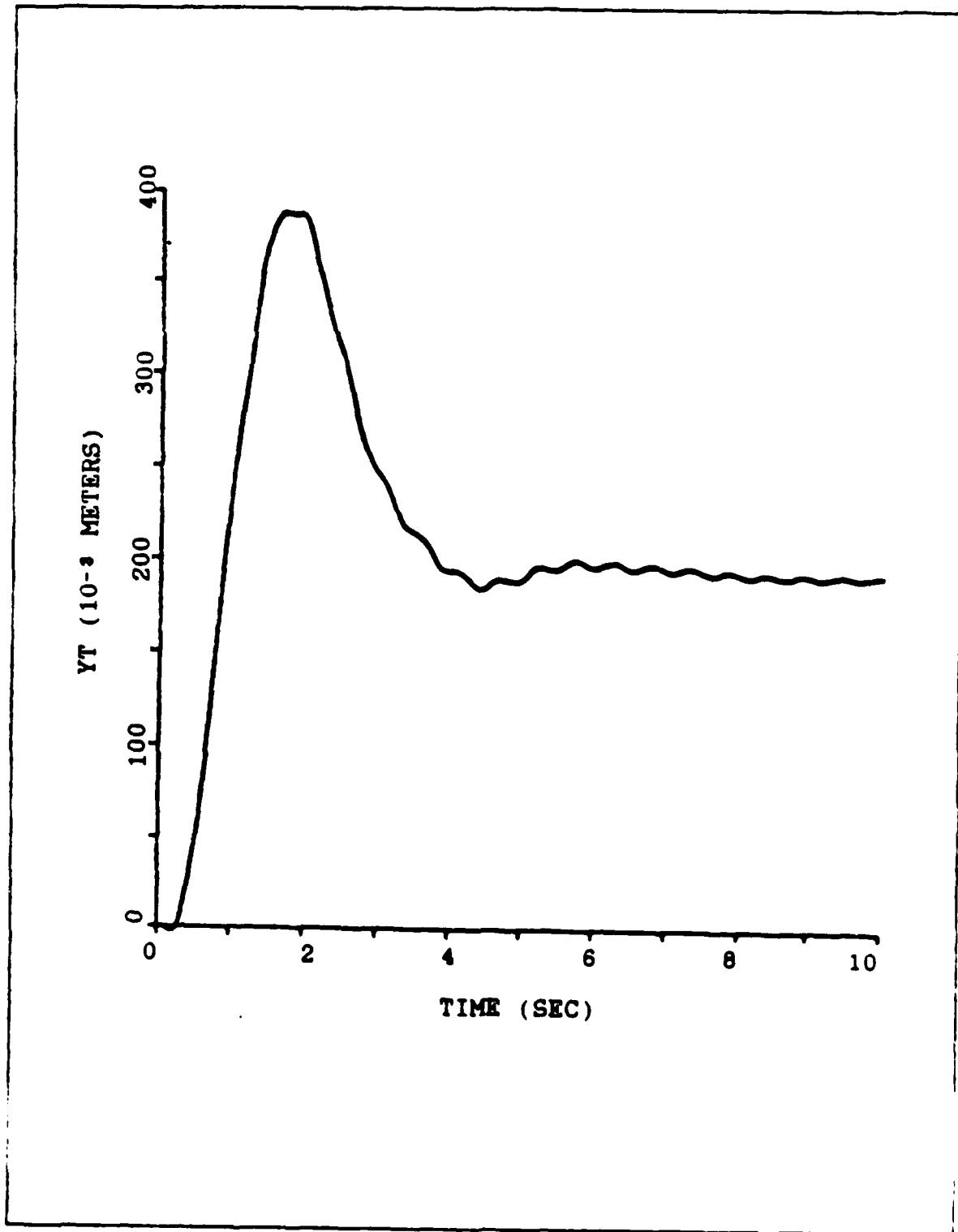


Figure 6.6 Tip Motion Switching To Linear Mode  
At 90% Of The Commanded Position.

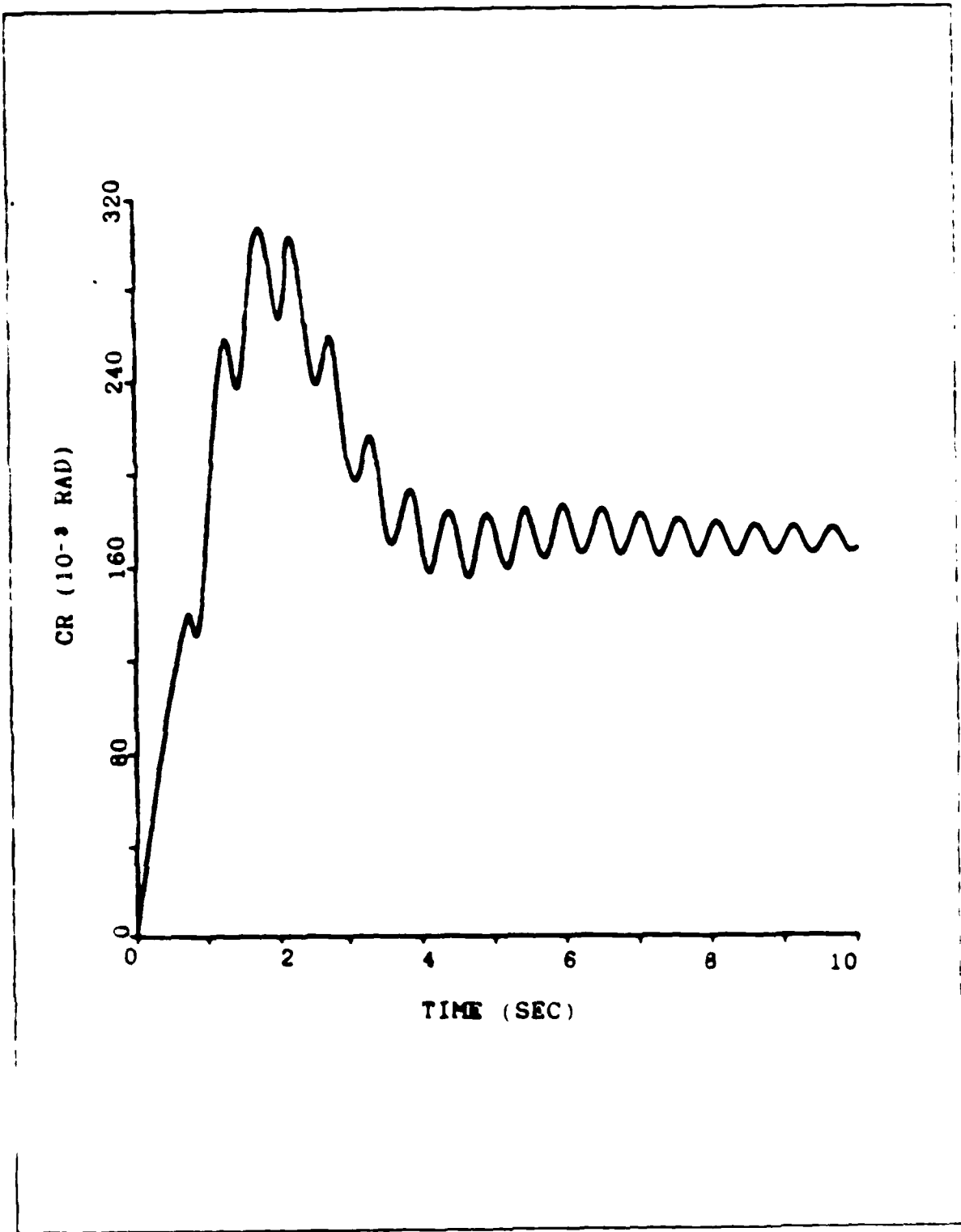


Figure 6.7 Hub Motion Switching To Linear Mode At 60% Of The Commanded Position.

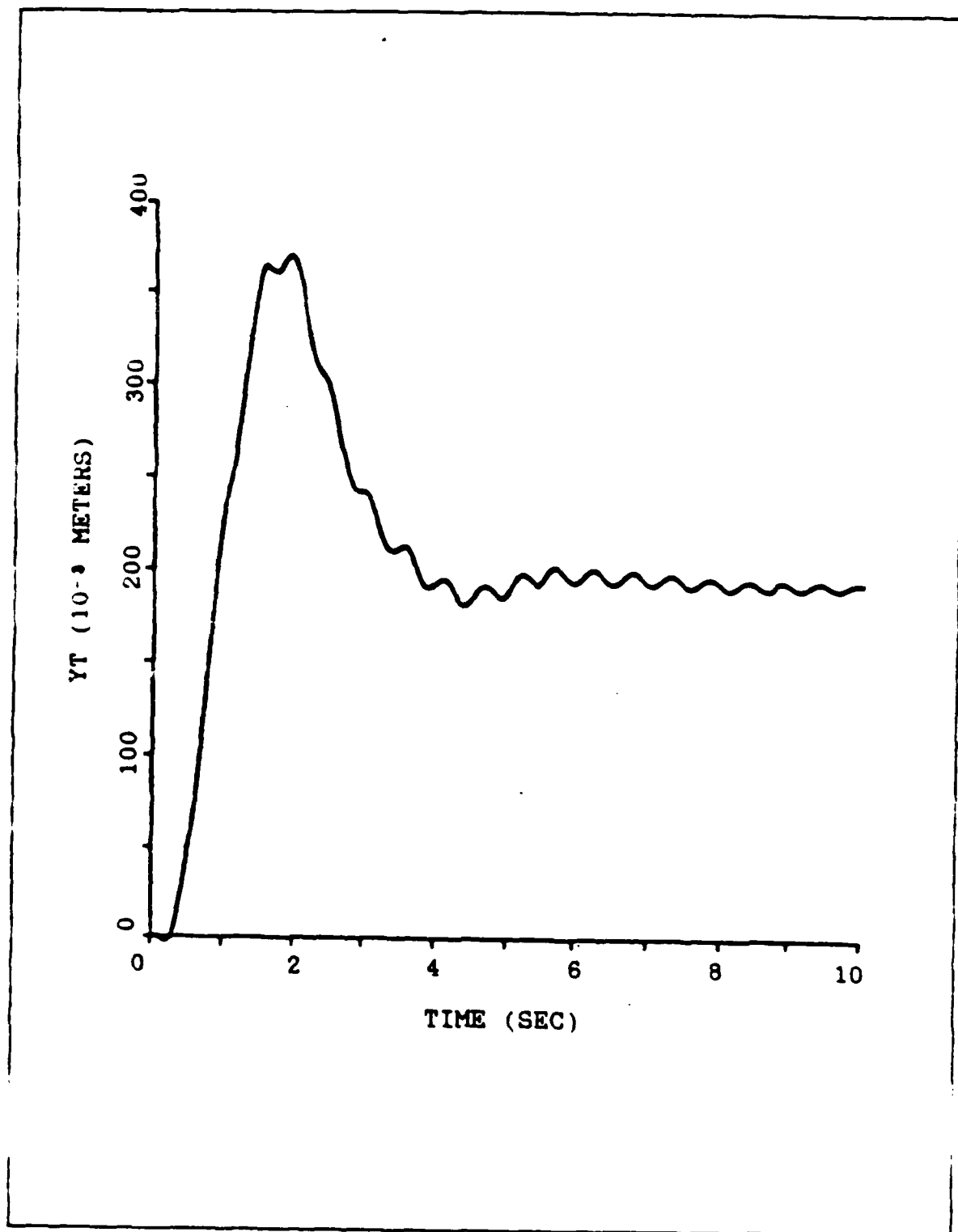


Figure 6.8 Tip Motion Switching To Linear Mode At 60% Of The Commanded Position.

overshoot, the output of the system is equal to the desired final position. When the output is at its peak, we add to the input the second fraction of the command. When this new input is seen by the system, the position error is zero, and the system's output stays at its overshoot value obtained by the first fraction of the command. The result is no overshoot at all and the settling time is considerably reduced.

Now in the case of the flexible arm this scheme might possibly work. If we imagine the arm as a circular spring, the energy is stored into the arm by winding that spring. When the tip reaches its maximum position, it reverses velocity and moves in the opposite direction. This motion unwinds the spring and through the spring's damping the energy stored in the arm is dissipated and the tip settles down.

When the tip is at its peak overshoot position, we can slow down (or hopefully stop) its motion, towards the opposite direction, if we find a way to unwind the spring. This can be accomplished by moving the hub towards the direction of the tip. Therefore, if we apply a predetermined input, so that the arm's tip overshooting reaches the desired position, and then add to the input the second fraction of the command, we can unwind the "spring" and hopefully make the motion of the tip acceptable.

Another factor that we have to consider, is the delay that the tip's motion undergoes. It may possibly be necessary

to apply the second fraction of the input a little bit earlier than the time that corresponds to the peak overshoot.

The DSL/VS program shown in Appendix D was used for the simulation of this idea and the results are shown in Figures 6.9 to 6.12 for different times of application of the second fraction of the desired command. We see that when the delay of the tip's response (280 msec) is taken into account (Figure 6.12), the motion of the tip is satisfactory, while the hub's motion is always very good (Figures 6.9 and 6.11). Comparing Figure 6.10 with Figure 6.12 we see how critical is the time of the application of the second portion of the input command. The optimal point of application of the second portion of the input cannot be found very accurately, and it changes with the operation conditions (load, speed, magnitude of the input, etc.). Therefore we do not expect so much from this control scheme, for a real application.

### C. USE OF A SHAPED INPUT

It is seen from the motion of the tip, that at the beginning of the application of the torque, there is energy given to the arm, without any motion of the tip. When this energy winds the "spring", the tip starts moving first in the opposite direction, and then quickly towards the desired direction (Figures 5.3, 5.6 and 5.9).

The energy supplied to the arm depends on the magnitude of the input command. If, therefore, we shape the input

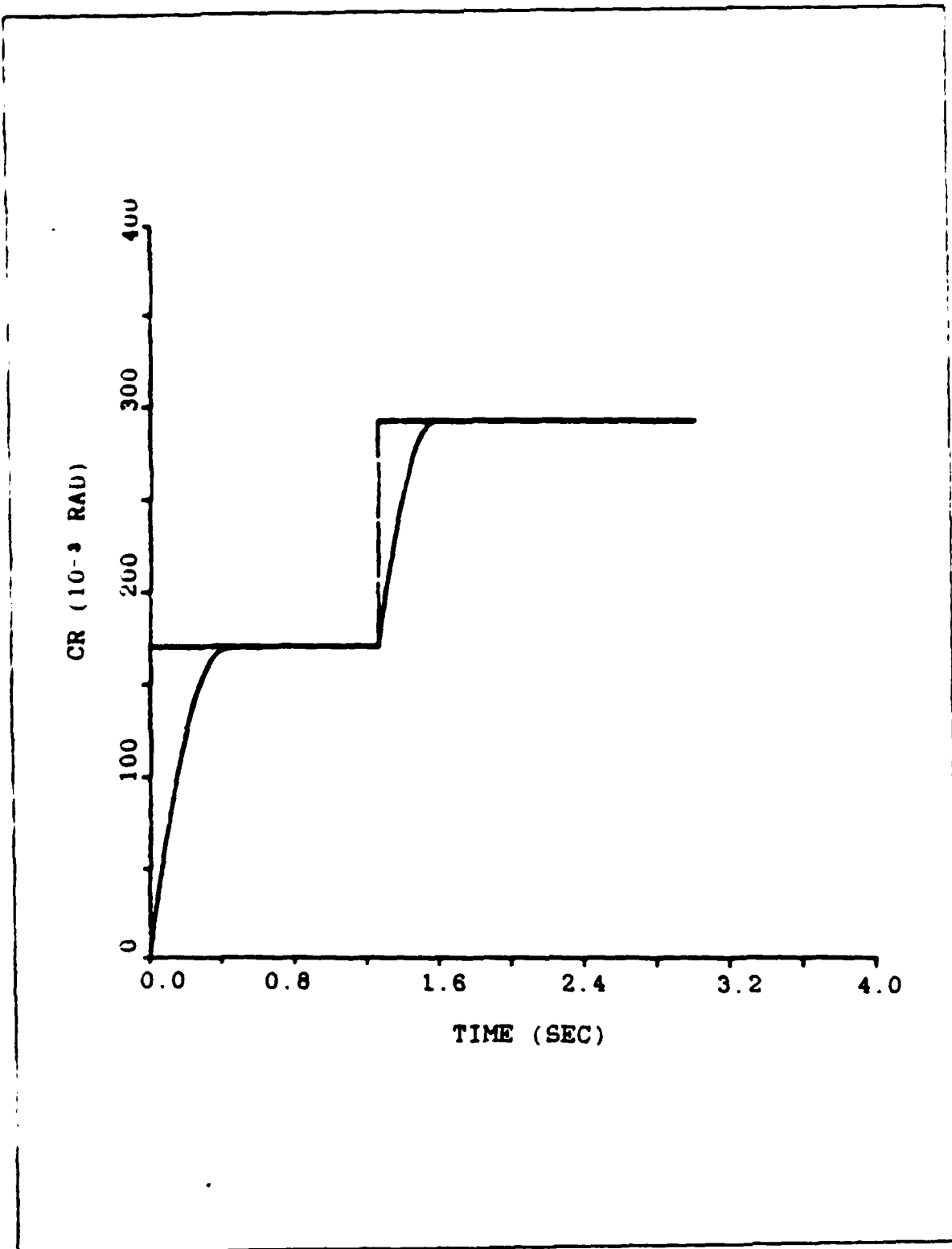


Figure 6.9 Posi-Cast Control (Hub Motion).

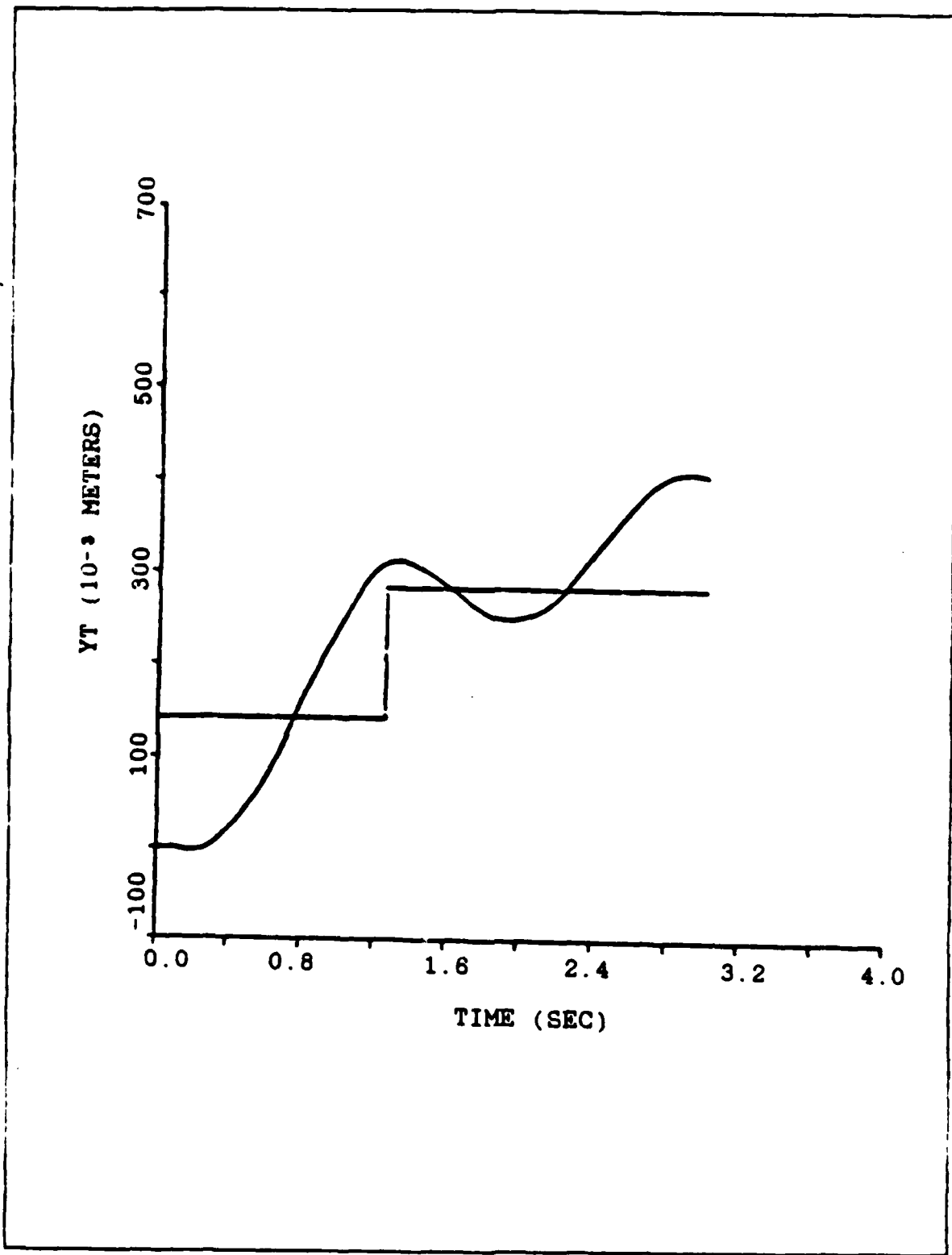


Figure 6.10 Posi-Cast Control (Tip Motion).

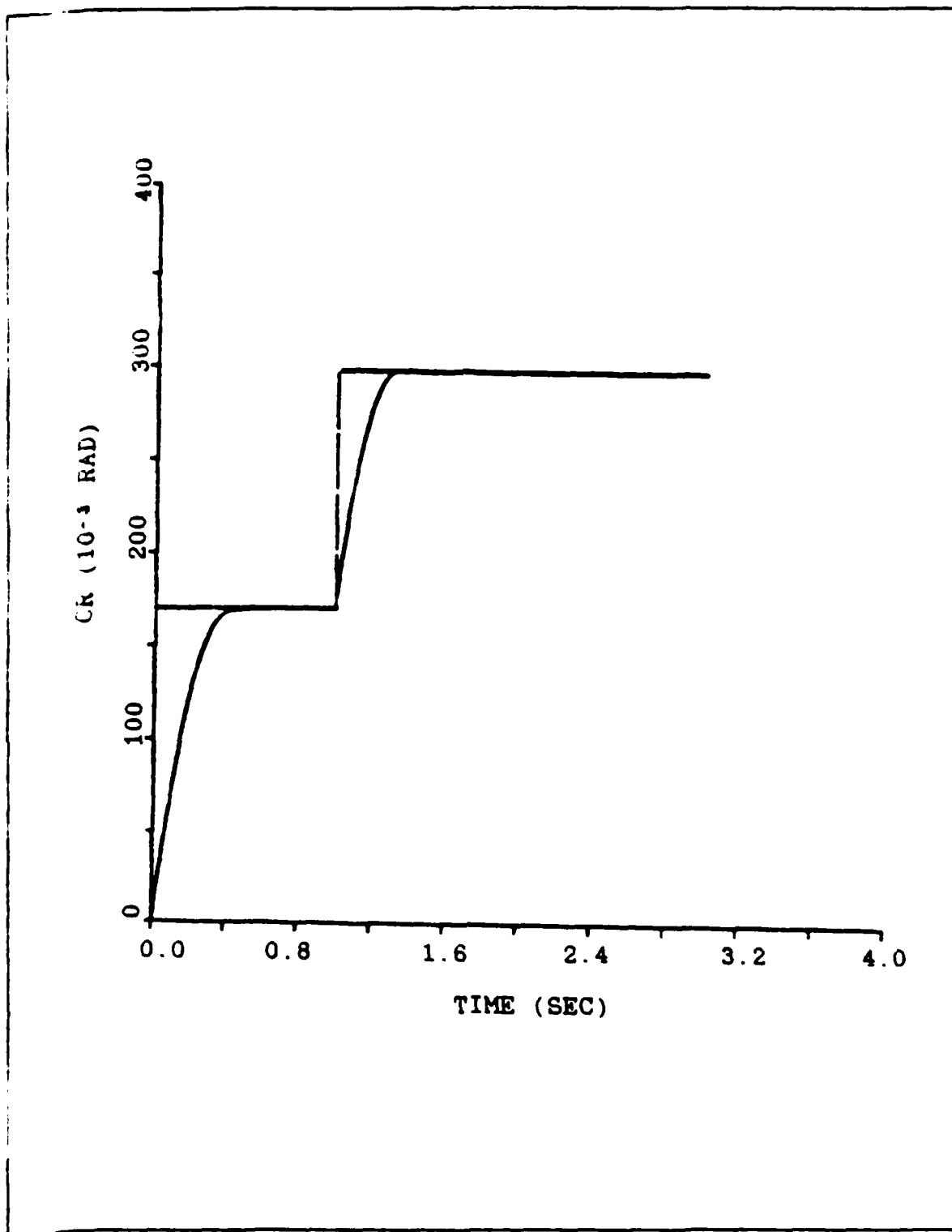


Figure 6.11 Posi-Cast Control (Hub Motion), Taking Into Account The 280 msec Delay Of The Tip's Response.

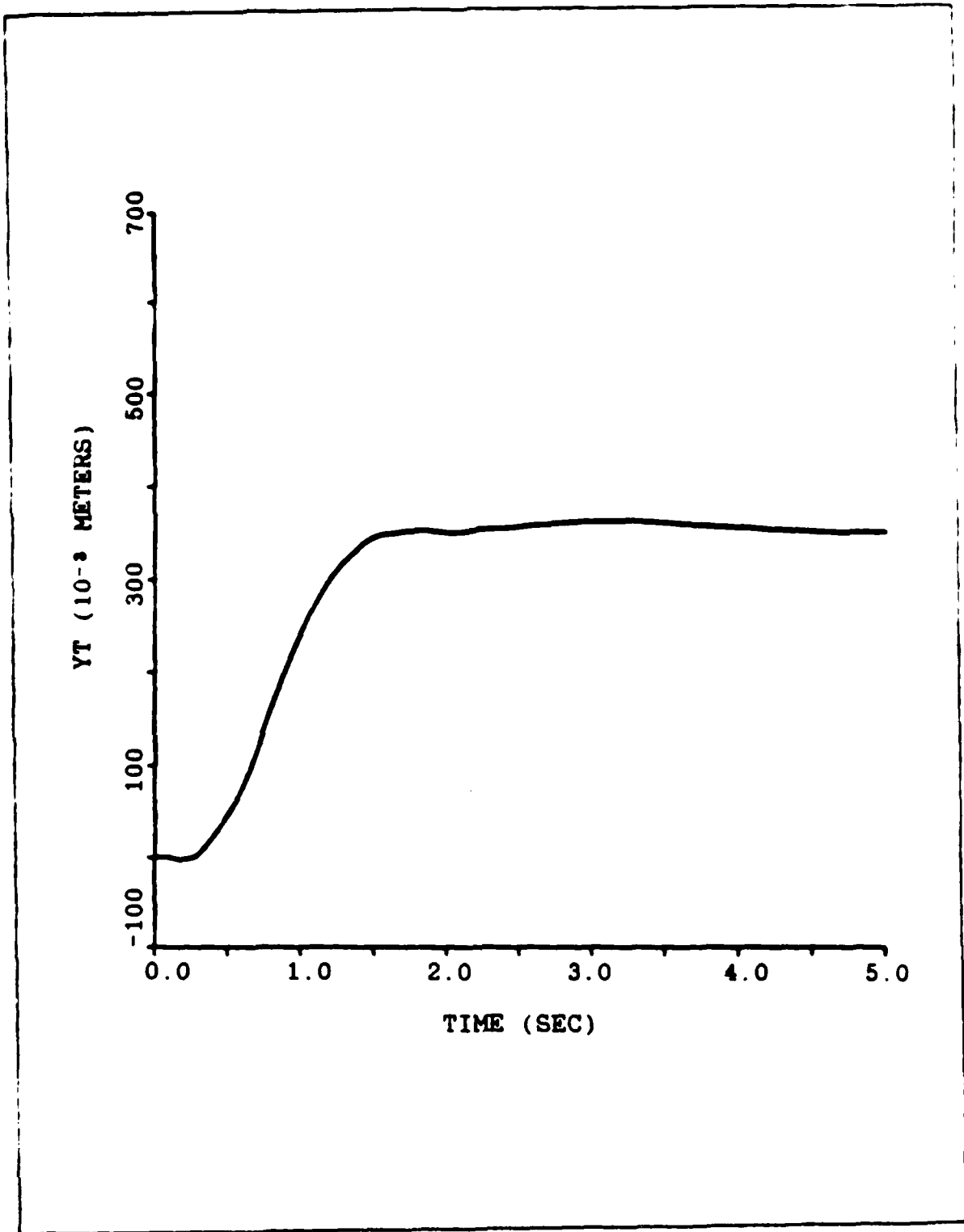


Figure 6.12 Posi-Cast Control (Tip Motion), Taking Into Account The 280 msec Delay Of The Tip's Response.

command, so that only a small amount of energy is supplied to the arm, during this early stage of the motion, it seems reasonable to assume that a better motion of the tip will result

For this purpose the input shape shown in Figure 6.13 was used. This shaped command has been found in Chapter IV (Figures 4.7, 4.8 and 4.9) to give good results when used as an input to the curve following system. The resulting motion of the hub and the tip of the arm are shown in Figures 6.14 and 6.15 respectively. Again we see that the resulting motion of the tip is not acceptable.

The input shape used is of course a very simple one and someone could expect that a different shape could probably give better results. This may be true, but it is also true that this different input shape may require complicated and time-consuming calculations, resulting in a complex system. The most systematic way to calculate the appropriate input shape is by the application of optimal control theory. The optimal input is then found as the one that minimizes the selected cost function.

In this and the previous sections we made use of various simple schemes for the control of the tip of the arm. We found that none of them gave satisfactory results, and we must have been convinced by now that we have to use more complex schemes in order to control the motion of the tip. However we must always keep in mind, that the arm used with

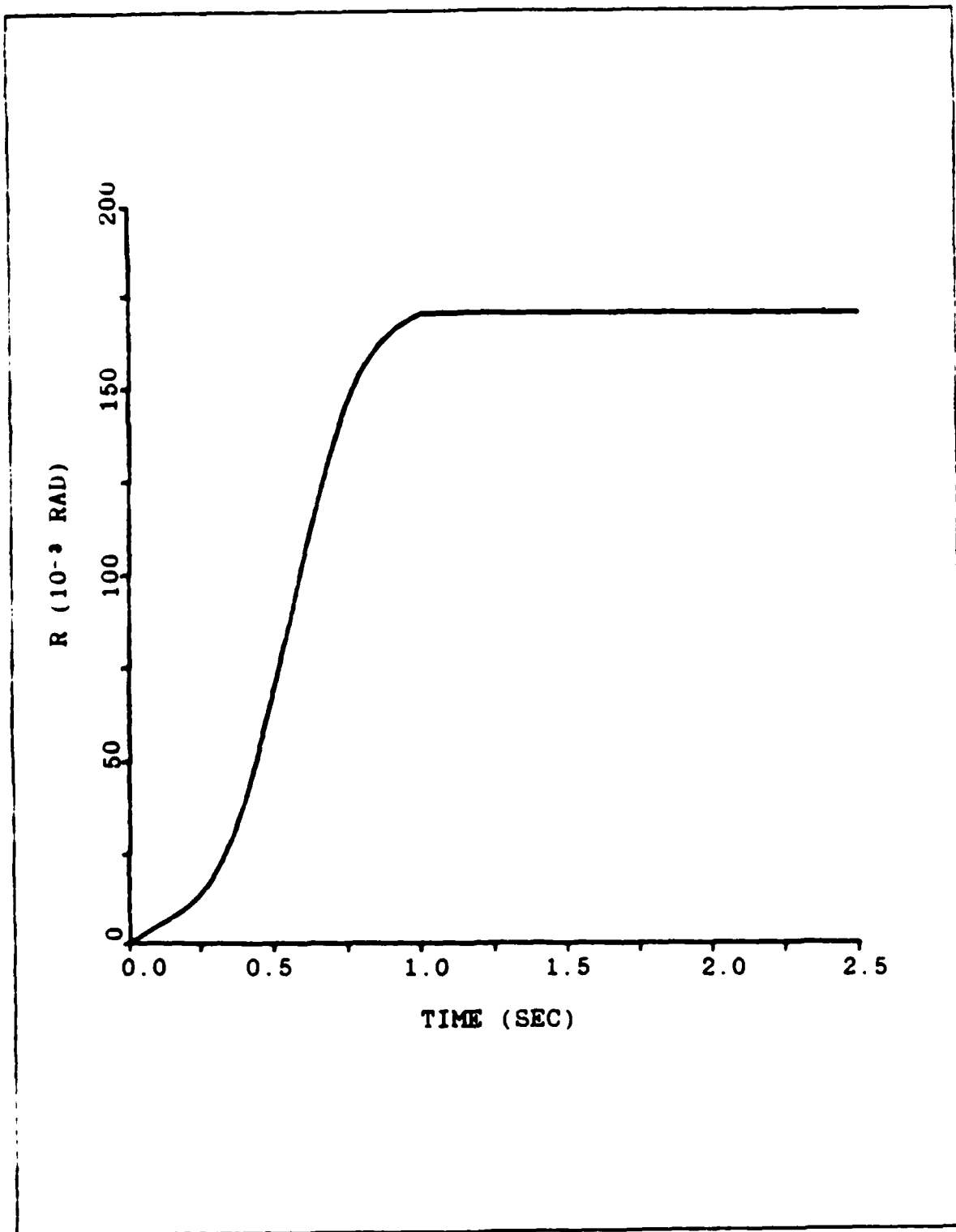


Figure 6.13 Input Shape For The Motions Shown  
In Figures 6.14 And 6.15

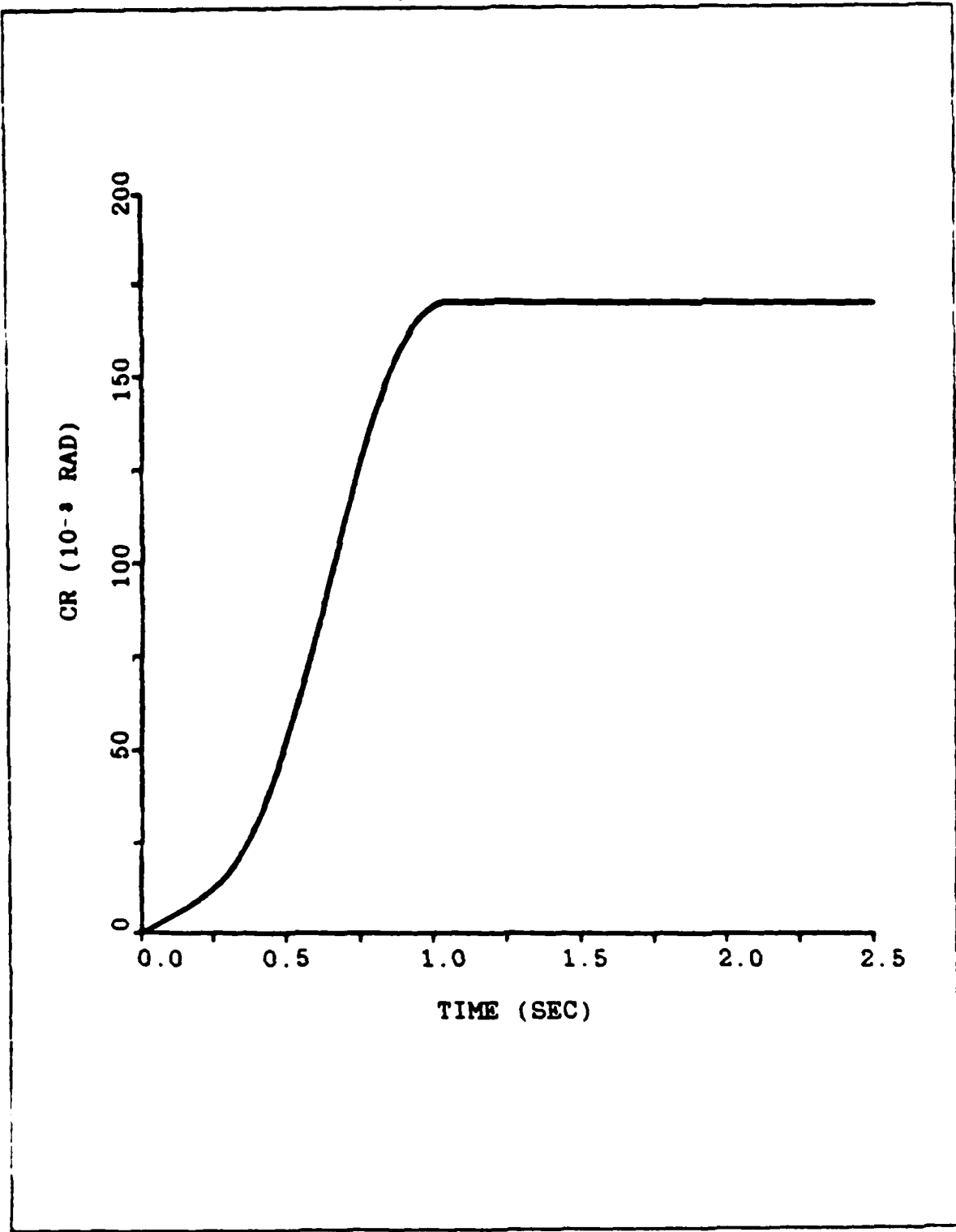


Figure 6.14 Hub Motion Subject To The Input Shown In Figure 6.13.

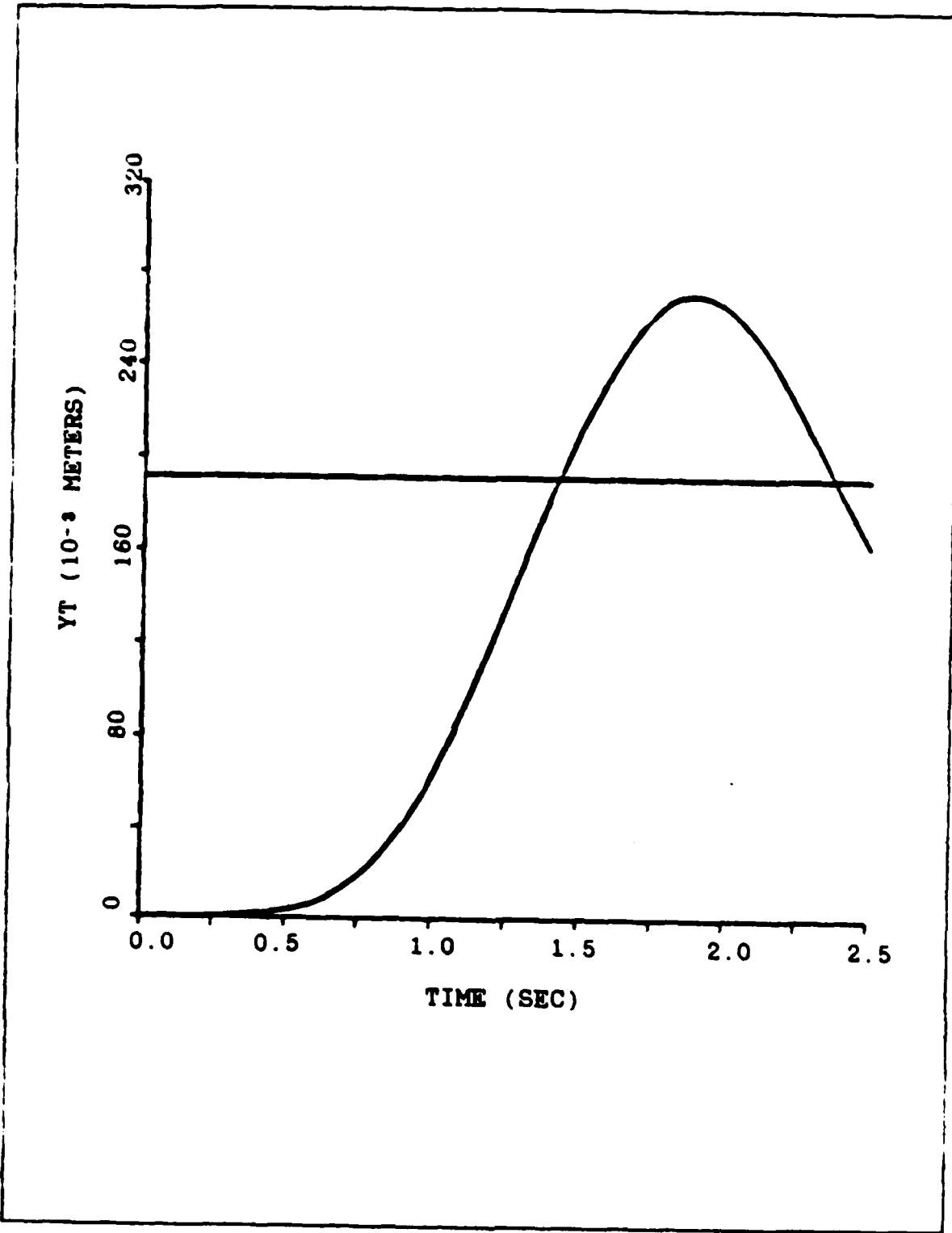


Figure 6.15 Tip Motion Subject To The Input Shown In Figure 6.13.

the previous schemes is a very flexible one. It is possible that some of the tested ideas may work satisfactorily when we use them for the control of a stiffer arm.

#### D. FEEDBACK COMPENSATION

##### 1. Overview

As already mentioned all the attempts made to control the tip of the arm by simple methods had no success. None of the previous methods provided the necessary damping to dissipate, in a reasonable time, the energy stored in the arm. Therefore we have to consider the application of more complex schemes.

In this section a feedback compensator, whose design is based on optimal control theory, will be used. This compensator is given in [Ref. 1]. The curve following scheme will be used in order to drive the arm quickly, over a large portion of the whole motion. Then we will switch off the curve following scheme, and we will leave the rest of the motion to be done under the linear regulator. This composite scheme offers a significant advantage, compared with the scheme used in [Ref. 1]. In [Ref. 1], the control of the arm is done by using only the linear system. Attention, however, has to be paid, in order to avoid driving the motor to saturation. If this happens the whole system is rendered inappropriate. To avoid this problem, [Ref. 1] uses only small displacements as inputs to the system. If a large

displacement is desired, it has to be applied through a number of smaller movements, resulting in large total time.

When we use the composite system, shown in Figure 6.16, the saturation of the motor is not a problem any more. The first stage of the motion, where large torques are required due to the large position error, is done by the curve following scheme, without worrying about the saturation of the motor. When the position error becomes small and therefore only small torques are required, we switch to the linear mode, which provides the necessary damping, to remove the energy stored into the arm and make the motion of the tip acceptable.

## 2. Design Of The Feedback Compensator

First of all we have to decide which signal we will feed back for the compensation of the system. If we use as a feedback signal the hub position or the hub velocity, we will lose all the information about the tip, because the tip does not follow the hub motion, as in the case of a rigid arm. Therefore we have to use tip feedback for the compensation of the system. To use tip feedback however, we need a sensor to measure the position of the tip. To build such a sensor is by no means a trivial problem, and extensive research has to be done on this area.

For the purpose of this thesis we will assume that such a sensor exists, which gives us accurate measurements



of the position of the tip. With this provision we can now proceed in the design of the feedback compensator.

The design of the compensator is given in chapter five of [Ref. 1]. At first a full state feedback regulator is designed, which minimizes the cost function:

$$J = \int (X^T A_c X + u^T B u) dt,$$

where  $X$  is the state of the system and  $u$  the input to the system.

Consequently a state estimator is designed in order to provide the states of the system, used by the regulator.

Three different compensators have been designed. The first uses only tip position feedback. The second uses tip position and hub velocity, while the third uses tip position, hub velocity and strain-gauge as feedback signals.

The latter two yield better results but they are very complex and it is questioned whether or not they can be used in a practical application. In order to keep our system as simple as possible, we will use the first compensator. It is the simplest one. Its transfer function is

$$H(s) = \frac{1160.3(s+1.5)(s-2.3 \pm j14.1)(s-2.3 \pm j14.1)}{(s+18.2 \pm j22)(s+12.2)(s-30)(s-30)}$$

This compensator consists of a lead filter, two notch filters and two notch filters. The notches are at the poles of the system.

AD-A185 835

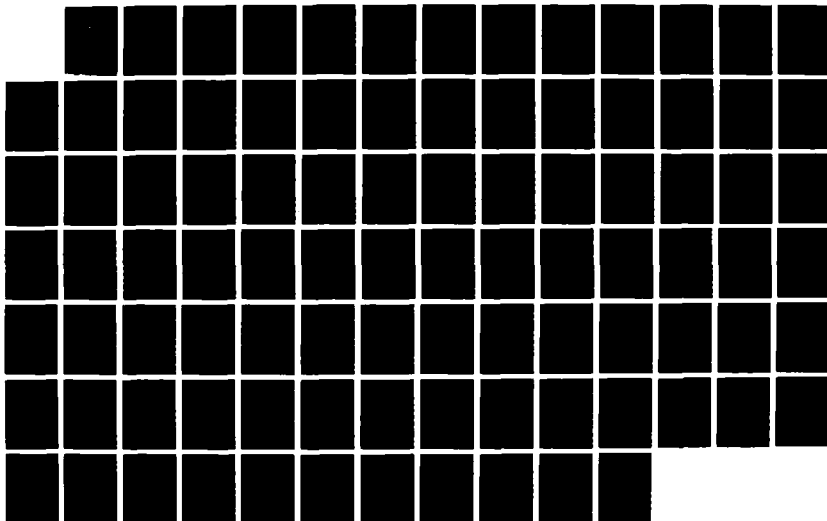
CONTROL OF A FLEXIBLE ONE-LINK MANIPULATOR(U) NAVAL  
POSTGRADUATE SCHOOL MONTEREY CA I E ZOUZIAS JUN 87

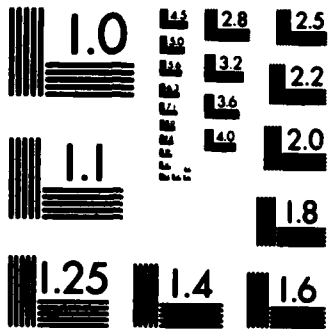
2/2

UNCLASSIFIED

F/G 13/9

NL





MICROCOPY RESOLUTION TEST CHART  
NATIONAL BUREAU OF STANDARDS-1963-A

exactly at the frequencies of the first and the second vibration mode of the arm. This makes the closed loop system very sensitive to errors or changes of the vibration frequencies. Especially in the case of the loaded arm, where the vibration frequencies are moved to the left by 0.4 rad/sec (Figures 3.3 and 3.4) we are going to face problems. The step response of the closed loop linear system is shown in Figure 6.17, where we see a very well damped motion of the tip of the arm, with zero overshoot.

### 3. Simulation Of The System

The composite system shown in Figure 6.16 was simulated by the DSL/VS program listed in Appendix E. Different values for the gain constant  $K_1$  and various points for the switching from the curve following to the linear system were used. The results of these simulations are shown in Figures 6.18 to 6.25. The Figures 6.18 through 6.23 correspond to a small commanded position equal to 0.17 rad (or  $10^\circ$ ). The Figures 6.24 and 6.25 correspond to a commanded position equal to one radian (large motion). From these simulations (and even more not included), the best value found for  $K_1$  was 0.06. The resulting system is very good for the control of the tip when "large motion" is used. When the motion is "small" we obtain almost the same settling time as when we use the linear system alone, but we have an overshoot of the order of 7% (for  $K_1 = 0.06$ ). This overshoot may or may not be acceptable, depending on the specific application.

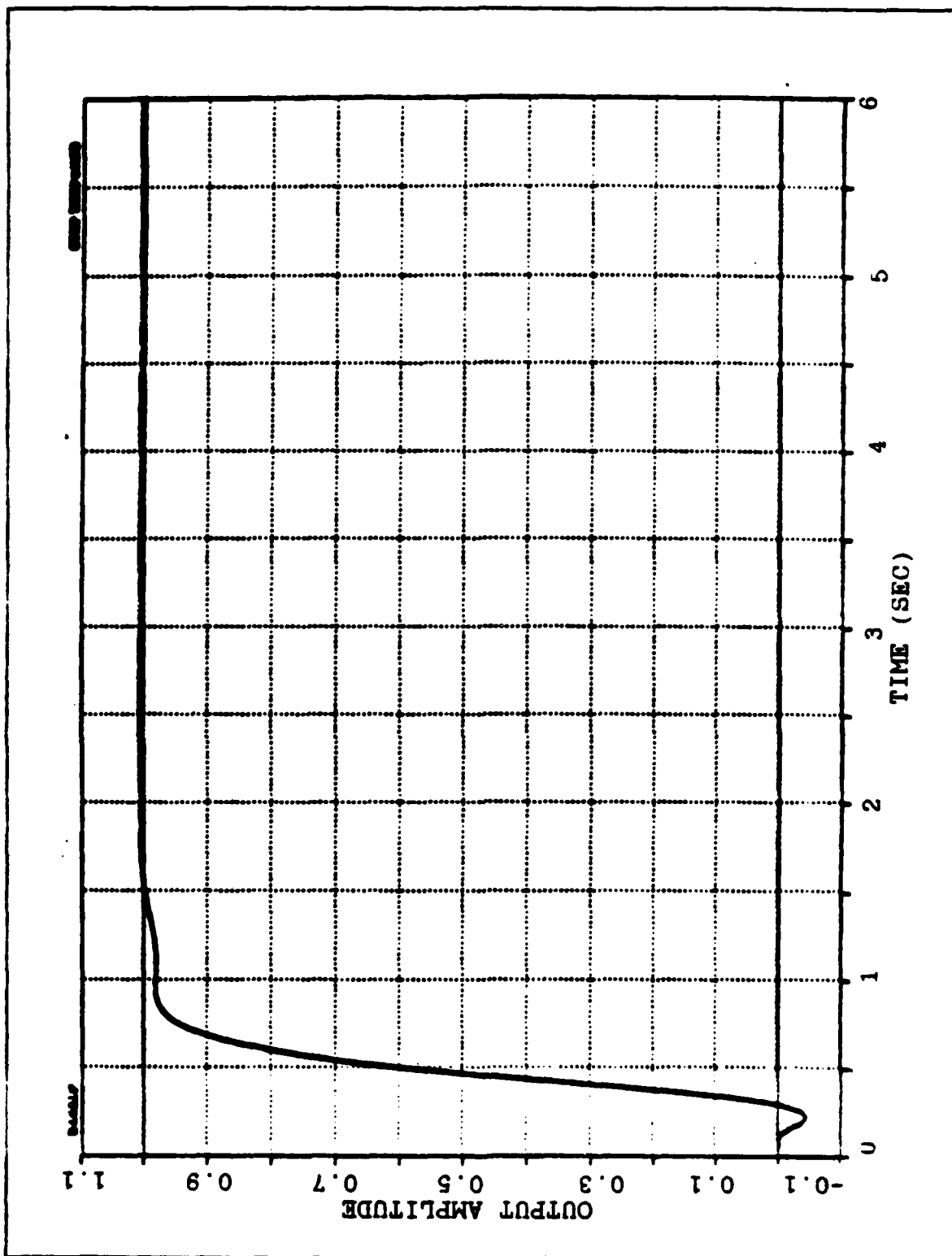


Figure 6.17 Step Response Of The Linear System

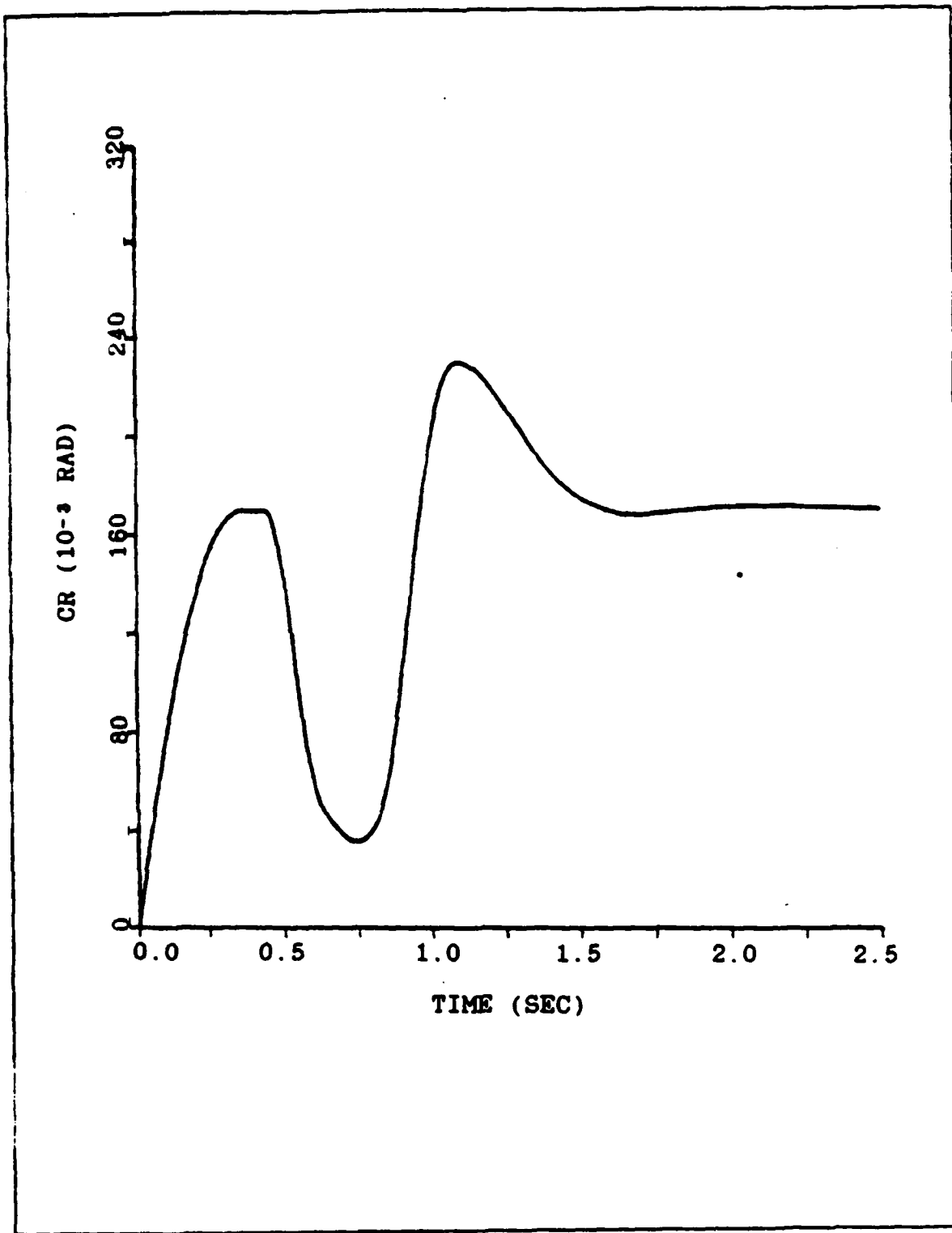


Figure 6.18 Hub Motion Using The System Shown In Figure 6.16 With  $K_1 = 0.2$  (Small Motion).

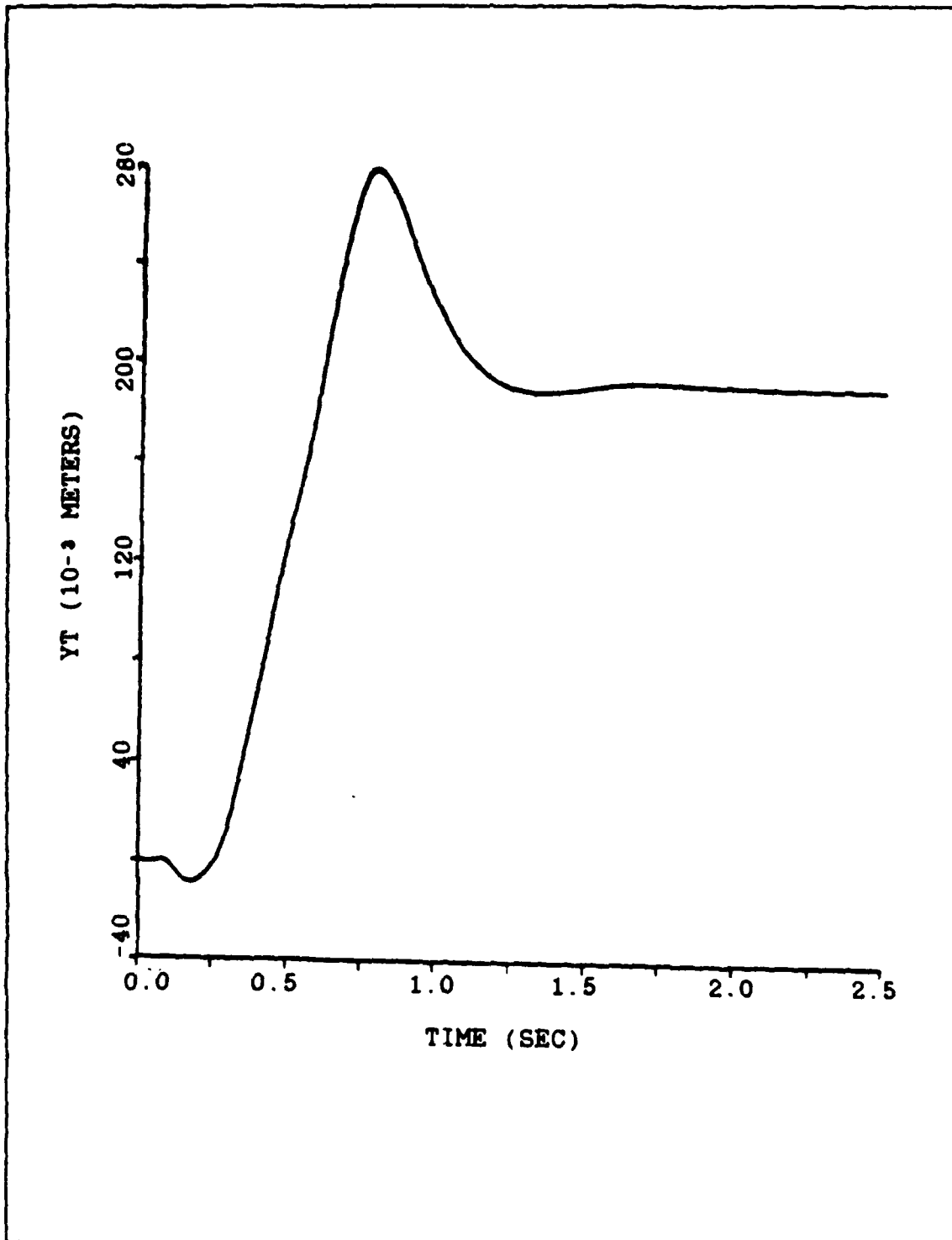


Figure 6.19 Tip Motion Using The System Shown In Figure 6.16  
With  $K_1 = 0.2$  (Small Motion).

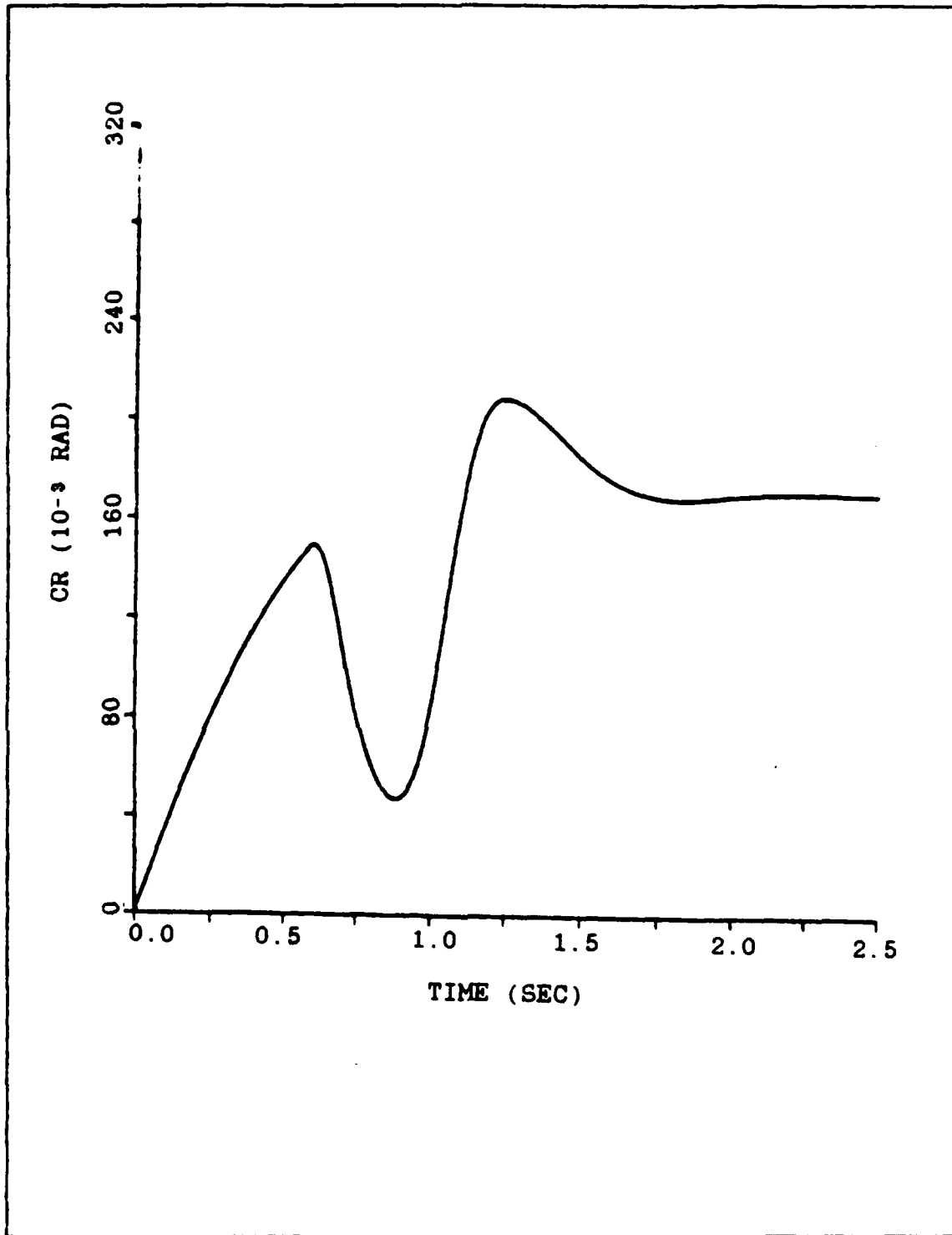


Figure 6.20 Hub Motion Using The System Shown In Figure 6.16  
With  $K_i = 0.08$  (Small Motion).

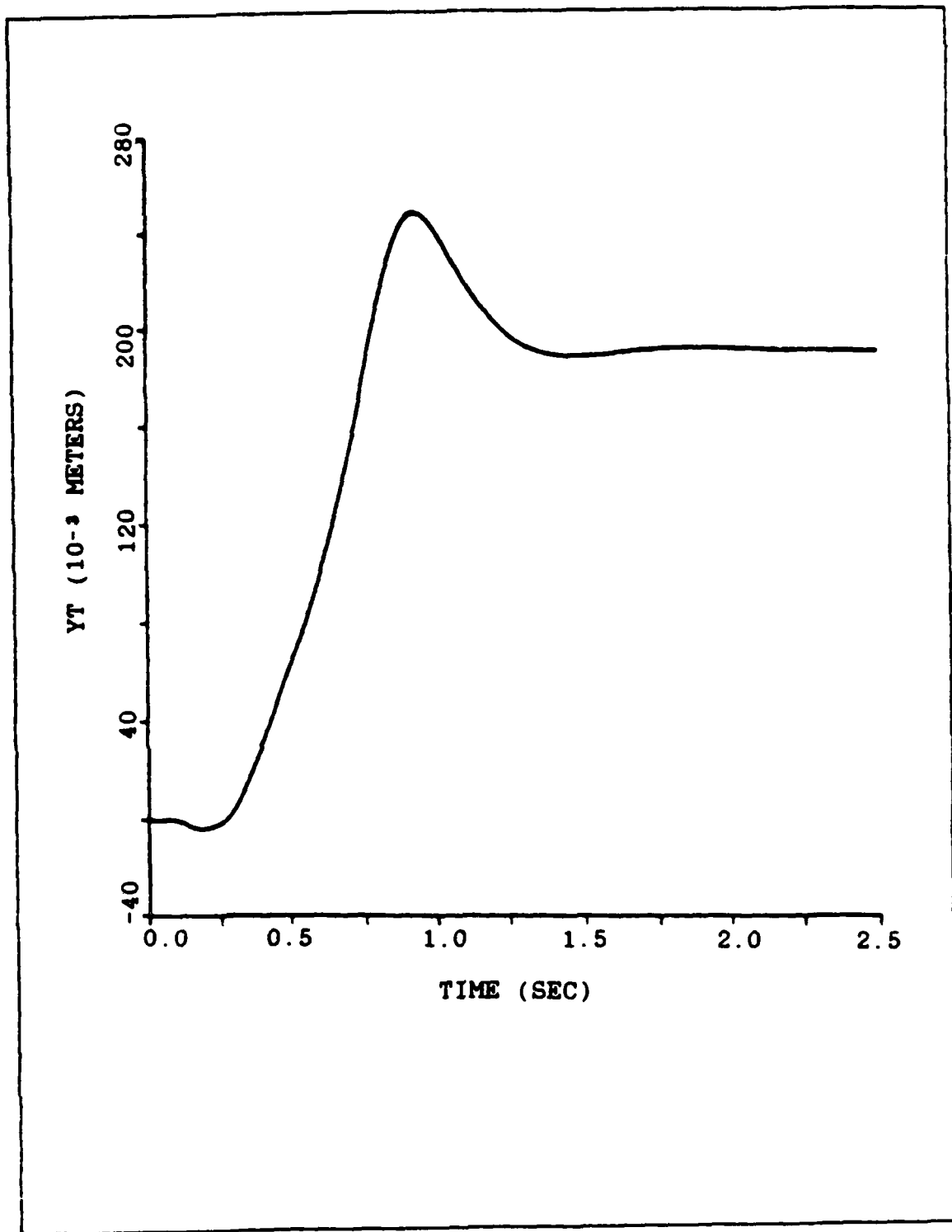


Figure 6.21 Tip Motion Using The System Shown In Figure 6.16  
With  $K_1 = 0.08$  (Small Motion).

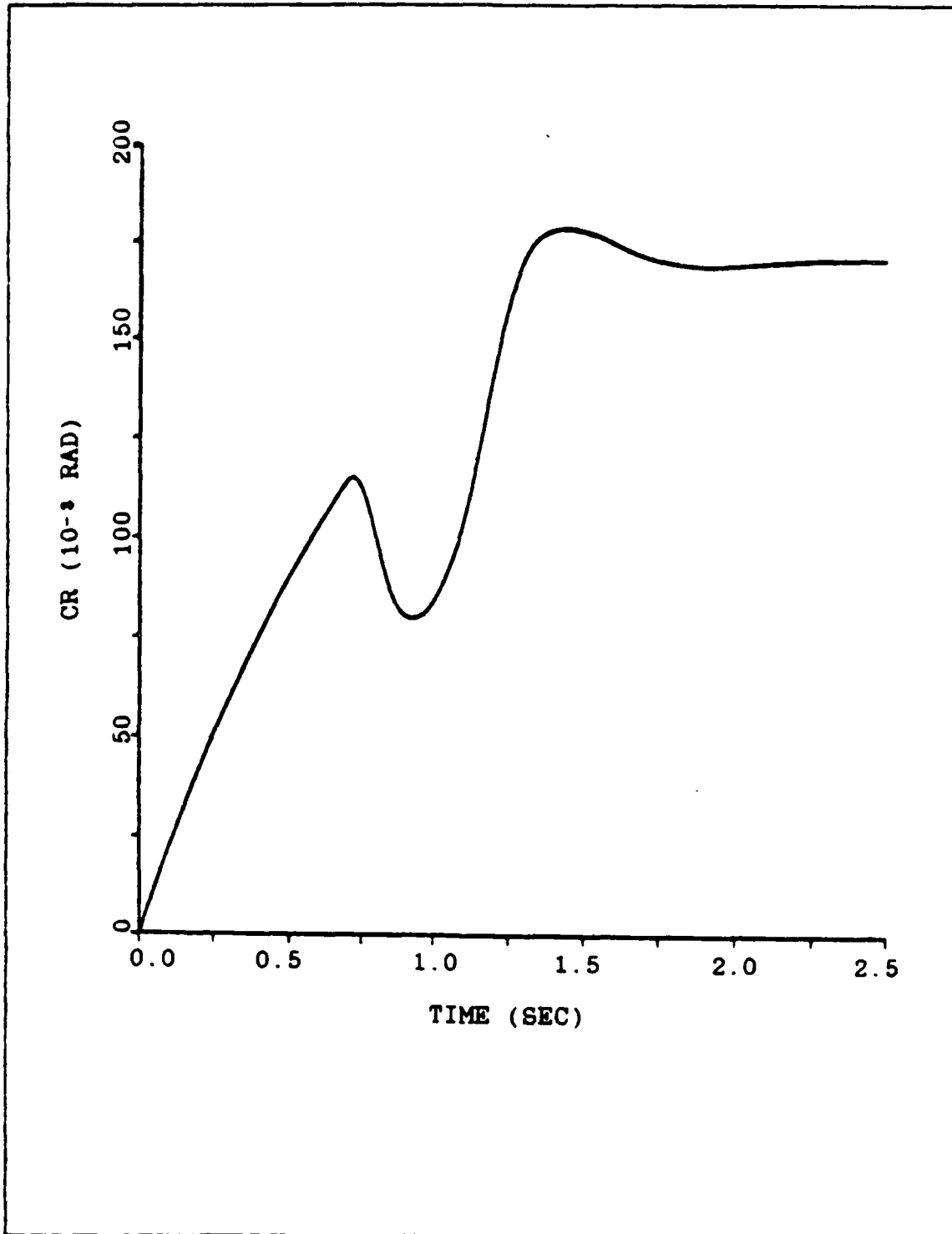


Figure 6.22 Hub Motion Using The System Shown In Figure 6.16  
With  $K_1 = 0.06$  (Small Motion).

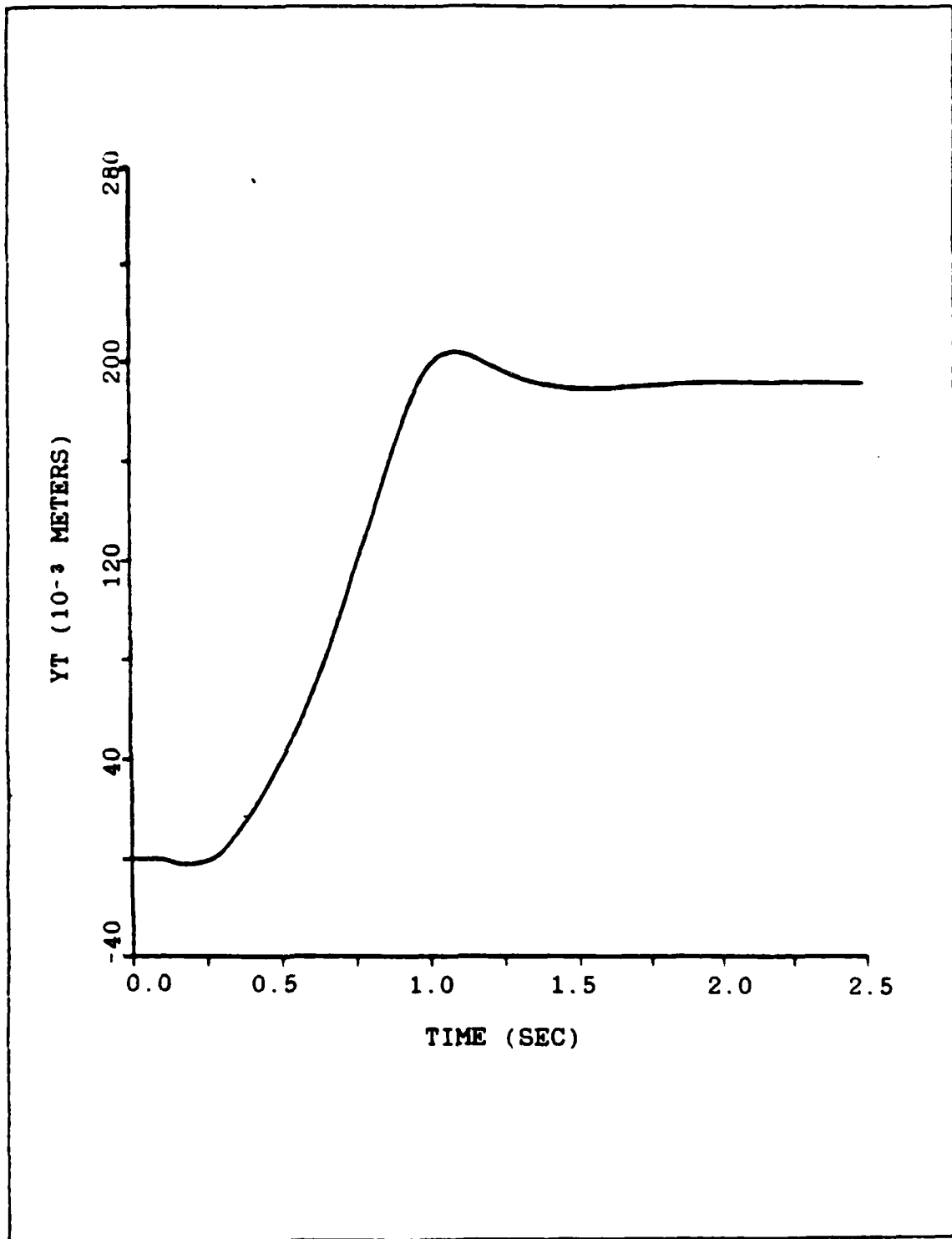


Figure 6.23 Tip Motion Using The System Shown In Figure 6.16  
With  $K_1 = 0.06$  (Small Motion).

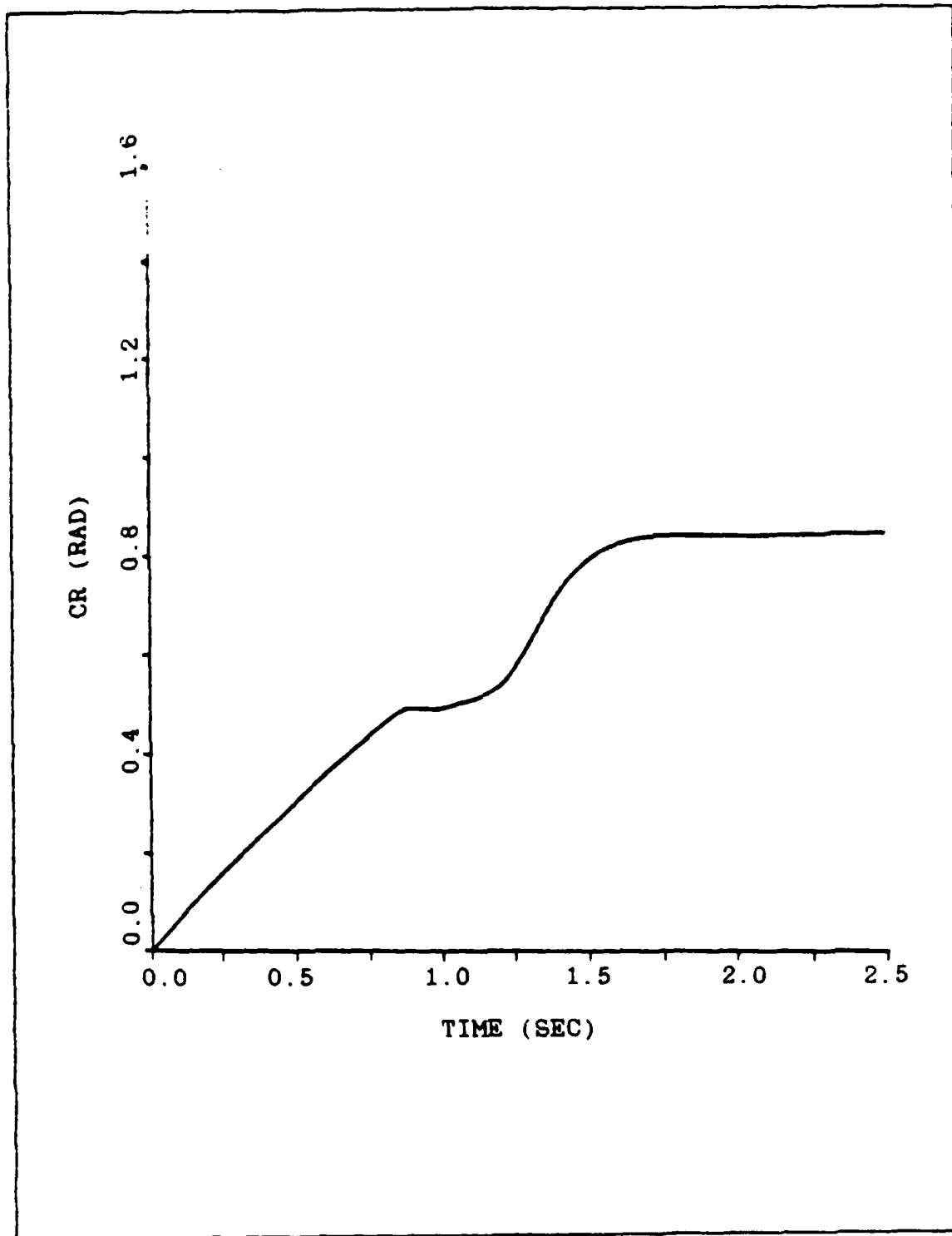


Figure 6.24 Hub Motion Using The System Shown In Figure 6.16  
With  $K_1 = 0.06$  (Large Motion).

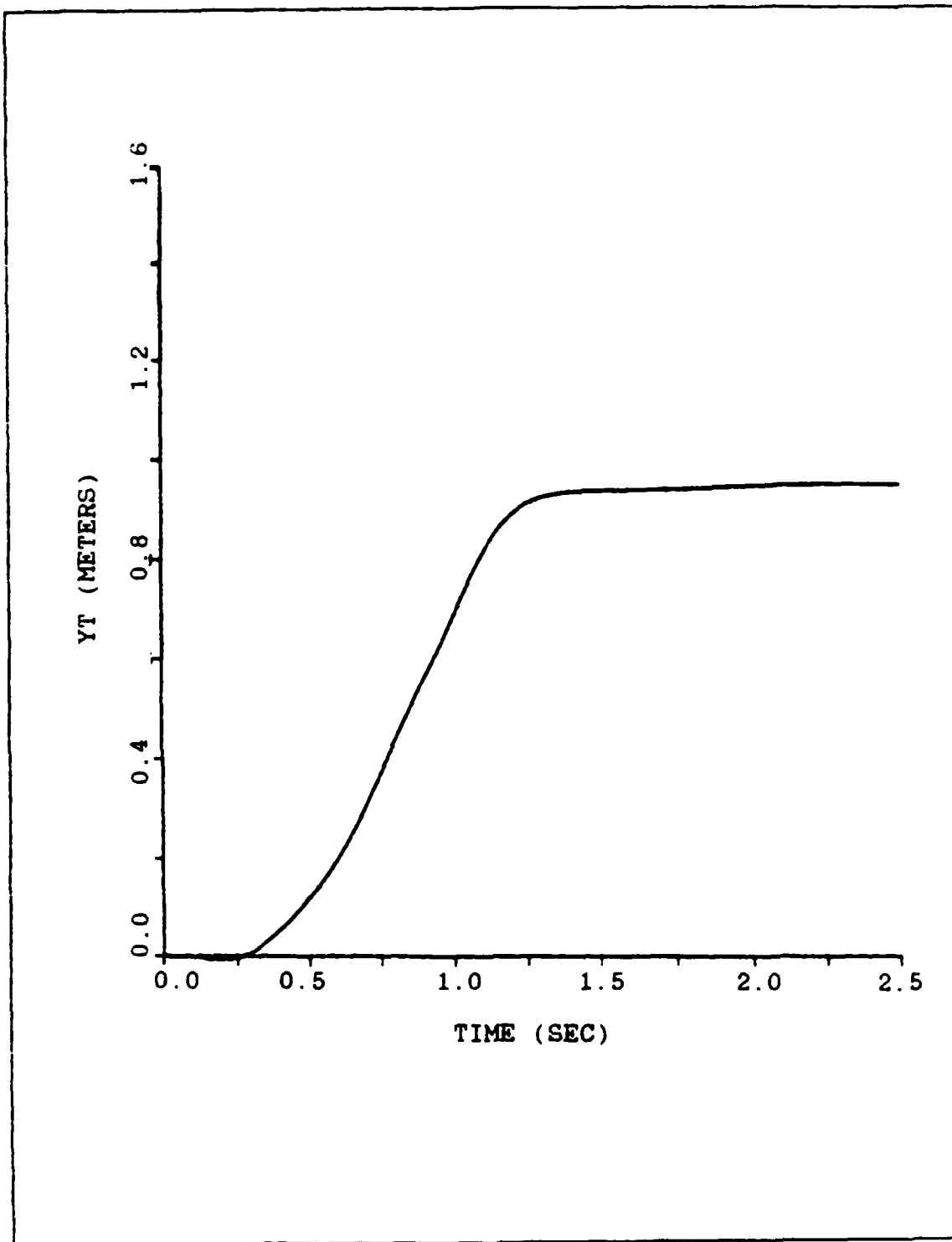


Figure 6.25 Tip Motion Using The System Shown In Figure 6.16  
With  $K_1 = 0.06$  (Large Motion).

Nevertheless, when the displacement is "small", there is no need to use the curve following scheme at all, because in this case there is no saturation problem for the motor. Therefore, we can use the system shown in Figure 6.16 for all applications, taking care to avoid the use of the curve following mode, when the commanded position is relatively small (of the order of  $5^\circ$  to  $10^\circ$ ).

## VII. EFFECT OF ARM'S STIFFNESS ON THE CURVE FOLLOWING SYSTEM

### A. INTRODUCTION

In the preceding chapters the control of a very flexible arm was studied, and we found that the most effective control scheme was the one given in section D of Chapter VI.

The use of a very flexible arm made the problem relatively difficult and from a theoretical point of view, it was a very good test for the various systems used. Due to the extremely high flexibility of the arm, we had to use the most complex and most demanding control scheme, whose design was based on optimal control theory. All simpler control schemes were found to be inappropriate for the control of the arm.

However as mentioned in earlier chapter, the arm used is 100 times more flexible than a "practical flexible" arm. It is therefore necessary to test our techniques on the case of that practical arm, and see if it is still necessary to employ such complex control schemes.

In the following the stiffness of the arm will be increased eventually. For each case the curve following system will be used, in order to see whether or not it can work effectively. When we arrive to the "practical flexible" arm (100 times stiffer), a simple linear regulator will be

used in combination with the velocity curve following system, for the final motion of the arm.

## B. BASIC THEORY OF ELASTICITY

Before we actually attempt to change the stiffness of the arm, it is considered necessary to have some understanding of what elasticity (or stiffness) means, and the basic physics behind it.

The measure of the stiffness of a material is given by the modulus of elasticity or the Young's modulus,  $E$ . This modulus describes the elastic deformation of a material subject to an applied stress. It tells us what stress we have to apply to the material in order to obtain a desired deformation, as long as the material is in its elastic region and has not plastically deformed. The higher the value of the Young's modulus the higher the stiffness of the material. The modulus of elasticity is related to the forces bonding the atoms in the material, and it is a property of each material. These bonding forces are higher for high density and high melting point materials.

Some indicative values of the modulus of elasticity are:

Magnesium (Mg)	(6.5)(10) <sup>6</sup>	psi
Aluminum (Al)	(10)(10) <sup>6</sup>	psi
Iron (Fe)	(30)(10) <sup>6</sup>	psi
Tungsten (W)	(58.9)(10) <sup>6</sup>	psi

We see that the modulus of elasticity varies over a large

range. The above values of E refer to pure metals. There exist many alloys with much higher E than the given values.

For the above materials the corresponding densities are as follows:

Magnesium (Mg)	1.74	g/cm <sup>3</sup>
Aluminum (Al)	2.9	g/cm <sup>3</sup>
Iron (Fe)	7.91	g/cm <sup>3</sup>
Tungsten (W)	19.25	g/cm <sup>3</sup>

If we compare the modulus of elasticity ratios, between these materials with the density ratios of the same materials, we find that they are almost equal. This means that the weight of a fixed size block of material (like an arm in our case), increases linearly with the modulus of elasticity.

From this result we see that a 50 times increase of the stiffness of the arm, means an increase of its weight by almost the same factor. This is not a favorable result, if we consider that in order to have a "practical flexible" arm, we must increase the stiffness, of the original arm, by a factor of 100.

Nevertheless, we can avoid the excess weight introduced by the change of the stiffness, by choosing appropriate geometrical shapes for the arm. For example, in the arm used in [Ref. 1], flexibility across the vertical plane was avoided by constructing the arm as a combination of two series of parallel vertical plates. If we were to place a

third series of plates, horizontally, between the two vertical ones, so that the final cross section of the arm was as the letter "H", we could increase the stiffness of the arm across the horizontal plane, without introducing so much weight. Depending on the motion the arm is designed to perform, in a real situation, a variety of geometrical shapes can be used, to reduce the flexibility of the arm in the direction of motion, and keep its weight as low as possible. It is therefore, not impractical to talk about stiffness reduction, since this does not necessarily mean an analogous weight increase. Having realized this fact we can now start changing the stiffness of the arm, and perform the tests for the curve following system, in each case.

#### C. CHANGE OF THE STIFFNESS OF THE ARM

The stiffness of the arm will be eventually increased until we reach the 100 times stiffer arm, which is considered to be a practical one. Intermediate stiffness will be used in order to see more clearly what is going on and how the stiffness affects the overall control scheme. Three different stiffness will be used. Namely, 20 times, 50 times and 100 times stiffer arms.

In Chapter II the mathematical model of the very flexible arm is given. [Ref. 1] states that the zeros and the complex poles of the transfer functions are proportional to the square root of the Young's modulus  $E$ . In order, therefore to

change the stiffness of the arm, we have to multiply all zeros and the complex poles, by the square root of the factor by which the stiffness is to be changed. Doing that the following transfer functions for the various stiffness result:

20 times stiffer arm - Hub transfer function:

$$\frac{\theta(s)}{T(s)} = \frac{46.321(s+0.49+j14.94)(s+1.3+j78.13)(s+3.9+j207.69)}{s(s+0.2)(s+0.76+j52.73)(s+1.79+j96.64)(s+3.22+j214.9)}$$

20 times stiffer arm - Tip transfer function:

$$\frac{Y_t(s)}{T(s)} = \frac{-2.177(s-53.84)(s+54.3)(s+100.1+j108.23)(s-96.24+j113)}{s(s+0.2)(s+0.76+j52.73)(s+1.79+j96.64)(s+3.22+j214.9)}$$

50 times stiffer arm - Hub transfer function:

$$\frac{\theta(s)}{T(s)} = \frac{46.321(s+4.88+j328.38)(s+2.05+j123.5)(s+0.78+j23.62)}{s(s+0.2)(s+1.2+j83.37)(s+2.83+j152.8)(s+5.1+j339.9)}$$

50 times stiffer arm - Tip transfer function:

$$\frac{Y_t(s)}{T(s)} = \frac{-2.177(s-85.1)(s+85.8)(s+158.3+j171.1)(s+152.2+j178.9)}{s(s+0.2)(s+1.2+j83.37)(s+2.83+j152.8)(s+5.1+j339.9)}$$

100 times stiffer arm - Hub transfer function:

$$\frac{\theta(s)}{T(s)} = \frac{46.321(s+1.1+j33.4)(s+2.9+j174.7)(s+6.9+j464.4)}{s(s+0.2)(s+1.7+j117.9)(s+4+j218.1)(s+7.2+j480.7)}$$

100 times stiffer arm - Tip transfer function:

$$\frac{Y_t(s)}{T(s)} = \frac{-2.177(s-120.4)(s+121.4)(s+223.8+j242)(s-215.2+j253)}{s(s+0.2)(s+1.7+j117.9)(s+4+j216.1)(s+7.2+j480.7)}$$

#### D. BASIC STUDIES OF THE STIFFER ARMS

As in Chapter II we again present here the results of some preliminary studies on the arms with different stiffness. These studies are intended to quantify our results and to reveal the basic characteristics of the arms. Also we will use them for the design of the linear regulator, that will be used in the case of the 100 times stiffer arm.

The results of these basic studies are shown in Figures 7.1 through 7.12 and they consist of the frequency and step response of each arm. For the derivation of these graphs the software package "CONTROLS" was used.

From comparison of the frequency response for each case, we see that the resonant frequencies are moving to the higher values by a factor equal to the square root of the factor by which the stiffness has been changed, as it was expected.

In the step response graphs we see the reduction of the oscillations as the stiffness is increased. In the tip's step response we still have a delay in the response of the tip of the arm of the order of 300 msec. Thereafter the tip moves initially towards the opposite direction than the desired and then it starts the desired motion.

It is clear that the arm maintains all the characteristic properties of the very flexible arm, even the most stiff one.

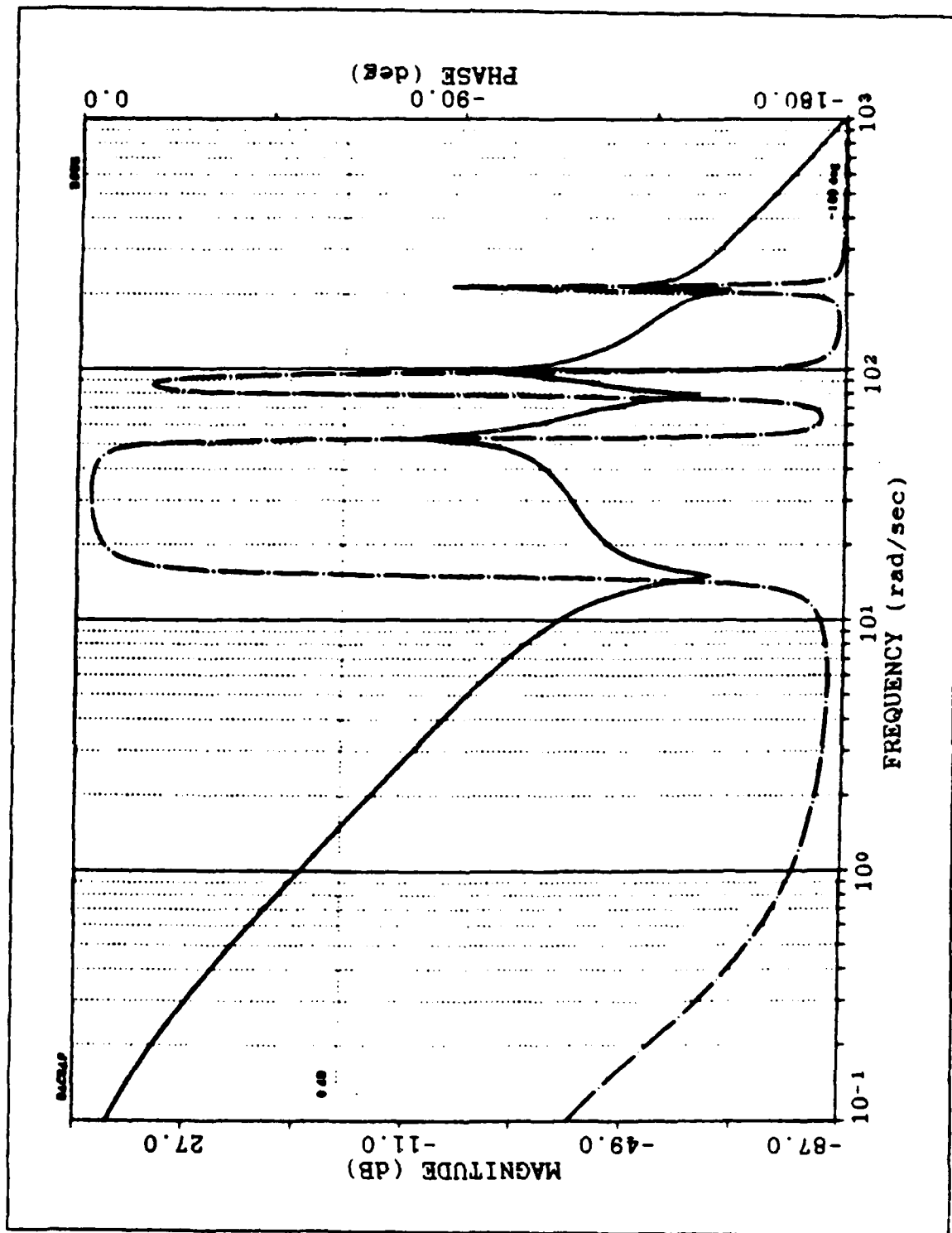


Figure 7.1 Open Loop Bode Plot Of The Hub Transfer Function Of The 20 Times Stiffer Arm.

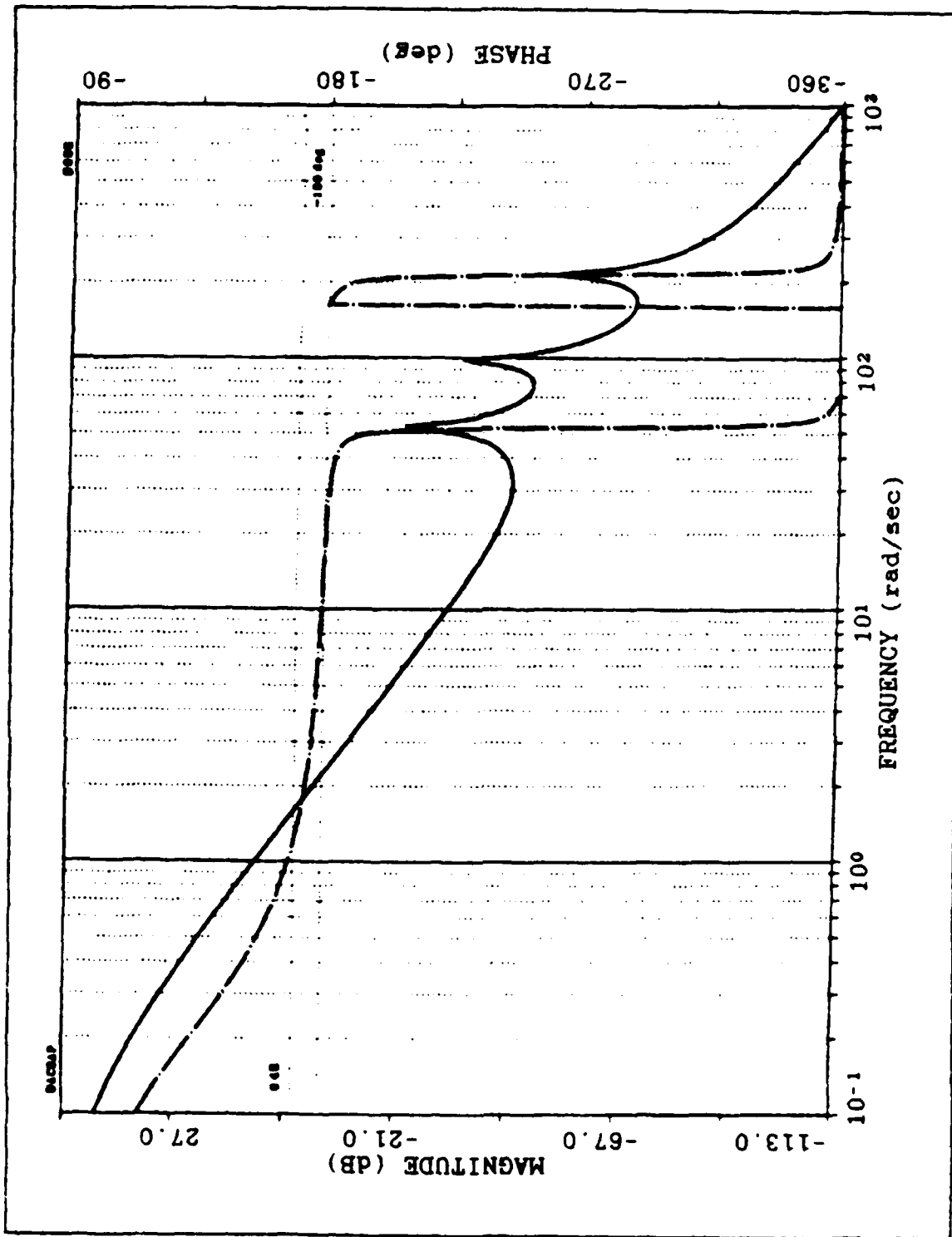


Figure 7.2 Open Loop Bode Plot Of The Tip Transfer Function Of The 20 Times Stiffer Arm.

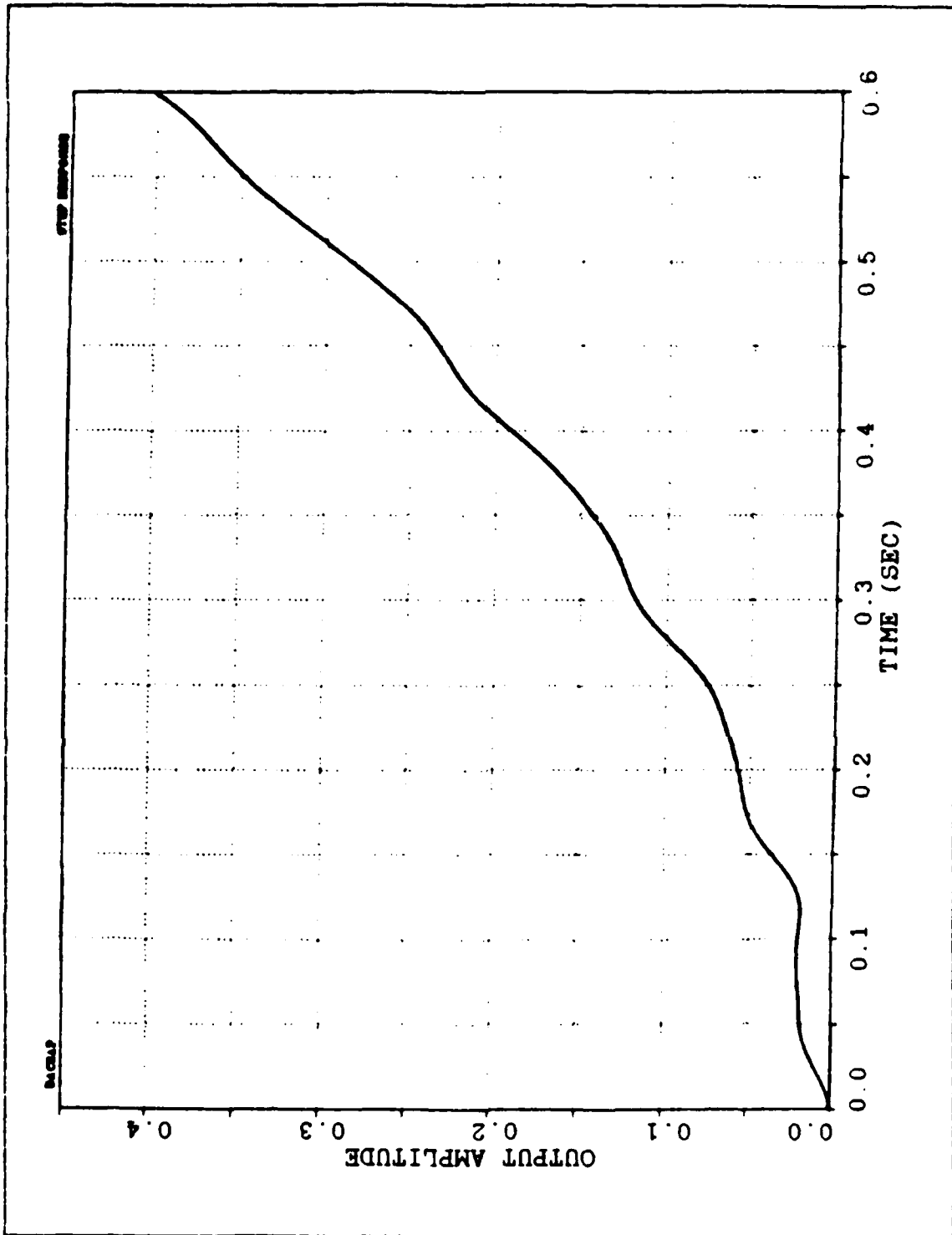


Figure 7.3 Step Response Of The Hub Transfer Function Of The 20 Times Stiffer Arm.

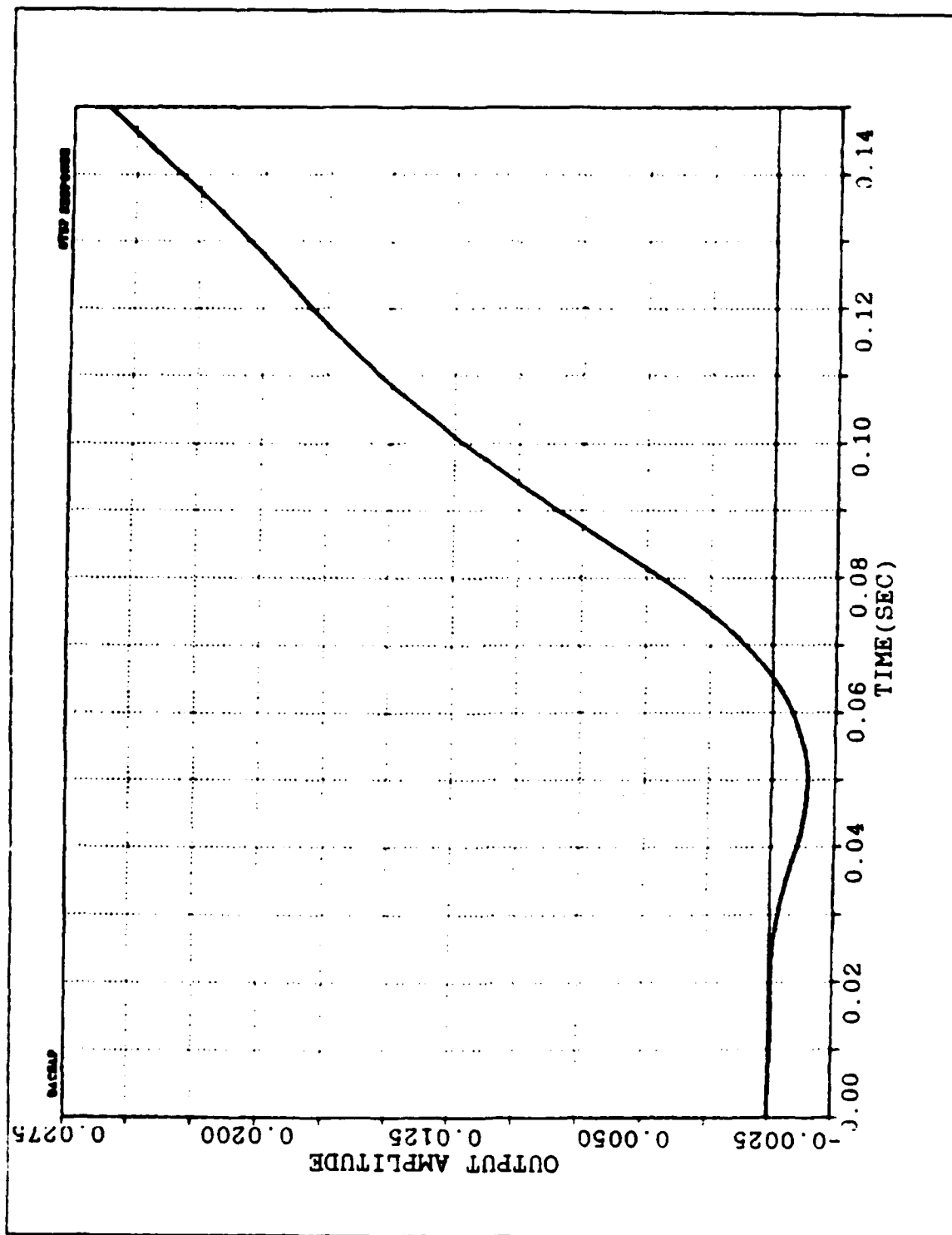


Figure 7.4 Step Response Of The Tip Transfer Function Of The 20 Times Stiffer Arm.

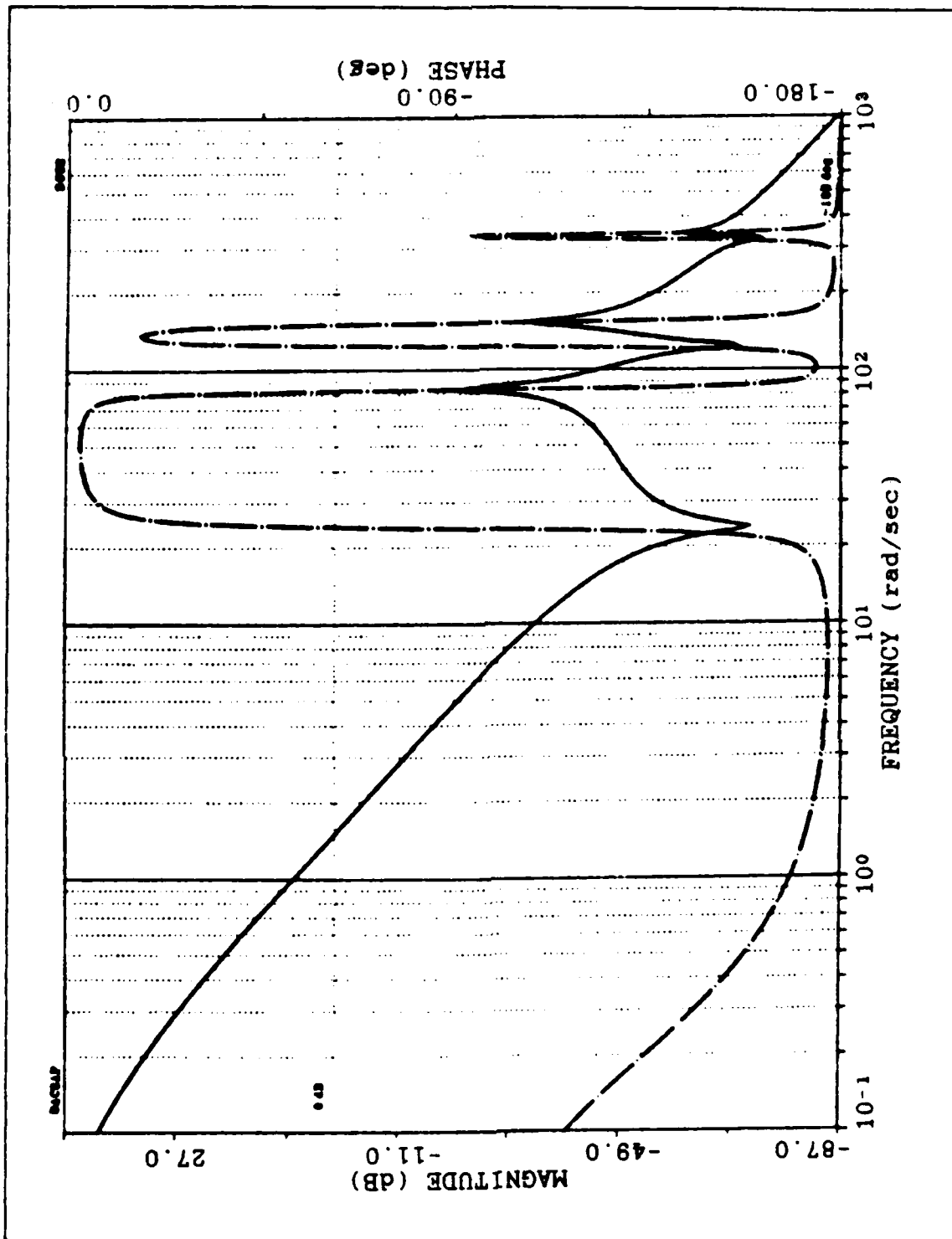


Figure 7.5 Open Loop Bode Plot Of The Hub Transfer Function Of The 50 Times Stiffer Arm.

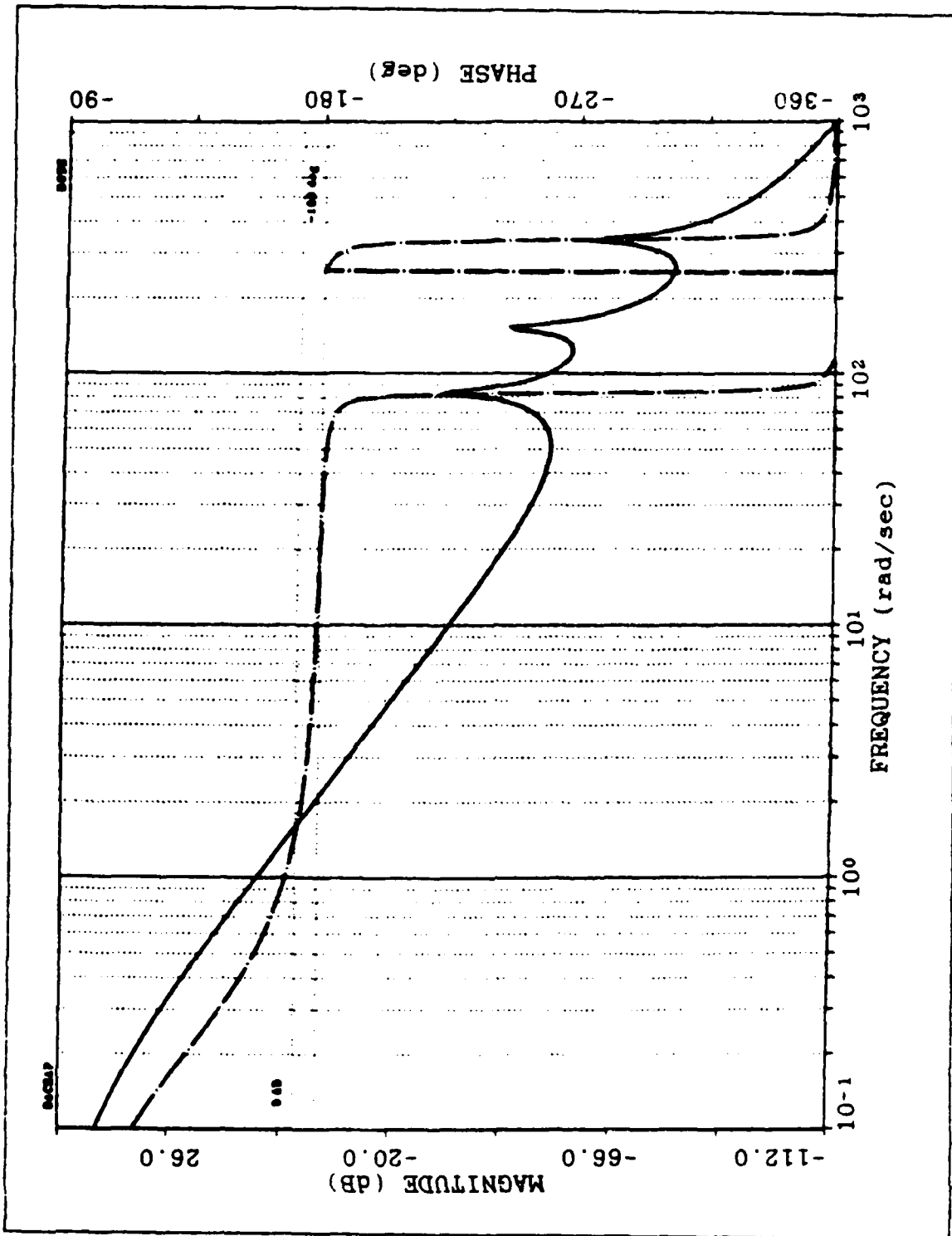


Figure 7.6 Open Loop Bode Plot Of The Tip Transfer Function Of The 50 Times Stiffer Arm.

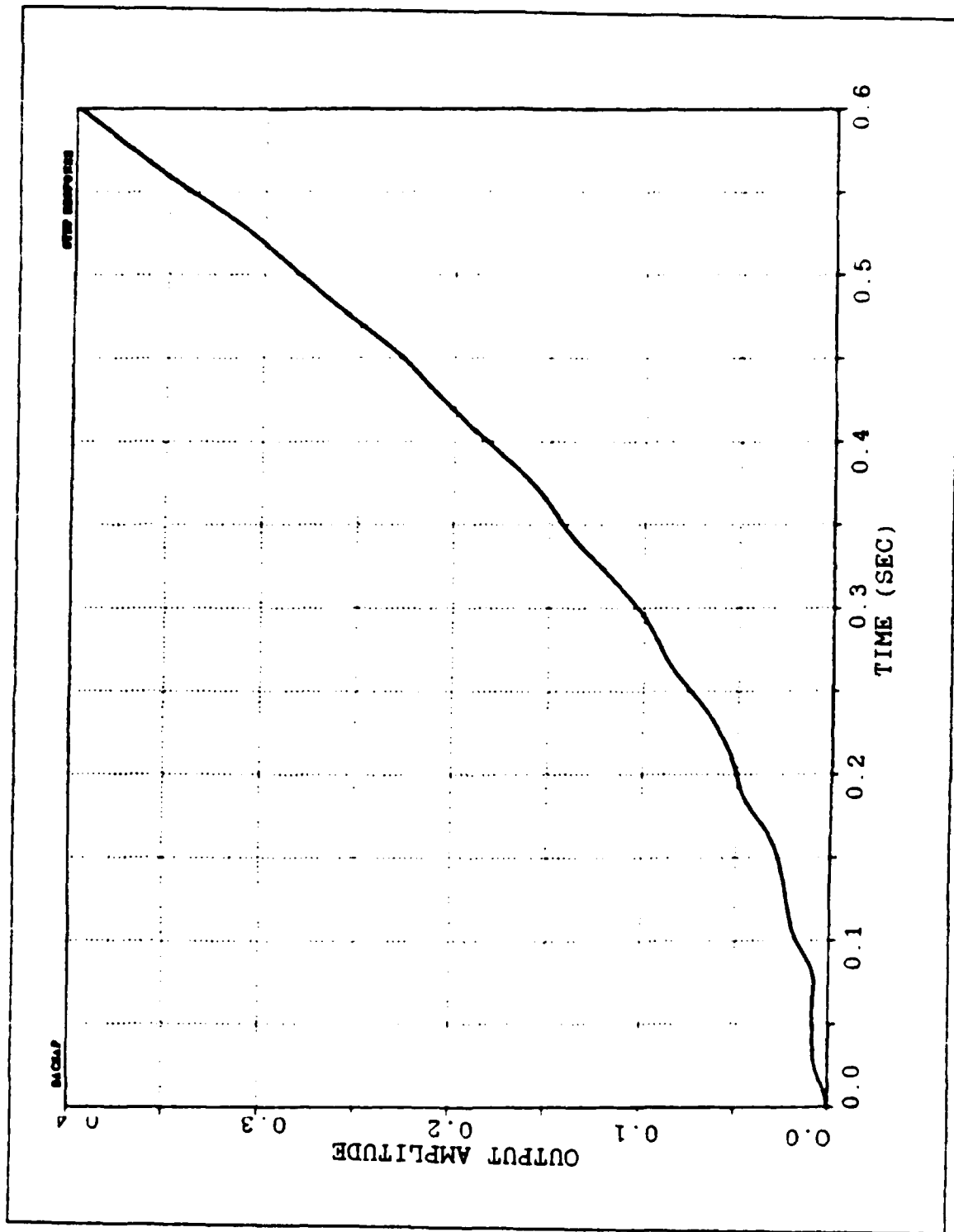


Figure 7.7 Step Response Of The Hub Transfer Function Of The 50 Times Stiffer Arm.

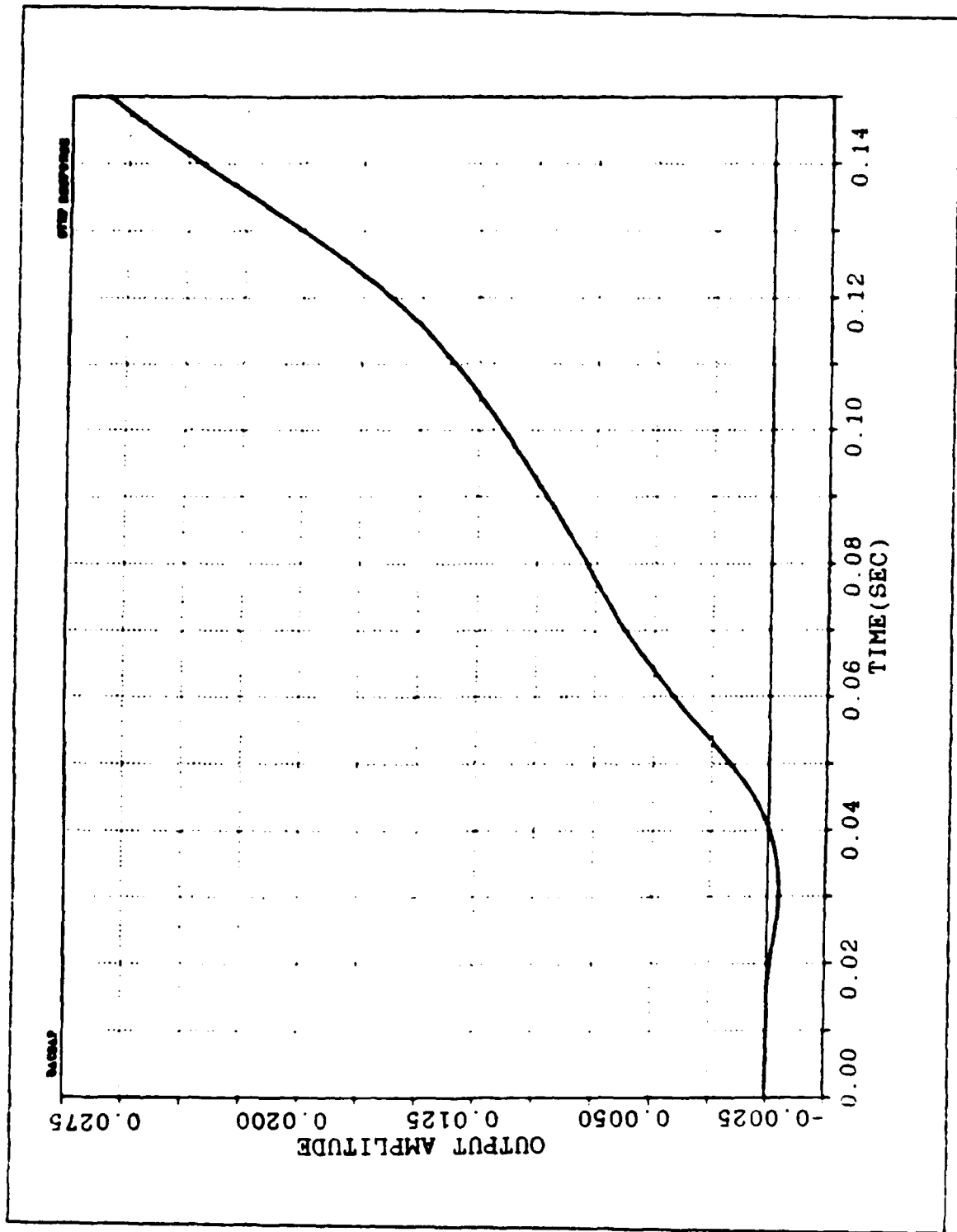


Figure 7.8 Step Response Of The Tip Transfer Function Of The 50 Times Stiffer Arm.

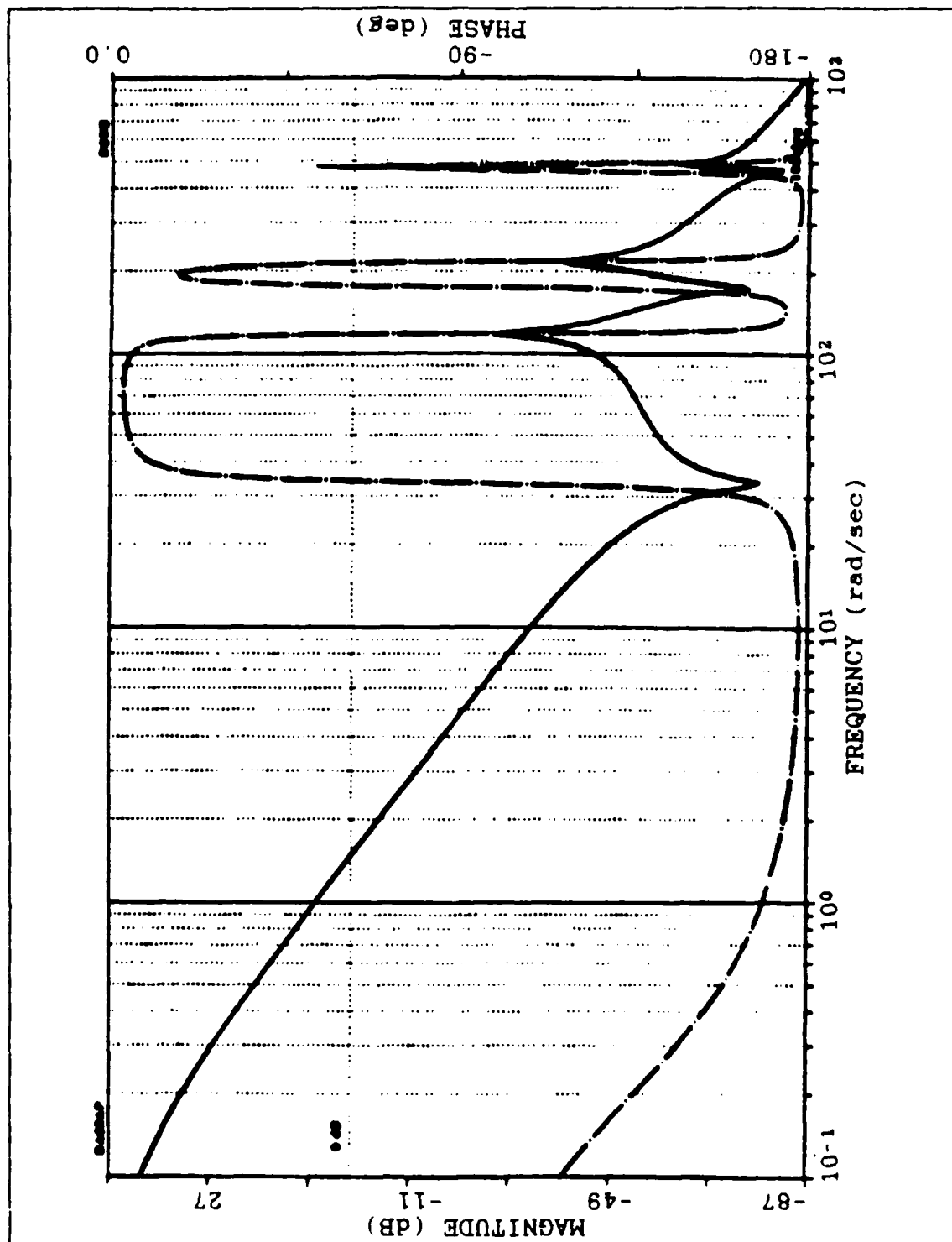


Figure 7.9 Open Loop Bode Plot Of The Hub Transfer Function Of The 100 Times Stiffer Arm.

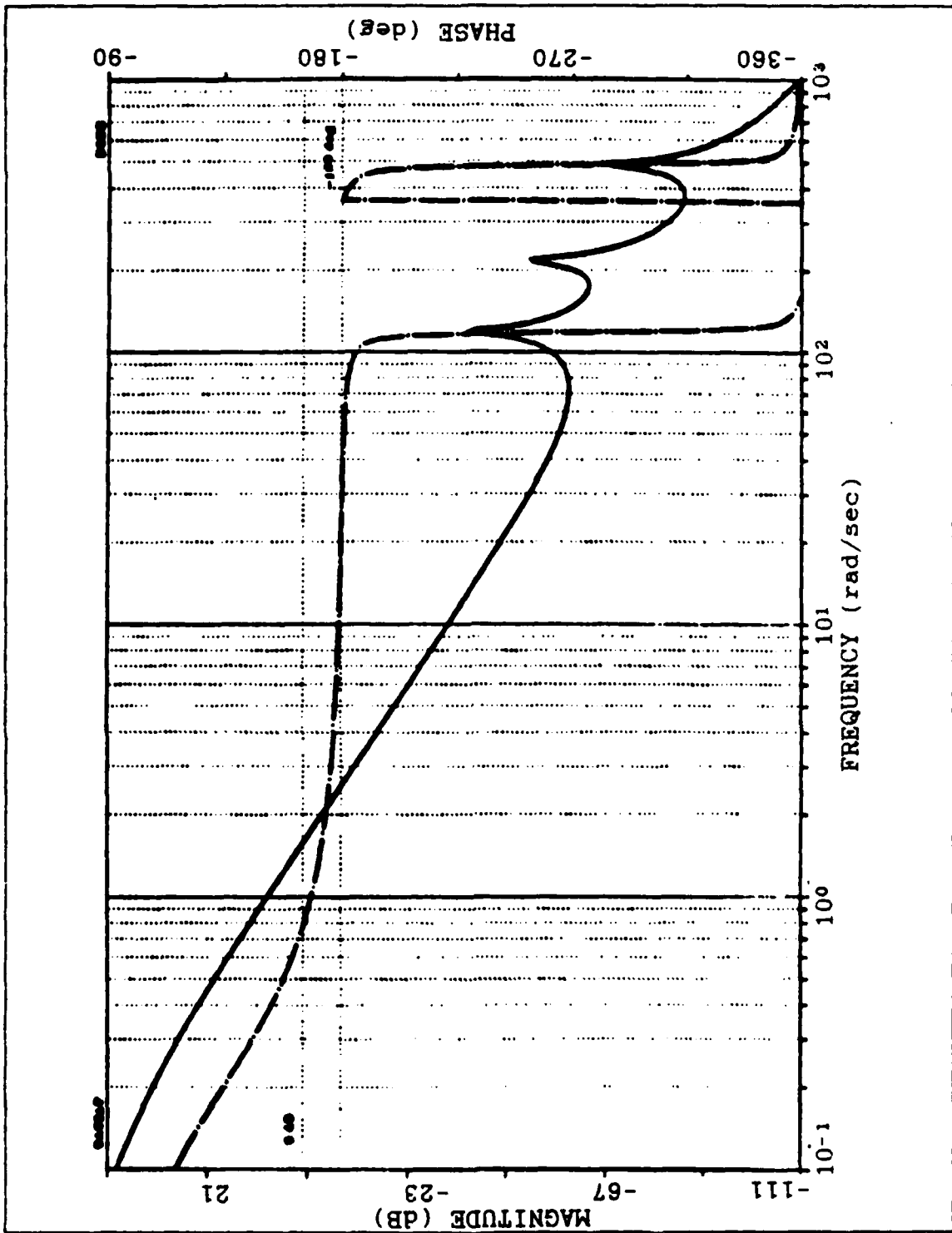


Figure 7.10 Open Loop Bode Plot Of The Tip Transfer Function Of The 100 Times Stiffer Arm.

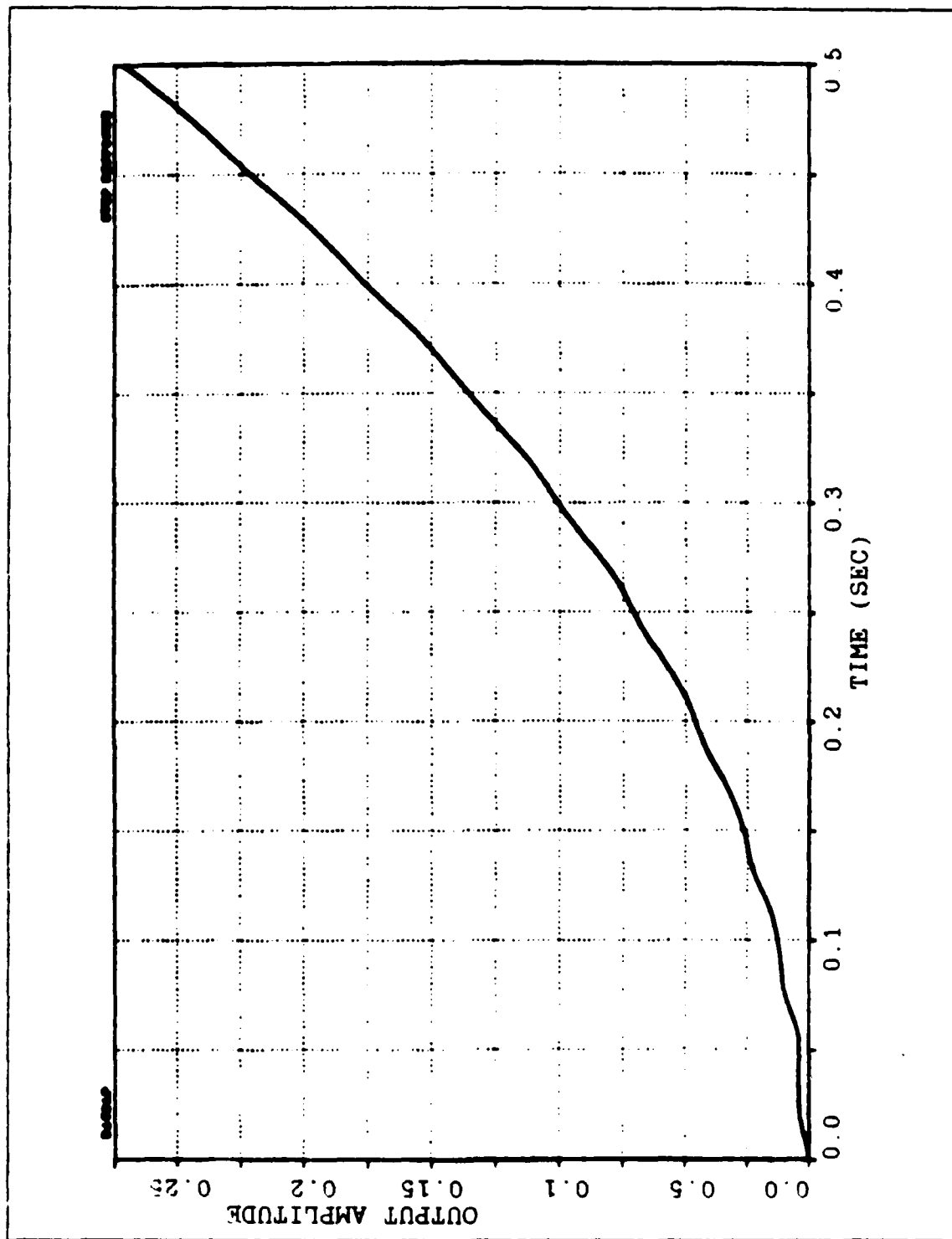


Figure 7.11 Step Response Of The Hub Transfer Function Of The 100 Times Stiffer Arm.

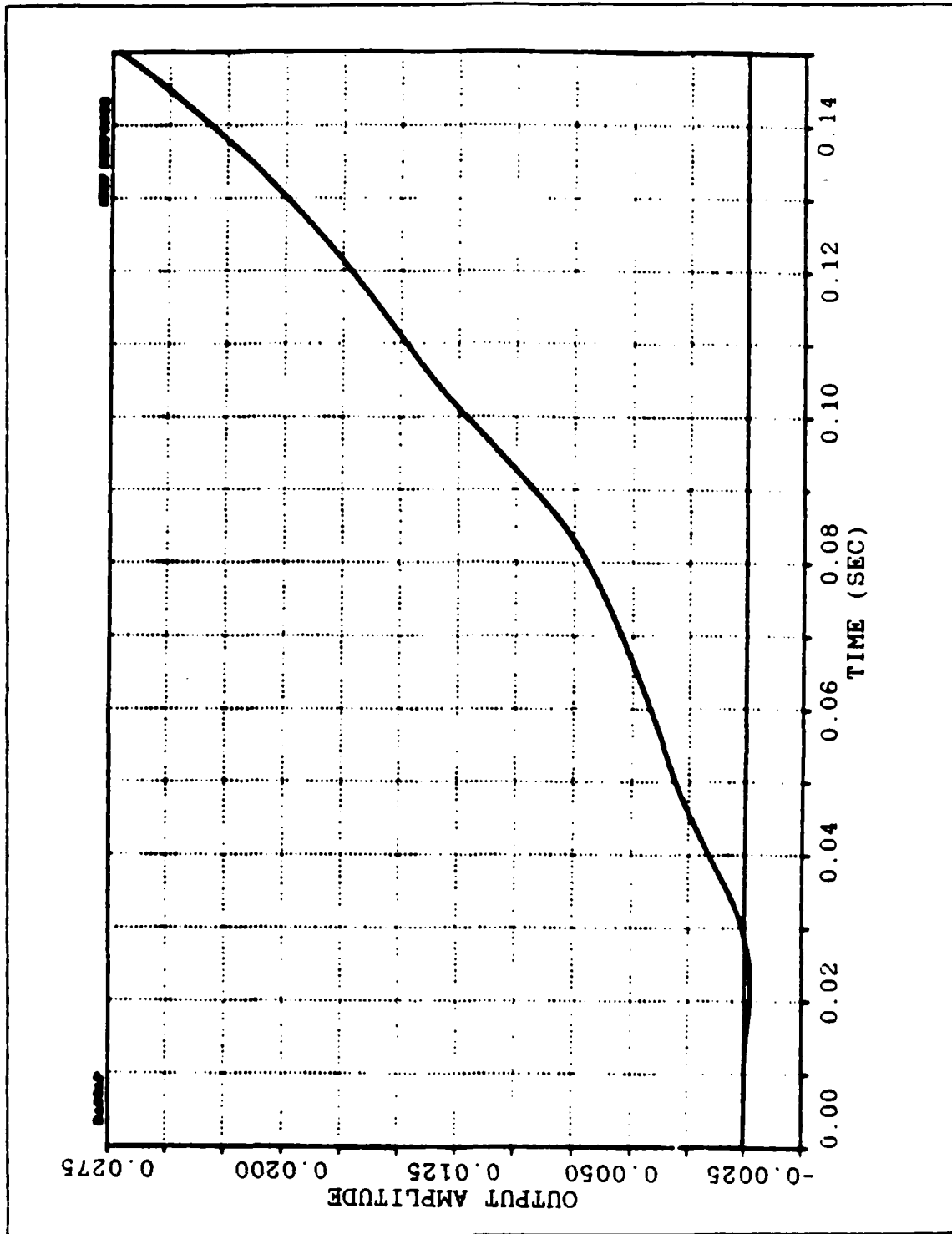


Figure 7.12 Step Response Of The Tip Transfer Function Of The 100 Times Stiffer Arm.

The only difference is that the intensity of these properties is being reduced as the stiffness is increased.

#### E. USE OF THE CURVE FOLLOWING SCHEME WITH THE STIFFER ARMS

The curve following scheme shown in Figure 4.10 was simulated using the DSL/VS programs shown in Appendices F through H with an arm of different stiffness in each case. The corresponding Hub and Tip motion for each case are shown in Figures 7.13 to 7.18. The time scale was intentionally left the same for all those figures in order to see more easily the resulting difference in the performance of the curve following system, as the stiffness of the arm is increased. For a more complete picture, the results presented in Figures 7.13 to 7.18 should be compared with Figures 5.8 and 5.9. From that comparison we see that the motion of the Hub is always excellent and is not affected by the change of the stiffness of the arm. The motion of the Tip, however, is dramatically improved as the arm is getting stiffer and stiffer. Especially in the case of the 100 times stiffer arm, the motion of the Tip is very nice and better than the motion shown in Figure 6.23 where the state feedback compensator was used for the final motion.

This is an encouraging result and indicates that the curve following system, whose advantages were outlined in Chapter IV, can be effectively used for the control of a "practical flexible" arm.

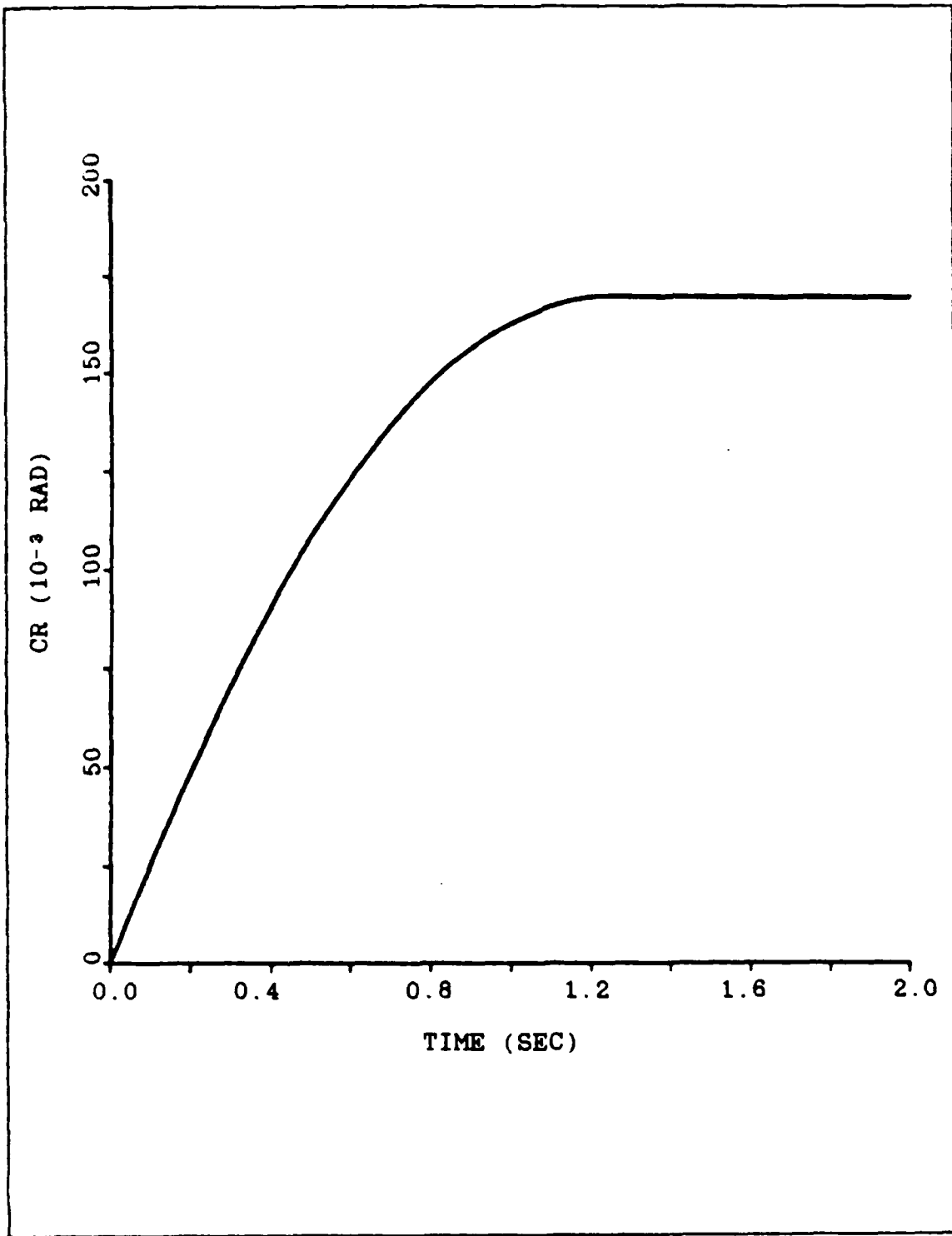


Figure 7.13 Hub Motion Of The 20 Times Stiffer Arm Using The Curve Following System.

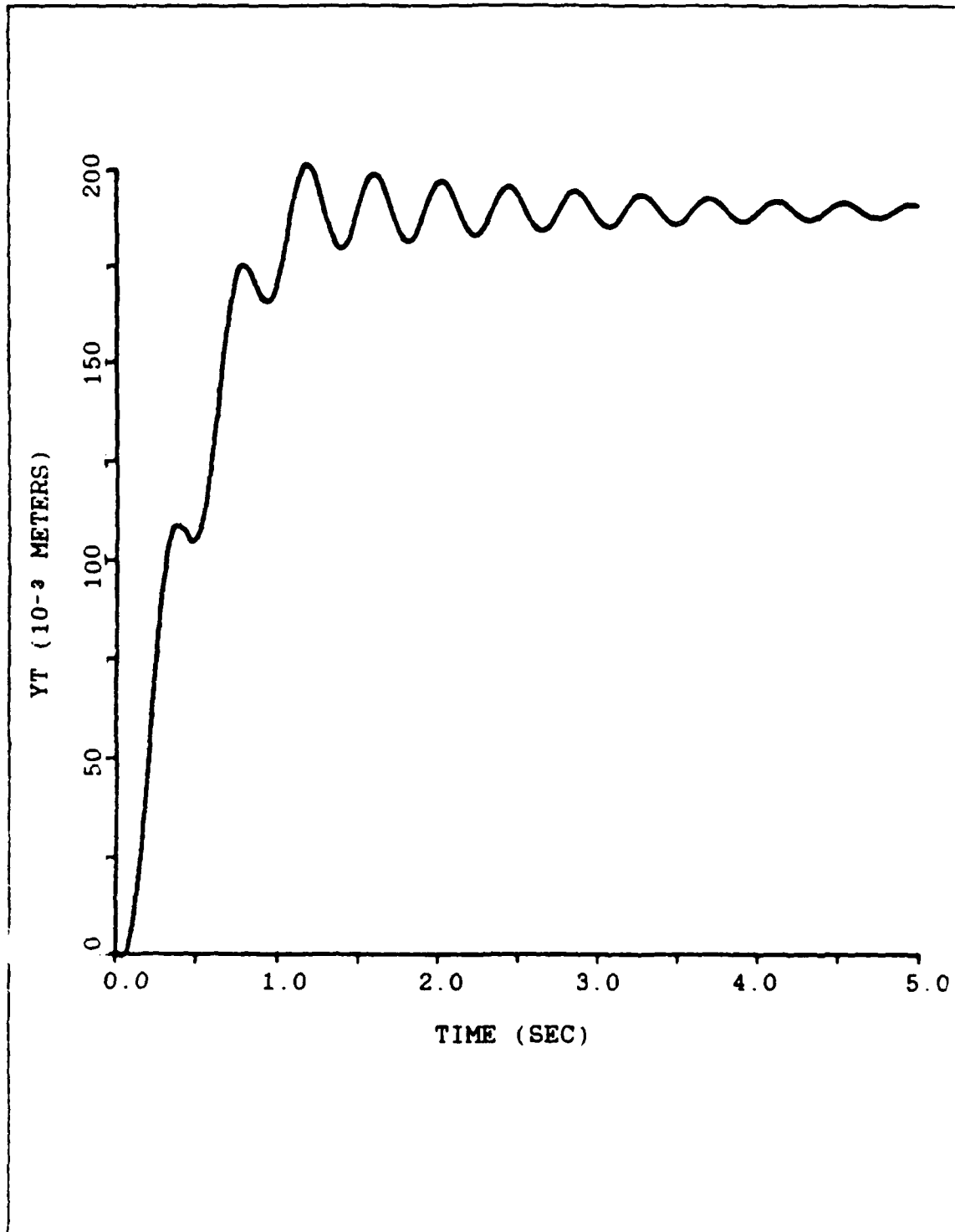


Figure 7.14 Tip Motion Of The 20 Times Stiffer Arm Using The Curve Following System.

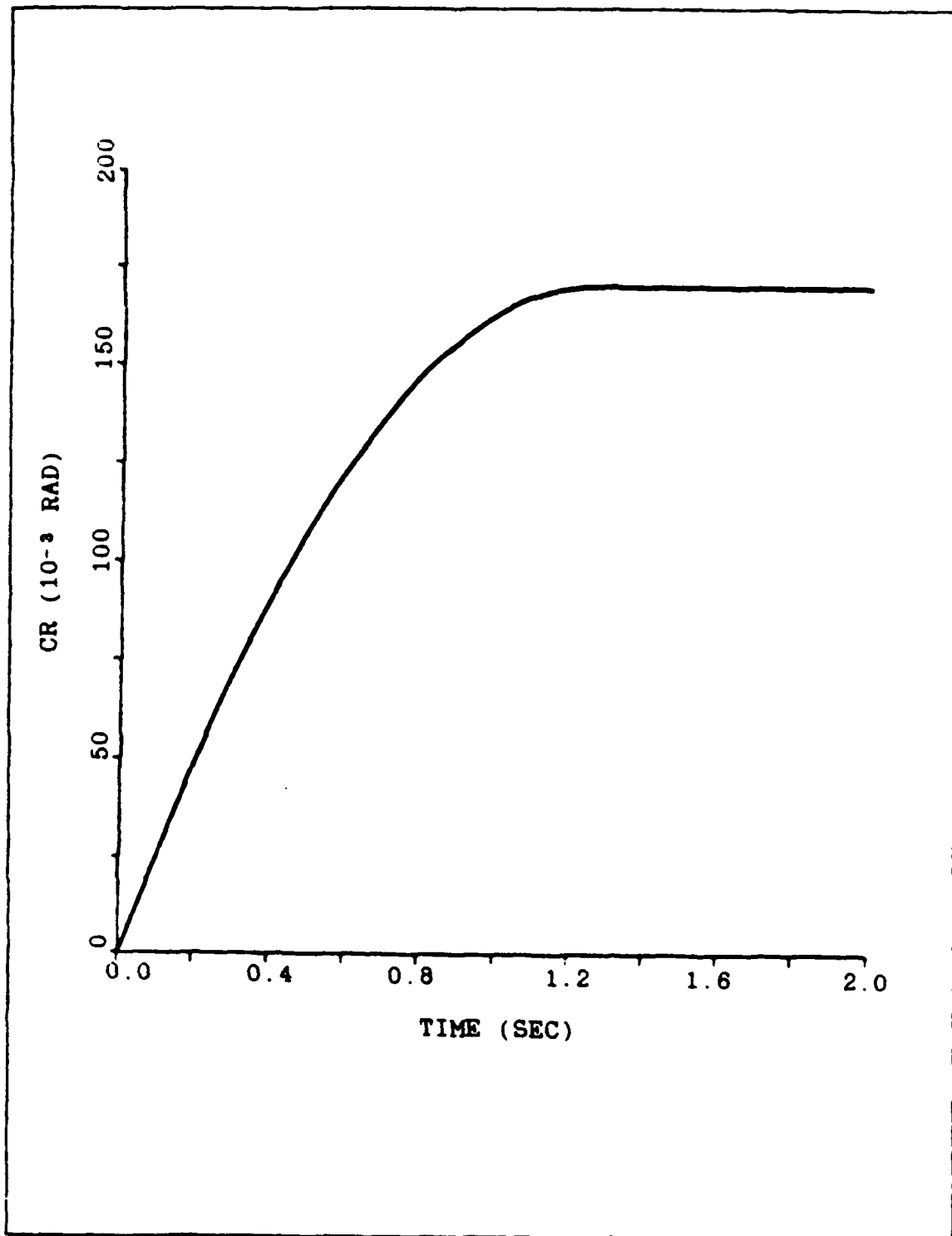


Figure 7.15 Hub Motion Of The 50 Times Stiffer Arm Using The Curve Following System.

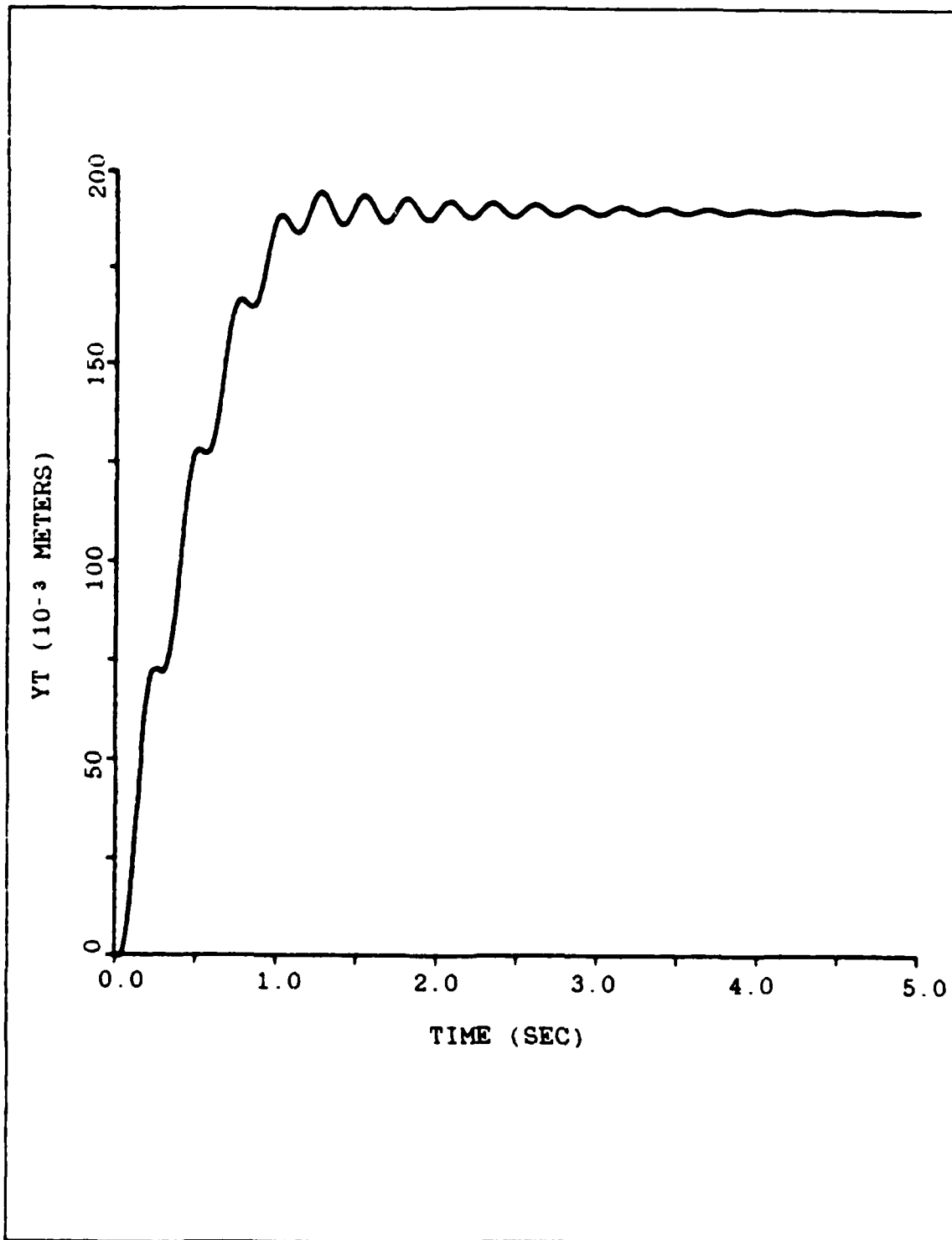


Figure 7.16 Tip Motion Of The 50 Times Stiffer Arm Using The Curve Following System.

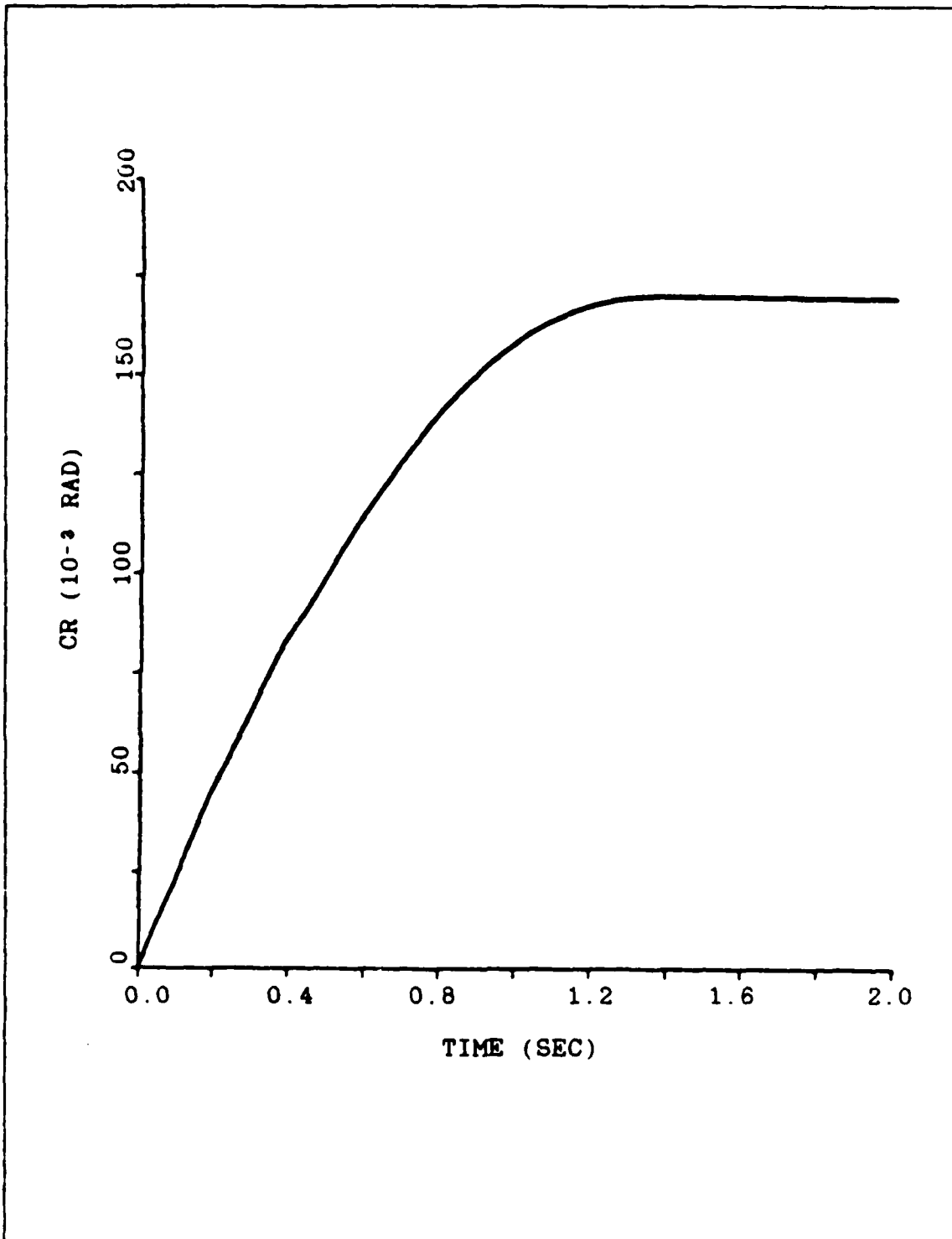


Figure 7.17 Hub Motion Of The 100 Times Stiffer Arm Using The Curve Following System.

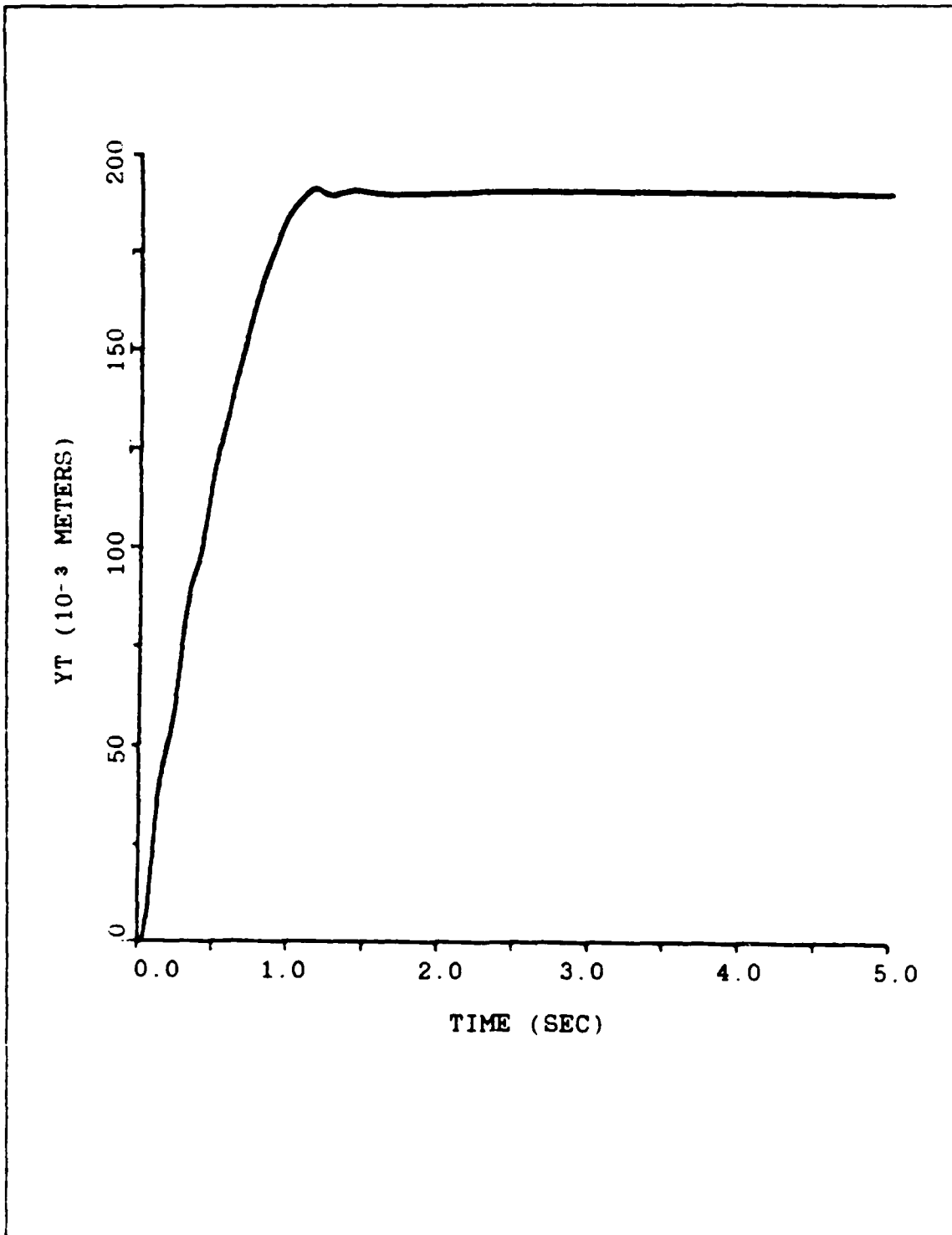


Figure 7.18 Tip Motion Of The 100 Times Stiffer Arm Using The Curve Following System.

#### F. LINEAR COMPENSATOR DESIGN FOR THE FINAL MOTION OF THE 100 TIMES STIFFER ARM

In section D of Chapter VI a state feedback compensator was used for the final motion of the very flexible arm. That compensator provided high damping so that the energy stored in the arm was dissipated, resulting in a good motion of the Tip of the arm.

In the case of the "practical flexible" arm, its natural damping is high enough, that dissipates the energy provided to the arm quickly, and the arm becomes more "controllable". However we need again a linear regulator for the final motion of the arm. Its purpose is not to provide damping to the system, but to switch off the curve following system and drive to zero any small remaining error.

As was explained in Chapter VI, the Tip position is the best feedback signal to be used with the linear regulator (in other words the loop of the linear system will be closed around the Tip).

The problem of designing the appropriate linear system in the case of the 100 times stiffer arm, is not difficult, since the resonant frequencies have now been moved to higher values as shown on Figure 7.10.

Classical control methods were employed for the design of the compensator to be used with the linear system for the final motion. The ultimate task of the design was to obtain the largest possible phase margin and the highest crossover frequency. After a trial-and-error process it was found that

the most effective compensator consists of two filters. One phase lead filter, whose transfer function is:

$$G1(s) = \frac{2s + 1}{0.005s + 1}$$

The second filter is a second order filter with transfer function:

$$G2(s) = \frac{1600}{s^2 + 72s + 1600}$$

These two filters were connected in cascade with the system, in a fashion similar to that shown in Figure 6.1. The arm will be first driven by the curve following system. When it reaches the commanded position the curve following system will be switched off and the arm will be left under the control of the linear regulator.

In the following the simulation results are presented. First, in Figure 7.19 the open loop Bode plot of the compensated linear system is shown. The phase margin is  $73^\circ$  and the crossover frequency 4 rad/sec. This phase margin corresponds approximately to a damping of 0.7, which is considered to be sufficient to keep the overshoot as low as possible. In Figure 7.20 the step response of the linear system is shown (tip motion). The motion of the tip is well damped and the overshoot is of the order of 4%. Finally in Figures 7.21 and 7.22, we see the resulting hub and tip

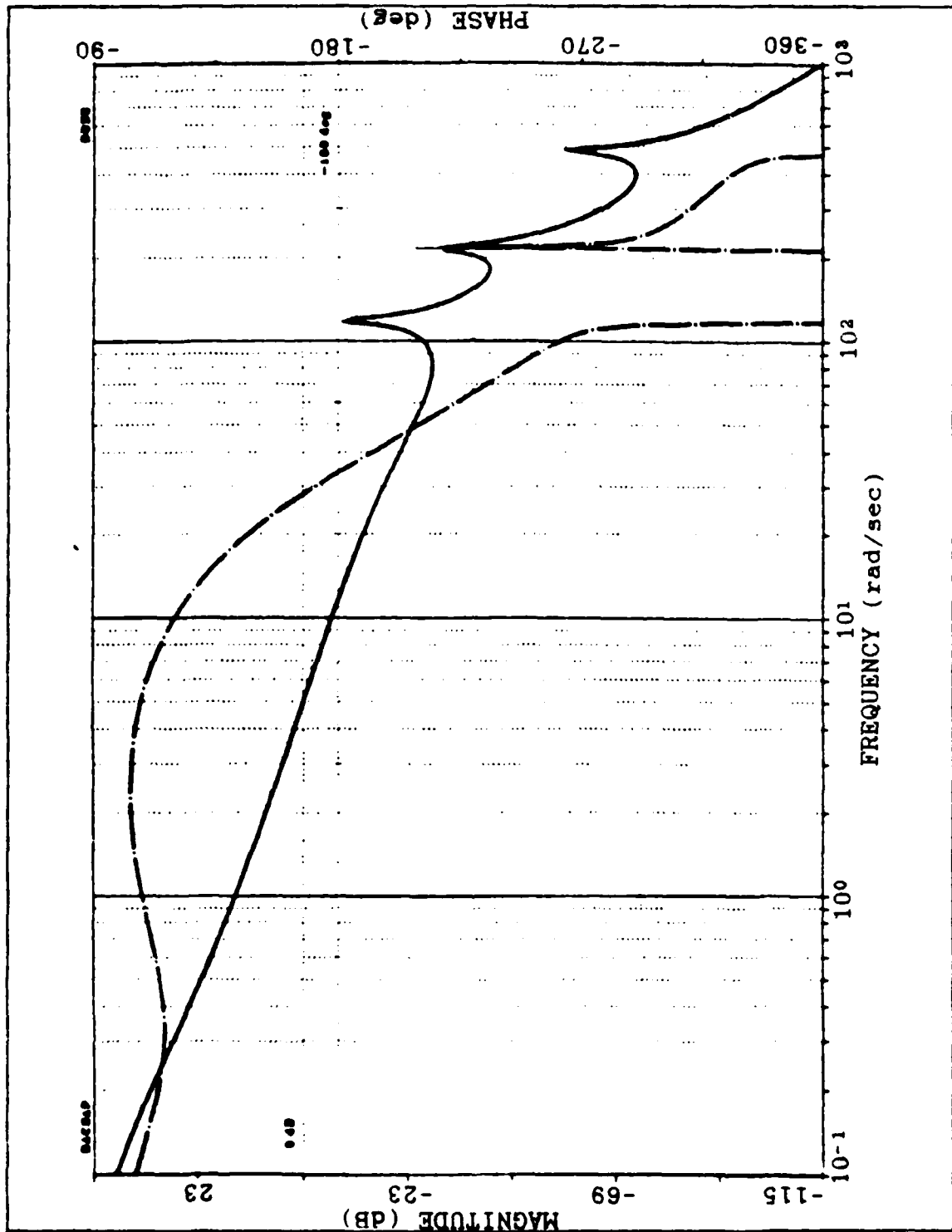


Figure 7.19 Open Loop Frequency Response Of The Linear System (Tip Feedback).

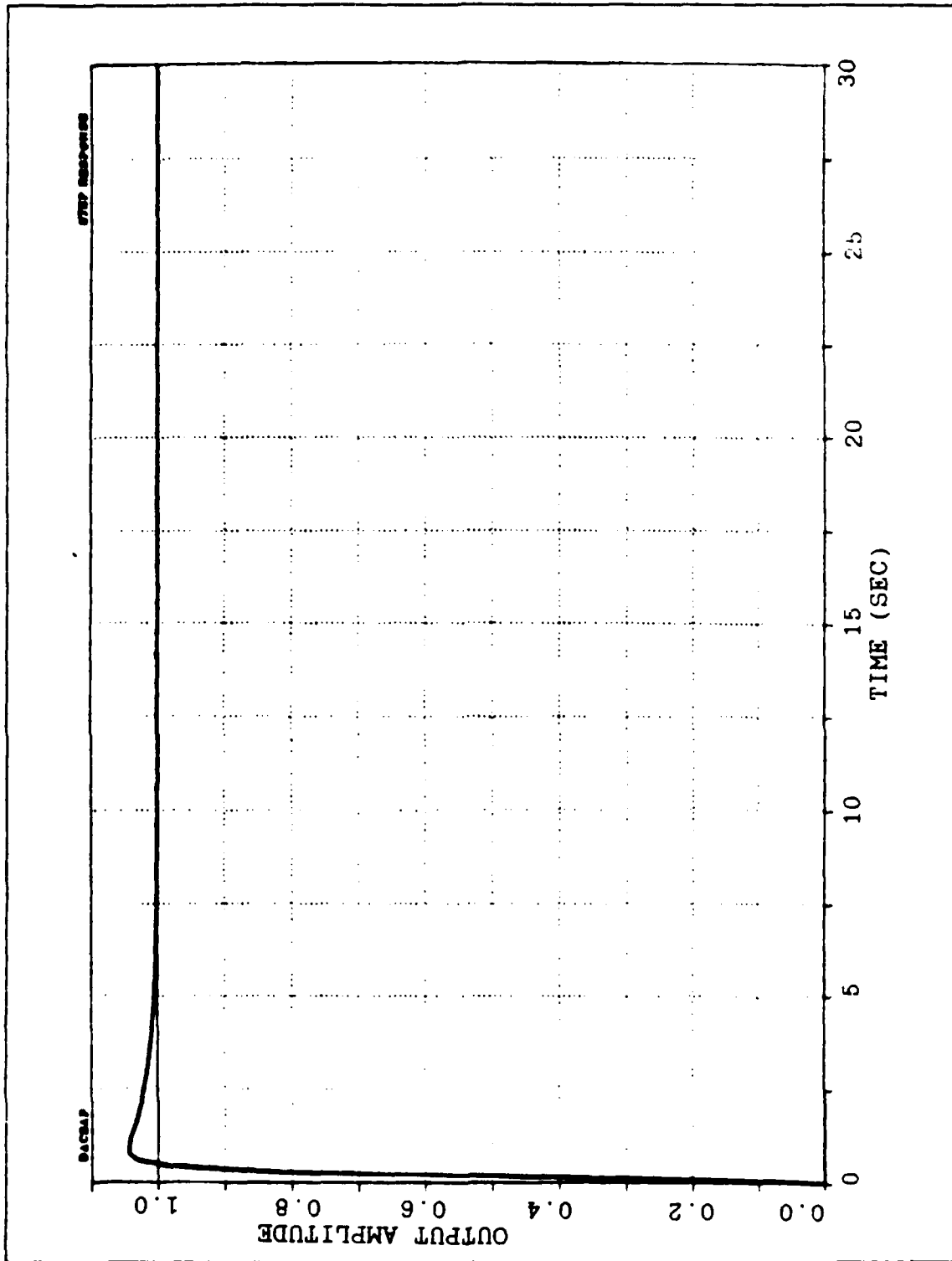


Figure 7.20 Step Response of The Linear System.

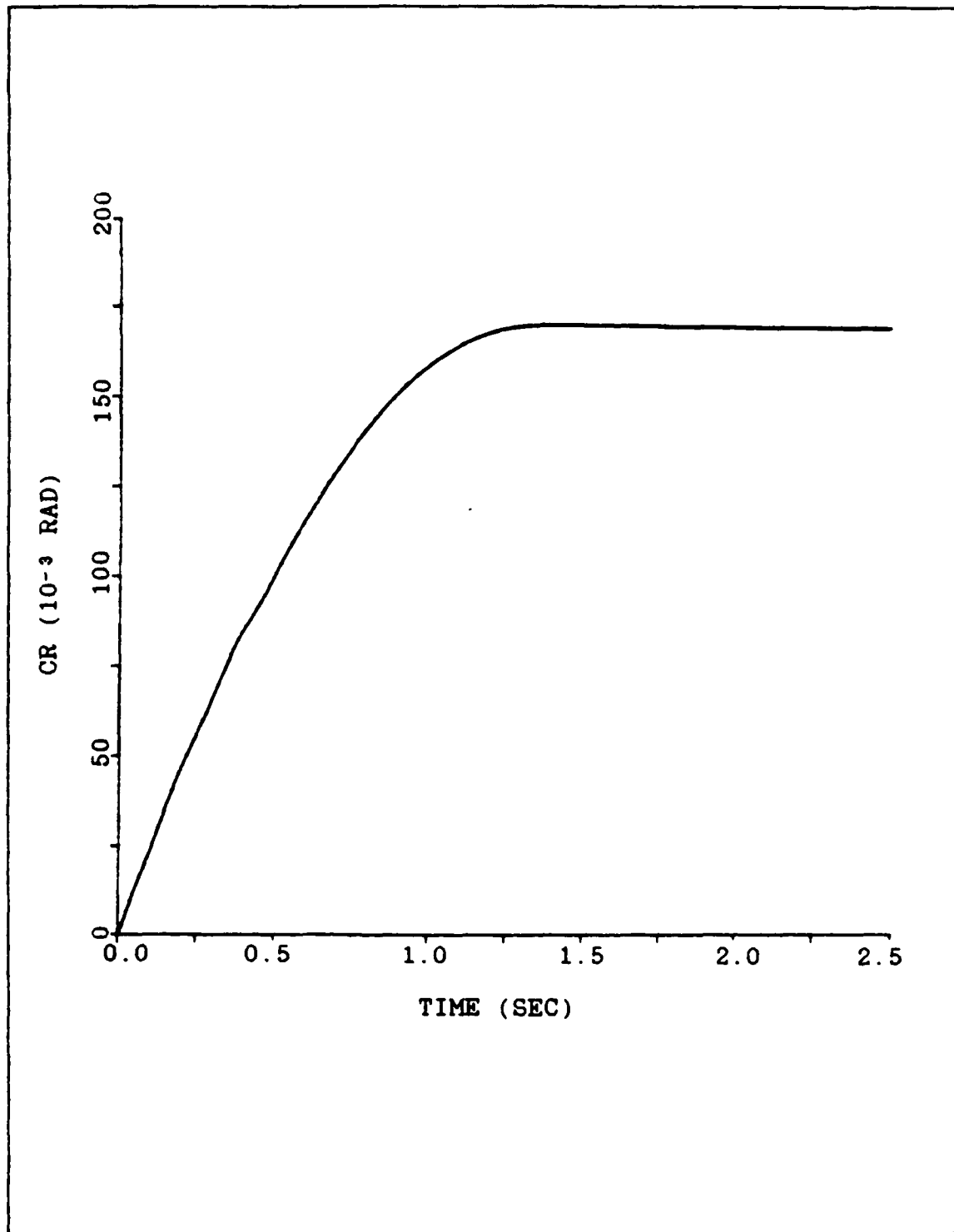


Figure 7.21 Hub Motion Using The Linear System For The Final Motion.

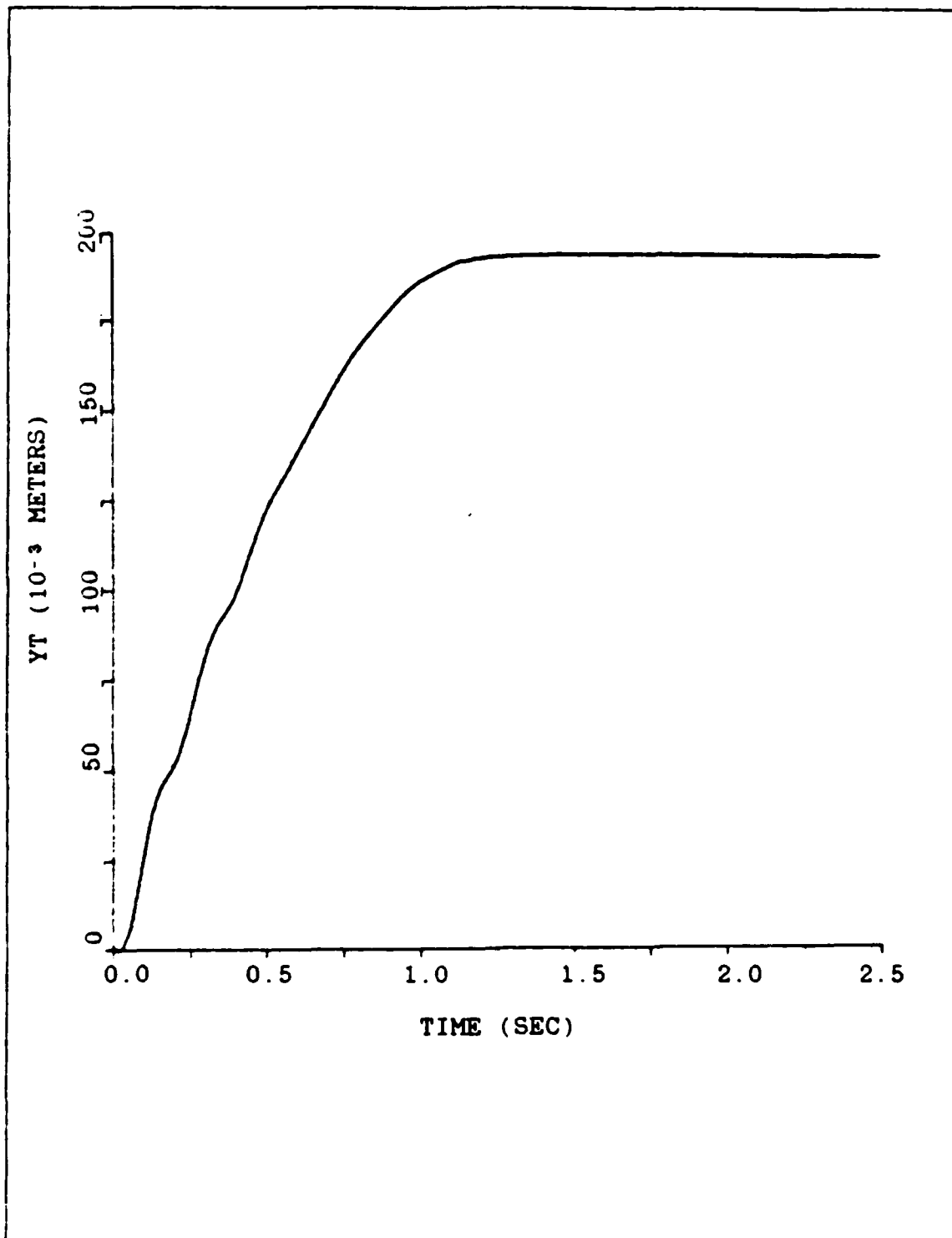


Figure 7.22 Tip Motion Using The Linear System For The Final Motion.

motion from the simulation of the system shown in Figure 6.1, where the appropriate transfer functions derived above have been substituted. The DSL/VS program used for this simulation is given in Appendix I. From Figure 7.22 we see that the motion of the tip is excellent and the oscillations that are shown in Figure 7.18, where the curve following system was used alone, have been completely eliminated.

This result leads us to the conclusion that the curve following system with the aid of a simple linear regulator, can be very effectively used for the control of a "practical flexible" arm.

## IIX. FLEXIBLE ARM WITH TIP LOAD

### A. OVERVIEW

In the preceding chapters, we studied in detail the case of an unloaded arm. We started with a very flexible arm, and we applied numerous techniques for its control. We saw that the problem is by no means trivial, and the employment of a very flexible control scheme, in section D of Chapter VI, was necessary, in order to achieve an acceptable motion of the tip of the arm.

Consequently the stiffness of the arm was changed, until we reached the 100 times stiffer arm, which is considered as a "practical flexible" arm. The control problem in that case was easier and the curve following system, with the aid of a very simple linear regulator, was sufficient to give us very good results.

The story, however, does not stop here. A big step towards the control of a flexible arm has been made, but what happens when the arm carries a tip load? Will our control schemes, derived for the unloaded arm, work as well when load is added?

These questions will be answered in the present chapter. We will start again with the case of the very flexible loaded arm and we will use the best control scheme, found for the unloaded arm. After that, we will change the stiffness of the

loaded arm, increasing it by 100 times, and we will use the control scheme which was applied in Chapter VII, where the arm (100 times stiffer) was unloaded.

#### B. VERY FLEXIBLE LOADED ARM

In Chapter II the transfer function of the very flexible loaded arm is given. The arm carries a load of 0.229 Kg, which is about half the mass of the arm. This load is arbitrary, and therefore, any conclusion drawn for this case, can be generalized for any load. Also, the load of 0.229 Kg, represents a big load for the arm, considering its mass (0.686 Kg). This is good, because we will test our system in extreme operating conditions.

Preliminary studies on the transfer function of the flexible loaded arm, are presented in Figures 3.3, 3.4, 3.7 and 3.8. The most important observation from Figures 3.3 and 3.4 is that the crossover frequency as well as the resonant frequencies have been moved to the left by 0.4 rad/sec, compared with the ones of the unloaded arm.

This loaded flexible arm, was "connected" to the curve following scheme, shown in Figure 4.10, and simulated using the DSL/VS program listed in Appendix B, having previously substituted the new transfer function. The motion of the tip was recorded for two different values of  $K_1$ . The first value was  $K_1=0.06$ , the same as the one used for the unloaded arm. The second value was  $K_1=0.02$ . The results are shown in

Figures 8.1 and 8.2 respectively, for the tip motion. In Figures 8.3 and 8.4 we see the hub motion for the above values of  $K_1$ .

The hub motion in both cases is excellent. Therefore the curve following system is not affected by the change of the tip load, as far as the hub motion is concerned. The tip motion, however, is unacceptable as it was in the case of the unloaded arm also. Certainly we should not hope for anything better.

The best control scheme, found for the case of the unloaded arm, will be used to "shape" the tip motion of the loaded arm. This scheme is shown in Figure 6.16. We must recall here, that the feedback compensator, used with the linear regulator for the final part of the motion, in Figure 6.16, was designed using the unloaded arm, employing optimal control theory. This compensator consists of a lead double-lag network and two notch filters. The notches of the filters are placed exactly at the frequencies of the first and second vibration mode of the unloaded arm. In the case of the loaded arm, where the vibration modes have been moved to the left by 0.4 rad/sec, we must expect poor results. This is shown in Figures 8.5 through 8.7 for  $K_1=0.06$ . In Figure 8.5 the hub motion is shown and in Figures 8.6 and 8.7 the tip motion (small and large displacement respectively).

Even though the motion of the tip has been dramatically improved, compared with Figure 8.1, it is not as good as it

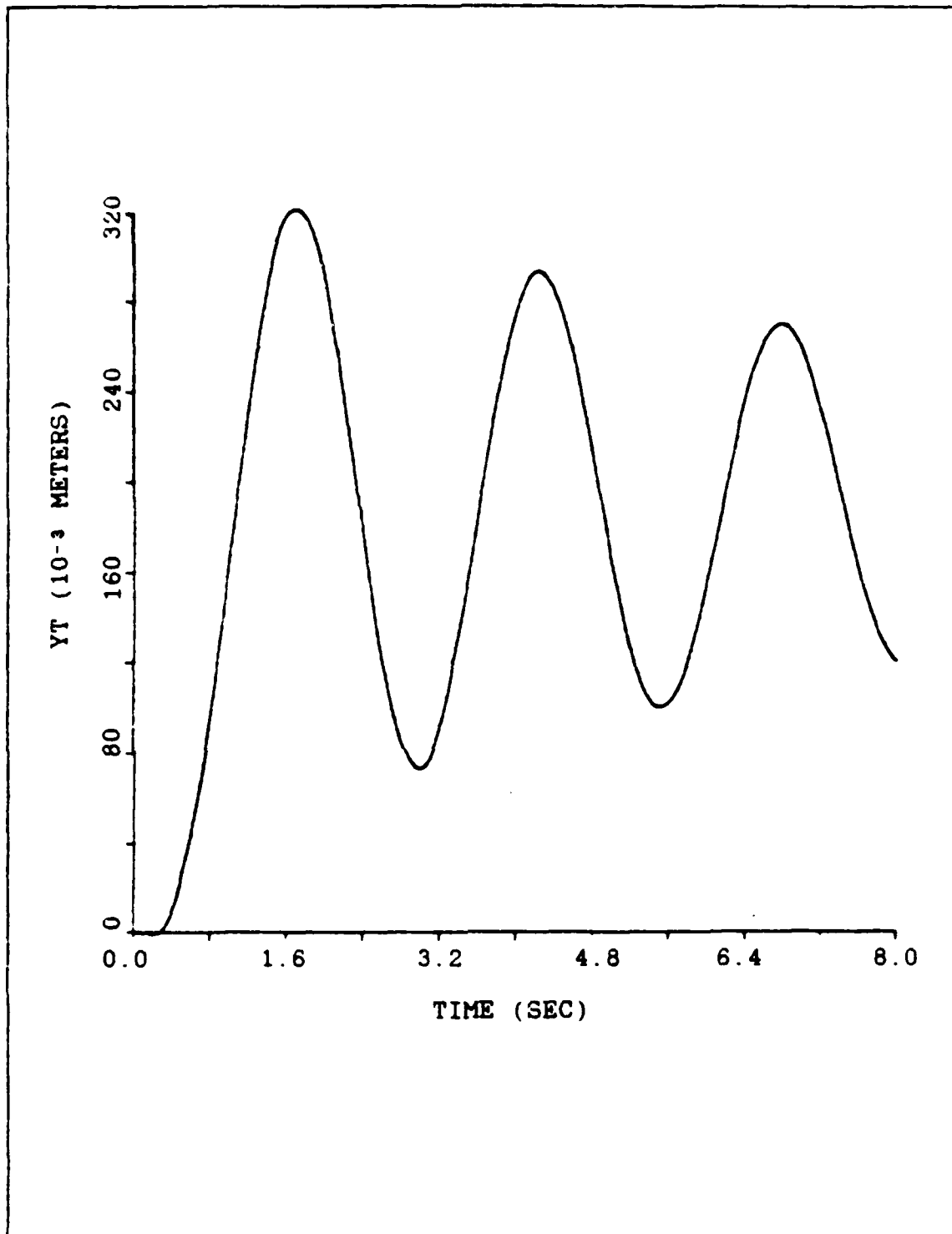


Figure 8.1 Tip Motion Of The Loaded Arm Using The Curve Following System Alone ( $K_1=0.06$ )

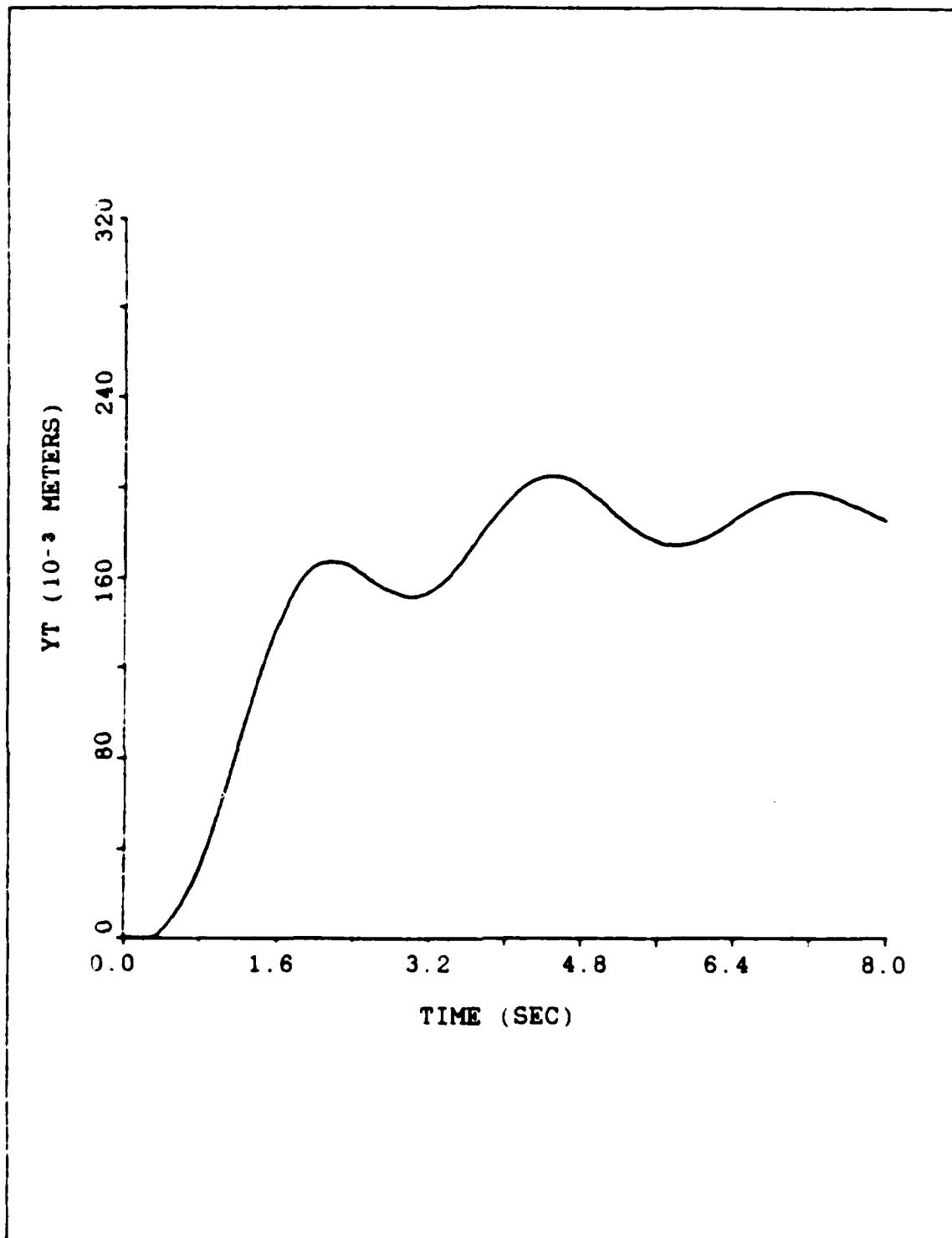


Figure 8.2 Tip Motion Of The Loaded Arm Using The Curve Following System Alone ( $K_i=0.02$ )

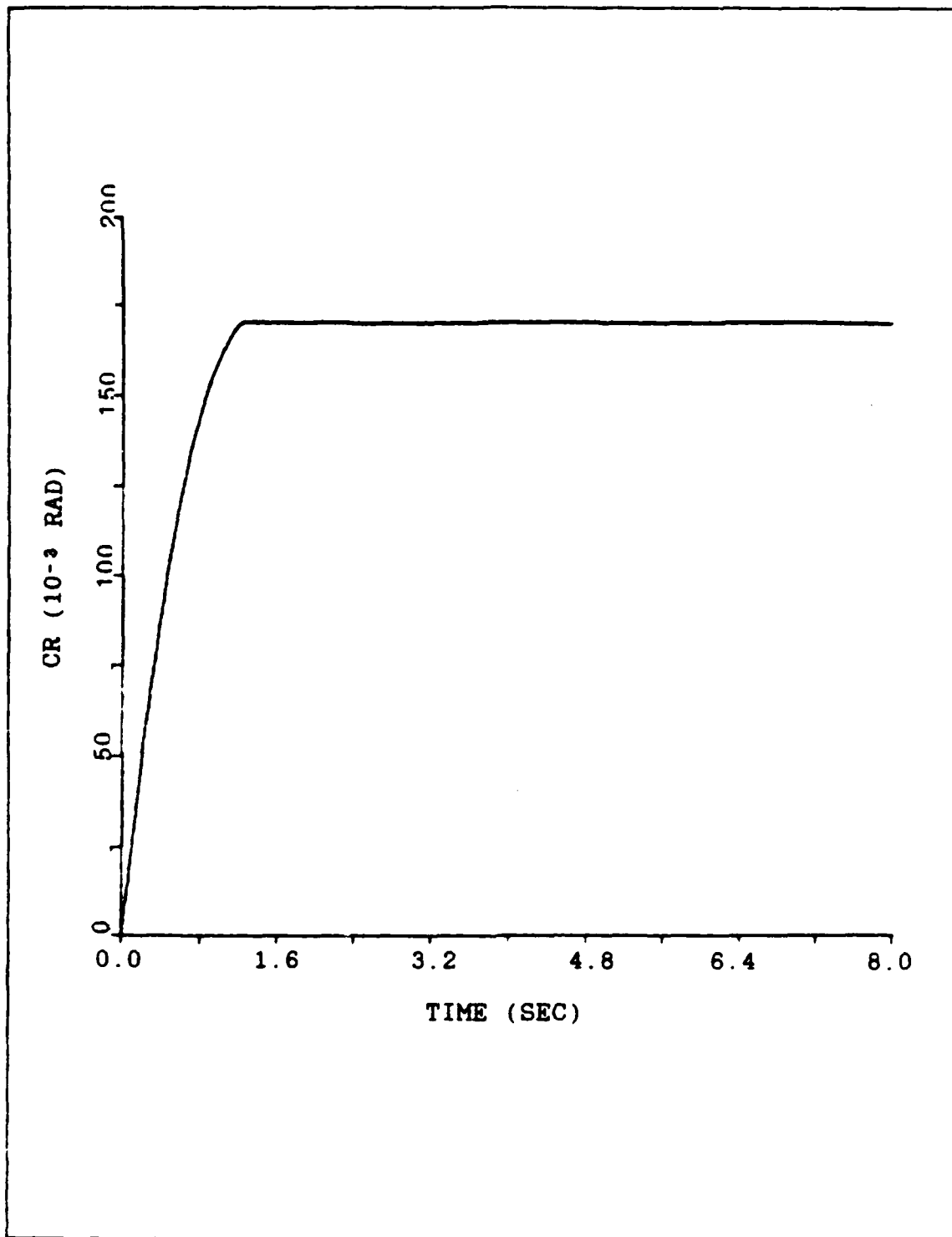


Figure 8.3 Hub Motion Of The Loaded Arm Using The Curve Following System Alone ( $K_1=0.06$ )

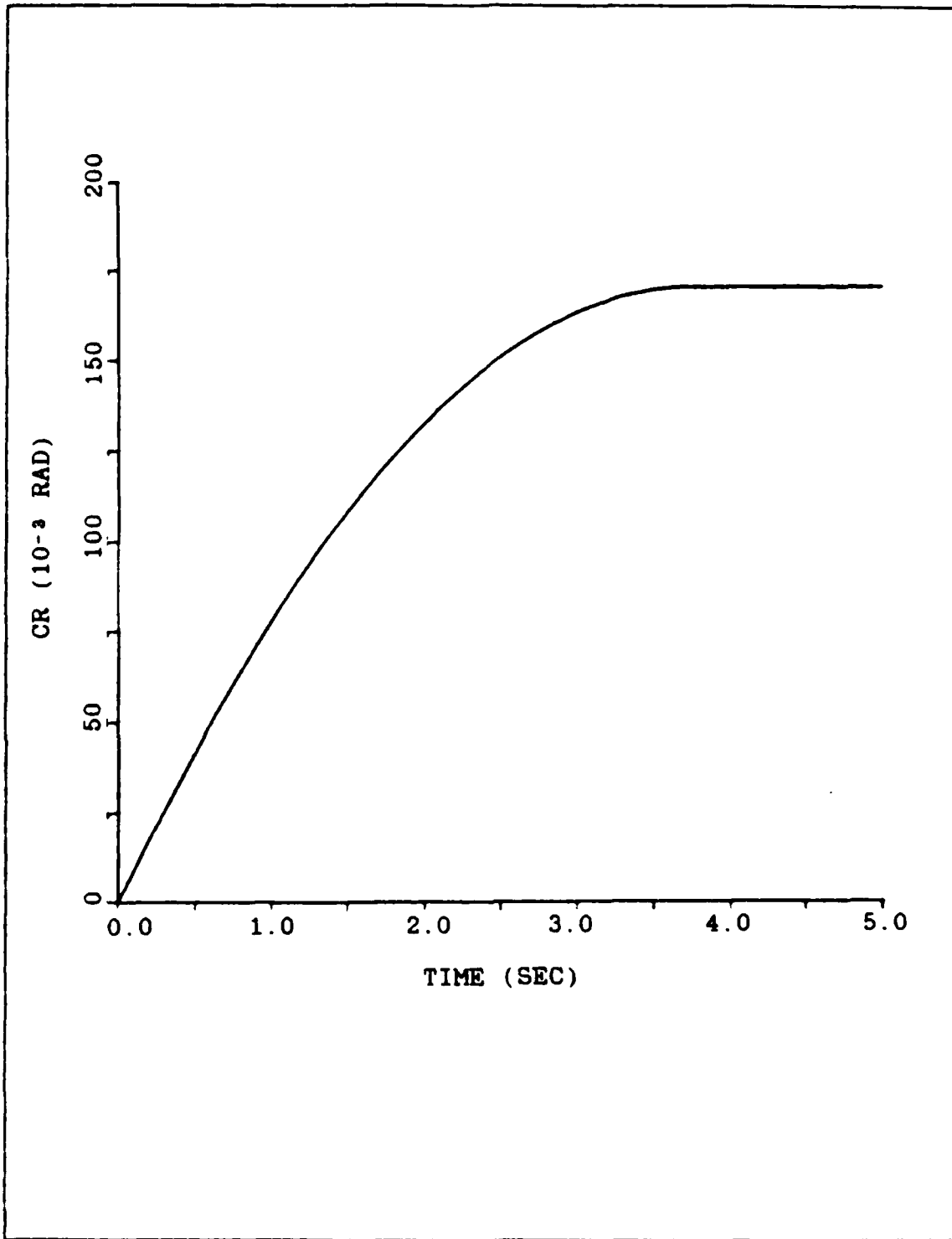


Figure 8.4 Hub Motion Of The Loaded Arm Using The Curve Following System Alone ( $K_1=0.02$ )

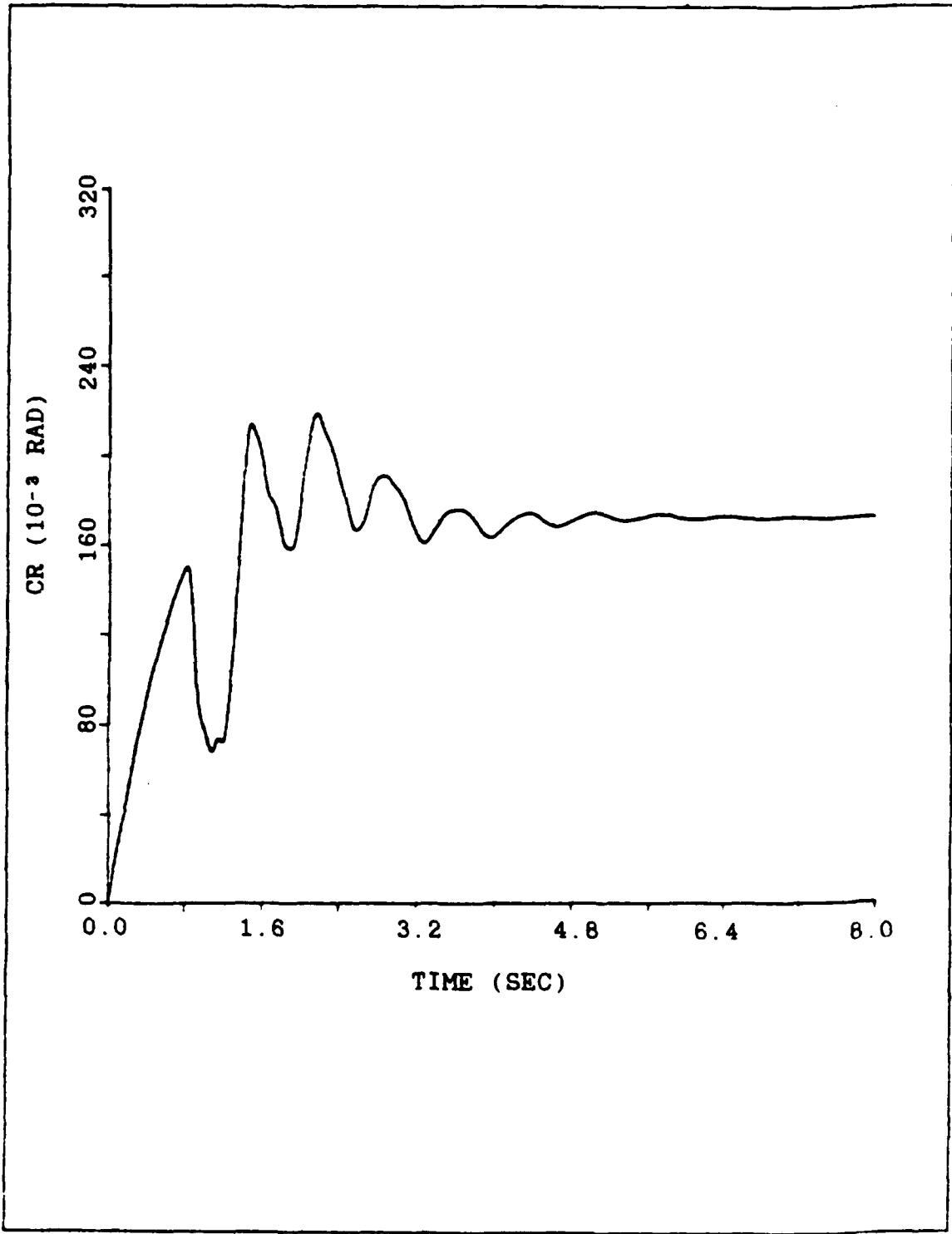


Figure 8.5 Hub Motion Of The Loaded Arm Using The System Shown In Figure 6.16 ( $K_1=0.06$ , Small Motion)

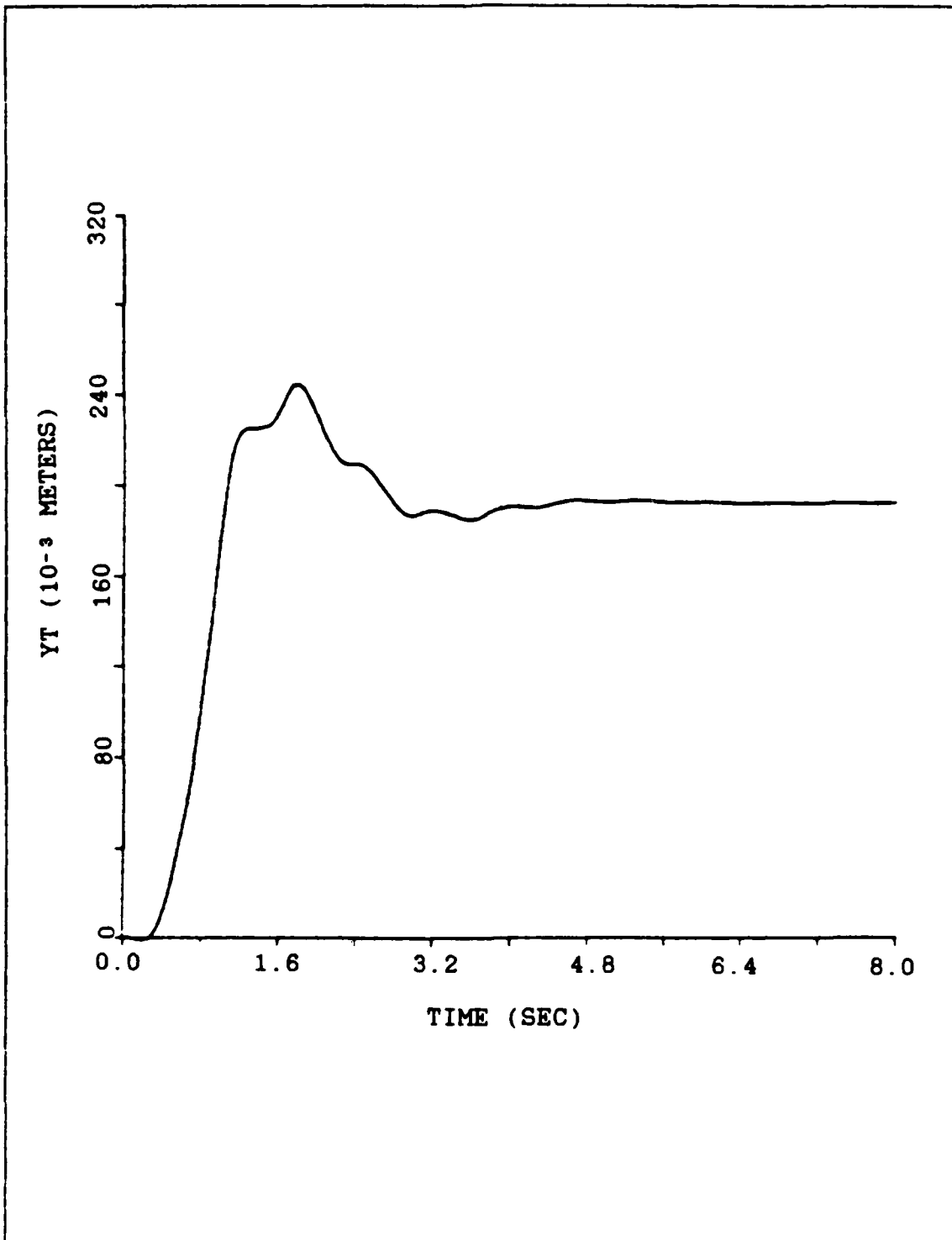


Figure 8.6 Tip Motion Of The Loaded Arm Using The System Shown In Figure 6.16 ( $K_1=0.06$ , Small Motion)

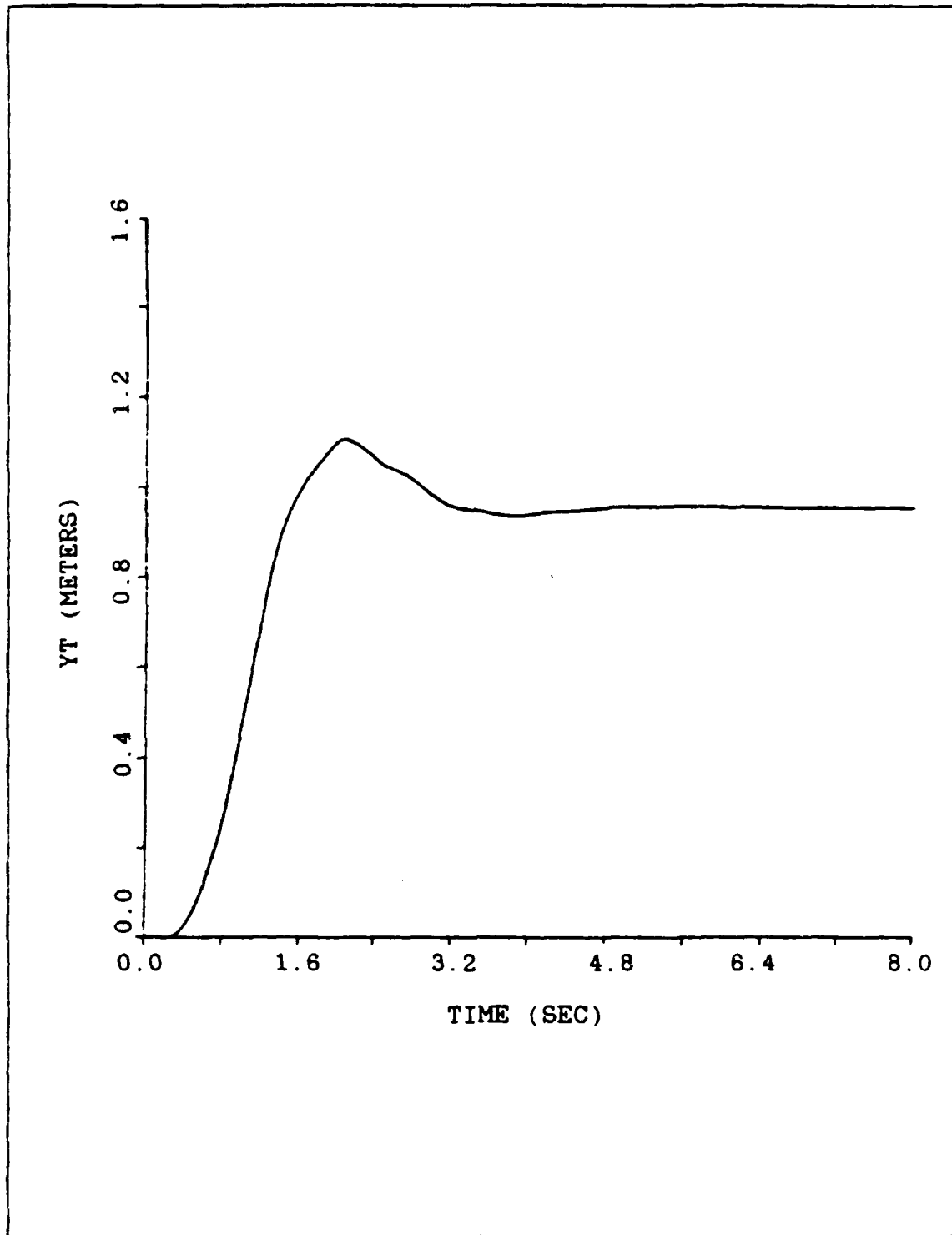


Figure 8.7 Tip Motion Of The Loaded Arm Using The System Shown In Figure 6.16 ( $K_1=0.06$ , Large Motion)

should be for the field of robotics. In an attempt to avoid the excitation of the vibration modes as much as possible, the constant  $K_1$  was reduced to 0.02. The simulation results for that value are shown in Figures 8.8, 8.9 and 8.10. The tip motion is better compared with Figures 8.6 and 8.7, but again is not as good as we would like it to be.

We could reduce the constant  $K_1$  further, but the settling time would be increased very much and the signals coming out of the curve could not be measured easily in a real situation. Therefore, one way out of this problem is to redesign the feedback compensator, making the width of the notches larger, so that they could cover the shift of the frequency of the vibration modes, when the load of the tip changes. Another possible solution is to leave the notches as they are now, but to move the center of the notches to the frequency of the vibration modes in each case. This requires a method to detect the frequency of the vibration modes and use this information to place the notch of the filters. This technique has been successfully used in [Ref. 8], to eliminate the bending modes of a missile.

Both ideas presented above, require a lot of work and are left as recommendations for future study.

### C. "FLEXIBLE PRACTICAL" LOADED ARM

In Chapter VII we studied the effects of the stiffness of the arm on the performance of the curve following system.

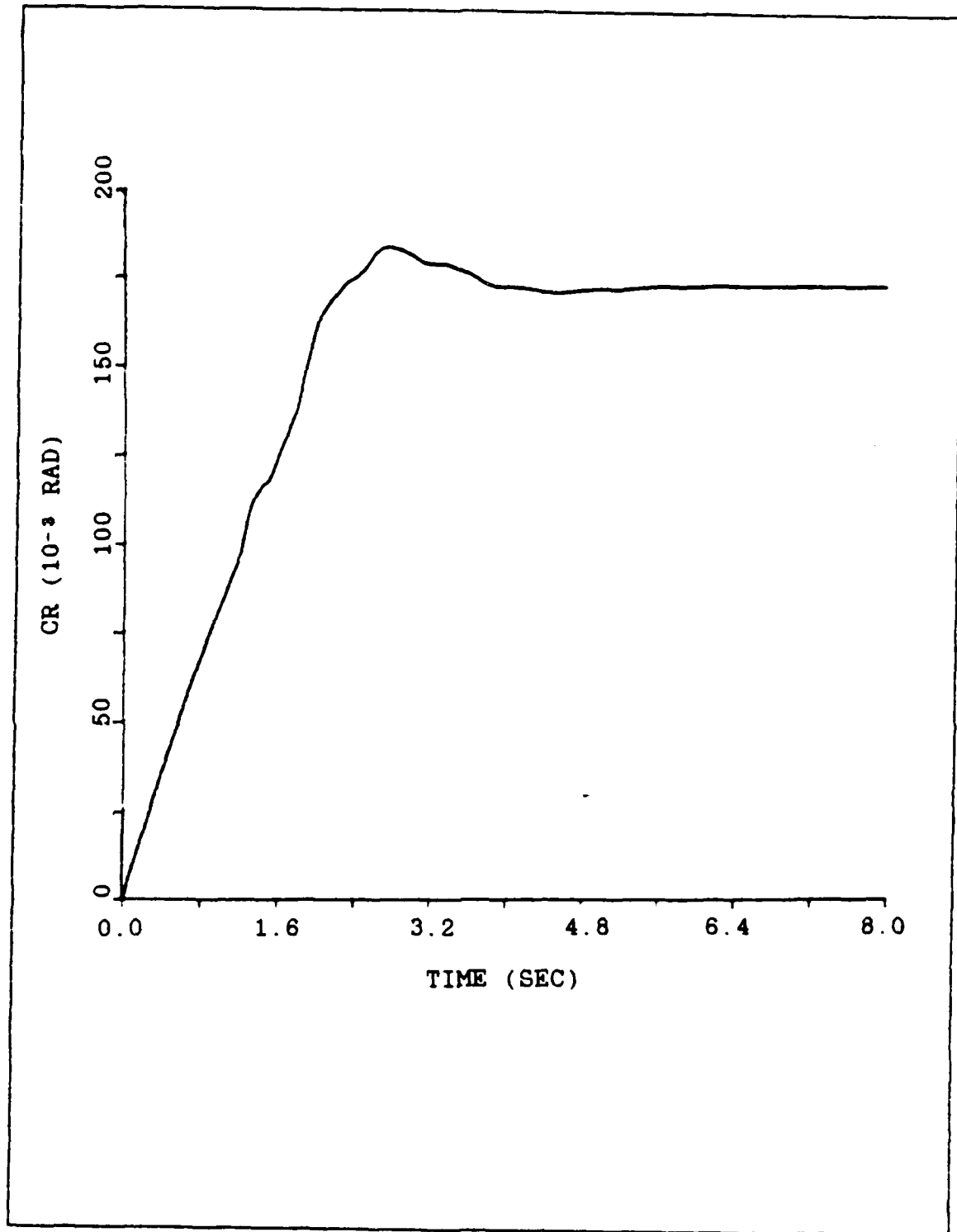


Figure 8.8 Hub Motion Of The Loaded Arm Using The System Shown in Figure 6.16 ( $K_1=0.02$ , Small Motion)

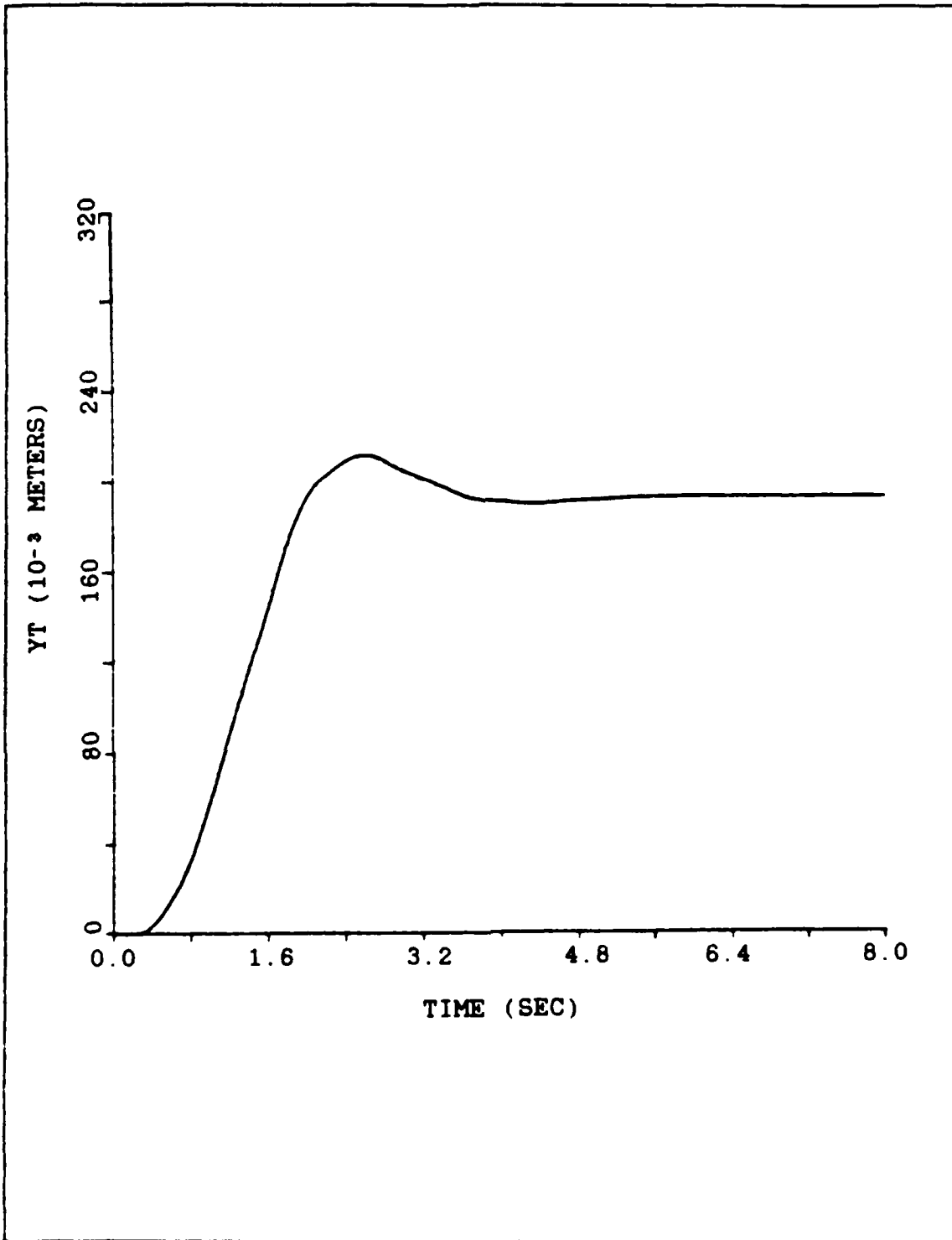


Figure 8.9 Tip Motion Of The Loaded Arm Using the System Shown In Figure 6.16 ( $K_1=0.02$ , Small Motion)

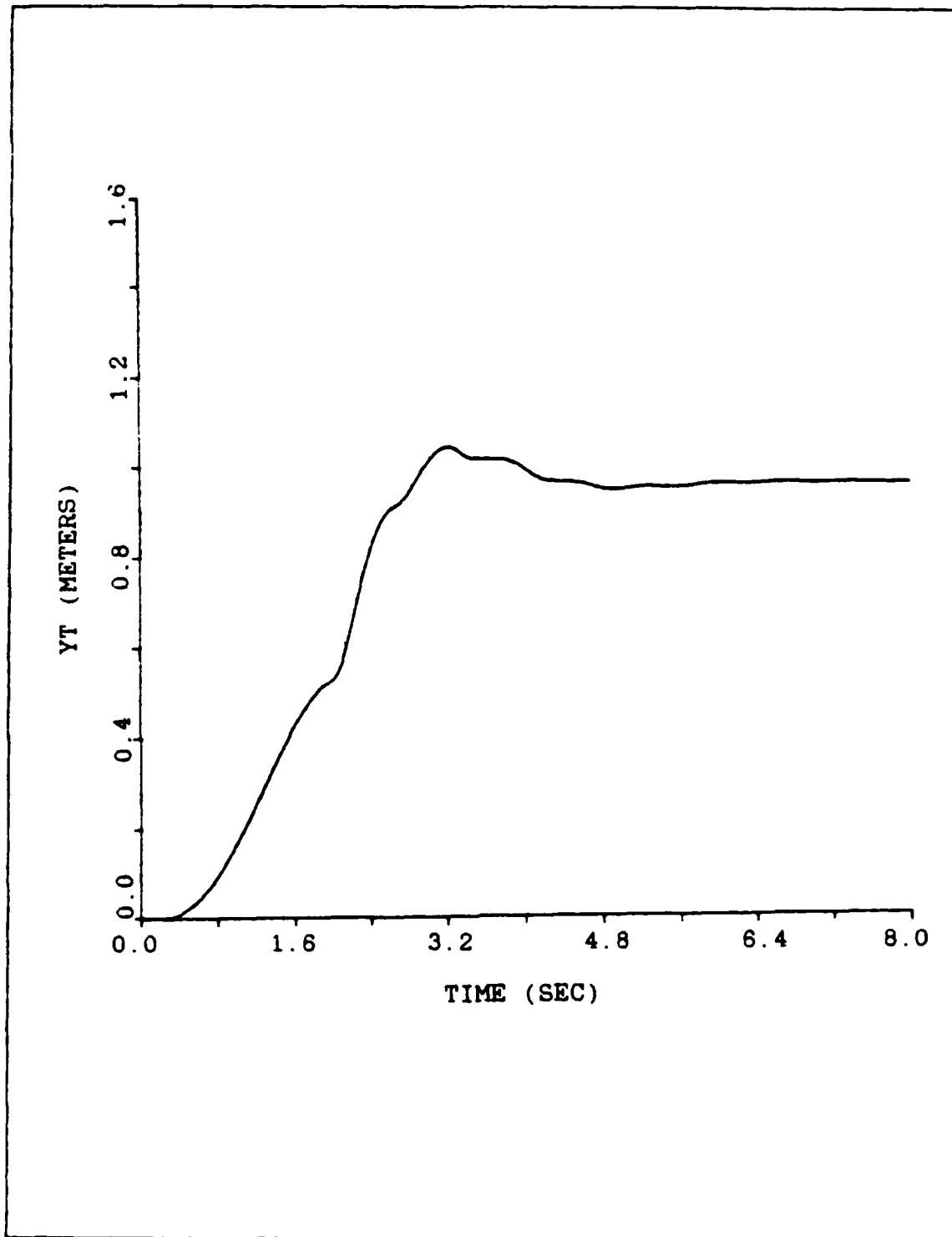


Figure 8.10 Tip Motion Of The Loaded Arm Using The System Shown In Figure 6.16 ( $K_1=0.02$ , Large Motion)

When the arm became 100 times stiffer, a simple linear regulator was used for the final part of the motion.

The same method used to change the stiffness of the unloaded arm, in Chapter VII, applies also for the case of the loaded arm. The resulting transfer functions for the 100 times stiffer arm are as follows.

Hub transfer function - Arm loaded:

$$\frac{\theta(s)}{T(s)} = \frac{44.314(s+1+j24.7)(s+2.4+j145.1)(s+82+j417)}{s(s+0.2)(s+1.5+j100.5)(s+4+j194.1)(s+8.7+j435.3)}$$

Tip transfer function - Arm loaded:

$$\frac{y(s)}{T(s)} = \frac{-0.714(s-127.4)(s+128.9)(s+207.2+j229.4)(s-199+j243.6)}{s(s+0.2)(s+1.5+j100.5)(s+4+j194.1)(s+8.7+j435.3)}$$

The curve following scheme, shown in Figure 4.10 was used again and the simulation results are shown in Figures 8.11 and 8.12 for the hub and the tip motion. The tip motion has still its oscillatory character but the amplitude of the oscillations has been reduced very much.

The same linear regulator as the one used in the case of the unloaded arm, in Chapter VII, was used here, for the final part of the motion of the 100 times stiffer loaded arm. The results of the simulation of the system shown in Figure 6.1, where the appropriate transfer functions have been substituted, are shown in Figures 8.13 and 8.14. From Figure 8.14 we see an excellent tip motion and all oscillations

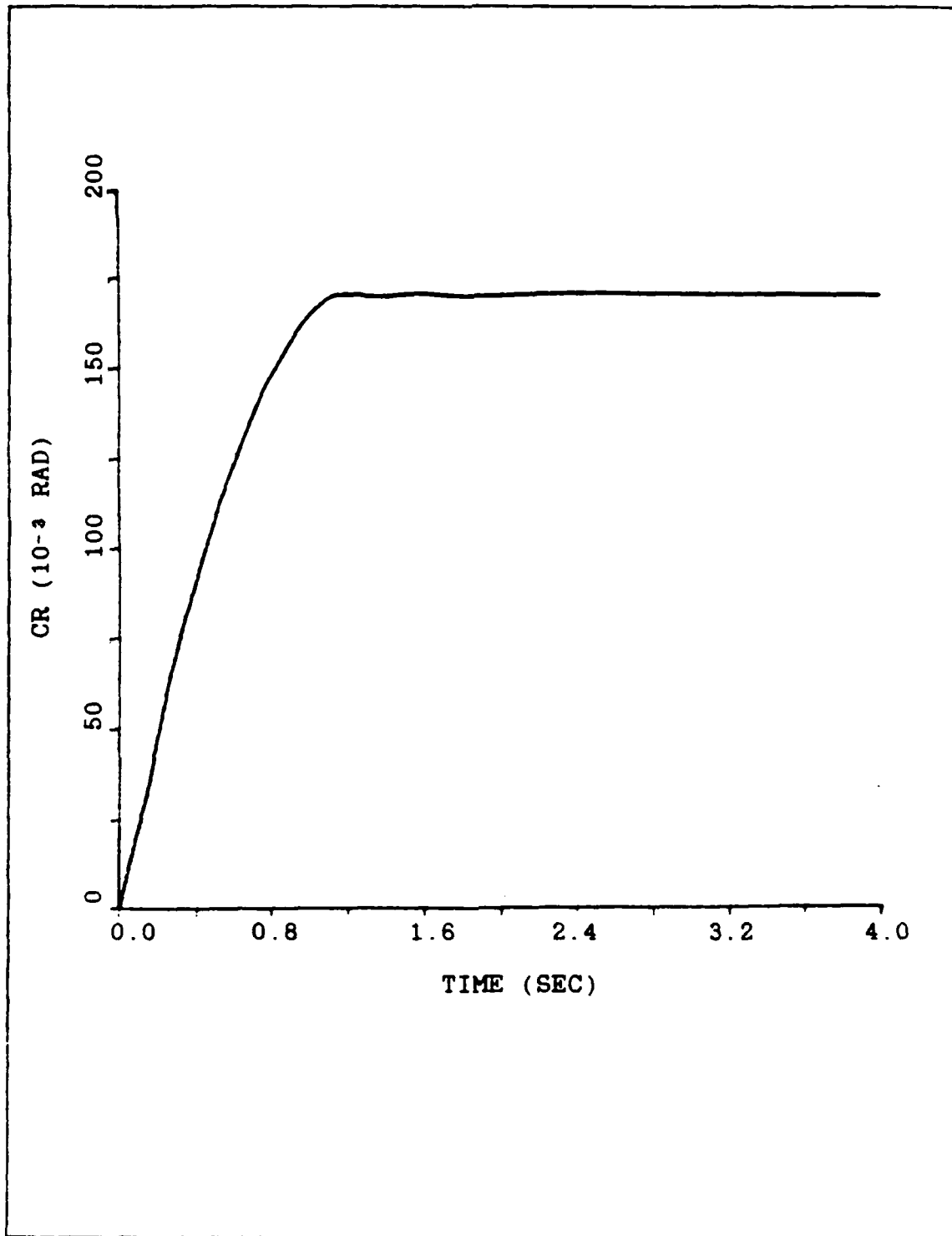


Figure 8.11 Hub Motion Of The 100 Times Stiffer Loaded Arm Using The Curve Following System Alone ( $K_1=0.06$ )

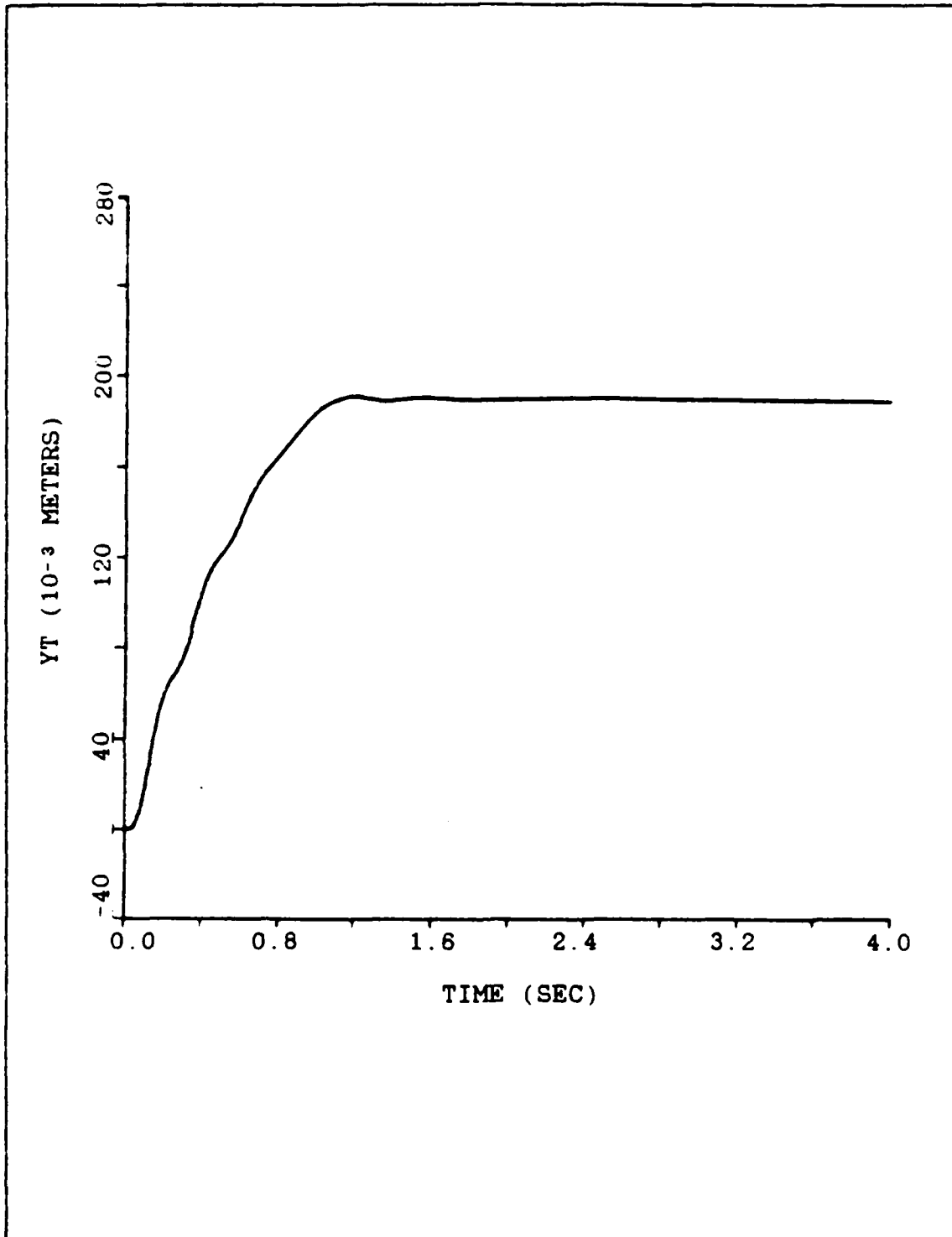


Figure 8.12 Tip Motion Of The 100 Times Stiffer Loaded Arm Using The Curve Following System Alone ( $K_1=0.06$ )

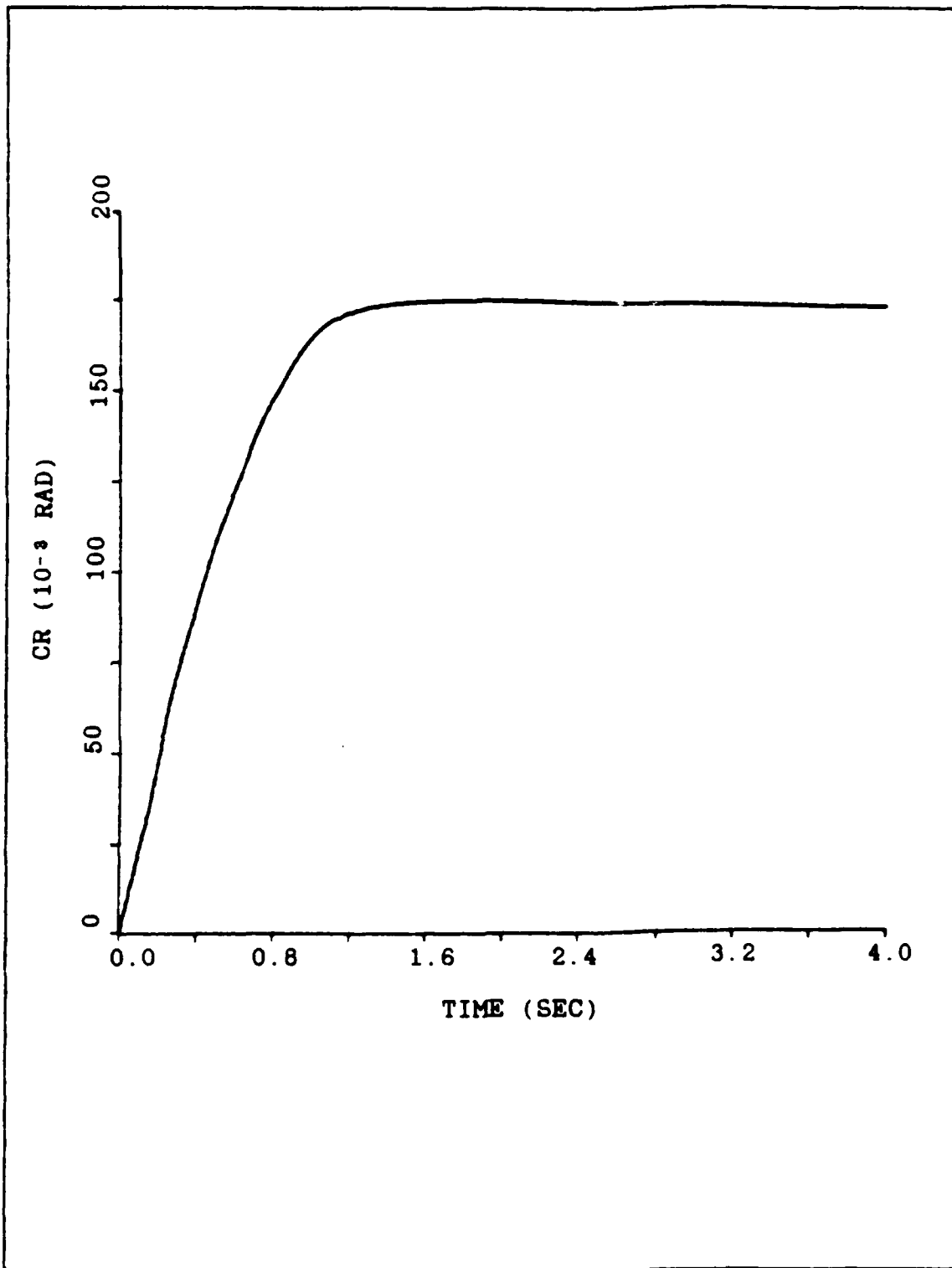


Figure 8.13 Hub Motion Of The 100 Times Stiffer Loaded Arm Using The Linear System For The Final Motion ( $K_1=0.06$ )

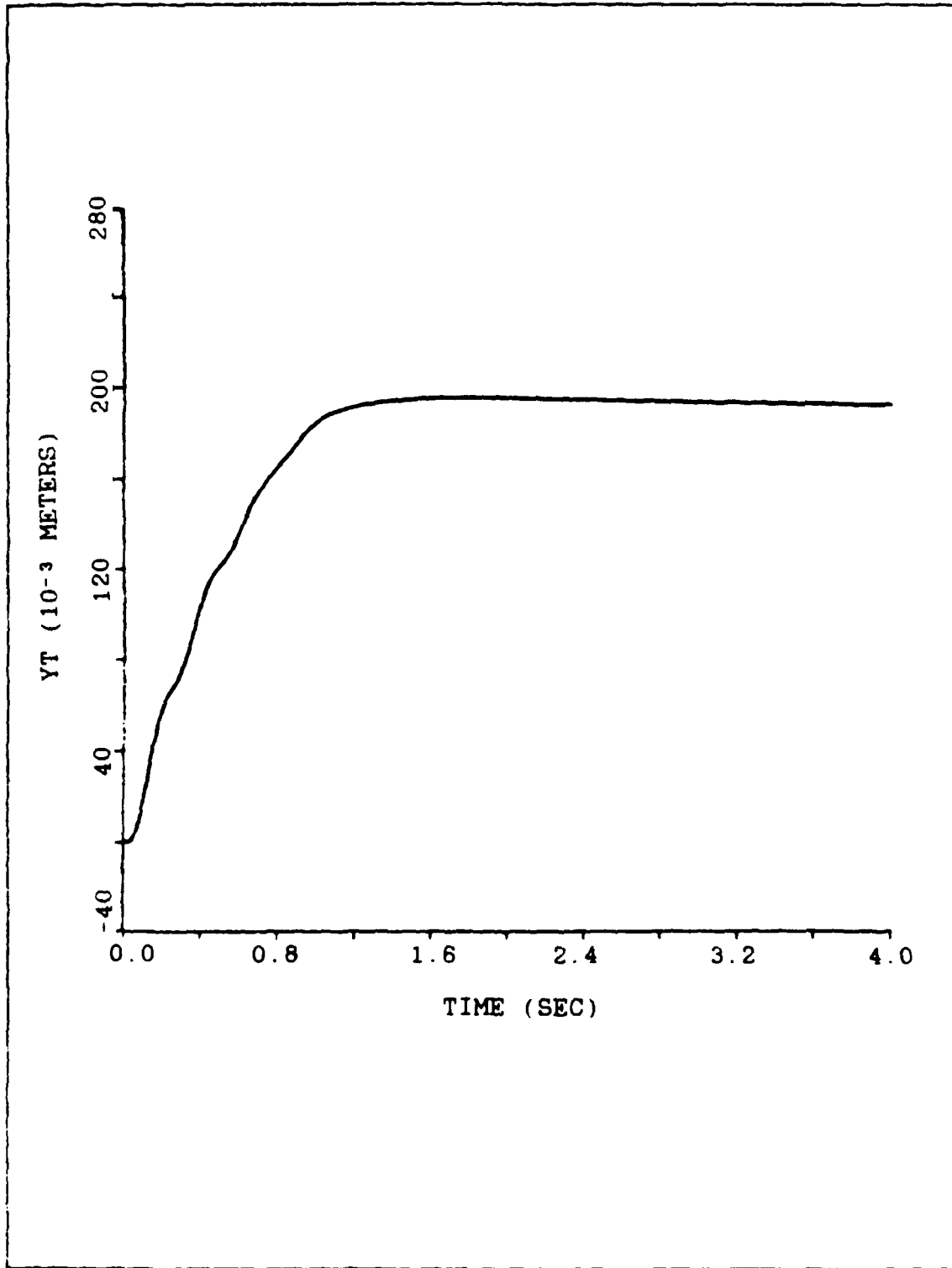


Figure 8.14 Tip Motion Of The 100 Times Stiffer Loaded Arm Using The Linear System For The Final Motion ( $K_1=0.06$ )

present in Figure 8.12 have been completely eliminated and the overshoot is zero.

We conclude again, as in Chapter VII, that the curve following system with the aid of a simple compensator, can be used very effectively for the control of a "practical flexible" arm, for any loading condition of the arm.

## IX. CONCLUSIONS / AREAS FOR FUTURE STUDY

As a result of the research conducted in this thesis, the control of a flexible arm, with the use of the curve following system, appears possible, when the appropriate linear regulator, for the final motion is used. If the arm is very flexible, the linear regulator has to be very complex. When the arm has a practical stiffness, however, the linear regulator is very simple. Furthermore, in this case the overall system is robust to changes of the loading conditions of the arm.

When the arm is very flexible, even though the proposed solution in Chapter VI works very well for the case of the unloaded arm, it does not work as well when the arm carries a tip load. Two possible solutions to this problem are proposed. First, the width of the notches of the feedback compensator, must become larger, so that they can cover any shift of the frequency of the vibration modes, occurring when the loading conditions change. As a second solution, the use of adaptive notch filters can be considered. In this case an algorithm must be derived to detect the resonance frequencies during the operation of the system, and one must use these frequencies to place the notch filters accordingly. A similar approach has been used in [Ref. 8], but the time required for the detection of the vibration modes there is of the order of

one second. This is a very large time for the area of robotics, and therefore [Ref. 8] is only a starting point. For our case a much faster detection of the vibration modes is required.

APPENDIX A

SIMULATION PROGRAM FOR THE BASIC CURVE FOLLOWING  
SYSTEM

```
TITLE THIS PROGRAM INVESTIGATES THE ABILITY OF THE BASIC
TITLE MODEL TO FOLLOW THE CURVE WHEN WE USE VELOCITY CURVE
TITLE FOLLOW TECHNIQUE.
PARAM K1=0.40,K2=10000.0,KM=17.000,VSAT=50.0,K=1.0
PARAM REF=0.1000
INITIAL
      A=SQRT(2.*KM*VSAT)
      XDOT=0.0
DERIVATIVE
      R=REF*STEP(0.0)
      E=R-C
NOSORT
      IF(E.LT.0.0)XDOT=-A*K1*SQRT(ABS(E))
      IF(E.GE.0.0)XDOT=A*K1*SQRT(E)
SORT
      XDOTE=XDOT-KCDOT
      KCDOT=CDOT*K
      V=LIMIT(-VSAT,VSAT,K2*XDOTE)
      CDDOT=KM*V
      CDOT=INTGRL(0.0,CDDOT)
      C=INTGRL(0.0,CDOT)
TERMINAL
METHOD RKSFX
CONTRL FINTIM=1.50000,DELT=0.00005,DELS=0.00025
SAVE (G1)0.00005,TIME,C,XDOT,CDOT
SAVE (G2)0.00005,TIME,C,REF
GRAPH(G1/G1,DE=TEK618,PO=0,.5) C(LE=8.0,UN='RAD') ...
      XDOT(LE=12,NI=12,LO=0,SC=0.7,AX=OMIT) ...
      CDOT(LE=12,NI=12,LO=0,SC=0.7,UN='RAD/SEC')
GRAPH(G2/G2,DE=TEK618,PO=0,.5)
TIME(LE=8.0,UN='SEC',SC=0.0045),...
      C(LE=12,NI=12,LO=0,SC=0.02,UN='RAD') ...
      REF(LE=12,NI=12,LO=0,SC=0.02,AX=OMIT)
LABEL (G1) PHASE PLANE
LABEL (G1) XDOT,CDOT VS C
LABEL (G2) STEP RESPONSE
LABEL (G2) C VS TIME
END
STOP
```

APPENDIX B

SIMULATION PROGRAM FOR THE WHOLE SYSTEM USING CURVE  
FOLLOWING TECHNIQUE

TITLE SIMULATION PROGRAM FOR THE WHOLE SYSTEM  
TITLE USING VELOCITY CURVE FOLLOW TECHNIQUE.  
TITLE THE ARM IS THE THEORETICAL VERY FLEXIBLE ONE.  
PARAM K1=0.06,K2=10000.0,KM=1.2000,VSAT=50.000,K=1.00  
PARAM REF=0.1700,CRO=0.0,T=0.00005,KT=1.00,L=1.13  
INTGER N,SW,SW1  
ARRAY NUMWM(7),DENWM(9),NUMTWM(7)  
\* K1: THE CURVE SCALLING CONSTANT  
\* K2: THE AMPLIFIER GAIN  
\* KM: THE INITIAL MOTOR CONSTANT OF THE IDEAL (MODEL) MOTOR  
\* VSAT: THE SATURATION LIMITS OF THE AMPLIFIER  
\* K: THE VELOCITY LOOP FEEDBACK GAIN (OF THE MODEL)  
\* REF: THE COMMANDED HUB ANGLE IN RAD  
\* T: THE SAMPLING INTERVAL  
\* L: THE ARM'S LENGTH  
\* NUMWM IS THE NUMERATOR OF THE HUB TRANSFER FUNCTION  
\* OF THE ARM WITHOUT MASS AT THE TIP.  
\* DENWM IS THE DENOMINATOR OF THE HUB TRANSFER FUNCTION  
\* OF THE ARM WITHOUT MASS AT THE TIP. THIS DENOMI-  
\* NATOR IS THE SAME FOR THE TIP TRANSFER FUNCTION.  
\* NUMTWM IS THE NUMERATOR OF THE TIP TRANSFER FUNCTION  
\* OF THE ARM WITHOUT MASS AT THE TIP.  
TABLE NUMWM(1-7)=4.362E1,...  
1.0097978E2,...  
1.146367857E5,...  
1.0358489805E5,...  
3.17957559456E7,...  
7.5761380523E6,...  
3.406649216313E8  
TABLE DENWM(1-9)=1,...  
2.78,...  
2.919858E3,...  
4.3620421E3,...  
1.4677639854E6,...  
1.01109904014E6,...  
1.502577700529E8,...  
3.002284611578E7,...  
0  
TABLE NUMTWM(1-7)=-2.177,...  
-3.96214,...  
-2.574372164E2,...  
-5.3041198658E3,...  
-2.52831210194E6,...

5.85687441282E5, ...  
3.817577560845E8

INITIAL

A=SQRT(2.\*KM\*VSAT)  
XDOT=0.0  
SW1=0  
R=REF\*STEP(0.0)

DERIVATIVE

E=R-C

\*\*\*\*\*  
\*\*\*\*\* CURVE CALCULATION \*\*\*\*\*  
\*\*\*\*\*

NOSORT

IF(E.LT.0.0)XDOT=-A\*K1\*SQRT(ABS(E))  
IF(E.GE.0.0)XDOT=A\*K1\*SQRT(E)

SORT

XDOTE=XDOT-KCDOT  
KCDOT=CDOT\*K  
V=LIMIT(-VSAT, VSAT, K2\*XDOTE)  
CDDOT=KM\*V  
CDOT=INTGRL(0.0, CDDOT)  
C=INTGRL(0.0, CDOT)  
OKU=KT\*V  
CR=TRNFR(6, 8, 0.0, NUMWM, DENWM, OKU)  
CRDOT=DERIV(0.0, CR)  
YT=TRNFR(6, 8, 0.0, NUMTWM, DENWM, OKU)

\*\*\*\*\*  
\*\*\*\*\* SAMPLING OF THE ARM'S HUB \*\*\*\*\*  
\*\*\*\*\* POSITION AND HUB RATE \*\*\*\*\*  
\*\*\*\*\*

SAMPLE

NOSORT

IF(N.EQ.0.0)GO TO 20  
IF(CDOT.GT.XDOT)SW=1  
IF(SW.EQ.1)GO TO 5  
KS=ABS(2.\*CR)/(((N\*T)\*\*2)\*V)  
KM=KS

5

CONTINUE  
C=CR

20

CDOT=CRDOT  
N=N+1  
CONTINUE

SORT

TERMINAL

METHOD RKSFX

CONTRL FINTIM=2.0000, DELT=0.00005, DELS=0.00005

\*RINT 0.05, YT

\*AVE (G1)0.0001, C, XDOT, CDOT, CRDOT

\*AVE (G2)0.0001, TIME, C, CR

SAVE (G3)0.0001, TIME, YT

GRAPH(G1/G1, DE=TEK618, PO=0, .5) C(UN='RAD', LE=8.0), ...

XDOT(LO=0, UN='RAD/SEC', LE=12.0), ...

```
CDOT(LO=0,UN='RAD/SEC',LE=12.0),...
CRDOT(LO=0,UN='RAD/SEC',LE=12.0)
GRAPH(G2/G2,DE=TEK618,PO=0,.5) TIME(UN='SEC',LE=8.0),...
CR(UN='RAD',LE=12.0)
* REF(SC=2.0,LO=0,AX=OMIT)
GRAPH(G3/G3,DE=TEK618,PO=0,0.5) TIME(UN='SEC',LE=8.0),...
YT(UN='METERS',LE=12.0)
LABEL (G1) PHASE PLANE
LABEL (G1) XDOT,CDOT,CRDOT VS C
LABEL (G2) STEP RESPONSE
LABEL (G2) C,CR VS TIME
LABEL (G3) MOTION OF THE ARM'S TIP
LABEL (G3) YT VS TIME
END
STOP
```

APPENDIX C

SIMULATION PROGRAM FOR THE WHOLE SYSTEM USING CURVE  
FOLLOWING TECHNIQUE FOR THE FIRST PART OF THE MOTION  
AND SWITCHING TO A SIMPLE LINEAR REGULATOR FOR THE  
FINAL MOTION

TITLE SIMULATION PROGRAM FOR THE WHOLE SYSTEM  
TITLE USING VELOCITY CURVE FOLLOW TECHNIQUE SWITCHING TO  
TITLE LINEAR MODE (SIMPLE SYSTEM) FOR THE FINAL MOTION.  
PARAM K1=0.06,K2=10000.0,KM=1.2000,VSAT=50.000,K=1.00  
PARAM REF=0.1700,CRO=0.0,T=0.00005,KT=1.00,L=1.13  
INTGER N,SW,SW1  
ARRAY NUMWM(7),DENWM(9),NUMTWM(7),NUMF1(2),DENF1(2)  
ARRAY NUMF2(1),DENF2(3)  
\* K1: THE CURVE SCALLING CONSTANT  
\* K2: THE AMPLIFIER GAIN  
\* KM: THE INITIAL MOTOR CONSTANT OF THE IDEAL (MODEL) MOTOR  
\* VSAT: THE SATURATION LIMITS OF THE AMPLIFIER  
\* K: THE VELOCITY LOOP FEEDBACK GAIN (OF THE MODEL)  
\* REF: THE COMMANDED HUB ANGLE IN RAD  
\* T: THE SAMPLING INTERVAL  
\* L: THE ARM'S LENGTH  
\* NUMWM IS THE NUMERATOR OF THE HUB TRANSFER FUNCTION  
\* OF THE ARM WITHOUT MASS AT THE TIP.  
\* DENWM IS THE DENOMINATOR OF THE HUB TRANSFER FUNCTION  
\* OF THE ARM WITHOUT MASS AT THE TIP. THIS DENOMI-  
\* NATOR IS THE SAME FOR THE TIP TRANSFER FUNCTION.  
\* NUMTWM IS THE NUMERATOR OF THE TIP TRANSFER FUNCTION  
\* OF THE ARM WITHOUT MASS AT THE TIP.  
\* NUMF1,DENF1,NUMF2,DENF2 ARE THE NUMERATORS AND THE  
\* DENOMINATORS OF THE FILTERS THAT COMPRISE THE  
\* LINEAR COMPENSATOR.  
TABLE NUMWM(1-7)=4.362E1,...  
1.0097978E2,...  
1.146367857E5,...  
1.0358489805E5,...  
3.17957559456E7,...  
7.5761380523E6,...  
3.406649216313E8  
TABLE DENWM(1-9)=1,...  
2.78,...  
2.919858E3,...  
4.3620421E3,...  
1.4677639854E6,...  
1.01109904014E6,...  
1.502577700529E8,...  
3.002284611578E7,...

```

0
TABLE NUMTWM(1-7)=-2.177,...
                -3.96214,...
                -2.574372164E2,...
                -5.3041198658E3,...
                -2.52831210194E6,...
                5.85687441282E5,...
                3.817577560845E8
TABLE NUMF1(1-2)=0.5,0.25
TABLE DENF1(1-2)=0.5,1
TABLE NUMF2(1)=16
TABLE DENF2(1-3)=1,1.6,16
INITIAL
    A=SQRT(2.*KM*VSAT)
    XDOT=0.0
    SW1=0
    YCOM=L*SIN(REF)
    R=REF*STEP(0.0)
    CRITL=(90.*YCOM)/100.
DERIVATIVE
    E=R-C
*****
***** CURVE CALCULATION *****
*****
NOSORT
    IF(E.LT.0.0)XDOT=-A*K1*SQRT(ABS(E))
    IF(E.GE.0.0)XDOT=A*K1*SQRT(E)
SORT
    XDOTE=XDOT-KCDOT
    KCDOT=CDOT*K
    V=LIMIT(-VSAT,VSAT,K2*XDOTE)
    CDDOT=KM*V
    CDOT=INTGRL(0.0,CDDOT)
    C=INTGRL(0.0,CDOT)
    INPUT=KT*V
*****
***** SWITCHING TO THE LINEAR MODE *****
*****
NOSORT
    IF(YT.LE.CRITL)OKU=INPUT
    IF(YT.GT.CRITL)OKU=OKU1
SORT
    CR=TRNFR(6,8,0.0,NUMWM,DENWM,OKU)
    CRDOT=DERIV(0.0,CR)
    YT=TRNFR(6,8,0.0,NUMTWM,DENWM,OKU)
    ER=YCOM-YT
    OUTF1=TRNFR(1,1,0.0,NUMF1,DENF1,ER)
    OKU1=TRNFR(0,2,0.0,NUMF2,DENF2,OUTF1)
*****
***** SAMPLING OF THE ARM'S HUB *****
***** POSITION AND HUB RATE *****
*****

```

SAMPLE  
NOSORT

IF(N.EQ.0.0)GO TO 20  
IF(CDOT.GT.XDOT)SW=1  
IF(SW.EQ.1)GO TO 5  
KS=ABS(2.\*CR)/(((N\*T)\*\*2)\*V)  
KM=KS

5 CONTINUE  
C=CR  
CDOT=CRDOT  
20 N=N+1  
CONTINUE

SORT

TERMINAL

METHOD RKSFY

CONTRL FINTIM=10.000,DELT=0.00005,DELS=0.00005

\*RINT 0.05,YT

\*AVE (G1)0.0001,C,XDOT,CDOT,CRDOT

SAVE (G2)0.001,TIME,CR

SAVE (G3)0.001,TIME,YT

GRAPH(G1/G1,DE=TEK618,PO=0,.5) C(UN='RAD',LE=8.0),...

XDOT(LO=0,UN='RAD/SEC',LE=12.0),...

CDOT(LO=0,UN='RAD/SEC',LE=12.0),...

CRDOT(LO=0,UN='RAD/SEC',LE=12.0)

GRAPH(G2/G2,DE=TEK618,PO=0,.5) TIME(UN='SEC',LE=8.0),...

CR(UN='RAD')

\* REF(SC=2.0,LO=0,AX=OMIT)

GRAPH(G3/G3,DE=TEK618,PO=0,0.5) TIME(UN='SEC',LE=8.0),...

YT(UN='METERS')

LABEL (G1) PHASE PLANE

LABEL (G1) XDOT,CDOT,CRDOT VS C

LABEL (G2) STEP RESPONSE

LABEL (G2) C,CR VS TIME

LABEL (G3) MOTION OF THE ARM'S TIP

LABEL (G3) YT VS TIME

END

STOP

APPENDIX D

SIMULATION SYSTEM FOR THE WHOLE SYSTEM USING CURVE  
FOLLOWING TECHNIQUE AND POSI-CAST CONTROL

TITLE SIMULATION PROGRAM FOR THE WHOLE SYSTEM  
TITLE USING VELOCITY CURVE FOLLOW TECHNIQUE,  
TITLE APPLYING POSY CAST CONTROL.  
PARAM K1=0.06, K2=10000.0, KM=1.2000, VSAT=50.000, K=1.00  
PARAM REF1=0.1700, REF2=0.320, CRO=0.0, T=0.00005, KT=1.00, L=1.13

INTGER N, SW, SW1

ARRAY NUMWM(7), DENWM(9), NUMTWM(7)

- \* K1: THE CURVE SCALLING CONSTANT
- \* K2: THE AMPLIFIER GAIN
- \* KM: THE INITIAL MOTOR CONSTANT OF THE IDEAL (MODEL) MOTOR
- \* VSAT: THE SATURATION LIMITS OF THE AMPLIFIER
- \* K: THE VELOCITY LOOP FEEDBACK GAIN (OF THE MODEL)
- \* REF: THE COMMANDED HUB ANGLE IN RAD
- \* T: THE SAMPLING INTERVAL
- \* L: THE ARM'S LENGTH
- \* NUMWM IS THE NUMERATOR OF THE HUB TRANSFER FUNCTION
- \* OF THE ARM WITHOUT MASS AT THE TIP.
- \* DENWM IS THE DENOMINATOR OF THE HUB TRANSFER FUNCTION
- \* OF THE ARM WITHOUT MASS AT THE TIP. THIS DENOMI-
- \* NATOR IS THE SAME FOR THE TIP TRANSFER FUNCTION.
- \* NUMTWM IS THE NUMERATOR OF THE TIP TRANSFER FUNCTION
- \* OF THE ARM WITHOUT MASS AT THE TIP.

TABLE NUMWM(1-7)=4.362E1, ...  
1.0097978E2, ...  
1.146367857E5, ...  
1.0358489805E5, ...  
3.17957559456E7, ...  
7.5761380523E6, ...  
3.406849216313E8

TABLE DENWM(1-9)=1, ...  
2.78, ...  
2.919858E3, ...  
4.3620421E3, ...  
1.4677639854E6, ...  
1.01109904014E6, ...  
1.502577700529E8, ...  
3.002284611578E7, ...  
0

TABLE NUMTWM(1-7)=-2.177, ...  
-3.96214, ...  
-2.574372164E2, ...  
-5.3041198658E3, ...

-2.52831210194E6, ...  
5.85687441282E5, ...  
3.817577560845E8

INITIAL

A=SQRT(2.\*KM\*VSAT)  
XDOT=0.0  
SW1=0

DERIVATIVE

R=REF1\*STEP(0.0)-REF1\*STEP(0.95)+REF2\*STEP(0.95)  
E=R-C

\*\*\*\*\*  
\*\*\*\*\* CURVE CALCULATION \*\*\*\*\*  
\*\*\*\*\*

NOSORT

IF(E.LT.0.0)XDOT=-A\*K1\*SQRT(ABS(E))  
IF(E.GE.0.0)XDOT=A\*K1\*SQRT(E)

SORT

YCOM=L\*SIN(R)  
XDOTE=XDOT-KCDOT  
KCDOT=CDOT\*K  
V=LIMIT(-VSAT, VSAT, K2\*XDOTE)  
CDDOT=KM\*V  
CDOT=INTGRL(0.0, CDDOT)  
C=INTGRL(0.0, CDOT)  
OKU=KT\*V  
CR=TRNFR(6, 8, 0.0, NUMWM, DENWM, OKU)  
CRDOT=DERIV(0.0, CR)  
YT=TRNFR(6, 8, 0.0, NUMTWM, DENWM, OKU)

\*\*\*\*\*  
\*\*\*\*\* SAMPLING OF THE ARM'S HUB \*\*\*\*\*  
\*\*\*\*\* POSITION AND HUB RATE \*\*\*\*\*  
\*\*\*\*\*

SAMPLE

NOSORT

IF(N.EQ.0.0)GO TO 20  
IF(CDOT.GT.XDOT)SW=1  
IF(SW.EQ.1)GO TO 5  
KS=ABS(2.\*CR)/(((N\*T)\*\*2)\*V)  
KM=KS

5 CONTINUE

C=CR  
CDOT=CRDOT

20 N=N+1

CONTINUE

SORT

TERMINAL

METHOD RKSF

CONTRL FINTIM=5.0000, DELT=0.00005, DELS=0.00005

PRINT 0.5, YT

\*AVE (G1)0.0001, C, XDOT, CDOT, CRDOT

\*AVE (G2)0.001, R, CR

SAVE (G3)0.001, YT

```

*AVE (G4)0.0001,CR,OKU
GRAPH(G1/G1,DE=TEK618,PO=0,.5) C(UN='RAD',LE=8.0),...
  XDOT(LO=0,UN='RAD/SEC'),...
*   CDOT(LO=0,UN='RAD/SEC'),...
  CRDOT(LO=0,UN='RAD/SEC')
GRAPH(G2/G2,DE=TEK618,PO=0,.5) TIME(UN='SEC',LE=8.0),...
  CR(UN='RAD'LO=0.0,SC=50E-3),...
  R(LO=0.0,SC=50E-3,AX=OMIT)
*   REF(SC=2.0,LO=0,AX=OMIT)
GRAPH(G3/G3,DE=TEK618,PO=0,0.5) TIME(UN='SEC',LE=8.0),...
  YT(UN='METERS',LO=-50E-3,SC=100E-3)
*   YCOM(LO=-50E-3,SC=100E-3,AX=OMIT)
GRAPH(G4/G4,DE=TEK618,PO=0,0.5) TIME(UN='SEC',LE=8.0),...
  OKU(UN='NM'),...
  CR(UN='RAD',AX=OMIT)
LABEL (G1) PHASE PLANE
LABEL (G1) XDOT,CDOT,CRDOT VS C
LABEL (G2) STEP RESPONSE
LABEL (G2) COMMAND AND CR VS TIME
LABEL (G3) MOTION OF THE ARM'S TIP
LABEL (G3) YT VS TIME
END
STOP

```

## APPENDIX E

### SIMULATION PROGRAM FOR THE SYSTEM USING CURVE FOLLOWING TECHNIQUE FOR THE FIRST PART OF THE MOTION AND SWITCHING TO A LINEAR SYSTEM CONTAINING A FEEDBACK COMPENSATOR FOR THE FINAL MOTION

TITLE SIMULATION PROGRAM FOR THE WHOLE SYSTEM  
TITLE USING VELOCITY CURVE FOLLOW TECHNIQUE SWITCHING TO  
TITLE LINEAR MODE FOR THE FINAL MOTION.  
TITLE ( USE OF THE FEEDBACK COMPENSATOR )  
PARAM K1=0.06,K2=10000.0,KM=1.2000,VSAT=50.000,K=1.00  
PARAM REF=0.1700,CRO=0.0,T=0.00005,KT=1.00,L=1.13  
PARAM KB=0.1012,BM=0.04297  
INTGER N,SW,SW1  
ARRAY NUMWM(7),DENWM(9),NUMTWM(7),NUMCOT(8),DENCOT(9)  
\* K1: THE CURVE SCALLING CONSTANT  
\* K2: THE AMPLIFIER GAIN  
\* KM: THE INITIAL MOTOR CONSTANT OF THE IDEAL (MODEL) MOTOR  
\* VSAT: THE SATURATION LIMITS OF THE AMPLIFIER  
\* K: THE VELOCITY LOOP FEEDBACK GAIN (OF THE MODEL)  
\* REF:THE COMMANDED HUB ANGLE IN RAD  
\* T: THE SAMPLING INTERVAL  
\* L: THE ARM'S LENGTH  
\* NUMWM IS THE NUMERATOR OF THE HUB TRANSFER FUNCTION  
\* OF THE ARM WITHOUT MASS AT THE TIP.  
\* DENWM IS THE DENOMINATOR OF THE HUB TRANSFER FUNCTION  
\* OF THE ARM WITHOUT MASS AT THE TIP.THIS DENOMI-  
\* NATOR IS THE SAME FOR THE TIP TRANSFER FUNCTION.  
\* NUMTWM IS THE NUMERATOR OF THE TIP TRANSFER FUNCTION  
\* OF THE ARM WITHOUT MASS AT THE TIP.  
\* NUMCOT IS THE NUMERATOR OF THE FEEDBACK COMPENSATOR USING  
\* FEEDBACK ONLY FROM THE TIP MOTION.  
\* DENCOT IS THE DENOMINATOR OF THE FEEDBACK COMPENSATOR  
ABOVE.  
TABLE NUMWM(1-7)=4.362E1,...  
1.0097978E2,...  
1.146367857E5,...  
1.0358489805E5,...  
3.17957559456E7,...  
7.5761380523E6,...  
3.406649216313E8  
TABLE DENWM(1-9)=1,...  
2.78,...  
2.919858E3,...  
4.3620421E3,...  
1.4677639854E6,...  
1.01109904014E6,...

```

1.502577700529E8,...
3.002284611578E7,...
0
TABLE NUMTWM(1-7)=-2.177,...
-3.96214,...
-2.574372164E2,...
-5.3041198658E3,...
-2.52831210194E6,...
5.85687441282E5,...
3.817577560845E8
TABLE NUMCOT(1-8)=1160.3,...
-2.517851E4,...
5.54202211E6,...
-1.721367358E7,...
4.95075585685E9,...
-1.0001002852E10,...
7.76281441950E11,...
1.20376275595E12
TABLE DENCOT(1-9)=1,...
107.1,...
8565.06,...
4.53977023E5,...
1.714597556E7,...
4.74104184707E8,...
9.174522576342E9,...
1.18930489797E11,...
6.64749102467E11

```

INITIAL

```

A=SQRT(2.*KM*VSAT)
XDOT=0.0
SW1=0
YCOM=L*SIN(REF)
R=REF*STEP(0.0)
YCOM1=L*SIN(REF)*1.81
CRITL=(50.*YCOM)/100.

```

DERIVATIVE

E=R-C

```

*****
***** CURVE CALCULATION *****
*****

```

NOSORT

```

IF(E.LT.0.0)XDOT=-A*K1*SQRT(ABS(E))
IF(E.GE.0.0)XDOT=A*K1*SQRT(E)

```

SORT

```

XDOTE=XDOT-KCDOT
KCDOT=CDOT*K
V=LIMIT(-VSAT,VSAT,K2*XDOTE)
CDDOT=KM*V
CDOT=INTGRL(0.0,CDDOT)
C=INTGRL(0.0,CDOT)
INPUT=KT*V

```

```

*****

```

\*\*\*\*\* SWITCHING TO THE LINEAR MODE \*\*\*\*\*

\*\*\*\*\*

NOSORT

IF(YT.LE.CRITL)OKU=INPUT

IF(YT.GT.CRITL)OKU=OKU1

SORT

CR=TRNFR(6,8,0.0,NUMWM,DENWM,OKU)

CRDOT=DERIV(0.0,CR)

YT=TRNFR(6,8,0.0,NUMTWM,DENWM,OKU)

FTIP=TRNFR(7,8,0.0,NUMCOT,DENCOT,YT)

OKU1=YCOM1-FTIP

\*\*\*\*\*

\*\*\*\*\* SAMPLING OF THE ARM'S HUB \*\*\*\*\*

\*\*\*\*\* POSITION AND HUB RATE \*\*\*\*\*

\*\*\*\*\*

SAMPLE

NOSORT

IF(N.EQ.0.0)GO TO 20

IF(CDOT.GT.XDOT)SW=1

IF(SW.EQ.1)GO TO 5

KS=ABS(2.\*CR)/(((N\*T)\*\*2)\*V)

KM=KS

5

CONTINUE

C=CR

CDOT=CRDOT

20

N=N+1

CONTINUE

SORT

TERMINAL

METHOD RKSFX

CONTRL FINTIM=2.0000,DELT=0.00005,DELS=0.00005

\*RINT 0.05,YT

\*AVE (G1)0.0001,C,XDOT,CDOT,CRDOT

\*AVE (G2)0.0001,TIME,C,CR

SAVE (G3)0.0001,TIME,YT

GRAPH(G1/G1,DE=TEK618,PO=0,.5) C(UN='RAD',LE=8.0),...

XDOT(LO=0,UN='RAD/SEC',LE=12.0),...

CDOT(LO=0,UN='RAD/SEC',LE=12.0),...

CRDOT(LO=0,UN='RAD/SEC',LE=12.0)

GRAPH(G2/G2,DE=TEK618,PO=0,.5) TIME(UN='SEC',LE=8.0),...

CR(UN='RAD',LE=12.0)

\* REF(SC=2.0,LO=0,AX=OMIT)

GRAPH(G3/G3,DE=TEK618,PO=0,0.5) TIME(UN='SEC',LE=8.0),...

YT(UN='METERS',LE=12.0)

LABEL (G1) PHASE PLANE

LABEL (G1) XDOT,CDOT,CRDOT VS C

LABEL (G2) STEP RESPONSE

LABEL (G2) C,CR VS TIME

LABEL (G3) MOTION OF THE ARM'S TIP

LABEL (G3) YT VS TIME

END

STOP

APPENDIX F

SIMULATION PROGRAM FOR THE SYSTEM USING CURVE FOLLOWING  
TECHNIQUE WITH THE ARM BEING 20 TIMES STIFFER

TITLE SIMULATION PROGRAM FOR THE WHOLE SYSTEM  
TITLE USING VELOCITY CURVE FOLLOW TECHNIQUE. THE ARM IS  
TITLE 20 TIMES STIFFER THAN THE THEORETICAL ONE  
PARAM K1=0.06,K2=10000.0,KM=1.2000,VSAT=50.000,K=1.00  
PARAM REF=0.1700,CRO=0.0,T=0.00005,KT=1.00,L=1.13  
INTGER N,SW,SW1  
ARRAY NUMWM(7),DENWM(9),NUMTWM(7)  
\* K1: THE CURVE SCALLING CONSTANT  
\* K2: THE AMPLIFIER GAIN  
\* KM: THE INITIAL MOTOR CONSTANT OF THE IDEAL (MODEL) MOTOR  
\* VSAT: THE SATURATION LIMITS OF THE AMPLIFIER  
\* K: THE VELOCITY LOOP FEEDBACK GAIN (OF THE MODEL)  
\* REF: THE COMMANDED HUB ANGLE IN RAD  
\* T: THE SAMPLING INTERVAL  
\* L: THE ARM'S LENGTH  
\* NUMWM IS THE NUMERATOR OF THE HUB TRANSFER FUNCTION  
\* OF THE ARM WITHOUT MASS AT THE TIP.  
\* DENWM IS THE DENOMINATOR OF THE HUB TRANSFER FUNCTION  
\* OF THE ARM WITHOUT MASS AT THE TIP. THIS DENOMI-  
\* NATOR IS THE SAME FOR THE TIP TRANSFER FUNCTION.  
\* NUMTWM IS THE NUMERATOR OF THE TIP TRANSFER FUNCTION  
\* OF THE ARM WITHOUT MASS AT THE TIP.  
TABLE NUMWM(1-7)=46.321,...  
1009.8,...  
1.1463678571E7,...  
1.03584898053E8,...  
3.17957559457E11,...  
7.57613805235E11,...  
3.40664921631E14  
TABLE DENWM(1-9)=1,...  
26.0,...  
2.9803594E5,...  
3.90728207E6,...  
1.50406090396E10,...  
7.64243888420E10,...  
1.54089763177E14,...  
3.08150159785E13,...  
0  
TABLE NUMTWM(1-7)=-2.177,...  
-3.96214E1,...  
-2.5523332216E4,...  
-5.20524865907E6,...  
-2.528229735E10,...

5.71507551855E10, ...  
3.81407740623E14

INITIAL

A=SQRT(2.\*KM\*VSAT)  
XDOT=0.0  
SW1=0  
YCOM=L\*SIN(REF)  
R=REF\*STEP(0.0)

DERIVATIVE

E=R-C

\*\*\*\*\*  
\*\*\*\*\* CURVE CALCULATION \*\*\*\*\*  
\*\*\*\*\*

NOSORT

IF(E.LT.0.0)XDOT=-A\*K1\*SQRT(ABS(E))  
IF(E.GE.0.0)XDOT=A\*K1\*SQRT(E)

SORT

XDOTE=XDOT-KCDOT  
KCDOT=CDOT\*K  
V=LIMIT(-VSAT, VSAT, K2\*XDOTE)  
CDDOT=KM\*V  
CDOT=INTGRL(0.0, CDDOT)  
C=INTGRL(0.0, CDOT)  
OKU=KT\*V  
CR=TRNFR(6, 8, 0.0, NUMWM, DENWM, OKU)  
CRDOT=DERIV(0.0, CR)  
YT=TRNFR(6, 8, 0.0, NUMTWM, DENWM, OKU)

\*\*\*\*\*  
\*\*\*\*\* SAMPLING OF THE ARM'S HUB \*\*\*\*\*  
\*\*\*\*\* POSITION AND HUB RATE \*\*\*\*\*  
\*\*\*\*\*

SAMPLE

NJSORT

IF(N.EQ.0.0)GO TO 20  
IF(CDOT.GT.XDOT)SW=1  
IF(SW.EQ.1)GO TO 5  
KS=ABS(2.\*CR)/(((N\*T)\*\*2)\*V)  
KM=KS  
5 CONTINUE  
C=CR  
CDOT=CRDOT  
20 N=N+1  
CONTINUE

SORT

TERMINAL

METHOD RKSFX

CONTRL FINTIM=2.0000, DELT=0.00005, DELS=0.00005

\*RINT 0.05, YT

\*AVE (G1)0.0001, C, XDOT, CDOT, CRDOT

\*AVE (G2)0.0001, TIME, C, CR

SAVE (G3)0.0001, TIME, YT, CR

GRAPH(G1/G1, DE=TEK618, PO=0, .5) C(UN='RAD', LE=6.0), ...

```
XDOT(LO=0,UN='RAD/SEC',LE=6.0),...
CDOT(LO=0,UN='RAD/SEC',LE=6.0),...
CRDOT(LO=0,UN='RAD/SEC',LE=6.0)
GRAPH(G2/G2,DE=TEK618,PO=0,.5) TIME(UN='SEC',LE=6.0),...
CR(UN='RAD',LE=6.0)
* REF(SC=2.0,LO=0,AX=OMIT)
GRAPH(G3/G3,DE=TEK618,PO=0,0.5) TIME(UN='SEC',LE=8.0),...
YT(UN='METERS',LE=7.5),CR
LABEL (G1) PHASE PLANE
LABEL (G1) XDOT,CDOT,CRDOT VS C
LABEL (G2) STEP RESPONSE
LABEL (G2) C,CR VS TIME
LABEL (G3) MOTION OF THE ARM'S TIP
LABEL (G3) YT VS TIME
END
STOP
```

APPENDIX G

SIMULATION PROGRAM FOR THE SYSTEM USING CURVE FOLLOWING  
TECHNIQUE WITH THE ARM BEING 50 STIFFER

TITLE SIMULATION PROGRAM FOR THE WHOLE SYSTEM  
TITLE USING VELOCITY CURVE FOLLOW TECHNIQUE. THE ARM IS  
TITLE 50 TIMES STIFFER THAN THE THEORETICAL ONE  
PARAM K1=0.06,K2=10000.0,KM=1.2000,VSAT=50.000,K=1.00  
PARAM REF=0.1700,CRO=0.0,T=0.00005,KT=1.00,L=1.13  
INTGER N,SW,SW1  
ARRAY NUMWM(7),DENWM(9),NUMTWM(7)  
\* K1: THE CURVE SCALLING CONSTANT  
\* K2: THE AMPLIFIER GAIN  
\* KM: THE INITIAL MOTOR CONSTANT OF THE IDEAL (MODEL) MOTOR  
\* VSAT: THE SATURATION LIMITS OF THE AMPLIFIER  
\* K: THE VELOCITY LOOP FEEDBACK GAIN (OF THE MODEL)  
\* REF: THE COMMANDED HUB ANGLE IN RAD  
\* T: THE SAMPLING INTERVAL  
\* L: THE ARM'S LENGTH  
\* NUMWM IS THE NUMERATOR OF THE HUB TRANSFER FUNCTION  
\* OF THE ARM WITHOUT MASS AT THE TIP.  
\* DENWM IS THE DENOMINATOR OF THE HUB TRANSFER FUNCTION  
\* OF THE ARM WITHOUT MASS AT THE TIP. THIS DENOMI-  
\* NATOR IS THE SAME FOR THE TIP TRANSFER FUNCTION.  
\* NUMTWM IS THE NUMERATOR OF THE TIP TRANSFER FUNCTION  
\* OF THE ARM WITHOUT MASS AT THE TIP.  
TABLE NUMWM(1-7)=46.321,...  
714.03,...  
5.7318392857E6,...  
3.6622791921E07,...  
7.94893898642E10,...  
1.33928464800E11,...  
4.25831152039E13  
TABLE DENWM(1-9)=1,...  
1.84433549E1,...  
1.45970748671E5,...  
1.36497954188E6,...  
3.66778803401E9,...  
1.34207211044E10,...  
1.87668162657E13,...  
3.75285576447E12,...  
0  
TABLE NUMTWM(1-7)=-2.177,...  
-28.016560,...  
-1.2761661E4,...  
-1.84033331229E6,...  
-6.31557433757E9,...

1.01029216354E10, ...  
4.76759675779E13

INITIAL

A=SQRT(2.\*KM\*VSAT)  
XDOT=0.0  
SW1=0  
YCOM=L\*SIN(REF)  
R=REF\*STEP(0.0)

DERIVATIVE

E=R-C

\*\*\*\*\*  
\*\*\*\*\* CURVE CALCULATION \*\*\*\*\*  
\*\*\*\*\*

NOSORT

IF(E.LT.0.0)XDOT=-A\*K1\*SQRT(ABS(E))  
IF(E.GE.0.0)XDOT=A\*K1\*SQRT(E)

SORT

XDOTE=XDOT-KCDOT  
KCDOT=CDOT\*K  
V=LIMIT(-VSAT,VSAT,K2\*XDOTE)  
CDDOT=KM\*V  
CDOT=INTGRL(0.0,CDDOT)  
C=INTGRL(0.0,CDOT)  
OKU=KT\*V  
CR=TRNFR(6,8,0.0,NUMWM,DENWM,OKU)  
CRDOT=DERIV(0.0,CR)  
YT=TRNFR(6,8,0.0,NUMTWM,DENWM,OKU)

\*\*\*\*\*  
\*\*\*\*\* SAMPLING OF THE ARM'S HUB \*\*\*\*\*  
\*\*\*\*\* POSITION AND HUB RATE \*\*\*\*\*  
\*\*\*\*\*

SAMPLE

NOSORT

IF(N.EQ.0.0)GO TO 20  
IF(CDOT.GT.XDOT)SW=1  
IF(SW.EQ.1)GO TO 5  
KS=ABS(2.\*CR)/(((N\*T)\*\*2)\*V)  
KM=KS

5

CONTINUE  
C=CR

20

CDOT=CRDOT  
N=N+1  
CONTINUE

SORT

TERMINAL

METHOD RKSFX

CONTRL FINTIM=5.0000,DELT=0.00005,DELS=0.00005

PRINT 0.05,TIME

\*AVE (G1)0.0001,C,XDOT,CDOT,CRDOT

\*AVE (G2)0.0001,TIME,C,CR

SAVE (G3)0.0001,TIME,YT

GRAPH(G1/G1,DE=TEK618,PO=0,.5) C(UN='RAD',LE=8.0),...

```
XDOT(LO=0,UN='RAD/SEC',LE=6.0),...
CDOT(LO=0,UN='RAD/SEC',LE=6.0),...
CRDOT(LO=0,UN='RAD/SEC',LE=6.0)
GRAPH(G2/G2,DE=TEK618,PO=0,.5) TIME(UN='SEC',LE=8.0),...
CR(UN='RAD')
* REF(SC=2.0,LO=0,AX=OMIT)
GRAPH(G3/G3,DE=TEK618,PO=0,0.5) TIME(UN='SEC',LE=8.0),...
YT(UN='METERS')
LABEL (G1) PHASE PLANE
LABEL (G1) XDOT,CDOT,CRDOT VS C
LABEL (G2) STEP RESPONSE
LABEL (G2) C,CR VS TIME
LABEL (G3) MOTION OF THE ARM'S TIP
LABEL (G3) YT VS TIME
END
STOP
```

APPENDIX H

SIMULATION PROGRAM FOR THE SYSTEM USING CURVE FOLLOWING  
TECHNIQUE WITH THE ARM BEING 100 STIFFER

TITLE SIMULATION PROGRAM FOR THE WHOLE SYSTEM  
TITLE USING VELOCITY CURVE FOLLOW TECHNIQUE ONLY.  
TITLE THE ARM IS 100 TIMES STIFFER THAN THE THEORETICAL ONE.  
PARAM K1=0.08, K2=10000.0, KM=1.2000, VSAT=50.000, K=1.00  
PARAM REF=0.1700, CRO=0.0, T=0.00005, KT=1.00, L=1.13  
INTGER N, SW, SW1  
ARRAY NUMWM(7), DENWM(9), NUMTWM(7)  
\* K1: THE CURVE SCALLING CONSTANT  
\* K2: THE AMPLIFIER GAIN  
\* KM: THE INITIAL MOTOR CONSTANT OF THE IDEAL (MODEL) MOTOR  
\* VSAT: THE SATURATION LIMITS OF THE AMPLIFIER  
\* K: THE VELOCITY LOOP FEEDBACK GAIN (OF THE MODEL)  
\* REF: THE COMMANDED HUB ANGLE IN RAD  
\* T: THE SAMPLING INTERVAL  
\* L: THE ARM'S LENGTH  
\* NUMWM IS THE NUMERATOR OF THE HUB TRANSFER FUNCTION  
\* OF THE ARM WITHOUT MASS AT THE TIP.  
\* DENWM IS THE DENOMINATOR OF THE HUB TRANSFER FUNCTION  
\* OF THE ARM WITHOUT MASS AT THE TIP. THIS DENOMI-  
\* NATOR IS THE SAME FOR THE TIP TRANSFER FUNCTION.  
\* NUMTWM IS THE NUMERATOR OF THE TIP TRANSFER FUNCTION  
\* OF THE ARM WITHOUT MASS AT THE TIP.  
TABLE NUMWM(1-7)=46.321, ...  
1009.8, ...  
1.1463678571E7, ...  
1.03584898053E8, ...  
3.17957559457E11, ...  
7.57613805235E11, ...  
3.40664921631E14  
TABLE DENWM(1-9)=1, ...  
26.0, ...  
2.9803594E5, ...  
3.90728207E6, ...  
1.50406090396E10, ...  
7.64243888420E10, ...  
1.54089763177E14, ...  
3.08150159785E13, ...  
0  
TABLE NUMTWM(1-7)=-2.177, ...  
-3.96214E1, ...  
-2.5523332216E4, ...  
-5.20524865907E6, ...  
-2.526229735E10, ...

5.71507551855E10, ...  
3.81407740623E14

INITIAL

A=SQRT(2.\*KM\*VSAT)  
XDOT=0.0  
SW1=0  
YCOM=L\*SIN(REF)  
R=REF\*STEP(0.0)

DERIVATIVE

E=R-C

\*\*\*\*\*  
\*\*\*\*\* CURVE CALCULATION \*\*\*\*\*  
\*\*\*\*\*

NOSORT

IF(E.LT.0.0)XDOT=-A\*K1\*SQRT(ABS(E))  
IF(E.GE.0.0)XDOT=A\*K1\*SQRT(E)

SORT

XDOTE=XDOT-KCDOT  
KCDOT=CDOT\*K  
V=LIMIT(-VSAT, VSAT, K2\*XDOTE)  
CDDOT=KM\*V  
CDOT=INTGRL(0.0, CDDOT)  
C=INTGRL(0.0, CDOT)  
OKU=KT\*V  
CR=TRNFR(6, 8, 0.0, NUMWM, DENWM, OKU)  
CRDOT=DERIV(0.0, CR)  
YT=TRNFR(6, 8, 0.0, NUMTWM, DENWM, OKU)

\*\*\*\*\*  
\*\*\*\*\* SAMPLING OF THE ARM'S HUB \*\*\*\*\*  
\*\*\*\*\* POSITION AND HUB RATE \*\*\*\*\*  
\*\*\*\*\*

SAMPLE

NOSORT

IF(N.EQ.0.0)GO TO 20  
IF(CDOT.GT.XDOT)SW=1  
IF(SW.EQ.1)GO TO 5  
KS=ABS(2.\*CR)/(((N\*T)\*\*2)\*V)  
KM=KS

5

CONTINUE

C=CR

CDOT=CRDOT

20

N=N+1

CONTINUE

SORT

TERMINAL

METHOD RKSFX

CONTRL FINTIM=2.0000, DELT=0.00005, DELS=0.00005

\*RINT 0.05, YT

\*AVE (G1)0.0001, C, XDOT, CDOT, CRDOT

\*AVE (G2)0.0001, TIME, C, CR

SAVE (G3)0.0001, TIME, YT

GRAPH(G1/G1, DE=TEK618, PO=0, .5) C(UN='RAD', LE=8.0), ...

```
XDOT(LO=0,UN='RAD/SEC',LE=12.0),...
CDOT(LO=0,UN='RAD/SEC',LE=12.0),...
CRDOT(LO=0,UN='RAD/SEC',LE=12.0)
GRAPH(G2/G2,DE=TEK618,PO=0,.5) TIME(UN='SEC',LE=8.0),...
  CR(UN='RAD',LE=12.0)
*   REF(SC=2.0,LO=0,AX=OMIT)
GRAPH(G3/G3,DE=TEK618,PO=0,0.5) TIME(UN='SEC',LE=8.0),...
  YT(UN='METERS',LE=12.0)
LABEL (G1) PHASE PLANE
LABEL (G1) XDOT,CDOT,CRDOT VS C
LABEL (G2) STEP RESPONSE
LABEL (G2) C,CR VS TIME
LABEL (G3) MOTION OF THE ARM'S TIP
LABEL (G3) YT VS TIME
END
STOP
```

## APPENDIX I

### SIMULATION PROGRAM FOR THE SYSTEM USING CURVE FOLLOWING TECHNIQUE FOR THE FIRST PART OF THE MOTION AND THEN SWITCHING TO A LINEAR REGULATOR FOR THE FINAL MOTION ( THE ARM IS 100 TIMES STIFFER )

TITLE SIMULATION PROGRAM FOR THE WHOLE SYSTEM  
TITLE USING VELOCITY CURVE FOLLOW TECHNIQUE SWITCHING TO  
TITLE LINEAR MODE FOR THE FINAL MOTION.  
TITLE THE ARM IS THE 100 TIMES STIFFER.  
PARAM K1=0.10,K2=10000.0,KM=1.2000,VSAT=50.000,K=1.00  
PARAM REF=0.1700,CRO=0.0,T=0.00005,KT=1.00,L=1.13  
INTGER N,SW,SW1  
ARRAY NUMWM(7),DENWM(9),NUMTWM(7),NUMCOT(2),DENCOT(4)  
\* K1: THE CURVE SCALLING CONSTANT  
\* K2: THE AMPLIFIER GAIN  
\* KM: THE INITIAL MOTOR CONSTANT OF THE IDEAL (MODEL) MOTOR  
\* VSAT: THE SATURATION LIMITS OF THE AMPLIFIER  
\* K: THE VELOCITY LOOP FEEDBACK GAIN (OF THE MODEL)  
\* REF:THE COMMANDED HUB ANGLE IN RAD  
\* T: THE SAMPLING INTERVAL  
\* L: THE ARM'S LENGTH  
\* NUMWM IS THE NUMERATOR OF THE HUB TRANSFER FUNCTION  
\* OF THE ARM WITHOUT MASS AT THE TIP.  
\* DENWM IS THE DENOMINATOR OF THE HUB TRANSFER FUNCTION  
\* OF THE ARM WITHOUT MASS AT THE TIP.THIS DENOMI-  
\* NATOR IS THE SAME FOR THE TIP TRANSFER FUNCTION.  
\* NUMTWM IS THE NUMERATOR OF THE TIP TRANSFER FUNCTION  
\* OF THE ARM WITHOUT MASS AT THE TIP.  
\* NUMCOT IS THE NUMERATOR OF THE LINEAR COMPENSATOR CONNECTED  
  
\* IN CASCADE WITH THE ARM.  
\* DENCOT IS THE DENOMINATOR OF THE LINEAR COMPENSATOR ABOVE.  
TABLE NUMWM(1-7)=46.321,...  
1009.6,...  
1.1463678571E7,...  
1.03584898053E8,...  
3.17957559457E11,...  
7.57613805235E11,...  
3.40664921631E14  
TABLE DENWM(1-9)=1,...  
26.0,...  
2.9803594E5,...  
3.90728207E6,...  
1.50406090396E10,...  
7.64243888420E10,...  
1.54089763177E14,...

```

3.08150159785E13,...
0
TABLE NUMTWM(1-7)=-2.177,...
-3.96214E1,...
-2.5523332216E4,...
-5.20524865907E6,...
-2.526229735E10,...
5.71507551855E10,...
3.81407740623E14
TABLE NUMCOT(1-2)=3200,...
1600
TABLE DENCOT(1-4)=0.005,...
1.36,...
80.0,...
1600

```

INITIAL

```

A=SQRT(2.*KM*VSAT)
XDOT=0.0
SW1=0
YCOM=L*SIN(REF)
R=REF*STEP(0.0)

```

DERIVATIVE

E=R-C

```

*****
***** CURVE CALCULATION *****
*****

```

NOSORT

```

IF(E.LT.0.0)XDOT=-A*K1*SQRT(ABS(E))
IF(E.GE.0.0)XDOT=A*K1*SQRT(E)

```

SORT

```

XDOTE=XDOT-KCDOT
KCDOT=CDOT*K
V=LIMIT(-VSAT,VSAT,K2*XDOTE)
CDDOT=KM*V
CDOT=INTGRL(0.0,CDDOT)
C=INTGRL(0.0,CDOT)
INPUT=KT*V

```

```

*****
***** SWITCHING TO THE LINEAR MODE *****
*****

```

NOSORT

```

IF(YT.LT.YCOM)OKU=INPUT
IF(YT.GE.YCOM)OKU=OKU1

```

SORT

```

CR=TRNFR(6,8,0.0,NUMWM,DENWM,OKU)
CRDOT=DERIV(0.0,CR)
YT=TRNFR(6,8,0.0,NUMTWM,DENWM,OKU)
IN=YCOM-YT
OKU1=TRNFR(1,3,0.0,NUMCOT,DENCOT,IN)

```

```

*****
***** SAMPLING OF THE ARM'S HUB *****
***** POSITION AND HUB RATE *****

```

\*\*\*\*\*

SAMPLE  
NOSORT

IF(N.EQ.0.0)GO TO 20  
IF(CDOT.GT.XDOT)SW=1  
IF(SW.EQ.1)GO TO 5  
KS=ABS(2.\*CR)/(((N\*T)\*\*2)\*V)  
KM=KS  
5 CONTINUE  
C=CR  
CDOT=CRDOT  
20 N=N+1  
CONTINUE

SORT

TERMINAL

METHOD RKSFX

CONTRL FINTIM=2.5000,DELT=0.00005,DELS=0.00005

PRINT 0.05,TIME

\*AVE (G1)0.0001,C,XDOT,CDOT,CRDOT

\*AVE (G2)0.0001,TIME,CR

SAVE (G3)0.0001,TIME,YT,YCOM

GRAPH(G1/G1,DE=TEK618,PO=0,.5) C(UN='RAD',LE=6.0),...

XDOT(LO=0,UN='RAD/SEC',LE=6.0),...

CDOT(LO=0,UN='RAD/SEC',LE=6.0),...

CRDOT(LO=0,UN='RAD/SEC',LE=6.0)

GRAPH(G2/G2,DE=TEK618,PO=0,.5) TIME(UN='SEC',LE=8.0),...

CR(UN='RAD')

\* REF(SC=2.0,LO=0,AX=OMIT)

GRAPH(G3/G3,DE=TEK618,PO=0,0.5) TIME(UN='SEC',LE=8.0),...

YT(UN='METERS'),YCOM(LO=0.0,SC=40.0E-3)

LABEL (G1) PHASE PLANE

LABEL (G1) XDOT,CDOT,CRDOT VS C

LABEL (G2) STEP RESPONSE

LABEL (G2) C,CR VS TIME

LABEL (G3) MOTION OF THE ARM'S TIP

LABEL (G3) YT VS TIME

END

STOP

## LIST OF REFERENCES

1. Schmitz, E. Experiments on the End-Point Position of a Very Flexible One-Link Manipulator, Ph.D. Thesis, Stanford University, Stanford, California, June 1985.
2. Scientific Systems, Inc., Final Report, Advanced Control of Flexible Manipulators, by P. B. Usoro, R. Nadira, S. S. Mahil and R. K. Mehra, Cambridge, MA 02140, April 1983.
3. Ozaslan, K., The Near-Minimum Time Control of A Robot Arm, Master's Thesis, Naval Postgraduate School, Monterey, California, December 1986.
4. Wikstrom, R. K., An Adaptive Model Based Disk File Head Positioning Servo System, Master's Thesis, Naval Postgraduate School, Monterey, California, September 1985.
5. Suza R., P., Real Time Programming of A Robot, Master's Thesis, Naval Postgraduate School, Monterey, California, December 1986.
6. Johnson, T., Progress in Modelling and Control of Flexible Spacecraft, J. Franklin Institute, February 1983.
7. Rossberg, K., A First Course in Analytical Mechanics, John Wiley & Sons, Inc., 1983.
8. Marks, L. W., Adaptive Notch Filter Suppression of Bending Modes, Master's Thesis, Naval Postgraduate School, Monterey, California, December 1980.

# INITIAL DISTRIBUTION LIST

	No. Copies
1. Defense Technical Information Center Cameron Station Alexandria, Virginia 22304-6145	2
2. Library, Code 0142 Naval Postgraduate School Monterey, California 93943-5002	2
3. Professor G. J. Thaler, Code 62Tr Department of Electrical & Computer Engineering Naval Postgraduate School Monterey, California 93943	5
4. Professor H. A. Titus, Code 62Ti Department of Electrical & Computer Engineering Naval Postgraduate School Monterey, California 93943	1
5. Hellenic Navy General Staff Branch/Direction: GEN/B2 Holargos, Athens, GREECE	4
6. Ioannis Zouzas Anagnostara 35 Kallithea Athens, Greece	4

END

11-87

DTIC